



BIPV boost

D5.2 Report on the project developments of specific performance-based laboratory testing procedures for BIPV products

T5.2 Development of specific performance-based laboratory testing procedures for BIPV products.

Report Name: BIPVBOOST-WP5-T5.2-D5.2_M43-SUPSI_20221104_v00.doc
Version Number: v00

Document Number: D5.2
Due Date for Deliverable: 30/04/2022
Actual Submission date: 04/11/2022
Lead Beneficiary: SUPSI
Document Dissemination Level: PU

BIPVBOOST

“Bringing down costs of BIPV multifunctional solutions and processes along the value chain, enabling widespread nZEBs implementation”

Start date: Month Year. Duration: 4 Years

Coordinator: TECNALIA Grant Agreement No: 817991
www.bipvboost.eu

Summary

This document describes the work conducted in WP5 Task 5.2. In this task, specific calculation and test methodologies have been developed that can describe and evaluate the needed requirements beyond the performance and safety of BIPV products. The task was divided into 4 main activities linked to 4 requirements for BIPV products (Energy economy - Mechanical performance of BIPV elements - Electrical performance in unconventional scenarios - Reaction to fire of BIPV components/systems). The document, therefore, describes what has been developed for the four requirements considering the safety of BIPV products and their performance and aims to define operating limit states in line with what was developed in D5.1. The document aspires to create the basis for considering new calculation and test methodologies in the regulatory framework of the BIPV.

Document Information

Title	D5.2 Report on the project developments of specific performance-based laboratory testing procedures for BIPV products
Lead Beneficiary	SUPSI
Contributors	TECNALIA, CSTB
Distribution	PU
Report Name	BIPVBOOST-WP5-T5.2-D5.2_M43-SUPSI_20221104_v00.doc

Document History

Date	Version	Prepared by	Organisation	Approved by	Notes
23/02/2022	v00	F. Parolini, P. Bonomo, G. Bellenda D. Valencia S. Boddaert	SUPSI TECNALIA CSTB	Jose M. Vega de Seoane (TECNALIA)	Submitted to the EC

Acknowledgements

The work described in this publication has received funding from the European Union's Horizon 2020 research and innovation programme under grant agreement N° 817991.

Disclaimer

This document reflects only the authors' view and not those of the European Community. This work may rely on data from sources external to the members of the BIPVBOOST project Consortium. Members of the Consortium do not accept liability for loss or damage suffered by any third party as a result of errors or inaccuracies in such data. The information in this document is provided "as is" and no guarantee or warranty is given that the information is fit for any particular purpose. The user thereof uses the information at its sole risk and neither the European Community nor any member of the BIPVBOOST Consortium is liable for any use that may be made of the information.

© Members of the BIPVBOOST Consortium



Contents

Document Information.....	2
Document History	2
Acknowledgements.....	3
Disclaimer.....	3
1 EXECUTIVE SUMMARY	13
1.1 Description of the deliverable content and purpose	14
1.2 Relation with other activities in the project.....	14
1.3 Reference material	15
1.4 Abbreviation list.....	15
2 BIPV PRODUCTS QUALIFICATION: FROM STATE-OF-ART TO NEW TEST PROCEDURES.....	17
2.1 Why: summary of state of art and missing gaps.....	17
2.2 How: methodology of NTP in a performance-based perspective	18
2.3 What: technical requirements investigated	19
3 ENERGY ECONOMY	20
3.1 Introduction	20
3.2 Objectives	21
3.3 NTP EE01: Determination of thermal transmittance (U value) for BIPV glazed components	22
3.3.1 Goal.....	22
3.3.2 Problem.....	22
3.3.3 Solution	22
3.3.4 Results.....	24
3.3.5 Discussion.....	25
3.4 NTP EE02: G value of BIPV glasses	26
3.4.1 Goal	26
3.4.2 Problem.....	26
3.4.3 Solution	26
3.4.4 Results.....	27
3.4.5 Discussion.....	28
3.5 Maximum temperature results and other.....	29
3.5.1 Goal	29
3.5.2 Results	29
3.5.3 Discussion.....	30
3.6 Conclusions and next steps	30
4 ELECTRICAL SAFETY.....	32
4.1 Introduction	32
4.2 Objectives	32
4.3 NTP EL01: BIPV operating temperatures in non-conventional scenarios	33

4.3.1	Goal	33
4.3.2	Problem	33
4.3.3	Solution	35
4.3.4	Results	37
4.3.4.1	Test procedure	38
4.3.4.2	Equipment	41
4.3.4.3	Test execution and main results.....	42
4.3.4.4	Discussion	43
4.4	NTP EL02: Electrical safety and durability of insulating materials for BIPV products	44
4.4.1	Goal	44
4.4.2	Problem	44
4.4.3	Solution	46
4.4.4	Results	47
4.4.4.1	Test procedure	53
4.4.4.2	Equipment	53
4.4.4.3	Test execution and main results.....	54
4.4.4.4	Discussion	55
4.5	NTP EL03: Suitability of protection devices for BIPV products.....	56
4.5.1	Goal	56
4.5.2	Problem	56
4.5.3	Solution	57
4.5.4	Results	59
4.5.4.1	Test procedure	60
4.5.4.2	Equipment	61
4.5.4.3	Test execution and main results.....	61
4.5.4.4	Discussion	64
4.1	Conclusions and next steps	64
5	MECHANICAL SAFETY	65
5.1	Introduction	65
5.2	Objectives	65
5.3	NTP ME01: BIPV impact resistance	66
5.3.1	Goal	66
5.3.2	Problem	66
5.3.3	Solution	67
5.3.4	Results	69
5.3.4.1	Test execution and main results.....	69
5.3.4.2	Discussion	70
5.4	NTP ME02: Static mechanical load resistance for BIPV products.....	71
5.4.1	Goal	71
5.4.2	Problem	71
5.4.3	Solutions.....	71
5.4.4	Results	73
5.4.4.1	Test execution and main results.....	73
5.4.4.2	Discussion	74
5.5	Conclusions and next steps	75
6	FIRE SAFETY	76
6.1	Introduction	76

6.2	Objectives	77
6.3	NTP FR01: Roof fire reaction for BIPV products with electric load in ultimate LS	79
6.3.1	Goal	79
6.3.2	Problem	80
6.3.3	Proposal.....	80
6.3.4	Results	85
6.3.4.1	Test procedure	85
6.3.4.2	Equipment	85
6.3.4.3	Test execution and main results.....	86
6.4	NTP FR02: Facade fire reaction for BIPV products with electric load in ultimate LS.....	89
6.4.1	Goal	89
6.4.2	Problem.....	90
6.4.3	Proposal.....	90
6.4.4	Results	96
6.4.4.1	Test procedure	96
6.4.4.2	Equipment	96
6.4.4.3	Test execution and main results.....	97
6.5	NTP FR03: Fire reaction for other BIPV products with electric load in ultimate LS	101
6.6	Conclusions and next steps	101
7	ANNEXES	103
7.1	Energy Economy	103
7.1.1	Standards review and its conclusions	103
7.1.2	New studies performed related to new BIPV effects.....	105
7.1.3	Operating temperatures, dynamic U value and dynamic G value of double IGU PV glass	106
7.1.3.1	PV glazing thermal model - description.....	107
7.1.3.2	PV glazing thermal model - results.....	110
7.1.3.3	PV glazing thermal model – maximum temperatures with worse boundary conditions.....	116
7.1.4	Finite-Element-Method thermal simulations.....	123
7.1.4.1	The purposes	123
7.1.4.2	The cases	124
7.1.4.3	The results	128
7.1.5	Junction box effect on U-value and G-value	136
7.1.5.1	U value calculation method.....	138
7.1.5.2	G value calculation method.....	140
7.1.5.3	Results for specific JB dimensions	142
7.1.5.4	Generalized U value results for different JB dimensions.....	144
7.1.5.5	Generalized G value results for different JB dimensions.....	147
7.1.6	Light transmittance of different solar cells technologies	149
7.2	Mechanical Safety	150
7.2.1	NTP_ME01: general procedure for impact resistance test procedure for BIPV products	150
7.2.1.1	Summary	150
7.2.1.2	Definitions	150
7.2.1.3	Scope	152
7.2.1.4	Applicability on use categories, product families and kits	153
7.2.1.5	Normative references.....	153
7.2.1.6	Limit states requirements	154
7.2.1.7	Equipment	155
7.2.1.8	Device under test – sample definition.....	155
7.2.1.9	Impact point determination and temperature control	156
7.2.1.10	Procedure workflow	158

7.2.1.11	Assessing and judging limit states thresholds and test results	158
7.2.1.12	Legal basis.....	159
7.2.2	NTP-ME01-VK- SC00: Impact resistance test and results for a Vecture KIT” in Scenario “O”	160
7.2.2.1	Scope	160
7.2.2.2	Applicability	160
7.2.2.3	Normative references.....	160
7.2.2.4	Equipment	160
7.2.2.5	Procedure	160
7.2.2.6	Uncertainty.....	161
7.2.2.7	Test results	161
7.2.3	NTP-ME01: results of impact resistance test with temperature effect on different product classes.....	167
7.2.3.1	Scope	167
7.2.3.2	Applicability	167
7.2.3.3	Normative references.....	167
7.2.3.4	Equipment	167
7.2.3.5	Test procedure	168
7.2.3.6	Result.....	169
7.2.4	NTP_ME02: Static mechanical load test for BIPV products	175
7.2.4.1	Purpose.....	175
7.2.4.2	Methodology	175
7.2.4.3	Results	177
7.2.4.4	Conclusions.....	180
8	CONCLUSIONS.....	180
9	REFERENCES.....	182
10	ACKNOWLEDGMENTS	188

Tables

Table 1.1	Relation between current deliverable and other activities in the project	14
Table 2	Activity 5.2.1: Energy economy (EE): thermal transmittance (U) value. Summary sheet	23
Table 3.	Summary of average operating gas temperature and ΔT from dynamic simulations of PV-IGU in vertical.....	24
Table 4	NTP EE02: G value of BIPV glasses. Summary sheet.....	27
Table 5	NTP EL01: BIPV operating temperatures in non-conventional scenarios. Summary sheet	34
Table 6.	Results of NTP01 tests	42
Table 7	Relation of test levels proposed in the IEC TS 61326 expected to operate at higher temperatures, with SLS thermal classes for the BIPV products	44
Table 8.	NTP EL02: Electrical safety and durability of insulating materials for BIPV products	45
Table 9.	Applicability of the new test procedure to all BIPV families and types.....	46
Table 10.	Preliminary results for NTP-EL02 electrical safety and durability of insulating materials for BIPV products.....	54
Table 11.	Suitability of protection devices for BIPV products. Summary sheet.....	57
Table 12	NTP 03 for suitability of protection devices for BIPV products within the PV test sequence 58	
Table 13.	BIPV impact resistance-summary sheet	68
Table 14.	Static mechanical load resistance for BIPV products. Summary sheet	72
Table 15	NTP FR01: Roof fire reaction for BIPV products with electric load in ultimate LS	84
Figure 16:	DC PV GENERATOR (10 kW DC) used in electric load NTP	86

Table 17. List of analyzed standards related to glazing thermal transmittance (U value).....	103
Table 18. List of conclusions from the analysis of the standards related to glazing thermal transmittance (U value)	104
Table 19. List of analyzed standards related to glazing solar factor (G value).....	104
Table 20. List of conclusions from the analysis of the standards related to glazing solar factor (G value)	104
Table 21. List of analyzed standards related to energy performance of buildings.....	105
Table 22. List of conclusions from the analysis of the standards related to energy performance of buildings.....	105
Table 23. Technical gaps and how they are studied in this work.....	106
Table 24. U value as function of IGU gas temperature and ΔT . Air case. [4mm + 4mm / 16 mm Air / 4mm].....	106
Table 25. U value as function of IGU gas temperature and ΔT . Argon case. [4mm + 4mm / 16 mm Argon / 4mm]	107
Table 26. U value as function of IGU gas temperature and ΔT . Argon with LowE glass case. [4mm + 4mm / 16 mm Argon / LowE - 4mm]	107
Table 27. Average dynamic solar factor compared to normal incidence steady-state solar factor of PV-IGU WITHOUT LowE.....	112
Table 28. Solar factor as function of PV ratio and PV efficiency. PV-IGU WITHOUT LowE.	113
Table 29. Average dynamic solar factor compared to normal incidence steady-state solar factor of PV-IGU WITH LowE.....	114
Table 30. Solar factor as function of PV ratio and PV efficiency. PV-IGU WITH LowE.	115
Table 31. Solar factor as function of PV ratio and temperature coefficient of PV efficiency. PV-IGU WITH LowE.	115
Table 32. Operating temperature, dynamic U and dynamic G of PV-IGU WITHOUT LowE [4mm_lowIron + 4mm / 16 mm Argon / 4mm].....	117
Table 33. Operating temperature, dynamic U and dynamic G of PV-IGU WITH LowE [4mm_lowIron + 4mm / 16 mm Argon / LowE - 4mm]	118
Table 34. Operating temperature as function of PV efficiency of PV-IGU WITH LowE [4mm_lowIron + 4mm / 16 mm Argon / LowE - 4mm]	120
Table 35. Dynamic U and dynamic G as function of PV efficiency of PV-IGU WITH LowE [4mm_lowIron + 4mm / 16 mm Argon / LowE - 4mm]	120
Table 36. Temperatures as function of Rse/Wind velocity and indoor temperature of PV-IGU WITHOUT LowE (MPP).....	121
Table 37. Temperatures as function of Rse/Wind velocity and indoor temperature of PV-IGU WITH LowE (MPP).....	122
Table 38. Maximum temperatures as function of Rse and PV occupancy ratio of PV-IGU WITH LowE. Indoor temperature 29 °C. Open-circuit state.	123
Table 39. List of thermal FEM simulations cases.....	124
Table 40. Diagram of material layers of PV-IGU in FEM simulations	127
Table 41. Material properties considered in FEM simulations	127
Table 42. Temperatures results of PV-IGU for FEM cases, both from FEM simulations and PV glazing thermal model. In grey, extreme cases with Rse = 0,13 m ² K/W.	133
Table 43. Temperatures and outwards radiation flux of different PV glass configurations	136
Table 44. Data for the calculation of the thermal resistance of the JB cavity. Example for 18 mm JB thickness and $\Delta T=7,5$ K (on IGU).....	139
Table 45. Thermal resistance of a squared shape JB (Height = Width) for different surfaces and thicknesses. 15 K as temperature difference between cavity faces, i.e. to be used with no-IGU PV glazing	144

Table 46. Thermal resistance of a squared shape JB (Height = Width) for different surfaces and thicknesses. 7,5 K as temperature different between cavity faces, i.e. to be used with one cavity PV IGU glazing.....	145
Table 47. Reduction of overall PV module U value due (ΔU) to junction box [W/m ² K] (4mm+4mm laminated).....	145
Table 48. Reduction of overall PV module U value (ΔU) due to junction box [W/m ² K] (4mm+4mm / 16mm / 4mm).....	146
Table 49. Reduction of overall PV module U value (ΔU) due to junction box [W/m ² K] (4mm+4mm / 16mm / 4mm LowE).....	147
Table 50. Reduction of overall PV module G value (ΔG) due to junction box [%].....	148
Table 51. Hard and soft body impact locations (Source EAD 040914-00-0404).....	156
Table 52. Impact locations (Source IEC 61215-2 (3)).	156
Table 53 . LS assessment criteria.....	159
Table 54. Test results NTP ME01-VK-SC00 – cat.IV.....	162
Table 55. Test results NTP ME01-VK-SC00 – cat.III.....	165
Table 56. Hard body impact made at room temperature.....	170
Table 57. Hard body impact made at high temperature (90°C).....	170
Table 58. Hard body impact made at low temperature (-30°C).....	171
Table 59. Hard body impact made at high and low temperatures for the PV Veture KIT.....	172
Table 60. Hard body impact made at different temperature for the PV Roof tile.....	173
Table 61. General test indications and strain results.....	178

Figures

Figure 1. Hardware equipment- Shading moveable mask (left) and smart rack (right).....	41
Figure 2. Example of software interface used for data acquisition and procedure automation.....	41
Figure 3. full combined IEC 61215-IEC 61730 testing sequence is shown, where the main accelerated ageing test are highlighted with red boxes.....	48
Figure 4. The newly designed test procedure combines such ageing tests in one item, while reducing the number of samples to be tested (from 6 to 2).	49
Figure 5. NTP – EL 02: profile of combined thermal cycle for BIPV-SLS Thermal class 0.....	51
Figure 6. NTP EL 02: profile of combined thermal cycle for BIPV-SLS Thermal class 1 (test points are highlighted with red circles)	52
Figure 7. NTP – EL 02: profile of combined thermal cycle for BIPV-SLS Thermal class 2 (test points are highlighted with red circles)	52
Figure 8. Source measure unit and control panel application for NTP EL-03.....	61
Figure 9. Datasheet of the NTP EL03 results.....	63
Figure 10. Hierarchical approach for NTP development. This procedure is related to “General NTP-MECH01”. Specific procedures “NTP MECH-01-CPXX” will be adopted for defined “product type” (PTX) and “test type” (TTX)	67
Figure 11 : Initial ratio determination stages to assess BIPV systems according the full NTP process....	78
Figure 12 : Ratio determination to assess BIPV exclusively with electrical load under NTP.....	79
Figure 13: Electric load setup applied during the fire test to stress electrically the BIPV solution.	81
Figure 14: Side view and top view of test bench with location of the firebrands according to the CEN TS 1187 requirements.	82
Figure 15: Configuration according to standard CEN TS 1187 recommendations.....	83

Figure 16 : configuration chosen according to the manufacturer's recommendations	83
Figure 17. DC PV GENERATOR (10 kW DC) – preliminary settings before mockup connection Load device and remote control to test load on CIGS module (left) / User interface with load level (right)	86
Figure 18. Before/during/after the fire test with DC PV GENERATOR load applied. During the test, current and voltage values are checked to identify possible breaks in the electrical circuit... ..	87
Figure 19. Example of electric load carried out during Broof test (roof shingle product)	88
Figure 20. No electrical breakage observed – no negative effects due to electric load	88
Figure 21 Electric load setup applied during the fire test to stress electrically the BIPV solution	91
Figure 22 : Left side view (long wing/wall) and right side view (short wing/wall) of test bench with module size details according to the <i>EN 13823: 2020</i> requirements.....	93
Figure 23 : Configuration according to standard <i>EN 13823: 2020</i> recommendations, example of veture kit layout	93
Figure 24 : Configuration CIGS flexible module on a veture kit façade cladding system according to the manufacturer's module size (red area). Blue area are halves cut modules (not operating)	94
Figure 25. DC PV GENERATOR (10 kW DC) used in electric load NTP	97
Figure 26. DC PV GENERATOR (10 kW DC) – SBI preliminary settings before mockup connection Load device and remote control to test load on CIGS module (left) / User interface with load level (right) – Same procedure is used for crystalline modules	97
Figure 27. Before/during/after the fire test with DC PV GENERATOR load applied on veture kit cladding system with a front glass-glass module	98
Figure 28. Before/during/after the fire test with DC PV GENERATOR load applied on veture kit cladding system with a front CIGS-based flexible module.....	98
Figure 29. Example of electric load carried out during SBI test (façade product)	99
Figure 30. No electrical breakage observed – no negative effects due to electric load during all SBI tests. (picture as an example)	100
Figure 31. Busbar status after fire test, continuity test are performed, and module are still working / glass-glass module on veture kit cladding (Left) – thin film module polymeric-based on veture kit cladding (Right)	101
Figure 32. Sketch of PV-IGU system and the thermal circuit defined for the model.....	109
Figure 33. Model of internal surface resistance (R_{si}) as function of glass inclination (90° is vertical). Red: Outer glass is colder than inner glass. Green: Outer glass is hotter than inner glass.	109
Figure 34. Information flux of PV glazing thermal model	110
Figure 35. Example of 100% PV occupancy or lower with homogeneous absorption of sun radiation (e.g. transparent thin film).....	126
Figure 36. Example of 80% PV occupancy with heterogeneous absorption of sun radiation in 156x156 mm solar cells.	126
Figure 37. Different positions of the concentrated solar cells (blue). The arrow is the gravity vector. Examples for PV-IGU configuration.	127
Figure 38. Temperature results of case 1 in FEM simulations	129
Figure 39. Temperature of the air in the PV-IGU cavity. Case 1. From left to right: Bottom, middle and top of the cavity.	130
Figure 40. Temperature results of case 3 in FEM simulations. All elements.	131
Figure 41. Temperature results of case 3 in FEM simulations. Solar cells and intermediate EVA.....	131
Figure 42. Temperature results of case 3 in FEM simulations. Internal (2^{nd}) glass layer. Outer face (top) and inner face (bottom).....	132
Figure 43. Outer PV glass temperature of PV-IGU calculated with stationary and transient conditions. Façade (FC) and 30° tilted skylight (SK). Meteorological data from 21 st January and 7 th September in Madrid.....	134

Figure 44. Radiative heat fluxes of outer surface of PV glass with 50% PV occupancy. Left: PV cells concentrated at the top. Right: PV cells concentrated at the bottom	135
Figure 45. Sketches of the four cases where the impact of the JB on the U value has been studied. The sun represents the external side.	137
Figure 46. Sketches of the six cases where the impact of the JB on the G value has been studied. The sun represents the external side.	137
Figure 47. Picture of the reference junction box and the surfaces for view factors calculation	138
Figure 48. Optical data of glass layers used for the calculation of the optical properties of the laminated PV glass, PV-IGU and PV-IGU Low E.	141
Figure 49. Optical data of the transparent areas of laminated glass, IGU and IGU Low E.	141
Figure 50. U and G value for PV double laminated glass with 4 mm Low iron and 4 mm normal glass. Results for JB with dimensions 80 x 69 x 18 mm (H x W x D)	143
Figure 51. U and G value for PV-IGU with previously PV laminated glass plus 16 mm cavity and back normal glass. Results for JB with dimensions 80 x 69 x 18 mm (H x W x D)	143
Figure 52. U and G value for PV-IGU LowE with previously PV laminated glass plus 16 mm cavity and back low emissivity glass. Results for JB with dimensions 80 x 69 x 18 mm (H x W x D)	144
Figure 53. Transmittance of different solar cell technologies (bare cells, not laminated)	149
Figure 54. Hierarchical approach for NTP development. This procedure is related to "General NTP-MECH01". Specific procedures "NTP MECH-01-CPXX" will be adopted for defined "product type"(PTX) and "test type" (TTX)	152
Figure 55. Hard bodies and soft bodies, as specified by the reference European Assessment Documents (EADs) derived from ISO 7892	155
Figure 56. Hail test impact locations for wafer/cell based technologies (Source: IEC 61215-2 (3)).	157
Figure 57. Hard body impact test.	163
Figure 58. Hard body impact test, detail.	163
Figure 59. Soft body impact test.	163
Figure 60. Soft body impact test, detail.	163
Figure 61. Electroluminescence before hard and soft body test.	163
Figure 62. Electroluminescence after a hard body impact. No damages on cells.	163
Figure 63. Electroluminescence after a soft body impact. No damages on cells.	163
Figure 64. Hard body impact equipment.	166
Figure 65. Hard body impact breakage of the rear glass (ID 1, position 05).	166
Figure 66. Hard body impact test on the edge (ID 2, position 02).	166
Figure 67. Glass breakage after hard body impact test (ID 2, position 02).	166
Figure 68. Electroluminescence before hard body test.	166
Figure 69. Electroluminescence after a hard body impact (ID 2, position 7). Dark response of a single cell.	166
Figure 70. Structure consisting of two rails that guarantee the attachment of the module on the long side	169
Figure 71. Structure consisting of two rails that are fixed in between the insulation layer and the mortar of the module	169
Figure 72. Temporary structure consisting of two railings on which four clamps are fixed to ensure the attachment of the module.	169
Figure 73. Aspect of the PV module before the impact.	171
Figure 74. Electroluminescence made on the "ID4" at high temperature (90°C).	171
Figure 75. Electroluminescence made on the "ID3" at room temperature (25°C).	171
Figure 76. Electroluminescence made on the "ID5" at high temperature (90°C).	171
Figure 77. Electroluminescence made on the "ID6" at high temperature (90°C).	172
Figure 78. Electroluminescence made on the "ID7" at high temperature (-30°C).	172

Figure 79. Electroluminescence made on the “ID8” at high temperature (-30°C).	172
Figure 80. Electroluminescence made on the “ID9” at high temperature (-30°C).	172
Figure 81. Aspect of the sample “ID1” module before the impact.	173
Figure 82. Electroluminescence made on the “ID1” at high temperature (90°C) for the category III... ..	173
Figure 83. Aspect of the sample “ID2” module before the impact.	173
Figure 84. Electroluminescence made on the “ID2” at low temperature (-30°C) for the category III... ..	173
Figure 85. Electroluminescence made on the “ID1” at room temperature (25°C).	174
Figure 86. Electroluminescence made on the “ID2” at high temperature (54°C).	174
Figure 87. Electroluminescence made on the “ID3” at low temperature (-30°C).	175
Figure 88. Detail of the circle formed on the polymer after the impact.	175
Figure 89. Static mechanical load test for BIPV products. Test description.	176
Figure 90. Equipment developed for the PV Veture KIT	177
Figure 91. Electroluminescence equipment developed.	177
Figure 92. Electroluminescence of a PV laminated module.	177
Figure 93. Deformation on PV roof tile under mechanical load.	179
Figure 94. Test made on BIPV glass-glass module.	179
Figure 95. Test made with push load on PV laminated glass during the cycles.	179
Figure 96. Test made with pull load on PV laminated glass during the cycles.	179
Figure 97. Concentrated load on PV laminate glass in the climatic room.	179
Figure 98. Permanent deformation due to concentrated load at high temperature on PV laminated glass.	179

1 EXECUTIVE SUMMARY

The increasing and urgent demand for decentralized renewable energy led to a growing need for integrating photovoltaics (PV) in the built environment. Building Integrated Photovoltaics (BIPV) is progressively achieving an advanced level of technical maturity and considerable market penetration, in synergy with ambitious EU targets for Green Deal and Renovation Wave. The main technical challenges to unlock its massive potential and installation capacity are today mostly related to cost-effectiveness and product quality. Integrating PV in construction products, requires an accurate performance assessment in accordance with construction norms and PV standards, depending on the type of use in building. Although the EN 50583 (1) introduced a reference framework in Europe, BIPV multifunctional products are currently stagnant in uncertain qualification processes with the lack of clear regulations and missing gaps in normative that could facilitate its diffusion and acceptance. Product placing on the market is articulated on the separate application of electrical standards (IEC 61215 (2) (3) and IEC 61730 (4) (5)) and the EU Construction Products Regulation 305/2011 (6). Multifunctional BIPV products can perform different functions, involving more and more the use of several materials that must coexist in the same unitized construction component. These elements, electrically active and non-active, assembled together, mutually induce and influence changes both in the energy performance and in the construction requirements, such as the energy yield, dissipation of heat, mechanical safety, fire behaviour, etc. This performance relations have been only partially investigated at the state of art of BIPV quality assessment.

However, due to the interaction between PV and building parts, the quality assessment requires to go further than the application of the test methodologies provided separately by the PV or by the building regulations. In the previous part of the project BIPVBOOST, deliverable D5.1 provided the overview of the current normative framework in the BIPV field, the definition of the relevant missing gaps, and the key-aspects for grounding a new testing approach. In order to overcome some of these barriers and challenges, in this report the authors progressed with newly developed procedures for the qualification of some BIPV product requirements, with the ambition of addressing a more complete qualification scheme and favour the product introduction into market. A performance-based approach based on Limit States (LS), where possible, has been used as ground scheme to formulate the main new procedural proposals in order to assess both the electrical and building aspects involved with an integrated and interdisciplinary standpoint. Such a performance-based approach, as the key-concept of the proposed approach, is intended to relate the test methodology with the growing use of design engineering principles, calculations, and/or appropriate software tools to substantiate the proposed solution and to satisfy the limit-states to ensure product compliance with reduced time and costs. The methodology and preliminary findings with the related threshold levels, taking into account the effect of the main operative conditions such as temperature or electricity effects, are presented and analysed. As a result, it is envisaged that the implementation will help operators and prospective normative upgrading, ensuring more outstanding product quality for BIPV's market and driving toward a reduction in life cycle costs.

1.1 Description of the deliverable content and purpose

The main scope of WP5 was to develop an advanced BIPV qualification framework based on performance and not on pre-established criteria. The identification of current missing gaps in the standards (T5.1 and D5.1 (7)) served as basis to develop a roadmap describing the principles and basic approaches for BIPV products qualification. In T5.2, starting from this framework, the scopes of the testing procedures were elaborated for each requirement, considering the main implications in terms of normative references, process, product family extension, etc. The work was done also in coordination with the active participation of SUPSI, TECNALIA and CSTB in other activities such as Task 15 IEA-PVPS Subtask C: "International framework of BIPV specifications" (8), Task 15 IEA-PVPS Subtask E: "Pre-normative international research on BIPV characterization methods" (9) (www.iea-pvps.org), Construct-PV (10) (www.constructpv.eu) and PVSITES (11) (www.pvsites.eu), as well as to other relevant groups, technical committees and EU networks.

In this document, the aspects concerning the proposals for qualifying BIPV products are reported with respect to four fundamental requirements: energy performance of glass, electrical and mechanical safety, fire prevention. For each specific requirement under investigation, the goal was to cover the existing gaps in the current standardisation framework, simplifying the procedures and considering also a cost reduction related to the overall qualification process. Definition of test methodologies and equipment are reported, in order to set and define which are the concrete tools and procedures set for the various product families, limit states, combined performance and the other aspects assumed in relation to the existing standardization framework. Also, the first output targets, namely the KPIs resulting as "value" describing the BIPV performance from the first sample test applied, are part of the results.

1.2 Relation with other activities in the project

The relation with other activities in the project are shown as followed. Table 1.1 depicts the main links of this deliverable to other activities (work packages, tasks, deliverables, etc.) within BIPVBOOST project.

Table 1.1 Relation between current deliverable and other activities in the project

Project activity	Relation with current deliverable
T1.3	Archetypes defined in D1.3 will support the product family definition
T5.1	D5.1 providing the state-of-the-art in BIPV standardisation and related missing gaps, addressed in Task 5.2
T5.3	The results obtained from standard test permit to compare the NTP results in order to verify the reliability
T5.4	The BIPV products developed will be tested according to new testing procedures in addition to standard procedures in T5.3
WP3-WP4	The testing methodologies developed are put in relation with the real product families and manufacturing/market needs (feedback from industries supported the deliverable)
WP8	The testing methodologies developed are put in relation with the real product families used in the demo sites

1.3 Reference material

IEA-PVPS Task 15, *Compilation and Analysis of User Needs for BIPV and its Functions*, February 2019 (www.iea-pvps.org)

IEA-PVPS Task 15, *International definitions of "BIPV"*, August 2018 (www.iea-pvps.org)

IEA-PVPS Task 15, *Analysis of requirements, specifications and regulation of BIPV*, July 2019 (www.iea-pvps.org)

PVSITES, *European regulatory framework for BIPV*, project report, July 2016 (www.pvsites.eu)

PVSITES, *Standardization needs for BIPV*, project report, September 2016 (www.pvsites.eu)

BIPVBOOST, *Report on standardization, performance risks and identification of related gaps for a performance-based qualification in BIPV* (www.bipvboost.eu).

1.4 Abbreviation list

AEC	Architecture, Engineering and Construction
BAPV	Building applied Photo Voltaic
BIPV	Building Integrated Photo Voltaic
CE	European Commission
CPR	Construction Products Regulation
DoP	Declaration of performance
EAD	European Assessment Document
EEA	European Economic Area
EDP	Early Design Phase
EOTA	European Organisation for Technical Assessment
EPBD	Energy Performance of Buildings Directive
ETAs	European Technical Assessments
ETAG	European Technical Approval Guidelines
FEM	Finite Element Method
hEN	Harmonized standard
IEA	International Energy Agency
LVD	Low Voltage Directive
MG	Missing Gap
NTP	New Testing Procedures
non c.s.	Non conventional scenario
nZEB	Nearly Zero Emission Building
PEB	Plus Energy Building
PV	Photovoltaic

PVB Polyvinyl Butyral

TABs Technical Assessment Body

Tn Task number

WPn Work package number

2 BIPV PRODUCTS QUALIFICATION: FROM STATE-OF-ART TO NEW TEST PROCEDURES

EN 50583-1:2016 “Photovoltaics in buildings” (1) states that the properties of a BIPV module should be evaluated with respect to both relevant building requirements as set in the European Construction Product Regulation CPR 305/2011, and electro-technical requirements as specified in the LVD 2014/35/EU. Generally, the active part consists of solar cells made of semiconductor material, normally silicon, which transform solar radiation into electricity. In some cases, the active part is made up of semiconductor materials deposited on the surface of the glass inside the laminate. The insertion of PV cells inside the laminated glass can potentially determine changes in the overall behavior for some requirements. This document takes into consideration such a variation provided by the PV active part on the BIPV performance, as the key-point for reviewing the current limits of the product qualification (or design and engineering in some cases), as the starting point towards the proposal of new combined testing and performance-based assessment approaches.

2.1 Why: summary of state of art and missing gaps

Any construction product placed on the market in the European Economic Area (EEA), deals with harmonizing performance information across the EU. By drawing up the declaration of performance, the manufacturer shall assume responsibility for the conformity with such declared performance. However, according to Art.5 CPR 305/2001, a manufacturer may refrain from drawing up a declaration of performance when placing a construction product covered by a harmonized standard on the market where it is individually manufactured or custom-made in a non-series process in response to a specific order, and installed in a single identified construction work, in compliance with the applicable national rules and under the responsibility of those responsible for the safe execution of the construction works designated under the applicable national rules. Specific Technical Documentation demonstrating compliance of that product with the applicable requirements and equivalence of procedures can be used.

On the other hand, for terrestrial photovoltaic (PV) modules, the IEC 61215-1:2021 sets that *“Changes in material selection, components and manufacturing process can impact the qualification of the modified product. Retesting shall be performed according to IEC TS 62915 (12). During retesting, tests that are performed on representative samples do not need to be repeated if the only change to a product is one of size, and the change in product size still allows use of the same representative sample size already tested.”* Thus, some modification in the design, materials, components or processing of the module may require a repetition of some or all the qualification tests to maintain type approval.

Thus, the current complexity among building and PV normative assets, as it is today, that are considered separately, as already reported (7), and also addressed in the report “Proposed Topics for Future International BIPV Standardization Activities” from Task 15 IEA-PVPS, identified areas where there is still a need for international standardization on multifunctional characterization of BIPV modules and systems and to recommend approaches which could be taken to meet this need (13). To date, the building codes do not consider the presence of active parts that produce energy, such as PV cells, while the standards regarding PV modules do not sufficiently cover the building requirements. In the lack of a clear normative the two functions (building and electrical) still remain separate in the original normative acts (CPR 305/2011 and LVD 2014/35/EU) and in the consequent harmonized standards, thus not providing a concrete specification supporting a multidisciplinary assessment of BIPV. Laboratory tests also remain on separate paths, sectors and qualification logics are disconnected (e.g. for CE-marking) and today there are no test procedures considering a combination of building and PV functionality as a matter of fact for complete performance assessment and product qualification. Designers, manufacturers and installers currently mainly overlap procedures developed for standard PV with other standards already defined for the building sector (for non-

active elements) such as norms related to glass, to fire safety, etc. Real examples provide evidence of the current difficulties in qualifying BIPV products and the correlated risks in terms of responsibility in which players today incur. Some performances don't have a clear reference in the actual normative so in many cases his lack become a "no go" for the decision making process with a negative impact on the market. Also, in cases favourable to BIPV, a crucial aspect is today the high time and cost of the certification and retesting process. This calls for further developments, where a first step of a possible path is considered achievable by developing a new approach for the qualification of BIPV products, as pre-normative support, coherently with the principles of CPR 305/2011.

2.2 How: methodology of NTP in a performance-based perspective

As introduced in D5.1 (7), in order to overcome the limitation of a prescriptive approach usually adopted for standard PV, a first design criterion of the procedures is the **performance-based approach**, with the goal to base them on the reliability-based principles that have to be defined as a number of limit states to be explicitly checked. The performance-based approach to design usually relies on the use of engineering principles, calculations and/or appropriate software modelling tools to substantiate the proposed solution and to satisfy the limit-state. When using the performance-based pathways to code compliance, values are entered into a model, allowing the building designer to optimize the various components, equipment and assemblies, saving money, time and operating expenses. To use the performance-based approach, **limit states (LS)** were defined to identify the different conditions beyond which the product no longer fulfills the relevant pre-defined criteria as a *"condition beyond which the work/component no longer meets the requirements listed in the standards"*.

Compared to traditional building products, BIPV products contain an electrical part that is not considered in building regulations. As an example, the regulatory framework for glass in building (ISO 12543 (14), EN 12600 (15)) does not include any specific reference to electrical limit states or to the presence of PV cells (e.g. as defined in IEC 61730 (4) (5) and IEC 61215 (2) (3)). This electrical part plays a fundamental role in defining the safety of the BIPV product such as for electrical safety, which is necessary to include in the definition of the limit state as a key requirement, in addition to the construction aspect, e.g. to evaluate performance also according to IEC 61730 standard (4) (5). Starting from these considerations, the approach also considered the **contemporaneity of effects/actions** in order to accurately describe the BIPV behavior aimed at reproducing the operating conditions. A typical BIPV specific characteristic is the higher operating temperature, compared to the standard PV module. The investigation of temperature impact on electrical safety, mechanical safety and energy economy aspects has been investigated on different scenarios e.g. by considering the combined effect of temperature during impact resistance tests (NTP ME01) or to set the thermal boundary on electrical safety tests (NTP EL02) or the adequacy of protective devices (NTP EL03). At the same time specific procedures were aimed at defining the operating temperature in non-conventional scenarios including shading (NTP EL01) or features of the IGU in relation with the energy economy.

The testing procedures proposed are developed in the perspective of supporting, in a long-term strategy, a higher design flexibility based on performance objectives, to constitute a beneficial and competitive concept for supporting a stronger BIPV engineering, ensuring a simplification of the testing procedures and a reduction of the needed time and costs for testing.

2.3 What: technical requirements investigated

At the European level, the REGULATION (EU) N. 305/2011 (16) *“lays down conditions for the placing or making available on the market of construction products by establishing harmonized rules on how to express the performance of construction products in relation to their essential characteristics”*.

According to CPR, a *“construction product”* is defined as *“any product or kit which is produced and placed on the market for incorporation in a permanent manner in construction works or parts thereof and the performance of which has an effect on the performance of the construction works with respect to the basic requirements for construction works”*. Furthermore, it defined as *“essential characteristics those characteristics of the construction product which relate to the basic requirements for construction works”*.

An important point of the CPR is that *“construction works as a whole and in their separate parts must be fit for their intended use, taking into account in particular the health and safety of persons involved throughout the life cycle of the works”* and they *“must satisfy basic requirements for construction works for an economically reasonable working life”*. Concerning the photovoltaic modules used as construction products, the EN 50583 (all parts) (17) (18) shall be considered as well. These standards refer to both construction and electrical characteristics, in fact, *“focuses on the properties of photovoltaic modules relevant to essential building requirements as specified in the European Construction Product Regulation CPR 305/2011, and on the applicable electro-technical requirements as stated in Low voltage Directive (LVD) 2014/35/EU (19) (ex Low Voltage Directive 2006/95/EC / (20)) or CENELEC standards”*.

Regarding building requirements, the EN 50583-1 (17) consider PV modules when *“they are considered to be building-integrated forming a construction product providing a function as defined in the European Construction Product Regulation CPR 305/2011 (16)”*.

According to EN 50583-1 (17) *“the BIPV module is a prerequisite for the integrity of the building’s functionality. If the integrated PV module is dismantled the PV module would have to be replaced by an appropriate construction product”*. The EN50583 (17) (18), following the same methodology of CPR, defines seven building’s functions specific for these PV products to be assessed. In addition to building requirements, *“as electrical components, BIPV modules are subject to the applicable electro-technical requirements as stated in Low voltage Directive (LVD) 2014/35/EU (19) (ex Low Voltage Directive 2006/95/EC / (20)) or CENELEC standards”* and they shall comply with the electrical standards. (2) In the International framework, the IEC 63092 (21) (22), similarly include the building product definition from CPR imposing respect to the basic building requirements expressed in the regulation. In the CPR, the performance-based approach is directly observable from CPR definitions where, the performances are related to the relevant essential characteristics, expressed by level or class, or in a description and the level is *“the result of the assessment of the performance of a construction product in relation to its essential characteristics, expressed as a numerical value”*. The class is defined as *“a range of levels, delimited by a minimum and a maximum value, of performance of a construction product”* and the threshold level is *“a minimum or maximum performance level of an essential characteristic of a construction product”*. These definitions intrinsically contain the use of the limit states that define the performance of the products based on their characteristics and uses. The CPR defines the product-type as a *“set of representative performance levels or classes of a construction product, in relation to its essential characteristics, produced using a given combination of raw materials or other elements in a specific production process”*. This definition opens the way to define a new methodology where a specific sample (product-type) could be tested and qualified as representative.

In the following, we are focusing on the main requirements of:

- Energy economy and heat retention
- Mechanical resistance and stability
- Safety and accessibility in use (electrical safety)
- Safety in case of fire

3 ENERGY ECONOMY

3.1 Introduction

The transparent areas of the building envelope, normally built with glazed systems, have a relevant impact on the final building energy performance, both due to the thermal transmittance and the energy gains related to the sun radiation transmitted into the building spaces. In this sense, several parameters that account for these phenomena are required to be considered as interacting aspects during the design of the building energy concept and as inputs for the building energy performance calculations.

The U value or thermal transmittance of a building envelope component is the magnitude that accounts for the energy transferred across the walls or windows due to the difference between the indoor and the outdoor temperature. It does not consider the solar irradiation, but only the temperature difference. The U value is strongly related with the energy performance of the building skin, namely to the thermal losses during the winter and the thermal gains during the summer. The U of glazings is normally decreased by adding one or two gas cavities using two or three gas layers respectively, and/or applying low emissivity coatings for decreasing the thermal radiation transfer between glass surfaces of the cavity. The reference code to calculate the U value for general construction elements is the EN ISO 6946, while for the calculation of glazing U value are, in the international context, ISO 15099 and ISO 10292 and, in the European context, EN 673.

The G value, also known as Solar Heat Gain Coefficient (SHGC) or Solar Factor, is the magnitude that accounts for the ratio of sun radiation energy that enters the building. The total G value is composed by the solar transmittance across the transparent area, and the heat absorbed by the glass layers that is reemitted indoors. It is a number between 0 and 1 (or 0% and 100%), where a high value (e.g. $G > 70\%$) means that most of the sun radiation energy is entering and heating up the building, so could be desired during the winter or cold climates; while a low value (e.g. $G < 30\%$) means that most of the radiation do not enter into the building, which could be desired during the summer or hot climates. The reference standards for the calculation of G value are, in the international context, ISO 9050 and ISO 15099, and EN 410 in the European context.

In addition, there are standards related to the calculation of the energy performance of buildings with recommendations to account for the U and G value of normal glazing (not photovoltaic). These standards are mainly EN ISO 52000-1 and EN ISO 52016-1, and they could potentially be updated to include equivalent recommendations for PV glazing.

Some years ago, Misara et al. (23) already demonstrated the non-suitability of the current standards to reproduce the thermal behaviour of PV modules, and the main energy-related characteristics of BIPV modules and systems have been recently reviewed in (24). Different aspects of the BIPV thermal behaviour and its implications with standards were studied in (25), where the results showed the importance of considering the irradiance in the thermal characterization of PV module. Other studies related to this topic are (26), (27), (28), (29), (30), (31), (32), (33).

Compared to the common glazing, the BIPV glazing include a few new elements that may cause different phenomena. First and more obvious are the new photovoltaic solar cells, or alternatively photovoltaic thin film coatings, and the elements for the electrical connection like the ribbons. This introduces an impact on the optical properties that leads to a higher radiation absorption, affecting the operating temperature of the PV glazing. The potentially different operating temperature may impact on several aspects. From the U value viewpoint, it affects the gas cavity temperature and convection properties, the radiation heat fluxes between cavity surfaces, the heat transfer coefficients of external and internal surfaces and the direction of heat flux from outer to inner glass layers in some moments. As the G value depends on thermal resistances used for U value, the G value is also affected by these phenomena. Moreover, G value calculation could be affected by the PV conversion effect because a part of the absorbed solar radiation is transformed into electricity

instead of heat. In addition, the temperature may impact on the ageing and pressure of the gas cavity, ageing of materials and mechanical properties of the laminated glass.

Other new elements like the junction box (JB) may impact on the optical and thermal properties of the PV glazing. The JB introduces an additional gas cavity in the thermal system that may affect the total thermal transmittance; it also can absorb a part of the radiation if located in the transparent area of the PV module. The framing is often used to hide the cables, so its thermal transmittance might be affected by holes required, that can communicate different chambers of the frames.

This work is mainly focused on glazing BIPV modules. BIPV modules based on other materials can be found in the market but their thermal impact on the building is limited and it is not object of this investigation. In many cases they are opaque, thin, and are attached to other envelope materials. Thus, its thermal resistance and the impact of the different radiation absorption are very low.

The present research is coordinated with the ongoing initiatives to update different standards related to energy economy aspects for BIPV elements. In this sense, the EN 50583 standard, which is the reference for BIPV products and systems in Europe, is under revision. There is also an international initiative to update the calculation and measurement of G value (IEC 63092-1-1) and, from a pre-normative technical viewpoint, there are several initiatives within the context of the IEA Task 15 Subtask E.

3.2 Objectives

The aim of this work is to clarify whether specific factors related to BIPV products can impact the energy economy procedures as defined in current construction standards and, if required, propose adaptations in the assumptions and boundary conditions to correctly evaluate the calculation models of the thermal performance of the BIPV systems.

The relevant features and elements associated to the PV technology that may impact on the existing procedures and methodologies, as presented and assessed in the following parts, have been considered in relation with glazing thermal transmittance (U value) and glazing solar factor (G value) calculations. After investigating the state-of-the-art with an extensive literature and standard review, analytical studies, FEM simulation and optical measurements have been performed, in order to define the specific BIPV-related characteristics to be considered. These studies are detailed in Section 7.1 of this document, while this section presents a summary of the results, discussion, and conclusions.

3.3 NTP EE01: Determination of thermal transmittance (U value) for BIPV glazed components

3.3.1 Goal

The goal is to determine the steady-state U-value differences between normal IGU and PV-IGU glazing and, if required, propose new calculation methodologies for PV-IGU glazing.

3.3.2 Problem

The most important standards related to the calculation and measurement of the thermal transmittance (U value) of the building envelope -especially related to glazing- have been reviewed. As there is not a specific standard or procedure for the calculation of the U value of PV glazing, the purpose was to detect the potential discrepancies when the current methodologies for normal glazing are applied to BIPV systems. The list of standards and the conclusions are detailed in Section 7.1.1 of this document. After this revision, the following key-points have been detected as significant for BIPV elements:

1. The **temperature of the gas** in the cavity is assumed to be 10 °C (in EN 673 and ISO 10292). However, this temperature could be different in PV-IGUs.
2. The **temperature difference between cavity surfaces (ΔT)** is assumed to be 15 °C (in EN 673 and ISO 10292). However, this temperature could be different in PV-IGUs.
3. The **heat flux direction can change** because the radiation absorbed will heat up the PV layer. This may impact on horizontal glazing convection effects.
4. **Junction boxes** may impact on the thermal transmittance
5. The **thermal transmittance of the framing** might be affected by the holes required for the cables.
6. The **higher operating temperature may impact on the cavity insulation** properties. Thus, adaptation of the ageing, moisture penetration or gas leakage tests might be needed.
7. The **heat transfer coefficients** of the internal and external surfaces depend on glazing position, wind velocity, external and internal temperatures, and surface temperatures of outer glass layers.

In this study, the points 1 to 4 have been studied, while the points 5 to 7 will require future investigation.

3.3.3 Solution

The topics related with the average and maximum operating temperature of the BIPV glazing have been studied by means of a PV glazing thermal model (PVGTM) and finite-element-method (FEM) thermal simulations. The PVGTM calculates the operating temperature of the different glass layers of a double-glazing PV-IGU according to the hourly meteorological data of a location, considering the incident radiation, the angle of incidence, the PV conversion with temperature dependent efficiency and the thermal resistance of the cavity according to the system temperature. It is based on the calculation procedures described in EN 673, EN ISO 6946 and EN 410. It has been checked and compared with FEM simulations and it is described in detail in Section 7.1.4.3.

The configuration of the simulated glazing system is a [4 mm Low-Iron + 4 mm glass / 16 mm Argon cavity / 4 mm glass] (depicted in Figure 34), with and without low emissivity coating. The hourly meteorological data of four years has been used in three different locations: Madrid, Brussels, and Stockholm. Several glazing orientations have been analysed, including E, S, W, N and skylights facing South tilted 5° and 30°; and different PV occupancy ratios of 100%, 80%, 50% and 0% (common glazing without PV).

In addition, the impact of the junction box (JB) on different PV glazing systems has been assessed. The JB has been considered as an additional element of the glazing system similar to the frames. Thus, the additional

thermal resistance of the JB is calculated according to EN ISO 10077-2, which describes a numerical method to calculate the thermal resistance of windows, doors, and shutters. The method described considers limited area of the surfaces and the different view factors. Then, its impact depending on the area occupied by the JB has been evaluated for the different glazing configurations (more details in section 7.1.5).

Table 2 Activity 5.2.1: Energy economy (EE): thermal transmittance (U) value. Summary sheet

Activity 5.2.1: Energy economy (EE): thermal transmittance (U) value
Leading partner: TECNALIA
Specific technical requirement covered by the new procedure (TR):
Determination of steady-state thermal transmittance (U value)
Product family (PF):
Laminated PV glass, Insulating PV glass units (PV IGUs)
New procedure code:
EE_PR_1_PF_1
Specific reference standards in force in PV and building domain for product qualification/markings:
EE_TECNALIA_PR_1_PF_1 EN 673, EN 674, EN 675, ISO 10292, ISO 15099, EN ISO 10077, EN ISO 6946, EN 50583
Innovation of the new procedure with reference to existing standards:
<p>It has been shown that, if a U value calculation methodology is applied to vertical normal IGU, it can be also applied to vertical PV-IGU with comparable results. The slightly higher operation temperature of PV-IGU does not impact significantly on its final U value.</p> <p>The T_{gas} and ΔT assumptions of current standards (EN 673 & ISO 10292) has been found to be not realistic compared to operational conditions. New values could be taken according to Table 29 and Table 30. However, the comparative purpose of the currently standardized boundary conditions should be considered.</p> <p>When calculating the U value of a specific glazing unit as per EN ISO 10077-2, the impact of the junction box should be considered in some cases.</p>
Methodology
PV optothermal modelling, analytical calculations
Equipment development
-
Expected impact for product certification according to CPR and/or LVD
- EN 673, ISO 10292, EN ISO 10077, EN 50583
Expected impact for cost reduction
-No impact on certification cost. Impact on the accuracy of U-value for building energy assessment. It may impact the long track record of U values under the current standardized boundary conditions.

3.3.4 Results

The results of all the cases regarding the dynamic U value are shown in Table 32, Table 33 and analysed in Section 7.1. As a summary, the main results obtained concerning the calculation of the U value of PV-IGU are described below:

- Yearly **average temperature of the gas in the cavity** among all PV glazing, locations and orientation cases is **17-18 °C**. The same average gas temperature for a **non-PV glass is 16-17 °C**. Thus, PV-IGU gas temperature is about 1 °C higher than NO-PV-IGU. Gas temperature proposed by EN 673 and ISO 10292 is 10 °C (see Table 3).
- Average temperature difference between cavity surfaces (**ΔT**) is **6,3 °C without LowE and 9,5 °C with LowE**, being the same for NO-PV-IGU in both cases. ΔT defined by EN 673 and ISO 10292 is 15 °C (see Table 3).
- The average dynamic U value of PV-IGU in vertical is 2,61 W/m²K without LowE and 1,06 W/m²K with LowE, while steady-state U value according to EN 673 is 2,56 W/m²K and 1,08 W/m²K respectively.
- The **differences of the yearly average dynamic U value of PV-IGU and NO-PV-IGU are negligible for vertical systems** (<0,04 W/m²K).
- The yearly average dynamic **U value of PV-IGU nearly horizontal (skylights) is reduced (about 0,05-0,1 W/m²K) compared to NO-PV-IGU**, because the outer glass is heated, and the heat flux changes from upwards to downwards thus reducing the convection effects.
- The yearly average dynamic U value of a PV skylight is 0,03 W/m²K higher than the steady-state calculated with the EN 673 standard for a system without LowE, but 0,24 W/m²K lower than the steady-state with LowE.

The Table 3 summarizes the results related to the average temperature of gas in the cavity, and the average temperature differences between cavity surfaces. The averages are for the whole year, the winter period (October to February) and summer period (April to August).

Table 3. Summary of average operating gas temperature and ΔT from dynamic simulations of PV-IGU in vertical

Magnitude	EN 673 & ISO 10292	Dynamic - Yearly	Dynamic - Winter	Dynamic - Summer
Gas temperature	10 °C	16-18 °C	12-14 °C	19-22 °C
Temp difference between cavity surfaces (ΔT)	15 °C	6,3 °C (w/o LowE) 9,5 °C (w LowE)	8-9 °C (w/o LowE) 12-13 °C (w LowE)	4-5 °C (w/o LowE) 6-7 °C (w LowE)

In addition, the main results from the analysis of the JB impact on the U value are:

- The impact of the JB on the U value of the module depends on the relative area occupied by the JB and the glazing configuration.
- The U value of the PV glazing is reduced due to the JB, as it adds another gas cavity to the area that it occupies.

- To reduce $0,01 \text{ W/m}^2\text{K}$ the U value, the JB should occupy more than 0,4%, 1% and 3% of the module total surface in laminated PV, PV-IGU without LowE, and PV-IGU with LowE respectively.

3.3.5 Discussion

In view of the results, the differences in average operating temperature between PV-IGU and common NO-PV-IGU are very small if they are in vertical position. For the operating gas temperature is about $1 \text{ }^\circ\text{C}$ while for ΔT is almost negligible. This result is found for every orientation, as this parameter does not significantly impact the average thermal behaviour. Thus, it can be concluded that, **if a U value calculation methodology is considered valid for common vertical IGU, it can be also applied to vertical PV-IGU with deviations lower than $0,02 \text{ W/m}^2\text{K}$.**

The average cavity gas temperature in operation is significantly higher than the gas temperature proposed by EN 673 and ISO 10292, while the value of ΔT is significantly lower. As seen in Table 25 and Table 26, the increase of both magnitudes increases the U value. Thus, **as ΔT is lower and gas temperature is higher, there is a kind of balance, and the difference between the steady-state U of EN 673 and the average dynamic U is relatively small** in most of the cases ($<0,05 \text{ W/m}^2\text{K}$). In other words, one deviation offset the other.

In the case of nearly horizontal glazing systems (skylights), the PV-IGU shows slightly lower average dynamic U value than the equivalent NO-PV-IGU. This is because the outer glass is heated due to the radiation absorption of the solar cells, and the heat flux changes from upwards to downwards thus reducing the convection effects in the cavity. This effect is slightly higher in summer than in winter. The current calculation procedure (EN 673) gives similar result for the system without LowE, but overestimates the U value of the system with LowE. Therefore, a determined IGU glazing configuration installed as skylight has slightly lower U value when including PV, so PV-IGU has better insulation properties that can reduce the building energy needs.

It should be pointed out that, even if it is not clear the origin of the temperature and other boundary conditions assumed by **EN 673 and ISO 10292, they are probably focused on reproducing the winter conditions** with about $20 \text{ }^\circ\text{C}$ as indoor temperature and $0 \text{ }^\circ\text{C}$ as outdoor temperature. This would make sense as the main purpose of reducing the U value is avoiding the thermal losses during cold seasons. In this sense, the average gas temperature found during the winter with PVGTM is $12\text{-}14 \text{ }^\circ\text{C}$, which is closer to the $10 \text{ }^\circ\text{C}$ assumed by the codes, but with ΔT of $7\text{-}9 \text{ }^\circ\text{C}$ which is still significantly lower than $15 \text{ }^\circ\text{C}$.

Therefore, as a conclusion regarding the standards, new temperature assumptions might be proposed for the calculation of the steady-state U value for yearly conditions, so the U value is calculated assuming that the gas temperature and ΔT are the yearly or winter values of Table 3. Also, specific values could be selected depending on the location, orientation, or PV ratio. However, the **purpose of the EN 673** is not only to calculate the U value, but to **provide a common methodology to compare the U value** among different glazing systems. In this sense, if the boundary conditions were changed, the ability to compare the U value from new and old glazing would be affected, losing the U value track record. Apart from this, it is important that the building energy performance calculations consider somehow the dynamic U value, or the U value calculated with average dynamic properties, in order to provide accurate energy results.

The addition, the JB at the backside of the module can decrease the U value of the PV glazing. As higher is the area ratio occupied by the JB in the module, higher is the reduction of the U value. In the case of PV laminated glass, the JB impact can be significant if it occupies more than 1% of the module surface. Thus, **for the calculation of the U value of small PV laminated glasses where the JB occupies a significant part of it, it is recommended to consider the insulation effect of the JBs.** The impact of the JB on the U value of PV-IGU systems is negligible, and only should be considered if the module is very small and the JB occupies a very important part of the module surface.

3.4 NTP EE02: G value of BIPV glasses

3.4.1 Goal

The goal is to determine the steady-state G-value differences between normal IGU and PV-IGU glazing and, if required, propose new calculation methodologies for PV-IGU glazing

3.4.2 Problem

As there is not a specific standard or procedure for the calculation of the G value of PV glazing, the purpose was to detect the potential discrepancies when the already existing codes are applied to BIPV systems. In this sense, the most important standards related to the calculation and measurement of the solar factor of the building envelope have been reviewed, most of them related to glazing. The list of standards and the conclusions are detailed in section 7.1.1 of this document. After this revision the following points have been detected:

1. **Heat reduction due to PV conversion.** The efficiency of the PV technology might be removed from the system. If thermal dependence of PV efficiency is considered, the incident radiation and boundary temperatures should be known.
2. The **spectral transmittance of the solar cell** is normally considered as zero. However, the optical properties of several solar cell technologies have been measured and show significant transmittance in the NIR region that should be considered for the G-value calculations.
3. The **junction box** on the rear side of the BIPV module will affect the optical and thermal properties in this area, so that the U and G values.
4. **G value** is a weighted average between opaque (with PV) and transparent (without PV) parts, but the thermal radiation effects **might depend on whether the cells are distributed or concentrated** in an area.

In this study, the points 1 to 4 are addressed.

3.4.3 Solution

The G value can be affected by changes on both optical and thermal properties. The changes in thermal properties of the glazing system have been already addressed in U value, and its impact on the G value are already included by pertinent modifications in PVGTM. In these thermal calculations, it is also included the effect of the PV conversion and its thermal dependency. Thus, the PVGTM calculations consider both the optical changes that impacts on the solar transmittance, and the thermal changes that impacts on the secondary heat. Actually, the impact of both phenomena on the G value and other parameters have been assessed (Table 28, Table 30, Table 31, Table 34, Table 35).

To evaluate the impact of the optical properties of the solar cells, the spectral transmittance and reflectance of different solar cell technologies have been measured. The results show an important transmittance of some solar cell technologies in the near infrared (NIR) region (Figure 53). The measurements have been done on bare solar cells and it has not been possible to perform G value calculations as its measurement encapsulated laminated glass is required. This point could be addressed in the future.

The impact of the junction box (JB) on different PV glazing systems has been assessed. The optical properties of the black silicone, used for the JB attachment, have been measured. Then, it has been calculated the optical properties of the different glazing system with the JB, considering that the JB is both behind cells or in transparent area (more details in section 7.1.5).

Finally, in order to evaluate the potentially different thermal behaviour of PV glazing with the same PV occupancy ratio but different distribution of the solar cells, several thermal FEM simulations have been performed. In particular, the thermal radiation of the external surface has been evaluated to detect potential differences at this point (more details in 7.1.4.3).

Table 4 NTP EE02: G value of BIPV glasses. Summary sheet

Activity 5.2.1: Energy economy (EE): thermal transmittance (U) value
Leading partner: TECNALIA
Specific technical requirement covered by the new procedure (TR):
Determination of the solar factor (G value)
Product family (PF):
Laminated PV glass, Insulating PV glass units (PV IGUs)
New procedure code:
EE_PR_1_PF_1
Specific reference standards in force in PV and building domain for product qualification/markings:
EN 410, ISO 9050, ISO 15099, EN 50583
Innovation of the new procedure with reference to existing standards:
It has been shown a reduction of the average dynamic solar factor (G-value) due to PV conversion. The PV conversion can be considered constant, as the impact of its reduction with temperature is negligible. The optical properties of the area covered with solar cells should be measured. It cannot be considered opaque.
Methodology
PV optothermal modelling
Equipment development
-
Expected impact for product certification according to CPR and/or LVD
EN 410, ISO 9050, ISO 15099, EN 50583
Expected impact for cost reduction
- No impact on certification cost. Impact on the accuracy of G-value for building energy assessment.

3.4.4 Results

Here, it is presented a summary of the results detailed in section 7.1.

- **The solar factor is reduced due to PV conversion effect.** This reduction can be **up to 1,7 percentage points for PV-IGU without LowE, and up to 0,7 percentage points for PV-IGU-LowE.** The reduction is higher as higher is the PV occupancy ratio.
- The impact of the **PV efficiency variation with temperature on the solar factor is negligible.**

- Conventional monofacial solar cells can be considered fully opaque, but **the optical transmittance of other technologies like back-contact or bifacial solar cells seems to be high enough (10-20% at NIR) to be considered.**
- It seems that the **different distribution of the solar cells does not impact significantly on the radiative heat flux** of the outer PV glass surface. Thus, it is not expected an impact on either U or G from this side.

Regarding the impact of JB on G value:

- The impact of the JB on the G value of the module depends on the relative area occupied by the JB, the glazing configuration and whether the JB is behind a solar cell or transparent area.
- The G value of the PV glazing is reduced due to the JB, as it adds another gas cavity to the area that it occupies and reduces the solar transmittance.
- **For reducing 1 percentage point the G value, the JB should be in the transparent area of the module and occupy more than 1,4%, 2,4% and 4,8% of the module total surface in laminated PV, PV-IGU without LowE, and PV-IGU with LowE respectively.**
- **If the JB is located behind the solar cell, its impact on the G value is not significant.**

3.4.5 Discussion

In view of the results, the **PV conversion effect may impact slightly but significantly on the final G value.** Considering 1 percentage point of the G value as the significant minimum, there have been found higher differences for PV-IGU, but lower for PV-IGU-LowE. Even though it has not been analyzed here, the impact on PV laminated glass would be probably higher. Thus, it is recommended to calculate the G-value taking into account the PV conversion according to its efficiency.

Besides, the PV efficiency of the solar cells decreases when its temperature increases according to the **temperature coefficient of Pmpp**. It has been shown that **the impact of this parameter on the G value is negligible.** Thus, it is recommended to not include a temperature dependent PV efficiency in the calculations. An option is to consider a constant efficiency value according to the average operation temperature during daytime. However, a preliminary analysis of the average PV production temperature losses shows a high variability depending on the cases. It can vary between -6.7% for a skylight in Madrid facing south 30° tilted 100% PV covered; and +4.0% for a north façade in Stockholm for the theoretical limit case of 0% PV covered.

Some PV cell technologies has shown a significant optical transmittance in the near infrared (NIR) area. Here, the impact of this transmittance on the G value has not been assessed. However, **the transmittance of some PV cells seems to be high enough to recommend its consideration on optical calculations of G value.** Specifically, significant transmittance has been found in back-contact solar cells and bifacial solar cells.

The impact of the junction box (JB) on the final G value seems to be only significant (> 1 percentage point) if it is in the transparent area of a PV laminated (not IGU) and occupies a significant part of the module area (>1,4%). Thus, **for the calculation of the G value of small PV laminated glasses where the JB is located in the transparent area and occupies a significant part of the module, it is recommended to consider the insulation effect of the JB's.** For other cases, the impact of JB on G value is negligible.

3.5 Maximum temperature results and other

3.5.1 Goal

Due to the development of the PVGTM (PV glass thermal model) and the thermal FEM simulations, it has been obtained also interesting results related to the maximum temperature that a PV-IGU can reach compared to a normal IGU. This point may impact on several standards and calculation procedures, including the ageing of IGU cavities tested under EN 1279 code series. This section summarizes and discusses these results.

3.5.2 Results

Regarding maximum temperatures of PV glass and gas in the cavity:

- **In worst conditions, maximum gas temperature can reach about 83 °C** (open circuit) while the **PV glass can reach up to 118 °C**. This is for PV-IGU-LowE skylight in Madrid with 100% PV occupancy, tilted 30°, oriented to South, assuming 29 °C as indoor temperature, and with very low external convection.
- **The PV-IGU in MPP state can significantly reduce the maximum temperatures** of the PV glass and the gas cavity compared to the open-circuit state. However, its impact on long period averages of temperatures, U and G seems to be very low.
- In worst conditions, the maximum temperature of the Argon in a PV-IGU-LowE could be up to 37 °C higher than equivalent NO-PV-IGU (Table 38).
- The temperature difference between the transparent area and the central area of the solar cells can reach about 8 °C, while the temperature difference between the centre and the edge of a solar cell can reach 5-6 °C. This is for high sun radiation (about 1000 W/m²) on a PV-IGU system with 80% PV occupancy.
- The maximum temperature reached in a PV-IGU with 80% PV occupancy with heterogeneous radiation absorption is slightly higher than homogeneous absorption case and significantly lower than 100% PV occupancy case. This means that **the temperature of 156x156 mm c-Si PV cells distributed** (not concentrated) in an IGU glazing are affected by the PV occupancy and **cannot be considered as thermally independent**.
- In a vertical 2 m height module, **temperature difference between bottom-top gas cavity can reach about 8-10 °C** and significant gas velocity (convection) in high radiation conditions (about 1000W/m²).
- Even though the PV module has the same PV occupancy, if the **PV cells are concentrated in an area of the module, they can reach significantly higher temperatures than the distributed ones** (12-14 °C in the analysed cases).

Other thermal effects:

- **The thermal inertia of a PV-IGU is relatively low**, producing maximum temperature deviations about 1 °C. Thus, when analysing long periods, steady-state calculations can be used instead of transient.

3.5.3 Discussion

The **maximum temperatures of 83 °C and 118 °C for the cavity gas and PV glass respectively should be considered as theoretical maximum temperatures** for Madrid climate and similar southern European climates. The assumptions made are strong enough to consider these values as an upper limit difficult to reach in real conditions but with maximum values that might be close. However, there is a strong dependency of maximum temperature on R_{se} , and thus on wind velocity, that may impact on these results.

The **maximum temperatures** reached by the cavity gas and, specially, at the PV glass **depends on the PV efficiency**, so that on whether the system is in MPP or open-circuit state. In other words, the energy removed from the system as electricity impacts on the punctual maximum temperatures. Thus, this **should be considered for dummy PV-IGU modules or unconnected PV-IGU installations**. Regarding the ageing and safety tests, it is recommended to assume that the systems will be in open-circuit state so that the worst case scenario is covered.

In the view of the results with c-Si cells, the maximum temperature of the PV-IGU will depend on whether the cells are distributed in the module or concentrated. If distributed, the maximum temperature will be slightly higher than the equivalent glass with same PV occupancy and homogeneous radiation absorption. Nevertheless, if the cells are concentrated, the maximum temperature of the PV glass will be like a 100% PV occupied module.

3.6 Conclusions and next steps

Several studies have been performed about the operating temperature of double PV-IGU and PV-IGU-LowE glazing systems. Its impact on the U and G values has been compared to equivalent NO-PV systems and to temperature assumptions made in the standards (EN 673, ISO 10292, EN 410). This analysis has been carried out with a developed PV glazing thermal model (PVGTM), mainly based on thermal laws described in those standards; using meteorological data from three representative climates of south, mid and north Europe; different façade and skylights orientations and different PV occupancy ratios of the glazing. Then, it has been complemented with FEM thermal simulations to validate the PVGTM, validate the steady-state calculations (instead of transient) and assess the impact of concentrating the solar cells on a specific area of the PV glazing. In addition, the optical properties of different PV solar cell technologies have been characterized.

According to this study, the assumptions made in the current steady-state U calculation codes EN 410 and ISO 10292 do not reflect properly the real gas temperature conditions and temperature difference between cavity surfaces (ΔT) of both common IGU and PV-IGU. According to this study, it would probably be more exact to consider 15 °C as gas temperature, instead of 10 °C; and 10 °C as ΔT instead of 15 °C. However, as the increase of both magnitudes increases the U value, with current assumptions one deviation offset the other, so the final U would probably be similar in both cases. Besides, it should be considered that the standards have used the assumptions from several years ago as a common methodology for the U value calculation. Therefore, it is not clear whether the change of this assumption would worth. Independently of the boundary conditions, it has been observed that the U value of the PV-IGU is similar to the equivalent glazing system without PV. Therefore, the current EN 410 and ISO 10292 standards can be used to calculate the U value of the vertical PV-IGU as it was a normal IGU without significant performance deviation between both, as the slightly higher average operation temperature of the PV-IGU do not induce significant impact on the U value. This is not applicable for horizontal glazing, where the new thermal effects of PV-IGU can impact on the average dynamic U. Besides the mentioned standards, these results may impact on other standards like EN 674 and EN 675 for the experimental determination of U. The JB may reduce slightly the U value, but this reduction is significant only in PV laminated (not IGU) if the JB occupies a significant area of the glazing.

It is recommended to separate the centre-of-glass U value calculations without JB and the overall PV glass U value considering the JB, because the area of the elements are involved in the last calculation.

The G value of PV-IGU seems to be slightly (but significantly) affected by the PV conversion effect, so it is recommended to perform the dynamic G value calculations considering this heat reduction due to the radiation energy transformed into electricity. It should be noted that this result is for average dynamic conditions, and the impact of PV efficiency with the boundary conditions described in the codes could be different. Both MPP and open-circuit G values could be defined depending on whether the PV system is working or not. The JB only can significantly impact the G value if it is in the transparent area of laminated (not IGU) small PV glazing. Like in the U value case, it is recommended to perform independent calculations for centre-of-glass, without the JB, and the whole glazing with the JB. The correction factor of G-value due to non-normal incidence of light described in Table 27 and Table 29 might be included in EN ISO 52016-1 (Tables B.22 and B.43).

The maximum temperatures found both for the cavity gas and PV glass layer of a PV-IGU unit are significantly higher than for NO-PV equivalent glazing. Therefore, this should be considered in the different ageing test of the system and the materials. Also, the pressure in the cavity can be significantly higher, and thus the risk of gas leakages and mechanical loads. For instance, this fact should be considered in EN 1279 standard series.

It should be considered that **the results described in these studies are linked to specific thermal assumptions, locations, orientations, PV ratios, glazing configurations, and other specificities of each study.** Thus, it is recommended to take these results with care and understanding their context.

Within the context of this project, it is expected to perform soon experimental studies of a PV-IGU unit installed as a curtain wall facing South. The system will be installed in KUBIK experimental building located in Tecnalia facilities, near Bilbao, Spain. The results from this experiment will be compared with the outputs obtained from this study.

Further similar studies are suggested to be performed by using other inputs. For instance, in terms of thermal properties, other existing PV optothermal modelling could be used, in particular the one described in ISO 15099. In terms of the thermal FEM simulations, further variations with different inputs and analysing different outputs could be performed. The impact of the junction box on the U and G values has been done assuming an empty box and further thermal studies could be done assessing the diode heat or describing the system with more details in thermal FEM simulations. Regarding the optical properties of the solar cell technologies, measurements of the cells encapsulated in glass are required to properly include this data in the G value calculations.

These results and conclusions are expected to be transferred to the scientific community, not only by the publication of this report, but also with active dissemination among stakeholders' communities. It is expected to discuss within the standardization groups related to the mentioned codes and IEA Task 15 activities.

4 ELECTRICAL SAFETY

4.1 Introduction

The evaluation of the electrical safety and performances of a BIPV system or component is a crucial aspect if we consider the transition from a traditional building product, which is a passive component, to an electrically active element: two historically separate “worlds” now meet each other.

4.2 Objectives

The general goal of the WP5 Task 5.2 is the development of New Testing Procedures (NTPs) and the design and assembly of dedicated laboratory equipment and control software, aimed to assess the essential safety and performance requirements of BIPV products, in the framework of a performance-based approach. The main technical requirements about electrical safety to be assessed are in particular:

1. Possibly increased operating temperatures of the BIPV products due to different thermal insulation conditions and shading scenarios (increased risks of overheating)
2. Suitability and durability of the materials and components used in the construction of the BIPV product to operate as intended at potentially higher temperatures (as defined in point 1.), while maintaining adequate safety and performance levels over time.
3. Suitability of the protective devices (bypass diodes) included in the PV product to withstand the increased thermal stresses, due to non-conventional shading conditions and reduced heat dissipation conditions.

Considering the particular operating conditions of BIPV products, which are subjected to more complex stress conditions (reduced cooling and different shading conditions) than traditional photovoltaic products, the New Test Procedure **NTP EL-01** is firstly finalized to define the **reference and max operating temperature of BIPV**, with regard to **mounting method and shading scenarios**. The definition of the temperature-related limit states (thermal classification) for performance assessment is thus a primary goal of this NTP.

Once the thermal classification (Thermal Serviceability Limit States) is done by means of the NTP – EL01, by combining stresses of external factors, and selecting the proper severity levels as defined by the IEC TS 63126, a new **highly accelerated ageing test** is developed in **NTP-EL02**. Such new ageing sequence allows to assess the relevant performance and safety limit states (electrical insulation according to MST 16, IEC 61730 as well as the relevant performance-related parameters) during thermal cycling and accelerated ageing tests. This method considerably reduces the test time and lab costs with respect to the standard PV ageing tests.

Finally, the **bypass diode thermal test** (MST 25-IEC 61730) can be performed in conjunction with the thermal ageing sequence according to NTP EL 02: the new test procedure **NTP EL-03** has been developed to assess the suitability of such fundamental protective devices (bypass diodes) in order to check electrical safety limit states in combined stress scenarios. The possibility to perform this NTP in combination with the ageing tests has a clear impact on the reduction of test time and lab costs as well.

4.3 NTP EL01: BIPV operating temperatures in non-conventional scenarios

4.3.1 Goal

The integration of electrical active parts in building elements has an impact on the **thermal behaviour** of the component in terms of operating temperatures when exposed to solar radiation and ambient temperatures. The BIPV shadowing scenarios that are not typical of standard PV modules (i.e., façades, curtain walls, balustrades, walking floors, BIPV roofs, etc.) may introduce additional stresses and degrading agents. The accurate determination of the BIPV operational temperatures, while considering the non-conventional shading scenarios and restricted cooling conditions as a normal serviceability condition, is the main goal of the New Test Procedure NTP EL01.

4.3.2 Problem

The BIPV products, as an integral part of the building skin within an urban environment, can be often subjected to unconventional conditions (e.g., variable shading) compared to the traditional PV module leading to long-term and cyclic stresses during operation, which can impact their electrical safety and performances and, in certain cases, lifespan. A BIPV product, for example, can have different heat dissipation properties, due to the integration in a multi-layered building skin system that alters the electrical performance related to temperature. Furthermore, very often then, a BIPV product undergoes the shading due to the conformation of the building, forcing a more frequent operation of the protective devices (diodes) to avoid the detrimental effects of hot spots. The actual standard framework in the PV sector (mainly based on IEC 61215-series and IEC 61730 series) does not fully cover the **shade tolerance** issue in terms of potential **overheating** of PV devices, which is instead a key topic to be considered in the BIPV sector. Only the safety aspects resulting from fixed shading conditions are covered by the hot-spot endurance test in IEC 61215-2 MQT 09 and IEC 61730-2 MST 22, which can be equated with the Safeguard Limit States assessment in the performance-based approach.

Hence, the main question we try to answer by this NTP is the following: “is the PV device as integrated in the BIPV end-product adequate to withstand, in terms of safety and reliability, the additional thermal stresses possibly induced by no-conventional shading scenarios in normal operation in the final installation?”

In recent studies, data from PV modules in hot climates and modelling were used to understand operating temperatures and resulted in the definition of two categories of high temperature operation (Level 1 and Level 2), which have been implemented in the IEC Technical Specification **IEC TS 63126** “*Guidelines for qualifying PV modules, components, and materials for operation at high temperatures*”. In the context of an introduction of such document, it is important to indicate, “*Level 2 temperatures were not found in field data but may result from insulated substrate modules on pitched roofs facing the sun when ambient air temperature exceeds 40 °C. This may be most consistent with BIPV module roofs*”.

In the IEC TS 63126, the 98th percentile temperature (T_{98th}) is defined as the temperature that a PV module would be expected to equal or exceed for 175.2 h per year. As reported in the guidelines, *the IEC 61215 series and IEC 61730 series International Standards demonstrated a good correlation with field ageing for an environmental temperature range of at least -40 °C to + 40 °C. For modules operating in such conditions for a 98th percentile (i.e., 175.2 hours per year), a module operational temperature of 70°C or less applies*. This environmental temperature range encompasses many locations and installation styles in these locations. As an example, it has been determined that thermally unrestricted, or “**open-rack-style**” structures, in most cases does not result in 98th percentile module operational temperatures exceeding 70 °C and as such, the originating standards are suitable as written. Module operating **temperatures exceeding 70 °C**, on the other

hand, at the 98th percentile typically will occur with **roof-parallel or building-integrated roof top** applications (BIPV) in climates with local environmental temperatures that exceed 40 °C.

For the scope of this NTP, the PV modules used in the construction of BIPV products are assumed to be operating at a higher temperature than the “open-rack” style structures for the following main reasons:

- Mounting conditions resulting in reduced thermal exchange with the environment
- Higher environment temperatures
- **Non-conventional shading scenarios (added by this NTP)**

The expected impact of this NTP-EL01 is hence the availability of a repeatable and robust test procedure, which combines the determination of the BIPV operating temperature in Serviceability Limit State (SLS), based on the standard existing methods, with the addition of the assessment of potential further overheating issues arising from non-conventional shading scenarios. Furthermore, a new test, aimed to evaluate the Safeguard Limit State (SfLS) due to moving shadows, has been implemented as well, in addition to the hot-spot endurance test (fixed shadows). In the following table, the preliminary one-sheet specifications for this NTP are reported:

Table 5 NTP EL01: BIPV operating temperatures in non-conventional scenarios. Summary sheet

Activity 5.2.2: Environmental and Electrical safety, performance, and yield in non-conventional scenarios
Leading partner: SUPSI
Specific technical requirement covered by the new procedure (TR):
1_ Environmental conditions and Electrical safety in Serviceability Limit State (SLS) and In Safeguard Limit State: electrical safety and performance at higher working temperature in variable shading scenarios
Product family (PF):
2_ All BIPV families
New procedure code:
TP_SUPSI_BIPV_EL_01 (Max Temperatures and Shadowing effects)
Specific reference standards in force in PV and building domain for product qualification/marketing:
<ul style="list-style-type: none"> • <i>Directive 2014/35/EU « Low voltage directive » (LVD); EN IEC 61730 series; IEC 61730-2: 2016, Cl. 10.15 “Temperature test – MST21” IEC 61730-2: 2016, Cl. 10.16 “Hot-spot endurance test – MST22”</i> • <i>IEC TS 61340 “Photovoltaic (PV) modules – partial shade endurance testing for monolithically integrated products”</i> • <i>IEC TS 63126 “Guidelines for qualifying PV modules, components and materials for operation at high temperatures”</i>
Innovation of the new procedure with reference to existing standards:
By means of the performance-based approach, the new testing procedure goes beyond the existing standards and allows evaluating the adequacy of the tested BIPV elements to operate in variable shading scenarios. In particular, the test conditions extend the normal use of the PV element as commonly specified by the manufacturers. The new indoor test procedure, starting from the “temperature test” according to IEC 61730-2 MST21, implements an assessment method of the additional thermal stresses introduced by variable shading scenarios.
Methodology

Definition of a normalized partial shading test condition applicable to all BIPV categories. The new test method excites similar levels of shading stress during an extended period of outdoor service life, to assess potential overheating issues and power loss

Equipment development

- TEST: Indoor temperature test with the addition of moveable shadowing system
- EQUIPMENT: Class CCC Steady state solar simulator -> SMART RACK #01
- TEST MODES: 3 test modes in combination with standard indoor temperature test

4.3.3 Solution

Starting from well-established IEC test methods, the new procedure has been developed in the framework of the performance-based approach, which encompasses the determination of the operating temperatures in normal service and in non-conventional shadowing scenarios typical of BIPV products (Thermal Serviceability Limit States). A new temperature test is proposed, aimed to determine the reference temperatures for various components and materials used to construct the BIPV module, to verify the suitability of their use. The additional potential temperature’s rise due to the non-conventional shading scenarios (shading here is assumed as a normal operational condition) is the key technical requirement assessed by this NTP (**temperature related shading tolerance**).

The new test procedure is so designed to assess the thermal behaviour of module installation methods that restrict cooling, potentially resulting in higher operational temperatures than anticipated in the originating standards, with the potential **additional thermal stresses introduced by moving partial shadows**.

The key points of the methodology adopted for the development of this NTP are then:

- Evaluation of the maximum temperatures according to IEC 61730-2:2016 – MST 21 – indoor method
- Definition of normalized moving shading masks (applicable to all BIPV product categories and PV technologies)
- Measurement of the impact of moving shades on the operational temperatures of the BIPV product

The applicable **Limit State in Serviceability conditions (SLS)**, in this NTP is the following:

BIPV-Serviceability Limit State (SLS)

“BIPV product under a frequent use condition can change the behavior/condition but it must remain reliable and functional for its intended use without damages”.

The SLS represents a condition in which the BIPV building skin module/system is useable as originally intended and designed in a frequent use condition. The system, under SLS actions, must remain reliable and functional for its intended use (e.g. energy production, building functions ensured, etc.) after being subjected to routine/typical loading/agent and it is not compromised in any of its building and electrical performances.

Based on the expected installation conditions for BIPV products, a specific **BIPV SLS –Thermal classification** is proposed, considering the additional contribution of the shading conditions, similar to as defined in the IEC TS 63126:

BIPV - Thermal Serviceability Limit States

SLS –BIPV Thermal class 0	SLS –BIPV Thermal class 1	SLS –BIPV Thermal class 2
$T_{98\% \text{ percentile}} < 70^{\circ}\text{C}$	$70^{\circ}\text{C} < T_{98\% \text{ percentile}} < 80^{\circ}\text{C}$	$80^{\circ}\text{C} < T_{98\% \text{ percentile}} < 90^{\circ}\text{C}$

The NTP allows defining also the **Safeguard Limit State (BIPV SfLS)**:

BIPV- Safeguard limit state (SfLS)

“BIPV under a rare event may suffer permanent damages but it must ensure a safe user evacuation for people and things. It does not maintain the initial functionality”.

After a rare event that induces a certain input action (e.g. mechanical action, electrical load, etc.) the system may suffer permanent damages and performance reduction, being also economically unrecoverable, but it should ensure a safe user evacuation and a certain residual protection against after possible shocks (e.g. avoiding collapses). The SfLS represents a condition in which the safety of a BIPV building skin system and its users is ensured. Safety, in terms of construction and electrical aspects, is safeguarded and it can be assumed as long as this state is fulfilled.

For the assessment of the Safeguard Limit States in the scope of this NTP, the events that could lead to permanent damages are the following:

BIPV - Thermal Safeguard Limit States

- **Failure of protective devices**, such as bypass diodes (possibly due to the increased operation time in forward mode originated by repetitive shading conditions)
- **Abnormal load conditions** of the BIPV module, such as operating point close to **short circuit** conditions (possibly due to severe mismatch among the BIPV modules connected in series within a string)
- Only in the case of monolithically integrated BIPV products (i.e., composed of multiple solar cells built on the same substrate or superstrate and integrated through scribing processes during fabrication, typically thin film technologies), the “**misuse**” and “**severe misuse**” conditions, as defined in the **IEC TS 61340**, are tested as well.

It is well known that small areas of a PV module may reach high temperatures (>150°C) during the “hot-spot” test or during partial shading of a module without bypass-diode protection, but the localized nature of this occurrence is different from the situation of prolonged operation in the hottest module operating environments, thermally adverse mounting configurations and partial shading (assumed here as serviceability limit states). In very hot environments, modules are known to reach temperatures in excess of 100°C. All the test conditions assessed by this NTP represent adverse shadow scenarios, but not necessarily the worst-case scenario, which varies by product.

The new test procedure is not equivalent to, and is not intended to replace, the hot-spot endurance test in IEC 61215-2 MQT 09 and IEC 61730-2 MST 22.

4.3.4 Results

The main results achieved by this **NTP – EL 01** are summarized in the following points:






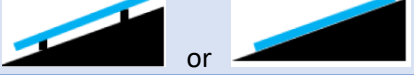



- Determination of the operating temperatures expected in normal serviceability conditions (SLS), including potential temperature rise due to the **non-conventional shading scenarios** and limited cooling conditions (repetitive partial shading here is assumed as normal operational conditions of a BIPV product).
- **Classification** of the BIPV products in **SLS-Level 0** ($T_{98}^{\text{th}} < 70^{\circ}\text{C}$), **SLS-Level 1** (T_{98}^{th} between 70°C and 80°C) or **SLS-Level 2** (T_{98}^{th} between 80°C and 90°C)
- Determination of the **shade tolerance** in terms of **temperature rise** in **SfLS**, due to either abnormal operation of protective devices (bypass diode open) or severe mismatch among the BIPV modules connected in series within a string.
- Definition of the **severity levels** for all the subsequent accelerated ageing tests (see NTP – EL 02) and bypass diodes thermal test (see NTP – EL 03), which are designed to verify the suitability of materials, components and protective devices in the BIPV product's construction over time, according to the IEC TS 63126.

Such results have been achieved by developing and assembling a dedicated **multi-functional test apparatus (Smart Rack #01)** and related control software (see par. 4.3.4.2 for more details).

The key innovation is then the availability of a quick and effective laboratory test procedure and related measuring equipment to guide the manufacturer/designer/installer as to which locations and shading scenarios might require the higher levels of temperature durability. The NTP EL01 is recommended especially for the R&D phase of a new BIPV product: based on the preliminary evaluation of the expected microclimate and shading scenarios of the final installation, the results of this NTP will help the manufacturer/designer/installer of the BIPV system to select the proper temperature levels to comply with. Note that it is not necessarily cost effective for module materials to comply with SLS-Level 1 or SLS-Level 2 requirements as defined in this document, unless the measured module temperature exceeds 70°C at the 98th percentile (Level 1) or 80°C at the 98th percentile (Level 2). Module materials capable of SLS-Level 1 or SLS-Level 2 are expected to impose higher expectations of endurance and cost than normal PV modules.

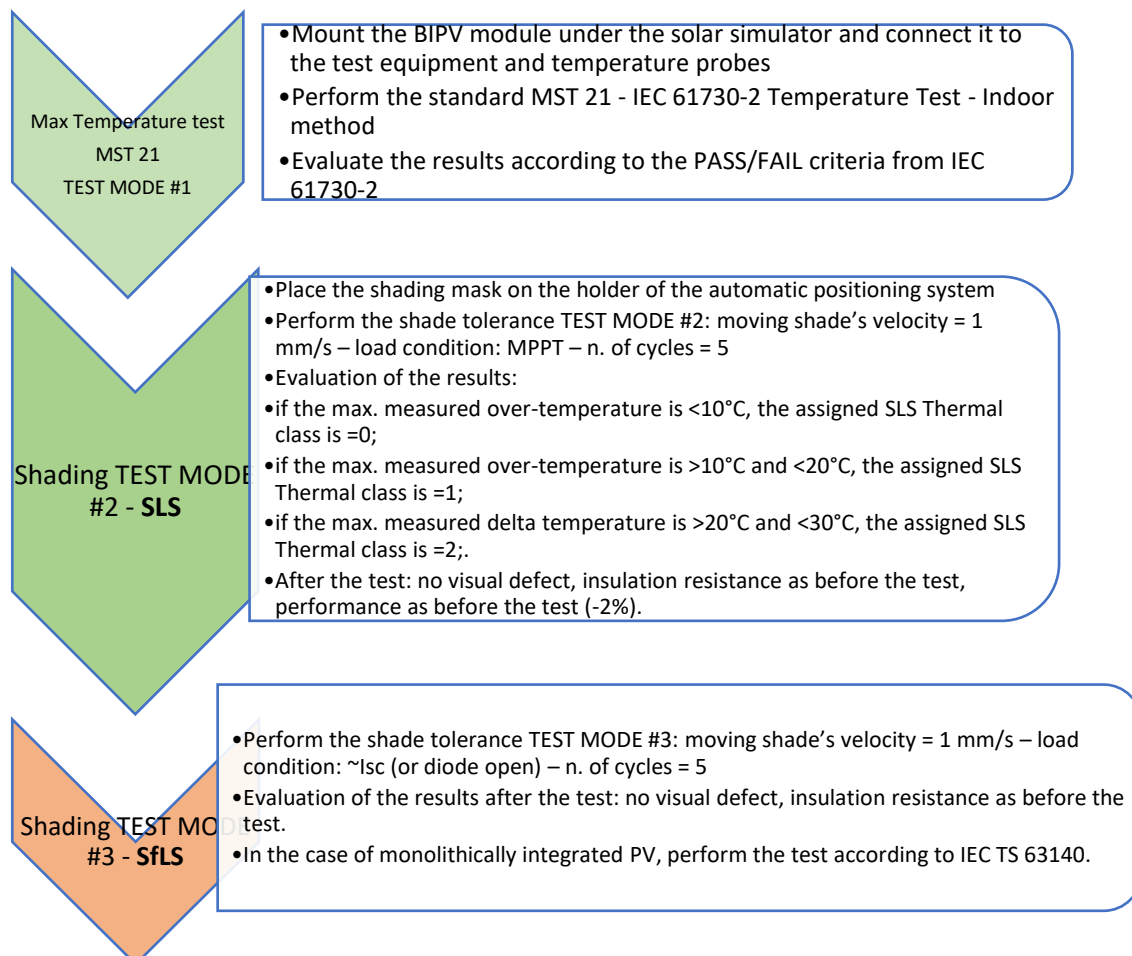
In the IEC TS 63126, the “Insulated-Backsheet constructions style” is the result of severely restricting, or precluding, air flow on the back side of a module and is assumed as the worst case condition by the thermal classification point of view. This construction style is intended to be consistent with building-integrated PV and would be similar to **roof-integrated PV modules**, but likely would exceed the actual field temperature of **vertical** building applications such as curtain walls, spandrel glass, or the like. A conservative approach for this NTP is adopted, since the BIPV products intended for vertical non-sloping installations (i.e. balustrades, curtain walls, cladding modules, etc.), are tested in a horizontal set-up, which is more demanding in terms of heat dissipation than the real installation mode.

The new test procedure can be applied to all BIPV families and types. In particular, it has been applied to the following BIPV product technologies:

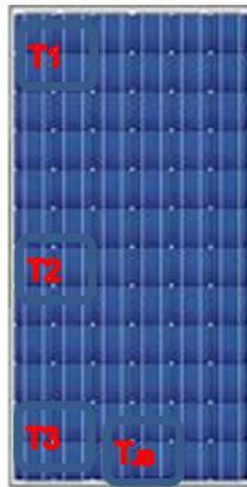
Product Type	BIPV Category – EN 50583-1 IEC 63092-1		Thermally equivalent installation mode - IEC TS 61326
Balustrade	E		
Ventilated Façade	C		
Roofing shingle	A		 or 
Facade (veture kit)	C		

4.3.4.1 Test procedure

The NTP's workflow is summarized in the following flowchart:



- The test specimen (DuT) is placed **horizontally** under a class CCB solar simulator and irradiated with $800 \div 1000 \text{ W/m}^2$.
- The cooling system of the test chamber is adjusted in order to stabilize the average temperature of the front surface of the DuT at $60^\circ\text{C} \pm 5^\circ\text{C}$, and the air temperature between the lamps and the DuT at approx. 40°C .
- The PV module is connected to an adjustable electronic load with MPP tracking functionality (included in the SMART RACK #01). The electronic load is able to adjust the working conditions of the DuT at any fixed point of the I-V characteristic.
- 4 temperature probes (Pt100) are attached on the **back side** of the PV laminate according to the following picture: T_1 on the top-left cell; T_2 on the centre-left cell, T_3 on the bottom-left cell, T_4 on the JB (best internally if applicable)



- The temperature sensors are connected to the datalogger included in the SMART RACK #01.
- The InfraRed Thermocamera (controlled by the SMART RACK #01) is adjusted to frame the area of interest on the surface of the module and to measure both the average surface temperature and local maxima.
- The shading mask (width of the mask = cell's width) is adjusted to cover 90% of the area of a single cell in the string
- The temperature test (measurement of the maximum temperatures) is performed for the 3 following operating modes:
 - Test Mode #1 (BIPV Serviceability Limit State): No Shading – Load Condition: MPPT (equivalent to MST21– Indoor method)
 - Test Mode #2 (BIPV Serviceability Limit State): moving shade's velocity = 1 mm/s – load condition: MPPT – n. of cycles = 5
 - Test Mode #3 (BIPV Safeguard Limit State): moving shade's velocity = 1 mm/s – load condition: $\sim I_{sc}$ (or Diode open) – n. of cycles = 5

TEST MODE #1 - SLS

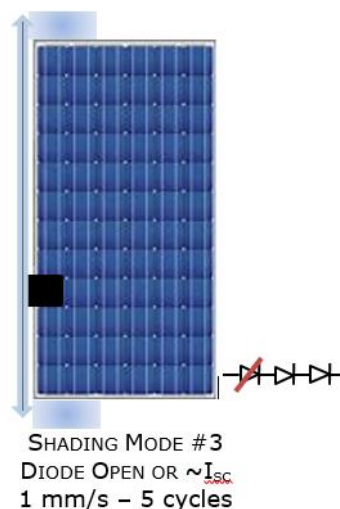
This test is basically equivalent to MST 21 – IEC 61730-2 performed under a steady state solar simulator (indoor method), in order to determine the maximum reference temperatures for various components and materials used to construct the PV module, to verify the suitability of their use. The serviceability temperature limit is assumed conservatively = 85°C in SLS Thermal Class 0, = 95°C in SLS Thermal Class 1 and = 105°C SLS Thermal Class =2, for all the measured points.

TEST MODE #2 -SLS

The scope of this test is the evaluation of the impact of slowly moving shades on the DuT when exposed to high irradiance levels and high ambient temperatures. The DuT is operated at the rated electrical load (maximum power point) and the shading mask is moved along the edge of the DuT according to the following figure:

**TEST MODE #3 - SfLS**

This test is designed to assess the thermal behavior of the DuT when exposed to high irradiance levels, high ambient temperatures and slowly moving shades, with an abnormal electric load condition (operating point close to short circuit or failure of a bypass diode):



4.3.4.2 Equipment

A new multifunctional laboratory test equipment (**SMART RACK #01**) has been designed and assembled, which embeds and controls all the instruments required for:

- Measurement and logging of the local module temperatures in at least 4 points on the back side of the DuT
- Measurement of the surface temperature of the DuT by means of an infrared camera, while exposed to artificial light from a steady state solar simulator
- Control of the electric load conditions of the DuT (i.e., Maximum Power Point, Short Circuit, Open circuit, Reverse power supply) and data acquisition system with full I_V tracking capabilities
- Control of the automatic shading mask positioning axis
- Measurement of the insulation resistance of the DuT in SLS and in SfLS.

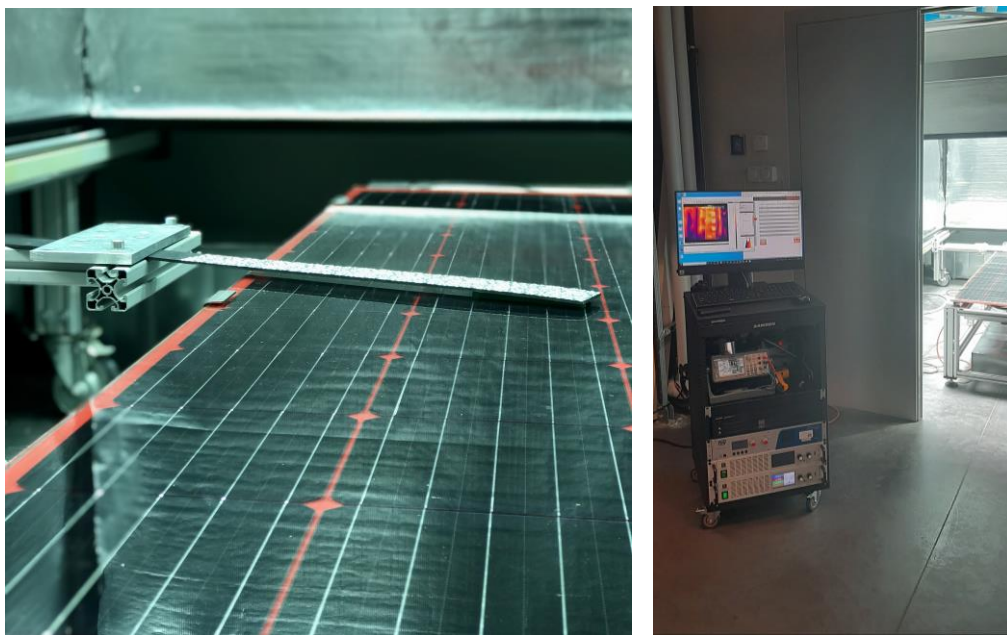


Figure 1. Hardware equipment- Shading moveable mask (left) and smart rack (right)

Software

The execution of the NTP is controlled by means of an in house developed NI Labview® software, which is an integral part of the Smart Rack #01 development:

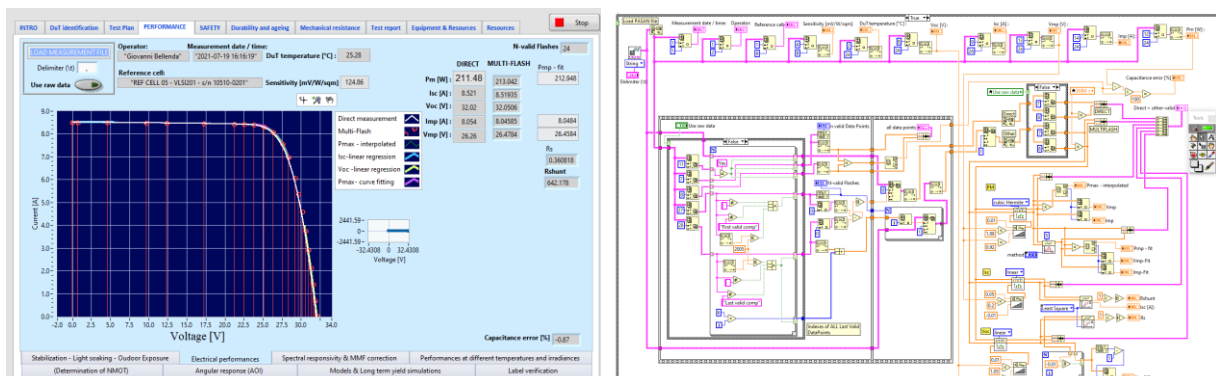


Figure 2. Example of software interface used for data acquisition and procedure automation

4.3.4.3 Test execution and main results

As part of the BIPVBOOST project, façade products such as ventilated façade elements, ventilated roofing shingles and balustrades glass-glass elements were tested according to the NTP EL 01. In addition, a cladding system (veture kit for cladding systems) is currently under test.

In the following table the main results achieved are summarized:

Product #	BIPV Category	Max-Temp-MST21 [°C]	Max Temp-SLS [°C]	SLS Thermal class
Balustrade	E	67.8	69.3	0
Ventilated Façade	E	76.4	78.2	0
Roofing shingle	C	78.6	82.6	0

Table 6. Results of NTP01 tests

The main result is that in none of the tested samples showed significant temperature rises in SLS Test Mode #2, resulting in a SLS thermal classification = 0 for all the tested products. As expected, the sample of roofing shingle, even in the ventilated backside configuration, showed the maximum temperature rise.

4.3.4.4 Discussion

The main innovative outcome of this NTP is the availability of a new method for the assessment and **classification of BIPV products in terms of thermal shade tolerance**, achieved by a completely new test procedure, even if based on well-demonstrated PV specific standard methods. Directly connected is also the development of a **state-of-the-art PV laboratory equipment** (Smart rack #01) and related control software, having a high potential of testing and measurement capabilities for the characterization of both performances and safety requirements of BIPV products. The definition of a new “normalized” shading mask, specifically designed to reproduce realistic shading conditions for BIPV, is an innovative outcome of this task as well.

The tests have been carried out on different BIPV typologies, both belonging to the project and not, with the aim of evaluating how a slowly moving shade can affect the operating temperature of the BIPV elements. The shadowing modes designed for this NTP are possibly originated in the field both by fixed elements in the surrounding of the installation (poles, chimneys, cables, antennas or the like), and by people walking or standing in front of a BIPV array. The proposed shading masks derive from the test conditions required by the “hot-spot” endurance test (MQT 09 – IEC 61215-2), where the over-heating could be provoked by faulty cells, mismatched cells, shadowing or soiling, and the worst-case shadowing conditions occur when the whole cell (or a large fraction) is shadowed. The slowly moving mask adopted in this procedure covers 90% of the cell area and can be either positioned accurately in a fixed position (so reproducing the test conditions of the hot-spot endurance test) or moved with an adjustable speed down to 1 mm/s.

The tests demonstrated a good correlation with outdoor measurements (mock-ups in the outdoor facilities - see WP8): for the Test Mode #1, the tested products showed that operating temperatures of the samples, corrected to the maximum expected temperature according to MST21-outdoor method, are in good correlation with the newly developed indoor method.

Limits of the research:

Mask definition and shading paths need of further investigations, step by step movements to be considered to better cover BIPV shading scenarios (close to the actual speed at which shadows move across the earth's surface).

The steady state sun simulator used for the development of the NTP is a class CCB sun simulator at the time being. In order to increase the accuracy of test method, a class BBB sun simulator should be used.

Temperature difference between the back and front sizes to be improved

Control software to be finalized.

Next STEPS

Perform the NTP on all the BIPV categories within the BIPVBoost project

Compare the results with outdoor data long term monitoring, in particular for back insulated vertical installation (validation of MST21 indoor method).

Perform the test on back insulated roofing (worst case in non-conventional shading scenarios).

4.4 NTP EL02: Electrical safety and durability of insulating materials for BIPV products

4.4.1 Goal

PV modules used for integration in building products include a certain amount of **polymeric materials**. The Electrical Insulation properties of such components are fundamental for the electrical safety and the reduction of electric shock and fire hazards of the whole BIPV system and must be reliable over time. The main goal of this New Test Procedure **NTP-EL 02** is the assessment of **long-term reliability** of all the materials and components in the BIPV product, based on their thermal classification as determined in the NTP-EL 01 (see par. 4.3). The main existing ageing tests methods as laid down in the PV IEC standards will be combined in **new highly accelerated thermal ageing sequence**, including the relevant performance and electrical safety measurements during the test, so allowing detecting any potential failure and excessive degradation rates at an earlier stage than the standard methods.

4.4.2 Problem

Sunlight, humidity, or other extreme conditions are important cause of damages to plastics, textiles, paints, and other organic materials. Short wavelength ultraviolet light exposure, alternated with thermal and humidity stresses, has been recognized as being responsible for most of these damages. Several R&D works demonstrated that UV exposure, Thermal Cycling, Damp Heat and Humidity and Freeze are able to accelerate ageing of PV modules, degrading their performance and electrical insulation resistance. The existing IEC accelerated ageing test sequences require to alternate long UV exposure, Thermal cycling, Damp heat and Humidity and Freeze cycling, and to measure the performances and the insulation resistance before and after the test. The main disadvantage of performing the standard IEC ageing sequence is that no information about the potential degradation of the relevant electrical parameters are available during the test, which can last several weeks. Especially in the R&D development phase of a new BIPV product, this could be expensive and time consuming.

As pointed out in the previous chapter, when a BIPV product is presumed to be operating at a higher temperature, according to its SLS thermal classification, the IEC TS 63126 suggests modifications to the well demonstrated IEC 61215 series and IEC 61730 series testing methods such as:

- Increasing testing temperatures
- Increasing testing duration
- Modifying test parameters, such as current injection.

In particular, the following test levels are proposed in the IEC TS 61326 for the BIPV products expected to operate at higher temperatures in SLS:

Standard	Test ref	Test name	SLS Thermal Class 0	SLS Thermal Class 1	SLS Thermal Class 2	
IEC 61215	MQT 09	Hot-spot endurance test	(50 ± 10) °C	+10 °C, (60 ± 10) °C	+20 °C, (70 ± 10) °C	
	MQT 10	UV preconditioning	(60 ± 5) °C	+10 °C, (70 ± 5) °C	+20 °C, (80 ± 5) °C	
	MQT 11	Thermal cycling test	(85 ± 2) °C	+10 °C, (95 ± 2) °C	+20 °C, (105 ± 2) °C	
	MQT 18	Bypass diode testing chamber	Part 1	(75 ± 2) °C	+15 °C, (90 ± 2) °C	+25 °C, (100 ± 2) °C
			Part 2	I_{SC}	1.15 * I_{SC} for diode T	1.15 * I_{SC} for diode T
			1.25 * I_{SC}	1.4 * I_{SC} for stress	1.4 * I_{SC} for stress	
IEC 61730		RTV/RTE/TI	min RTI 90 °C	min RTI 100 °C	min RTI 110 °C	
	MST 22	Hot spot endurance	(50 ± 10) °C	+10 °C, (60 ± 10) °C	+20 °C, (70 ± 10) °C	
	MST 37	Material creep test	105 °C	no change	110 °C	
	MST 51	Thermal cycle	(85 ± 2) °C	+10 °C, (95 ± 2) °C	+20 °C, (105 ± 2) °C	
	MST 54	UV test	(60 ± 5) °C	+10 °C, (70 ± 5) °C	+20 °C, (80 ± 5) °C	
	MST 56	Dry heat conditioning	105 °C	no change	110 °C	

Table 7 Relation of test levels proposed in the IEC TS 61326 expected to operate at higher temperatures, with SLS thermal classes for the BIPV products

The expected impact of this NTP-EL02 is hence the availability of a repeatable and robust highly accelerated ageing test procedure, which combines the basic relevant IEC ageing methods in a single test sequence, keeping into account the SLS thermal classification arising from non-conventional shading scenarios, as determined by means of the NTP EL 01. The test levels recommended by the IEC TS 63126 are transposed in the corresponding temperature limits in the UV exposure test and in the thermal cycling chamber. In the following table, the preliminary one-sheet specifications for this NTP are reported.

Activity 5.2.2: Environmental and Electrical safety, performance, and yield in non-conventional scenarios
Leading partner: SUPSI
Specific technical requirement covered by the new procedure (TR):
1_ Electrical safety in Serviceability Limit State (SLS): electrical insulation and durability of insulating materials
Product family (PF):
2_ All BIPV families
New procedure code:
TP_SUPSI_BIPV_EL_02 (Electrical insulation durability)
Specific reference standards in force in PV and building domain for product qualification/markings:
<ul style="list-style-type: none"> • <i>Directive 2014/35/EU « Low voltage directive » (LVD): EN IEC 61730 series; IEC 61730-2: 2016, Cl. 10.31 “UV test MST 54” IEC 61730-2: 2016, Cl. 10.29 “Humidity freeze test - MST 52” IEC 61730-2: 2016, Cl. 10.13 «Insulation test – MST16” IEC TS 63126 “Guidelines for qualifying PV modules, components, and materials for operation at high temperatures”</i>
Innovation of the new procedure with reference to existing standards:
The new testing procedure is based on the performance-based approach with new test sequences combining thermal cycling, damp-heat test and Humidity and Freeze test with electrical safety tests. Other PV degradation phenomena (i.e., PID and LeTID) can also be investigated with the same set-up.
Methodology
The purpose of this test is to determine whether the PV module is sufficiently well insulated between current carrying parts and the frame or other outside accessible components while exposed to extreme temperature conditions. The extended humidity and freeze test according to IEC 61730 is performed after the standard UV preconditioning test. With both the thermal and UV ageing, the electrical insulation properties will be measured on a real time basis.
Equipment development
<ul style="list-style-type: none"> - TEST: Insulation test during humidity and freeze - EQUIPMENT: Thermal chamber, UV chamber + Smart Rack #01 - TEST MODES: combination of standard Damp-Heat, Thermal cycling and extended Humidity and Freeze test

Table 8. NTP EL02: Electrical safety and durability of insulating materials for BIPV products

4.4.3 Solution

The New Test Procedure allows monitoring the main **electrical safety parameters** (i.e., insulation resistance and leakage current from PV circuit to ground) **during a new highly accelerated ageing sequence**, where the temperature limits are adapted to the SLS thermal classification of the BIPV product, as determined in the NTP EL 01.

The key-points of the methodology adopted for the development of this NTP are:

- Definition of a combined Damp Heat + Humidity and Freeze + Thermal cycling ageing test sequence, derived by the standard test methods, as laid down in IEC 61215-2:2021 – MQT 12 and MST 13
- Assessment of the degradation rate and failure detection of the relevant electrical parameters of the BIPV product under test
- Measurement of the insulation resistance to ground of the DuT both at low and high temperatures, including the humidity stress

The rationale at the basis of this NTP is that the IEC Damp Heat has been long demonstrated for ageing polymeric materials with a good correlation with actual field data. In such a test, the main driver for ageing the polymeric materials is still the **temperature**, while the IEC Humidity and Freeze test superimposes an additional stress, to determine the ability of the module to withstand the effects of high temperature and humidity followed by sub-zero temperatures. The Humidity & Freeze combination has been demonstrated to be particularly demanding to assess not only the ageing mechanism of the polymeric materials, but also the construction related parameters, such as the adhesion force of the adhesives and edge sealants, with regard to potential humidity paths inside the PV laminate, which may reduce the insulation resistance of the DuT.

The new test procedure can be applied to all BIPV families and types. In particular, it has been applied to the following BIPV product technologies (same as in NTP EL 01, see chapter 4.3.1):






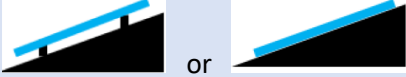



Product Type	BIPV Category – EN 50583-1 IEC 63092-1		Thermally equivalent installation mode - IEC TS 61326
Balustrade	E		
Ventilated Façade	C		
Roofing shingle	A		 or 
Facade (veture kit)	C		

Table 9. Applicability of the new test procedure to all BIPV families and types.

4.4.4 Results

The new ageing test procedure combines in a single sequence the IEC Damp Heat test, the IEC Humidity and Freeze and the IEC thermal cycling test, with maximum temperature levels modified according to IEC TS 61326, depending on the required SLS –BIPV thermal class:

- Total ageing time at 85°C - 85%RH = 1000 h
- Total number of freezing cycles from 85°C (or 95°C or 105°C) down to -40°C = 200
- Electrical parameters and insulation resistance measurements at different temperatures 8 times every cycle

The total duration of the ageing sequence is about 60 days, during which the main electrical performance and safety parameters (insulation resistance and leakage current) are monitored on a real time basis. In the following picture the **full combined IEC 61215-IEC 61730** testing sequence is shown, where the main accelerated ageing test are highlighted with red boxes:

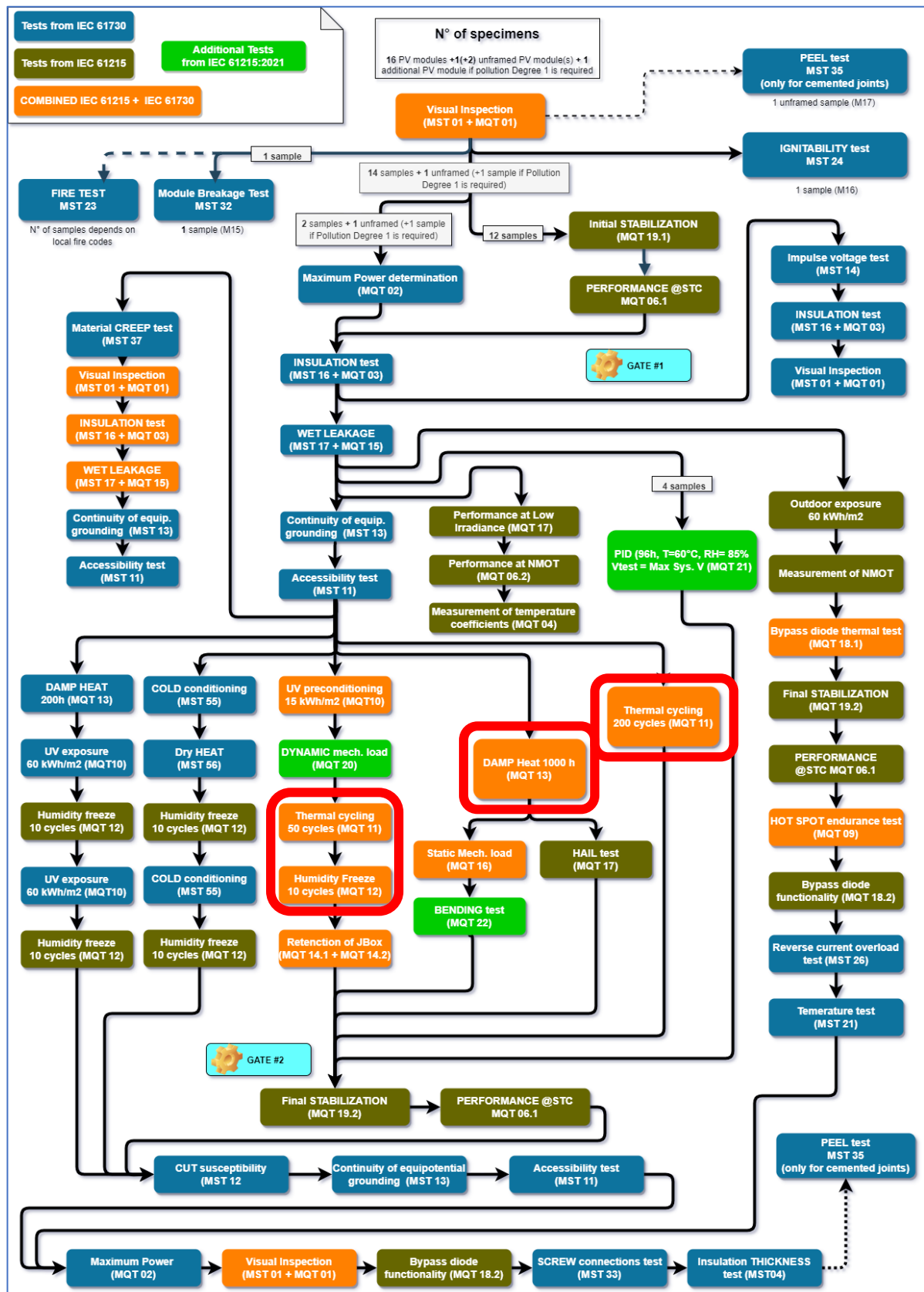


Figure 3. full combined IEC 61215-IEC 61730 testing sequence is shown, where the main accelerated ageing test are highlighted with red boxes.

The newly designed test procedure combines such ageing tests in one item, while reducing the number of samples to be tested (from 6 to 2). Moreover, the overall laboratory test time is significantly reduced:

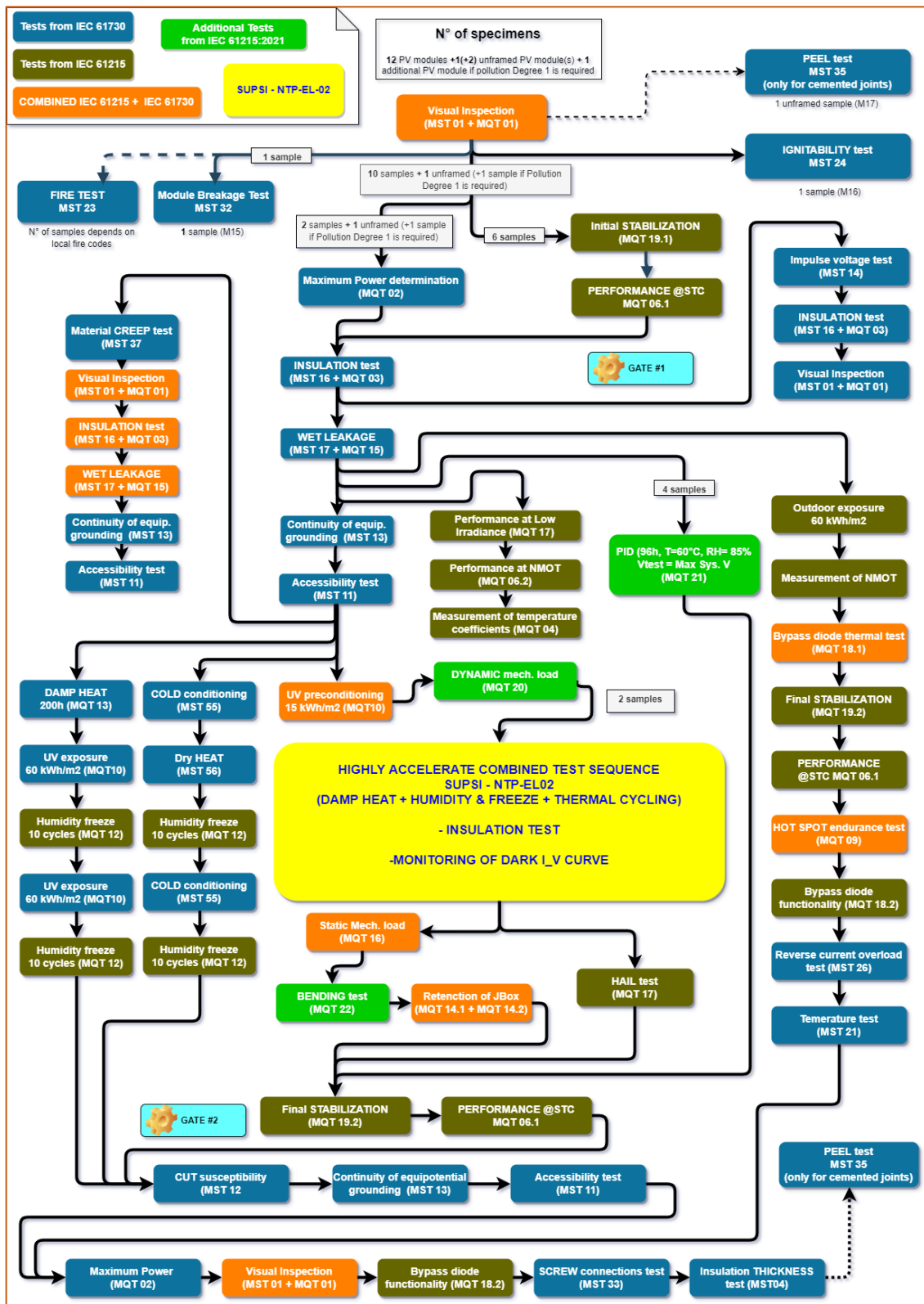
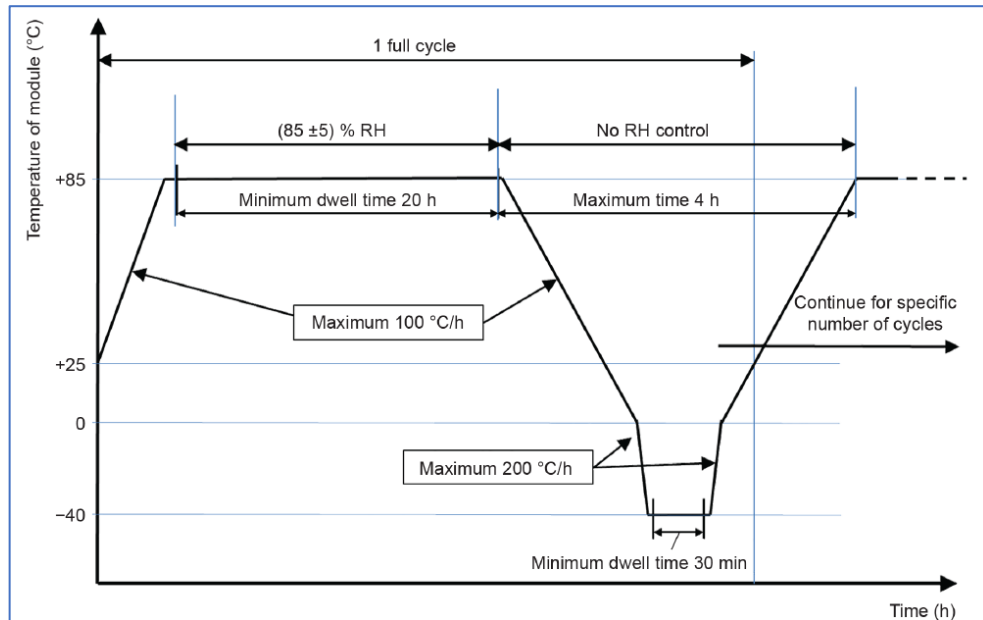


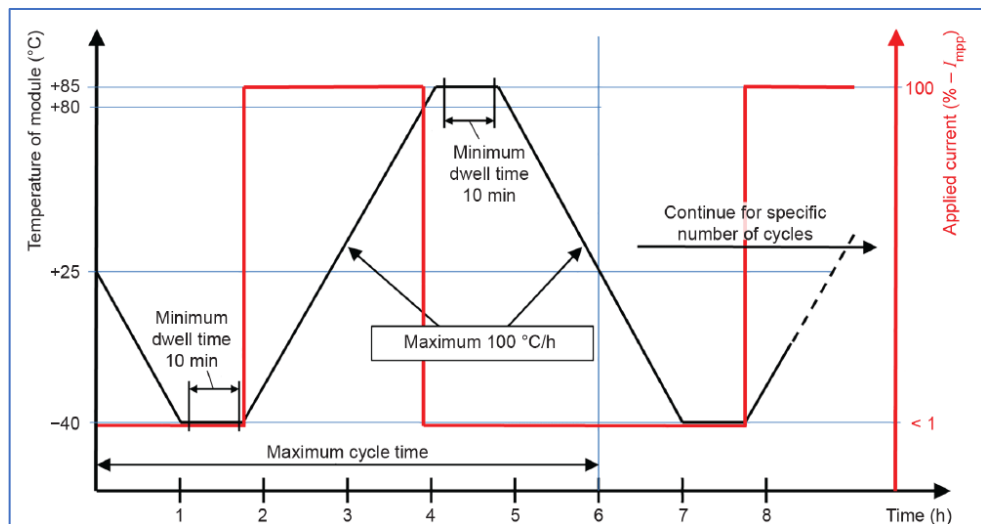
Figure 4. The newly designed test procedure combines such ageing tests in one item, while reducing the number of samples to be tested (from 6 to 2).

The base IEC ageing cycles are shown in the following pictures:

1. Humidity and Freeze test – IEC 61215-2:2021 – cl. 4.12 (MST 12)



2. Thermal cycling test – IEC 61215-2:2021 – cl. 4.11 (MST 11)



3. Damp Heat test – IEC 61215-2:2021 – cl. 4.13 (MST 13)

At least 1000 hours at $T_{MOD} = 85^{\circ}C$, RH% = 85

Noting that the increased temperature levels in the IEC TS 61326 are recommended only for the thermal cycling test according to IEC 61215-1 MST 11, in this NTP, the thermal cycling test is integrated along an extended Humidity and Freeze test. In the following diagrams, the test conditions and the key test points are reported:

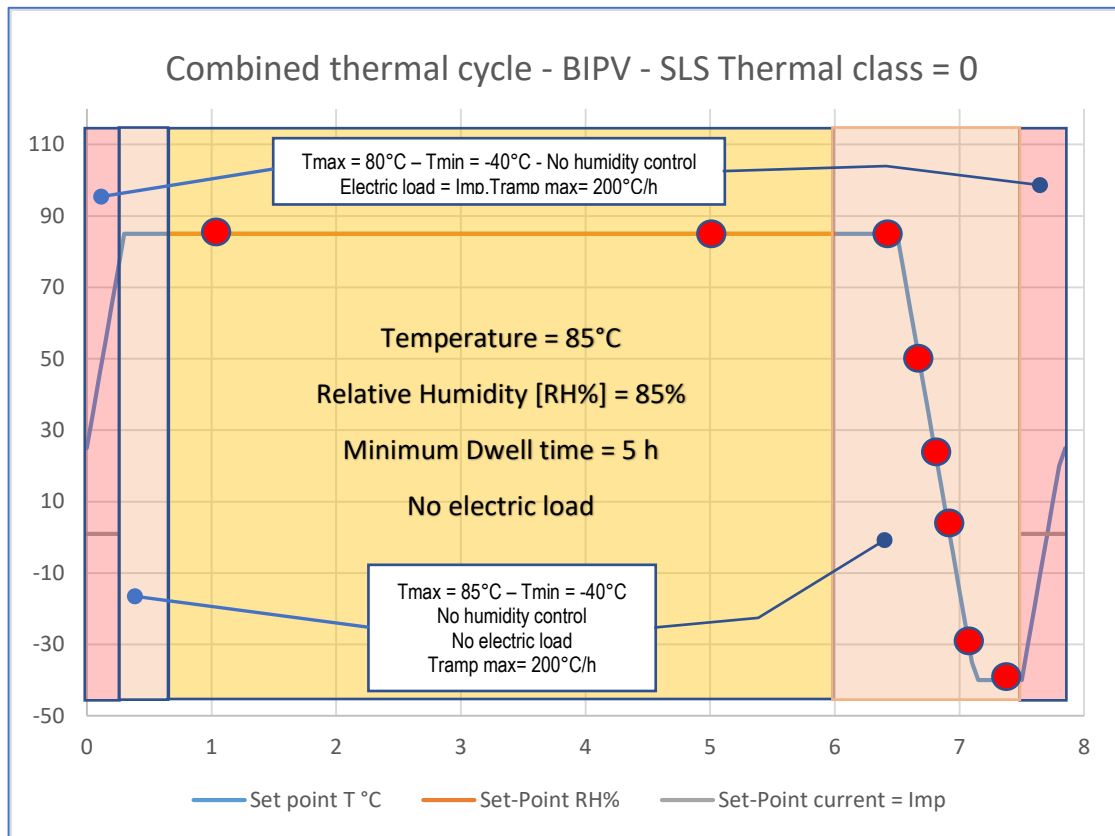


Figure 5. NTP – EL 02: profile of combined thermal cycle for BIPV-SLS Thermal class 0

● ->Test points

When the Test Point conditions are reached in the thermal chamber and in the temperature sensors, the following measurements are automatically performed by means of the **SMART RACK #01**:

- **Insulation resistance** according to IEC 61215-2:2021 (MQT 03) – IEC 61730-2:2016 (MST 16)
- Measurement of the **reverse voltage** needed to force the **rated I_{mp}** current level in the DuT. Such parameter is directly correlated to the temperature and to the series resistance of the PV-circuit and is used to evaluate the **degradation rate**.

The newly defined thermal cycle is repeated **200** times in order to cover 1000h of Damp Heat test conditions and 200 thermal cycles.

For BIPV products classified in **SLS Thermal class 1** by means of the NTP EL 01, the thermal cycle is shown in the following diagram, where the maximum temperature is $T_{MAX} = 95^{\circ}\text{C}$ for the thermal cycling phase:

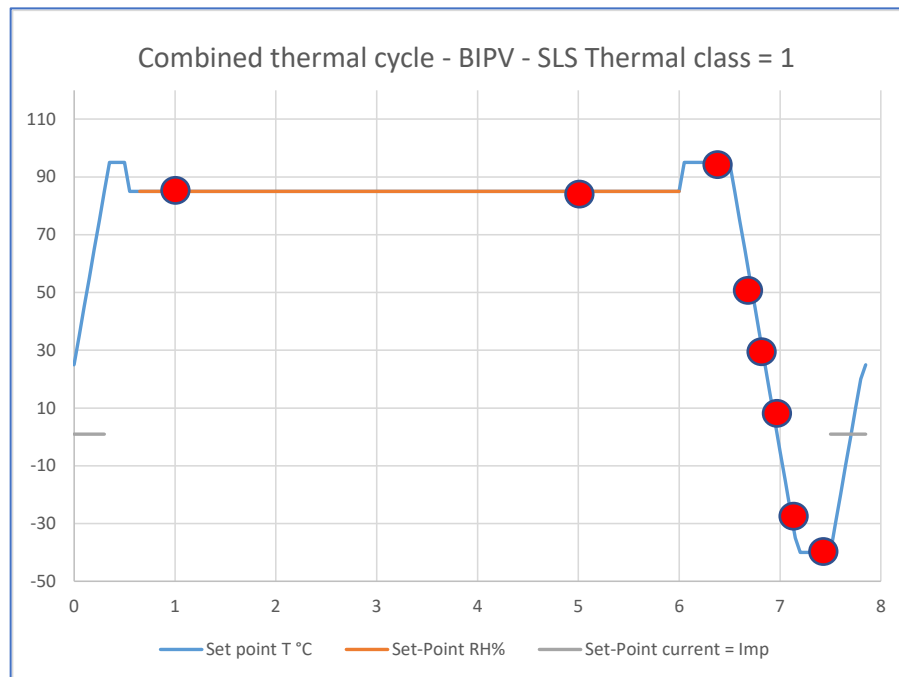


Figure 6. NTP EL 02: profile of combined thermal cycle for BIPV-SLS Thermal class 1 (test points are highlighted with red circles)

For SLS Thermal class 2 products, the maximum temperature in the thermal cycle is $T_{MAX} = 105^{\circ}\text{C}$

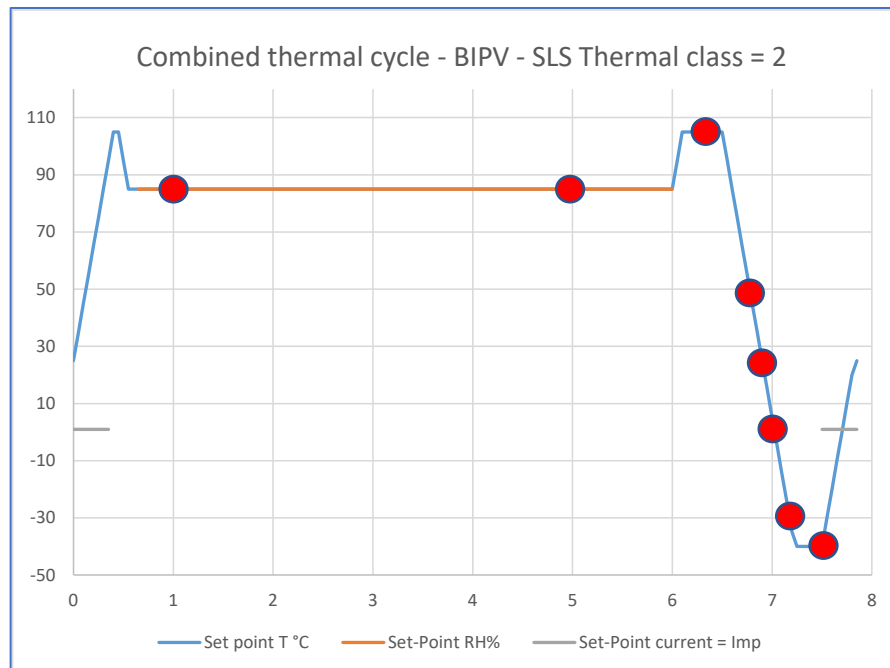


Figure 7. NTP – EL 02: profile of combined thermal cycle for BIPV-SLS Thermal class 2 (test points are highlighted with red circles)

4.4.4.1 Test procedure

- a) Install the module(s) at room temperature in the chamber and attach a single 5 N weight to the junction box as described in IEC 61215-2:2021 – MST 11 (the internal volume of the chamber shall be in dark conditions during the test)
- b) Connect the output terminals of the module to the PV terminals of the Smart Rack #01
- c) Connect the exposed metal parts of the module to the ground terminal of the Smart Rack #01. If the module has no frame or if the frame is a poor electrical conductor, wrap a conductive foil around the edges. Connect all foil-covered parts to the negative terminal of the Smart Rack #01 (ground terminal).
- d) Attach the temperature sensor(s) of the temperature-monitoring equipment of Smart Rack #01 to the DuT.
- e) Close the chamber and subject the module(s) to cycling between measured module temperatures of $(-40 \pm 2)^\circ\text{C}$ and $(+85 / 95 / 105 \pm 2)^\circ\text{C}$, in accordance with the profiles in Fig. 1, Fig. 2 or Fig. 3, depending on the SLS – Thermal Class of the DuT. The rate of change of temperature between the low and high extremes shall not exceed 200°C/h and the module temperature shall remain stable at each extreme for a period of at least 10 min. Air circulation around the module(s) has to ensure compliance with each module under test meeting the temperature cycling profile.
- f) Throughout the test, the module temperature, the rated I_{mp} current flow through the module(s) and the corresponding reverse voltage levels are automatically recorded, as well as the insulation resistance values in the eight test points defined in the previous chapter.

4.4.4.2 Equipment

A fully programmable thermal chamber is used in conjunction with the new multifunctional laboratory test equipment (**SMART RACK #01**) described in cl. 4.3.4.2, which embeds and controls all the instruments required for:

- Measurement and logging of the local module temperatures in up to 4 points on the back side of the DuT
- Measurement of the insulation resistance of the DuT by means of a programmable hi-pot tester, with up to 10 kV test voltage capabilities
- Control of the electric load conditions of the DuT (i.e., Maximum Power Point, Short Circuit, Open circuit, Reverse power supply) and data acquisition system with full Dark I_V tracking capabilities

4.4.4.3 Test execution and main results

As a part of the BIPVBOOST project, some samples of façade products for ventilated façade elements, ventilated roofing shingles, veture kit for cladding systems and glass-glass balustrades have been tested according to the NTP EL 02. At the time being, almost one third of the full thermal ageing sequence (70 cycles out of 200) has been completed on 4 test samples belonging to the above categories.

The preliminary results demonstrated a good correlation with the degradation rate as evaluated in T5.3 after the Damp Heat test. Moreover, three out of four tested samples maintain the same insulation resistance as in the preliminary measurements also during the thermal cycling (including high and low temperature Test Points and high temperature/ high humidity Test Points). One sample shown a significant reduction of the insulation resistance in damp heat test conditions (probably due to humidity paths in the PV circuit), which is not detected in all the other test points of the cycle. In the following table, the main results achieved so far are reported:

Product #	BIPV Category	Power degradation after 1000 h Damp Heat in T5.3 [%]	Power degradation after 1/3 rd of the NTP EL 02 [%]	Insulation resistance at 85°C / 85% RH [MΩ]
Balustrade	E	-2.9	-1.2	> 500
Ventilated Façade	E	-0.95	-0.4	<1

Table 10. Preliminary results for NTP-EL02 electrical safety and durability of insulating materials for BIPV products

4.4.4.4 Discussion

The main innovative outcome of this NTP is the availability of a **new highly accelerated ageing test sequence** tailored for the assessment of the durability of BIPV products, with regard to the ageing of **polymeric materials** and to the reliability over time of all the **adhesion interfaces** of the product, in the framework of a performance-based approach.

The new test procedure, even if based on well-demonstrated PV specific ageing standard methods, goes beyond the standards procedures, introducing a combined recipe of thermal, electrical, and environmental stresses, yet covering and exceeding the overall IEC ageing procedures and including the modifications on the test levels as laid down in IEC TS 61326, for the different SLS Thermal classes.

Directly connected is also the development of a **state-of-the-art PV laboratory equipment (SMART RACK #01)** and related control software, having a high potential of testing and measurement capabilities for the characterization of both electrical performances and safety requirements of BIPV products, which is used in conjunction with a fully programmable thermal chamber.

The tests are currently ongoing on different BIPV typologies, with the aim of assessing the behaviour of the insulation resistance of a BIPV product in extreme environmental conditions, together with the degradation rate of the performances.

The preliminary tests performed so far demonstrate a good correlation in terms of estimated degradation rate with the standard IEC ageing procedures carried out in T5.3. Moreover, the total time needed to complete the ageing sequence is significantly reduced, since a complete ageing test can be performed in only one thermal chamber, and using only 2 identical samples instead of 6. Moreover, any potential insulation failure or excessive degradation of the performances can be detected at an earlier stage, so avoiding expensive and time consuming re-testing procedures.

Limits of the research:

Despite the total testing time is reduced by the NTP EL 02 if compared with a full IEC ageing sequence, the duration is still about 2 months in the thermal chamber. To achieve a full validation of the ageing procedure, further experimental tests are needed to demonstrate the reproducibility of the test results.

The fully automatic mode of the control software has to be finalized.

Next STEPS

Perform the NTP on all the BIPV categories within the BIPVBOOST project

Compare the results of the NTP with the results obtained in T5.3 (validation of the method).

4.5 NTP EL03: Suitability of protection devices for BIPV products

4.5.1 Goal

This new testing procedure is designed for the assessment of the **suitability and long-term reliability of bypass diodes and complete junction boxes** used in BIPV products, which can be subjected to higher operating temperatures, due to limited thermal dissipation and more frequent operation of the bypass diodes (shading stress).

4.5.2 Problem

BIPV systems embed protective devices, such as bypass diodes, in order to limit the detrimental effects of hot spot susceptibility. Non-conventional shading scenarios, together with limited heat-dissipating enclosures, could lead to an excessive overheating of the bypass diodes, introducing additional risks. Consequently, the adequacy of the thermal design and relative long-term reliability of the bypass diodes used in BIPV products is a key-topic.

Activity 5.2.2: Electrical safety, performance and yield in non-conventional scenarios
Leading partner: SUPSI
Specific technical requirement covered by the new procedure (TR):
1_Electrical safety in Serviceability Limit State (SLS): suitability of protection devices (bypass diodes)
Product family (PF):
2_All BIPV families
New procedure code:
TP_SUPSI_BIPV_EL_03 (bypass diodes)
Specific reference standards in force in PV and building domain for product qualification/markings:
<ul style="list-style-type: none"> • <i>CPR 305/2011: applicable harmonized standards</i> • <i>Directive 2014/35/EU « Low voltage directive » (LVD): EN IEC 61730 series; IEC 61730-2: 2016, Cl. 10.19 «Bypass diodes thermal test – MST25” IEC 61730-2: 2016, Cl. 10.20 « Reverse current overload test – MST26” IEC 62979:2017, “Photovoltaic modules - Bypass diode - Thermal runaway test” IEC 63092-1:2020 “Photovoltaics in buildings – Part 1: Requirements for building-integrated photovoltaic modules IEC TS 63126 “Guidelines for qualifying PV modules, components and materials for operation at high temperatures”</i> <p>The test method according to IEC 61730 is combined with the test from IEC 62979.</p>
Innovation of the new procedure with reference to existing standards:
<p>The new testing procedure follows the performance-based approach and introduce a simplified test methodology based on State of the Art thermal characterization methods of semiconductor devices:</p> <ul style="list-style-type: none"> • Combination of Bypass diode thermal test according to IEC 61215-2 – MST 18.1 and Bypass diode functionality test (IEC 61215-2 – MST 18.2) by means of the measurement of the total Forward Mode Voltage of the bypass diodes.

Methodology
<p>Due to the expected increase of bypass diodes' stress in BIPV and in non-conventional scenarios, the test procedure verifies the adequacy of the thermal design and relative long-term reliability of the bypass diodes used to limit the detrimental effects of module hot-spot susceptibility.</p> <p>BIPV modules contain electrically conductive material contained in an insulating system. Under reverse current fault conditions the electrical conductors and the cells of the BIPV module are forced to dissipate energy as heat prior to circuit interruption by an over-current protector installed in the system. This test is intended to determine the acceptability of the risk of ignition or fire from this condition.</p> <p>Development of new equipment suitable to coordinate with the thermal cycling - Some of the diodes utilized as bypass diodes in BIPV modules have characteristics where the reverse bias leakage current increases with the diode temperature. So if the diode is already at an elevated temperature when reverse biased, there may be a substantial leakage current and the diode junction temperature can increase considerably. The worst case occurs when this heating exceeds the cooling capability of the junction box in which the diode is installed. As a result of this increasing temperature and leakage current, the diode can break down. These phenomena are called "thermal runaway".</p>
Equipment development
<ul style="list-style-type: none"> - TEST: Diodes test - EQUIPMENT: Thermal chamber + Smart Rack #02. - TEST MODE: in combination with thermal cycling in NTP EL 02

Table 11. Suitability of protection devices for BIPV products. Summary sheet

4.5.3 Solution

In the project framework, a new test procedure and dedicated equipment have been developed in consideration of the suitability of protection devices (bypass diodes) and reverse current overload test in non conventional scenarios, based on IEC 61215-2:2016, cl. 10.18, with software-controlled monitoring of the maximum temperatures reached by the bypass diodes. The testing conditions of the thermal bypass diode test as laid down in IEC 61215-2 – MQT18 have been implemented in a new simplified testing procedure, which allows strongly reducing the complexity of the test set-up. Thanks to State-Of-the-Art specialized test equipment (**Pulsed Current Source and Measuring Unit** included in the **SMART RACK #02**), it is possible dramatically simplifying the assessment of suitability of by-pass diodes as integrated in the junction boxes, without any bespoke sample preparation. Moreover, the test can be performed within a fully programmable test sequence.

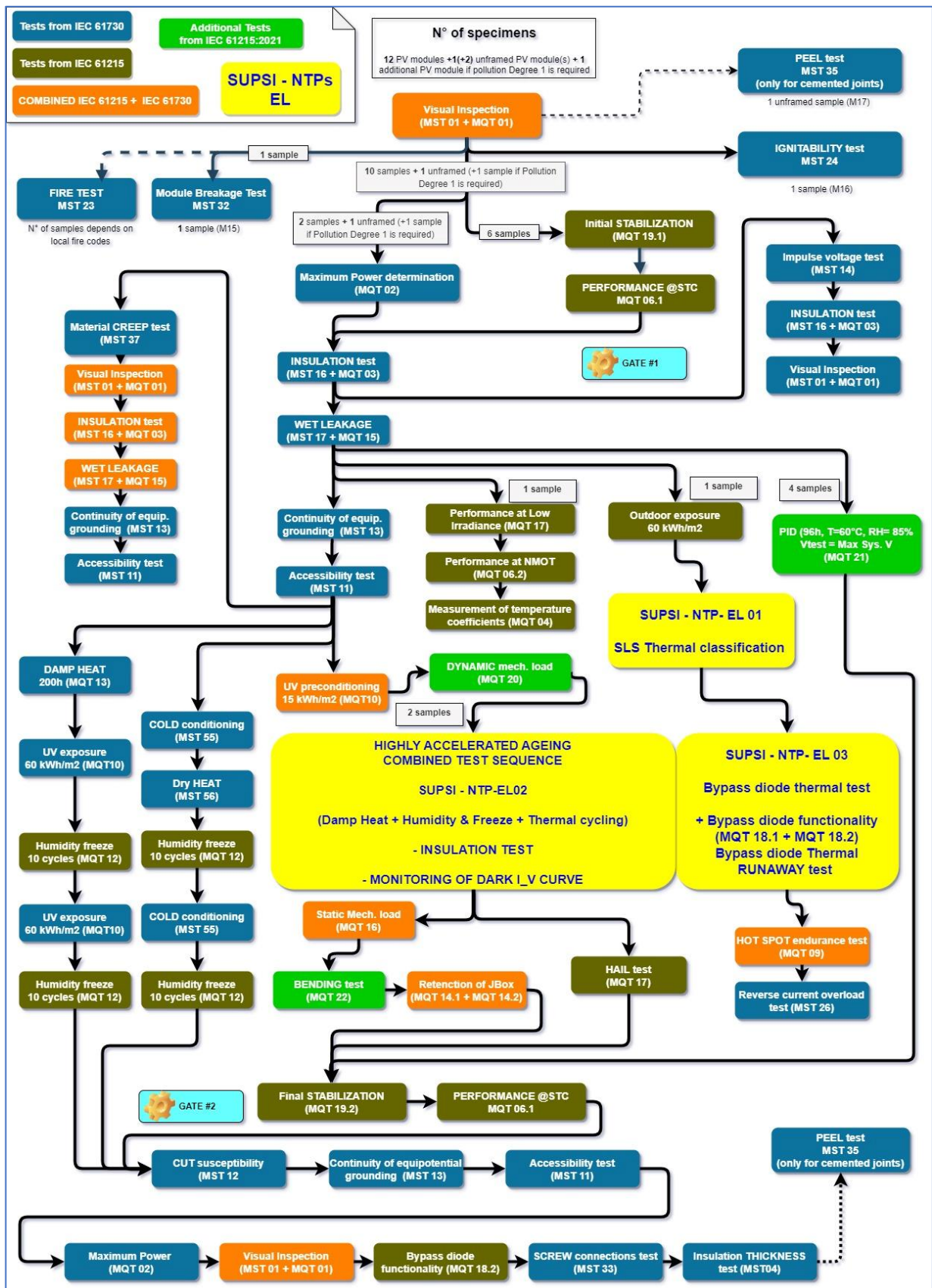
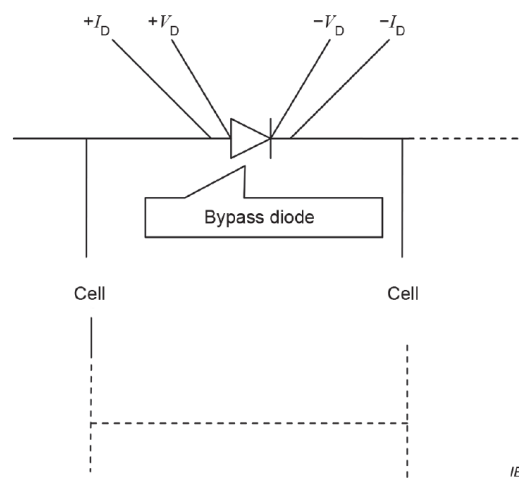


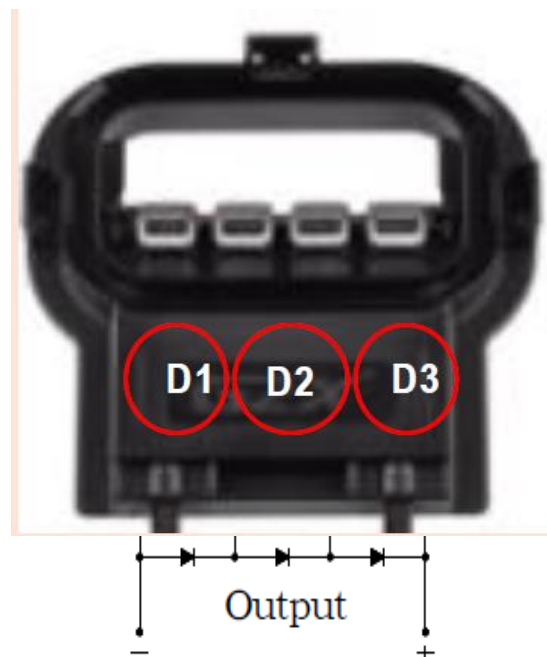
Table 12 NTP 03 for suitability of protection devices for BIPV products within the PV test sequence

4.5.4 Results

The NTP EL 03 allows to significantly reduce the laboratory efforts in terms of sample preparation: for the most common case of a PV junction box containing 3 bypass diodes, the IEC standard method IEC 61215-2 (MST 18.1) requires to measure separately the forward voltages of each diode: the voltage measurement implies to prepare special samples with additional terminals connected within the junction box and wired out of the thermal chamber. Such sample preparation method can also alter the thermal resistance of the diodes surfaces to the external air. Indeed, special care shall be taken that the lead wires do not cause heat dissipation from the terminal box, leading to misinterpretation of the test results. Thus, current connections should be made as far as possible away from the terminal box, and voltage probes made as small and thin as possible, according to the following picture:



In the NTP EL 03, the Source and Measuring Unit can be connected directly to the PV module's connectors, according to the following scheme:



4.5.4.1 Test procedure

Step 0: calibration of the VFM vs. TJ:

$$VFM = (N \times V_{FMrated}) \pm 10 \%$$

where:

N is the number of bypass diodes;

$V_{FMrated}$ is the diode forward voltage as defined in diode data sheet for 25 °C.

- a) After the SLS thermal classification achieved by NTP EL 01, select the max temperature according to IEC TS 63126, for the part 1 of the bypass diode thermal test (MST 18.1):

Test ref	Test name	SLS Thermal Class 0	SLS Thermal Class 1	SLS Thermal Class 2
MQT 18	Bypass diode testing chamber	(75 ± 2) °C	+15 °C, (90 ± 2) °C	+25 °C, (100 ± 2) °C
	Part 1	I_{SC}	1.15 * I_{SC} for diode T	1.15 * I_{SC} for diode T
	Part 2	1.25 * I_{SC}	1.4 * I_{SC} for stress	1.4 * I_{SC} for stress

- b) Install the DuT within the thermal chamber and connect it to the Smart Rack #02 (no need of additional wiring to each single diode in the Junction Box), taking care the DuT is in dark conditions during the test
- c) Determine the forward mode voltage vs. temperature characteristic of the series of the bypass diodes VFM vs. TJ (TJ is assumed to be the ambient temperature of the junction box in thermally stabilized conditions).
- d) Determine the rated STC short-circuit current of the module from its label or instruction sheet. For bifacial modules, use the value of the short-circuit current at elevated irradiance BSI, as defined in IEC 61215-1:2021.
- e) Heat the module and junction box up to a temperature of (30 ± 2) °C.
- f) Apply the pulsed current (pulse width <1 ms) equal to the STC short-circuit current of the module, measure the forward voltage VFM1 of the junction box. For bifacial modules, use the value of the short-circuit current at elevated irradiance BSI.
- g) Using the same procedure, measure VFM2 at (50 ± 2) °C.
- h) Using the same procedure, measure VFM3 at (70 ± 2) °C.
- i) Using the same procedure, measure VFM4 at (90 ± 2) °C.
- j) If an SLS Thermal class >0 has been determined for the DuT, measure additionally VFM5 at (110 ± 2) °C.
- k) Then, obtain the VFM versus TJ characteristic by a least-squares-fit curve from VFM1, VFM2, VFM3, VFM4 and VFM5

Step 1: calibration of the VFM vs. TJ:

- l) Heat the module to (75 ± 2) °C. Apply a current to the module equal to the short-circuit current $I_{sc} \pm 2 \%$ as determined in step d). After 1 h measure the total forward voltage

- m) Using the VFM versus TJ characteristic obtained in item k), obtain TJ from VFM at $T_{amb} = 75 \text{ }^\circ\text{C}$, $I = I_{sc}$.

Bypass diode thermal test Part- 2:

- n) Increase the applied current to 1.25 times the short-circuit current of the module, while maintaining the module temperature at $(75 \pm 5) \text{ }^\circ\text{C}$.
- o) Maintain the current flow for 1 h.
- p) The diode junction temperature TJ as determined in 4.18.1.4 k) shall not exceed the diode manufacturer's maximum junction temperature rating for continuous operation

4.5.4.2 Equipment

The fundamental piece of equipment for this NTP is a Pulsed Current Source and Measuring unit included in the Smart Rack#02, which allows performing accurate voltage measurements while forcing the required pulsed current through the diodes in forward mode. The SMU is a precision pulsed source measure unit that precisely sources pulsed current and simultaneously digitizes voltage. Optimized for precise and repeatable high-power diode, LED and laser testing, SMU (Source Measure Unit) delivers precise pulsing with low microsecond rise times, and integrated digitizer for more accurate and repeatable measurements.

The High Power Precision Source Measure Unit



Easy-to-Use Control Panel Software Application

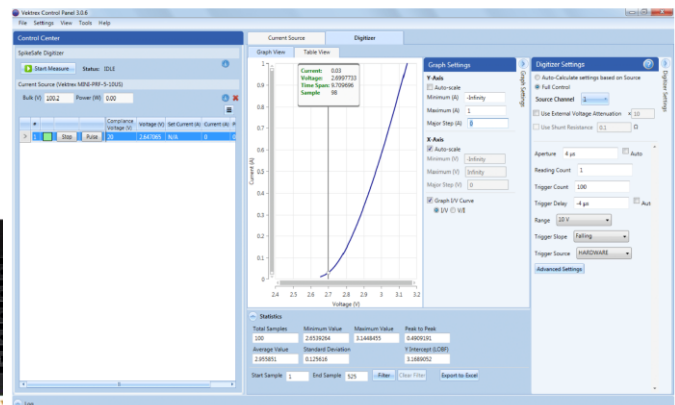


Figure 8. Source measure unit and control panel application for NTP EL-03

4.5.4.3 Test execution and main results

Three commercially available Junction Boxes with different thermal designs (not belonging to the BIPVBoost project) have been tested, in order to assess their suitability for use for SLS Thermal classes 1 and 2 as defined in NTP EL 01. The main result is that **none of the tested JB's was found suitable for SLS thermal class 2**, while **only one out of three was found suitable for SLS thermal class 1**. Moreover, the thermal runaway test was passed only for SLS thermal class 1 for all the three tested devices.

Bypass Diode Thermal Testing - IEC 61215-2:2021; IEC TS 63126; IEC 62979		Drawings of the Device under Test - Junction Box									
Test Date [YYYY.MM.DD] start/end :	2021.12.27 / 2021.12.30										
Number of diodes in junction box :	3										
Diode manufacturer :	*****										
Diode type designation :	*****										
Max. junction temp. T_{jmax} (from datasheet) [°C] :	200										
Max. V_{FM} @25°C (from datasheet) [V] :	0.55										
Max. rev. current @25°C (from datasheet) [mA] :	0.2										
Max reverse bias voltage (from datasheet) [V] :	45										
Designated I_{sc} [A] :	9.1										
Designated rev. bias voltage of JB (= V_{oc}) [V] :	40										
Bypass diode thermal RUNAWAY test @ 90°C - IEC 62979											
	Diode 1	Diode 2	Diode 3	Result / remarks							
Measured reverse current @25°C [μ A] :		24.0		68 μ A @ 120V							
Continuous current @90°C for 40 min $\Delta T < 0.3^\circ\text{C}/\text{min}$. (I_{sc}) [A] :		9.1		PASS							
Reverse voltage applied within 10 ms @90°C (V_{oc}) :		40.0		Verified up to 120 V							
Measured reverse current in reverse mode @90°C [μ A] :		960		1300 μ A @ 120V							
Measured reverse current I_{RM} @90°C < 5 x I_{RM} @25°C? (YES/NO) :		YES		PASS *							
Temperature rise after switching to reverse mode in 10s? (YES/NO) :	NO	NO	NO	PASS							
Measured reverse current @25°C (V_{oc}) [μ A] :		26.2		69 μ A @ 120V							
Difference of reverse current final-initial @25°C [μ A] :		2.2		* If Max rev. current @25°C assumed as initial value							
Determination of V_D versus T_J characteristic - $V_D(T_J)$ - IEC 61215-2:2021 (extended to 110/+5°C as per IEC TS 63126)											
	Diode 1		Diode 2		Diode 3						
Temp. set point [°C] :	30 \pm 2	50 \pm 2	70 \pm 2	90 \pm 2	110 \pm 5						
Pulsed (<1ms) current (I_{sc}) [A] :	9.1		9.1		9.1						
JB's ambient temp. [°C] :	30.4	49.9	69.6	90.4	110.2						
Voltage drop [mV] :	398	383	370	352	331						
V_D vs. T_J characteristic :	VD1 = 424.17 - 0.817 x T_J		VD2 = 433.94 - 0.8703 x T_J		VD3 = 470.37 - 1.2713 x T_J						
	Slope:	-0.8170	Intercept:	424.17	Slope:	-0.8703	Intercept:	433.94	Slope:	-1.2713	Intercept:
Bypass diode thermal test @ 90°C - IEC 61215-2:2021 (MQT 18.1)											
	Diode 1	Diode 2	Diode 3	Result / remarks							
Continuous DC current flow applied @75°C for 1h (I_{sc}) [A] :		9.10		Measured ambient temperature [°C] : 75.1							
Measured V_{FM} at terminals @75°C after 1h [mV] :	292	281	276	Measured JB temperature [°C] : 91.1							
Measured T_J (thermocouples) [°C] :	n/a	n/a	n/a								
Calculated max. junction temp. $T_{jcalc@75}$ [°C] :	161	175	153	PASS							
$T_{jcalc} < T_{jmax}$ (test passed)? [YES/NO] :	YES	YES	YES								
Current flow (1.25 * I_{sc}) applied for 1h @75°C [A] :		11.38		Measured ambient temperature [°C] : 75.0							
Measured V_{FM} at terminals @75°C after 1h [mV] :	290	276	284	Measured JB temperature [°C] : 95.3							
Measured T_J (thermocouples) [°C] :	n/a	n/a	n/a								
Calculated max. junction temp. $T_{jcalc@75}$ [°C] :	165	182	147	—							
Bypass diode remain(s) functional MQT 18.2 (YES/NO) :	YES	YES	YES	PASS							
Visual inspection according to IEC 61215-2:2021 (MQT 01) and IEC 61730-2:2016 (MST01) :	PASS										
Bypass diode thermal test @ 100°C - IEC 61215-2:2021 + IEC 63126 (Level 1)											
	Diode 1	Diode 2	Diode 3	Result / remarks							
Continuous current flow applied (1.15 * I_{sc}) [A] :		10.47		Measured ambient temperature [°C] : 90.0							
Measured V_{FM} at terminals @90°C after 1h [mV] :	276	264	272	Measured JB temperature [°C] : 108.0							
Measured T_J (thermocouples) [°C] :	n/a	n/a	n/a								
Calculated max. junction temperature $T_{jcalc@90}$ [°C] :	182	195	156	PASS							
$T_{jcalc} < T_{jmax}$ (test passed)? YES/NO :	YES	YES	YES								
Current flow (1.4 * I_{sc}) applied for 1h @90°C [A] :		12.74		Measured ambient temperature [°C] : 90.0							
Measured V_{FM} at terminals @90°C after 1h [mV] :	277	262	270	Measured JB temperature [°C] : 112.7							
Measured T_J (thermocouples) [°C] :	n/a	n/a	n/a								
Calculated max. junction temperature $T_{jcalc@90}$ [°C] :	180	197	157	—							
Bypass diode remain(s) functional MQT 18.2 (YES/NO) :	YES	YES	YES	PASS							
Visual inspection according to IEC 61215-2:2021 (MQT 01) and IEC 61730-2:2016 (MST01) :	PASS										
Bypass diode thermal test @ 110°C - IEC 61215-2:2021 + IEC 63126 (Level 2)											
	Diode 1	Diode 2	Diode 3	Result / remarks							
Continuous current flow applied (1.15 * I_{sc}) [A] :		10.47		Measured ambient temperature [°C] : 100.0							
Measured V_{FM} at terminals @100°C after 1h [mV] :	266	254	261	Measured JB temperature [°C] : 118.3							
Measured T_J (thermocouples) [°C] :	n/a	n/a	n/a								
Calculated max. junction temperature $T_{jcalc@100}$ [°C] :	193	207	165	FAIL							
$T_{jcalc} < T_{jmax}$ (test passed)? YES/NO :	YES	NO	YES								
Current flow (1.4 * I_{sc}) applied for 1h @100°C [A] :		12.74		Measured ambient temperature [°C] : 100.0							
Measured V_{FM} at terminals @100°C after 1h [mV] :	269	254	261	Measured JB temperature [°C] : 122.4							
Measured T_J (thermocouples) [°C] :	n/a	n/a	n/a								
Calculated max. junction temperature $T_{jcalc@100}$ [°C] :	190	207	165	—							

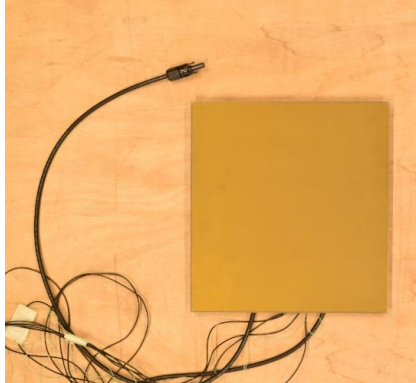



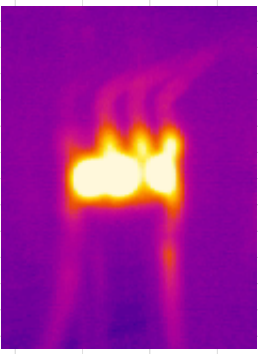
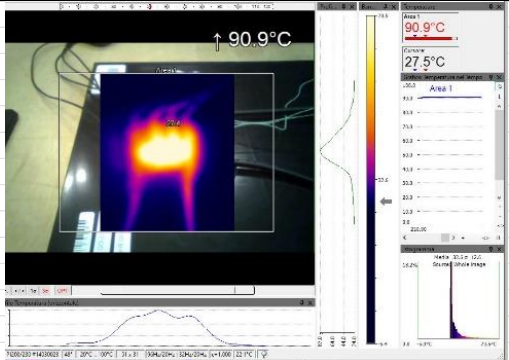
Bypass diode remain(s) functional MQT 18.2 (YES/NO) :	YES	YES	YES	PASS
Visual inspection according to IEC 61215-2:2021 (MQT 01) and IEC 61730-2:2016 (MST01) :	PASS			
FINAL MEASUREMENTS				
Wet leakage current measurement according to IEC 61730-2:2016 - MST 17	PASS			
FINAL Visual inspection according to IEC 61215-2:2021 - MQT 01				
				
Front view	Rear view: the lid is detached		Internal view	
Major defects according to IEC 61215-1:2021			Defect found ? (YES/NO/Not Applicable N/A)	Remarks – supplementary information
a) Broken, cracked, or torn external surfaces			NO	
b) Bent or misaligned external surfaces, including superstrates, substrates, frames and junction boxes to the extent that the operation of the PV module would be impaired			NO	
c) Bubbles or delaminations forming a continuous path between electric circuit and the edge of the module			NO	
d) If the mechanical integrity depends on lamination or other means of adhesion, the sum of the area of all bubbles shall not exceed 1 % of the total module area			N/A	
e) Evidence of any molten or burned encapsulant, backsheet, frontsheet, diode or active PV component			NO	The potting material show signs of browning, but the diodes are still functional
f) Loss of mechanical integrity to the extent that the installation and operation of the module would be impaired			NO	
g) Cracked/broken cells which can remove more than 10 % of the cell's photovoltaic active area from the electrical circuit of the PV module			N/A	
h) Voids in, or visible corrosion of any of the layers of the active (live) circuitry of the module extending over more than 10 % of any cell			N/A	
i) Broken interconnections, joints or terminals			NO	
j) Any short-circuited live parts or exposed live electrical parts			NO	
k) Module markings (label) are no longer attached or the information is unreadable			N/A	
FINAL - Infrared thermal imaging				
				
About 10 s after applying Isc (JB without lid)	About 1 min. after applying Isc (JB without lid)	About 10 min. after applying Isc (JB without lid)		

Figure 9. Datasheet of the NTP EL03 results

4.5.4.4 Discussion

The currently available IEC test procedures for the conformity assessment of the bypass diodes are still rather complex and normally require specific preparation of the test samples. The main innovative outcome from this NTP EL 03 is the evaluation of the suitability of the thermal design of the junction boxes (which embeds one or more bypass diodes), used in BIPV products, by means of a strongly simplified test set-up and a significant reduction of the test duration.

The proposed test method allows TJ to be measured at full current under actual operating conditions. It uses a two-step process. First, the bypass diodes' forward voltage versus temperature characteristic is profiled. A short pulse DC current is used for this step, not long enough to produce significant heating (<200 μ s). After characterization, the bypass diodes are driven at a much higher heating currents, maintained long enough to stabilize the full junction box at its operating temperature. After stabilization, the current is briefly pulsed and forward-voltage (V_{fm}) samples are taken.

Limits of the research

Due to different thermal designs of commercially available Junction boxes, BIPV manufacturers struggle with by-pass diodes' junction temperature measurement because the available methods are not possible to implement with complete junction boxes, especially when the thermal dissipation conditions are further limited in the BIPV end-product. These challenges have led to measurement compromises – such as estimating junction temperature using an average thermal resistance – that often produce inaccurate results.

The proposed test method does not consider the possible temperature deviations among the diodes integrated within a junction box.

Next STEPS

Full validation of the test procedure by means of an intercomparison between the IEC standard method and the new testing procedure.

Further investigation on the thermal runaway test.

4.1 Conclusions and next steps

The NTPs developed in this task 5.2 for the electrical safety and performance assessment of BIPV products, bridge the gap between the two separate paths for the assessment of the building and electrical technical requirements, by means of a comprehensive evaluation of the thermal requirements, including by-pass diodes, and ageing procedures in the framework of a performance-based approach. Laboratory tests now can follow one single comprehensive testing program, which covers all the relevant electrical safety and long-term performance requirements for a BIPV product, while avoiding overtesting. Need for a more extensive validation, especially for durability test (NTP EL02) and further improvement of the equipment are the next steps.

5 MECHANICAL SAFETY

5.1 Introduction

BIPV system and its construction parts should be designed, executed, and maintained in such a way that the product during its intended life, with appropriate degrees of reliability and in an economical way, will remain fit for the use for which it is required. The system has to sustain all actions and influences likely to occur during execution and use; it will not be damaged or will have controlled damage by pre-defined events, impacts, or consequences. The levels of reliability that apply to a particular BIPV product may be specified by classifying the system as a whole (BIPV system) or by classifying its components (e.g. BIPV module). The system's "working life" represents the assumed period for which it has to be used for its intended purpose with anticipated maintenance but without major repairs necessary. The notion of design working life is useful for selecting design actions (e.g. mechanical load, temperature, etc.), considering material property deterioration (e.g. fatigue, ageing), evaluating the life cycle cost, and developing maintenance strategies. Mechanical requirements in this report are meant basically as requirements of "safety and accessibility in use" among the essential characteristics for the products covered by the CPR such as wind load resistance, resistance to horizontal point loads, impact resistance, mechanical resistance of the cladding and its fixings or subframe components. As reported by authors (34), different investigations in the literature report discussions around this topic. Saretta et.al (35) evaluated the deflections of a laminated BIPV glass resulting from the IEC mechanical test aimed at comparing such an approach with the one of the Eurocode. Hemmerle (36) presented experimental research work on glass based on PV modules aiming to analyze whether the integration of various types of PV cells into glass products essentially changes the material characteristics defined in the harmonized product standards. Weller et.al (37) (38) discussed the verification of applicability for non-regulated building products like BIPV in the absence of harmonized standards. Kim et al. (39) examined the mechanical strength and bending strength of glass/glass modules according to encapsulant type and operating temperature. Misara et al (40) discussed the post-breakage-integrity of the BIPV module in the framework of the approval of the use of BIPV module for the overhead-glazing application. However, by examining these contributions, technical topics still highlight missing gaps, which call for further testing approaches.

5.2 Objectives

The essential requirements concerning mechanical resistance for building products are well described in the harmonized regulations, in the testing procedures for the product certification, and in CE marking. In many cases, such as the kits for external walls mechanically fixed, the EAD reports all the methods and criteria for assessing product's performance to its essential characteristics by specifying the tests for the kits family and reference procedures to get the declaration of performance. Different factors can introduce variation in the mechanical behavior of the BIPV products, compared to construction products without any active part, related to the presence of solar cells and the operating temperature. BIPV products usually operate at higher temperatures than traditional products (41) (42). This chapter introduces procedures for assessing essential mechanical characteristics of BIPV products, by combining the main criteria originated by the building standards with the essential characteristics for electrical safety.

In detail the essential characteristics investigated are:

- **Impact resistance** of the cladding component, considering hard and soft body impacts according to EOTA TR001 test methods of panel and panel assemblies considering serviceability and safety in use.
- **Static load resistance** (safety in use) of the cladding component

5.3 NTP ME01: BIPV impact resistance

5.3.1 Goal

The procedure is basically intended to introduce a testing approach to combine the photovoltaic limit states with the limit states related to the construction part for BIPV technology assessment. The NTP01 aims to evaluate the integrity of the product after stresses due to the impact of an external body, not only in terms of mechanical properties related to the requirements of "safety in use", but also of the consequences that the impact could generate on the "electrical safety". Thus, the effects of actions are not only in terms of mechanical properties related to the construction of the cladding but also considering the consequences that the impact could generate on the PV part. Moreover, by ensuring the control of the device temperature simulating operating conditions, different limit state levels can be affected by the characteristics of the BIPV product material.

5.3.2 Problem

Currently, impact test is executed both in PV and building product certification by performing different test procedures. The test to determine impact resistance is the PV qualification expressed by MST 32 module breakage test reported in IEC 61730-2 (5). The purpose of the test *"is to provide confidence that risk of physical injuries can be minimized if the PV module is broken in its specified installation"*. The criteria for passing the test are defined by three prescriptive criteria that do not consider the performance and status of the product but only the values to be respected. However, it is important to highlight that IEC 61730-2 (5) explicitly states that: *"For building integrated or overhead applications additional tests may be required according to relevant building codes"* thus referring to the requirements for the building part.

For glass components, EN 12600 (43) specifies a pendulum impact method. The test classifies flat glass products into three classes defined by impact performance and failure mode but does not specify application requirements or durability requirements. In fact, depending on the different applications of the components, specific standards are used. For glass elements with an anti-fall function inserted in curtain walls and windows, reference should be made to EN 14019 (44) and EN 13049 (45). These tests define different impact heights and energies based on categories of exposure and location in the building and do not provide a single prescriptive value. Where there are no specific European standards, for example, parapets, reference is made to national references. In Italy, for example, UNI 11678 (46) *"defines the test methods for determining the behavior to distributed linear static loads and dynamic loads of glass elements having an anti-fall function"*. The Italian standard defines for impact tests to determine their mechanical strength, the mode of impact, the size and type of the impactor, and the mode of execution of the test for both hard body and semi-rigid body.

In the case of ventilated facades, the EAD 090062-00-0404 *"kits for external wall claddings mechanically fixed"* is used as a reference (47). In this EAD (47), concerning the Essential characteristic and relevant assessment methods and criteria, regarding the impact resistance, it is clearly stated that the assembled cladding kit shall be tested concerning the category of impact use. It also established the impact use categories to correspond to the degree of exposure to impact use and requested curtain walls.

This EAD, in turn, refers to the EOTA TR 001 (48) *"Determination of impact resistance of panels and panel assemblies"* where the number of tests, conditioning and test condition, test assembly, test procedure, and test results are reported. The expected influence, in the present form, is to orientate the product development and its TRL enhancement and with the perspective of defining a possible future reference procedure for BIPV products qualification and market introduction.

5.3.3 Solution

In this framework, the test to qualify the BIPV product will be performed starting with the basic test requirements expressed in the relevant building code, but the result will also be evaluated in relation to electrical safety performance. The main innovation of this NTP is the combination of construction requirements of "safety in use" with "electrical safety" limit states.

The developed general procedure describes a general test method, equipment, and configuration used to determine the limit state for impact resistance of a BIPV product. For a detailed description, refer to **Annexes**. The method aims at evaluating a product's integrity after stresses due to an impact of an external body, not only in terms of mechanical proprieties related to "safety in use" requirements but also the consequences that impact could generate on "electrical safety". The workflow is valid for each type of BIPV and, as described in Figure 10, based on this general procedure, other specific tests are developed (and valid) to be applied to specific test types/ requirements (TT) as well as to specific product-types or kit or parts thereof (PT) by referencing the harmonized EN standards (hEN) or ETAG/EAD in force. In order to reproduce the effect of impacts on vertical construction elements from an external body (for example, for cladding system kits), reference originated by construction harmonized standards (refer to EAD 040914-00-0404 (49) and ISO 7892 (50) for more details).

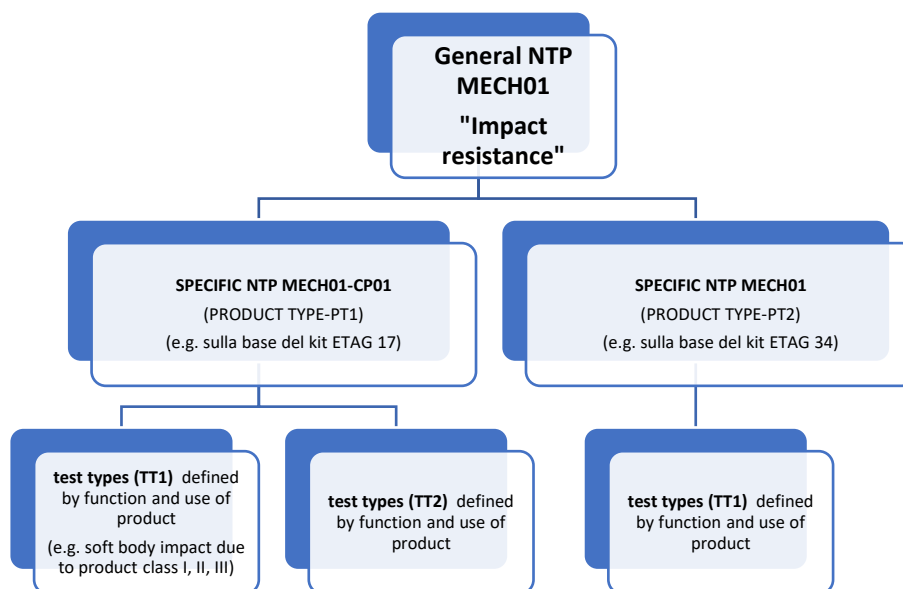


Figure 10. Hierarchical approach for NTP development. This procedure is related to "General NTP-MECH01". Specific procedures "NTP MECH-01-CPXX" will be adopted for defined "product type" (PTX) and "test type" (TTX)

The methodology is applied at the BIPV component level (single module), not at the system level, e.g. as requested in the harmonized standard EN 13830 (51) that "*specifies the requirements for curtain walls used as building envelope*", in the test methods/assessment/calculation and performance criteria for impact resistance refers to the conformity of EN 14019 (44). Testing a portion of the façade and not the component has a different value than testing a single component. The proposed methodology tests how the single component reacts following the impact, considering the PV part. It should be noted that even in EN 13049 (45) for windows, this difference is expressed: "*the test refers to all panes of any material, including glass. The intention is not to evaluate the strength of glass if it is used as a panel. Rather, the intention is to evaluate the interactions between all components of a window with particular regard to safety in use*". EN 14019 (44) "*defines performance requirements of curtain walling under impact load*" and takes as a reference not the component but a portion of the facade. EN 14019 (44) specifies that "*the test specimen should be a section*

of curtain wall a minimum of one storey height and a sufficient size to permit testing at all the specified test positions". As a type of impact, EN 14019 (44) refers to EN 12600 (15): "the impactor as specified in EN 12600 shall be mounted on a horizontal or vertical axis, as best befits the requirements of access to the impact point. In addition, wires, pulleys, hooks, and suitable height adjusting devices are needed, as specified in EN 12600". Therefore, as expressed above, the impactor described by the specific reference standard will be used and applied to the procedure.

Table 13. BIPV impact resistance-summary sheet

Impact resistance
Leading partner: SUPSI
Specific technical requirements covered by the new procedure (TR):
Impact resistance in Serviceability Limit State (SLS), Safeguard Limit State (SfLS), and Ultimate Limit State (ULS);
Product family (PF):
All families – (for each family different tests could be made)
New procedure code:
NTP_ME_01
Specific reference standards in force in PV and building domain for product qualification/markings:
<ul style="list-style-type: none"> • EN 50583-1 Photovoltaics in buildings - Part 1: BIPV modules; • EN 50583-2 Photovoltaics in buildings - Part 2: BIPV systems; • IEC 63092-1:2020 Photovoltaics in buildings - Part 1: Requirements for building-integrated photovoltaic modules • IEC 63092-2:2020 Photovoltaics in buildings - Part 2: Requirements for building-integrated photovoltaic systems • Regulation (EU) No 305/2011 named as Construction Products Regulation (CPR) and related Harmonised standards or harmonised technical specification in use as European Assessment Documents (EAD) originated by; • EN 12600:2002 Glass in building - Pendulum test - Impact test method and classification for flat glass; • EN 356:1999 Glass in building - Security glazing - Testing and classification of resistance against manual attack; • EN 13049:2003 Windows - Soft and heavy body impact - Test method, safety requirements and classification; • EN 14019:2016 Curtain Walling - Impact resistance - Performance requirements; • EAD 090062-00-0404 "Kits for external wall claddings mechanically fixed" chapter 2 "Essential characteristics and relevant assessment methods and criteria" paragraph 2.2.11 "Impact resistance" - Annex G "Impact resistance test" • EAD 040914-00-0404 "Veture kits – prefabricated units for external wall insulation and their fixing devices" chapter 2 "Essential characteristics and relevant assessment methods and criteria" - paragraph 2.2.17 "Impact resistance" – Annex L "Impact resistance test"

<ul style="list-style-type: none"> • EAD 220010-01-0402 “Flat plastic roofing sheets made of recycled plastic for self-supporting and/or fully supported discontinuous roofing and/or external cladding” • EOTA TR001 “Determination of impact resistance of panels and panel assemblies” • ISO 7892:1988 “Vertical building elements — Impact resistance tests — Impact bodies and general test procedures”; • M.O.A.T. No 43:1987 UEAtc “Directives for Impact Testing - Opaque Vertical Building Components” • Directive 2014/35/EU «Low voltage directive » (LVD) – relevant standards EN IEC 61730 series; • European Committee for Standardization, EN 1990:2002 - Basis of structural design, CEN, 2002
Innovation of the new procedure with reference to existing standards:
<p>Assessment criteria considering the combination of construction requirements of "safety in use" with "electrical safety" limit states. Moreover, by ensuring the control of the device temperature by simulating operating conditions, different limit state levels can be affected by the characteristics of different materials (e.g. laminated glass), especially in relation to the interlayer adhesion and stiffness.</p>
Methodology
<p>Evaluating a product’s integrity after stresses due to an impact of an external body, not only in terms of mechanical proprieties related to “safety in use” requirements but also the consequences that impact could generate on “electrical safety”. Ensure that the sample and the impact point stabilized in the controlled temperature scenario.</p>
Equipment
<p>Thermal chamber, impactor, electroluminescence apparatus, controller unit, leakage current measurement systems, software system.</p>
Expected impact for product certification according to CPR and/or LVD
<p>Possibility of harmonize a procedure for the impact resistance under the CPR and LVD</p>
Expected impact for cost reduction
<p>Avoiding a double testing</p>

5.3.4 Results

This chapter is organized into two main sections including i) test execution and main results and ii) discussion. The detailed NTP01 procedure flow as well as specific test results for the BIPV products tested will be presented as an example in Annexes 7.2.1 and 7.2.2 and 7.2.3.

5.3.4.1 Test execution and main results

This section aims to present some preliminary considerations obtained from applying NTP01.

The new test procedure for impact resistance was applied to the following types of products:

-prefabricated BIPV modules for exterior wall insulation (Veture KIT);

- BIPV plastic tiles for discontinuous roofing;
- BIPV glass-glass module.

Impact tests were performed considering the relevant CPR standards for the specific product using the impactors for the evaluation of rigid-body and soft-body impact resistance. Specific equipment inserted in the climatic chamber was created for the variation of test temperatures. This allowed the impact test to be carried out by defining the temperature conditions of the tested product.

Preliminary results on "safety in use" and "electrical safety" after stress due to mechanical impact showed that the performance of BIPV products depends on their design and materials but also depends on boundary conditions such as test temperature.

Results at different temperatures on BIPV products exposed to mechanical stress reveal that temperature affects their mechanical behavior by influencing the material properties of BIPV products. In particular, temperature variations alter the properties of polymeric materials used for layering the active part of photovoltaic modules, causing their performance to vary.

For example, the low-temperature impact test showed that glass breakage occurs at lower impact energies due to its brittleness. The results of specific tests at different temperatures are presented in 7.2.37.2.3.

The limit state condition also may be different in the case of "safety in use" (mechanical limit state) and "electrical safety" (electrical limit state). For example, after the stress caused by the impact, the breakage of the photovoltaic glass (mechanical limit state) without the breakage of the photovoltaic cells (electrical limit state) has been found in some cases.

It should also not be overlooked that by applying the performance approach, different performance requirements are required according to the product's intended use. The results showed that complying with a certain building category from the material point of view, such as admitting rupture but not penetration or detachment of parts or the product, cannot be considered as an acceptable requirement from the electrical point of view for insulation loss. This result supports the procedure by making it necessary to correlate both requirements under test.

5.3.4.2 Discussion

The results show the influence of impact resistance from the material from which the BIPV product is made and the test conditions. The temperature and the polymer used as encapsulant play a significant role in the strength characteristics of the laminated glass used in BIPV. Normally, for example, amorphous polymers are used to encapsulate BIPV-glazed products because they have more transparent characteristics than crystalline polymers (52). These amorphous polymers exhibit "rubbery" behavior at room temperature and are characterized by deeply temperature-dependent viscoelastic behavior (53). However, each polymer has its own characteristics that determine behavior and must be considered in testing (verification) and design. Impact tests also are affected by a large variety of factors. The fastening system is one of them. The fastening system significantly influences the impact resistance of the product. For the same size, materials, and thickness, impact resistance varies as fastener specifications change, and to validate it is important that the test is performed under the same installation and intended use conditions following the fastener rules expressed by the manufacturer. Impact resistance also is affected by the material and its treatments. For laminated glass with thermal tempering treatment, for example, the resistance value cannot be considered to be of a specific value but within a range of resistance probability. The characteristics of the tempering equipment, temperature value, positioning on the rollers, cooling time, as well as specific characteristics of the component determine the strength value of each individual glass product.

Research is currently being conducted on a limited number of BIPV samples. Further tests are needed to be carried out on a larger number of BIPV product samples to confirm and demonstrate these results to validate the results. Therefore, the preliminary results should be viewed with caution.

However, the results show that the path taken could be adopted to validate the impact resistance of the products by allowing a reduction in the number of tests currently required by different industry regulations allowing a reduction in costs. The expected influence, in its current form, is to guide product development and TRL enhancement and in the perspective of defining a possible future reference procedure for BIPV product qualification and market introduction.

5.4 NTP ME02: Static mechanical load resistance for BIPV products

5.4.1 Goal

The NTP ME02 aims to define a procedure to assess the integrity of the product after applying a static mechanical load, both in terms of mechanical properties related to the requirements of "safety in use", and in relation to the "electrical safety". In particular, this procedure refers to the mechanical resistance of the product to bending, verifying the integrity of the component and that there are no changes in the active part such as the breakage of the solar cells or of the contacts of the electrical connections.

5.4.2 Problem

Construction products shall comply with mechanical safety requirements, defined in the standards specifications, such as durability after load cycles, stress, and fatigue due to external loading conditions. Products shall be tested to demonstrate that they comply with the intended conditions of use as defined by the harmonized standards to be commercialized, as well as with the applicable legislation in each country to be incorporated in permanently in construction works. In the European Union, methods and criteria for validating the performance of construction products are defined in relation to essential characteristics according to CPR 305/2011 (16). In the absence of harmonized standards, the specific EAD shall be taken as a reference. For mechanical verifications concerning wind load resistance, the adhesion strength of product layers and tensile strength in composite products, load resistance, and impact resistance are typical verifications required to ensure safety in using the most used classes of products.

For a photovoltaic product, the evaluation of mechanical resistance to uniformly distributed static load is described by IEC 61215 (3) using the Static mechanical load test (MQT 16). The test aims to determine the module's ability to withstand a minimum static load (prescriptive approach) while determining limit state conditions load is not part of it. On the other hand, building material tests, are tests to check safety according to certain limit states that represents e.g. the ultimate strength value (performance-based approach). Another difference is that IEC 61215 (3) is based on the capacity of the single module to withstand the mechanical load while tests developed for construction products generally refer to the safety of the system or unit of a specific kit for mechanical resistance or safety in use. In both cases, tests must be performed according to the manufacturer's instructions that identify the intended installation conditions.

In the current scenario, BIPV manufacturers are in the condition to perform both tests for photovoltaic modules and building components separately. A harmonized procedure for BIPV products is unavailable, and the lack of specific instructions to clarify the applicability of existing standards for active multifunctional products implies uncertainty and in many cases major risks and costs for BIPV products.

5.4.3 Solutions

In order to evaluate the integrity of the electrical circuits of a BIPV product under the action of a mechanical load, a test procedure was developed for the resistance to mechanical load. The procedure is derived from the Static Mechanical Load Test (MQT 16) contained in IEC 61215 (3). The test proposal does not use prefixed load values but values derived from category and intended use indicated in the reference construction-related norms of the product. The test was developed as an indoor laboratory test and was chosen to apply it to a single component. The choice is dictated by the fact that the test's purpose is mainly to verify if the deformation due to mechanical action may affect the active part, rather than assessing structural safety.

The test can be performed with distributed or concentrated load on a single module and simultaneously evaluate whether deformations cause changes to the electrical part. According to the capacity of the supporting part to sustain mechanical deformations and stresses, different electrical limit states could occur as a consequence of mechanical actions (breakage, large displacement/permanent deformation, etc.) such

as loss of electrical insulation resistance, cell fracture, etc. Finally, tests were carried out with concentrated load application at different temperatures in the climatic chamber to assess whether temperature variation could make further impact.

Table 14. Static mechanical load resistance for BIPV products. Summary sheet

Mechanical load (Leading partner SUPSI)
Specific technical requirements covered by the new procedure (TR): Impact resistance in Serviceability Limit State (SLS), Safeguard Limit State (SfLS), and Ultimate Limit State (ULS);
Product family (PF): All families – (for each family different tests could be made)
New procedure code: NTP_ME_02
Specific reference standards in force in PV and building domain for product qualification/markings:
<p><i>EN 50583-1 Photovoltaics in buildings - Part 1: BIPV modules;</i></p> <p><i>EN 50583-2 Photovoltaics in buildings - Part 2: BIPV systems;</i></p> <p><i>IEC 63092-1:2020 Photovoltaics in buildings - Part 1: Requirements for building-integrated photovoltaic modules</i></p> <p><i>IEC 63092-2:2020 Photovoltaics in buildings - Part 2: Requirements for building-integrated photovoltaic systems</i></p> <p><i>IEC61215-2 Terrestrial photovoltaic (PV) modules – Design qualification and type approval – Part 2: Test procedures - Edition 2.0 – 2021</i></p> <p><i>Regulation (EU) No 305/2011 named as Construction Products Regulation (CPR) and related Harmonised standards or harmonised technical specifications in use as European Assessment Documents (EAD) originated by;</i></p> <p><i>EAD 090062-00-0404 “Kits for external wall claddings mechanically fixed” chapter 2 “Essential characteristics and relevant assessment methods and criteria” paragraph 2.2.9 “Wind load resistance” and paragraph 2.2.12 “Mechanical resistance” - Annex E “Wind suction and pressure load tests” – Annex J “Mechanical resistance of the cladding fixing”</i></p> <p><i>EAD 040914-00-0404 “Veture kits – prefabricated units for external wall insulation and their fixing devices” chapter 2 “Essential characteristics and relevant assessment methods and criteria” - paragraph 2.2.9 “Wind load resistance” – Annex E “Wind suction and pressure load tests”</i></p> <p><i>ISO 1288-3:2016 “Glass in building — Determination of the bending strength of glass — Part 3: Test with specimen supported at two points (four point bending)”.</i></p> <p><i>Directive 2014/35/EU «Low voltage directive » (LVD) – relevant harmonised standards EN IEC 61730 series;</i></p> <p><i>European Committee for Standardization, EN 1990:2002 - Basis of structural design, CEN, 2002</i></p> <p><i>NF EN 12179 « Curtain walling — Resistance to wind load — Test method”</i></p>
Innovation of the new procedure with reference to existing standards: addition to the conventional Static mechanical load test (MQT 16), by considering safety in use and in particular the electrical safety during and after a mechanical load. Using the performance based-approach and defining <i>limit states</i> it is possible to determine different limit states with respect to the electrical and the material parts.

Methodology: Evaluate electrical safety (insulation loss) by also considering the integrity of solar cells and electrical connections during the application of an external load on the products, as expressed by IEC::

- (a) No intermittent open-circuit fault was detected during the test.
- b) No evidence of major visual defects as defined in IEC 61215-1 (2).
- c) Wet leakage current shall meet the same requirements as for the initial measurements.

Equipment: Mechanical load test (IEC 61215 (3) compliant equipment (MQT16)), electroluminescence apparatus, electrical controller unit, leakage current measurement systems, software system.

Expected impact for cost reduction: Tests unification avoiding double testing

5.4.4 Results

In this chapter, two main sections include (i) test execution and main results, and (ii) discussion are reported. The detailed flow of the NTP02 procedure as well as the specific test results related to BIPV products can be found in 7.2.4.

5.4.4.1 Test execution and main results

The equipment used to perform the tests is mechanical load equipment conforming to the IEC 61215-2 standard (3) and other systems specially made and developed to perform mechanical load tests, which do not follow any regulatory standard. The choice to use such systems falls on the fact that the interest of the test is to verify that, as a result of load and consequent deformation, there is no loss of insulation (electrical safety) and the integrity of all photovoltaic components (cells and circuits) is maintained. For this reason, tests are carried out with both uniformly distributed loads (e.g., wind or snow stress) and concentrated loads (concentrated weight).

Tests were performed on individual modules, not on systems or assemblies of modules, using the mounting systems used specifically for the products.

The BIPV products for which the tests were conducted are as follows:

- prefabricated BIPV modules for exterior wall insulation (Veture KIT);
- BIPV plastic tiles for discontinuous roofing;
- BIPV glass-glass modules.

The tests involved a limited number of samples per product so further testing will be necessary to validate the results. Initial results show that no insulation loss occurred during flexing and at the end of the test, and both circuits and solar cells show no damage. Insulation leakage was detected by the Insulation test (MQT 03) and the Wet leakage current test (MQT 15) provided by IEC 61730-2 (3). The integrity of the electrical circuits and solar cells was verified by analyzing photographic images made by the electroluminescence technique and comparing the modules before and after the tests were performed.

Tests performed on the glass-glass and prefabricated modules were conducted with loads that would achieve the maximum bending conditions allowed by the construction requirements for individual products. For glass-glass modules, for example, the maximum deflection used in accordance with the reference standard corresponds to 50 mm (EN 16612 (54)) Indeed, the standard states "in the absence of specific requirements, the deformations must be limited to the lower value between span / 65 or 50mm." It was judged that pushing further deflections did not make sense because it was contrary to the mechanical safety requirement expressed in the building codes.

The tests on the roof tiles (BIPV modules made without the use of glass, with the active photovoltaic part consisting of CIGS) were carried out at very high deflection values. This is because the photovoltaics used

were specially made for flexible modules, and in fact, although high deflection values in the order of 20 cm were reached, as a result of the deflection there was no loss of insulation and changes with respect to the integrity of cells and circuits. Refer to 7.2.3 for details of the test.

Finally, low, high, and intermediate temperature tests were conducted to assess how temperature may affect the electrical part. The test consisted of inserting a module into a special flat sealing system developed for the glass-glass product and the subsequent application of a concentrated load. The load consists of 12-cm square bricks. As known for polymeric materials, the stiffness changed with temperature providing different deformations in line with the material characteristics. Again, both for insulation and the integrity of PV components. It should be noted, however, that the deformation of the PV glass that occurred with the application of the high-temperature load became permanent. In fact, after the end of the test, following the cooling that occurred by leaving the glass at room temperature, permanent deformation was found, and the glass no longer returned to its pre-test state of flatness. Full details of the tests can be found in the Annexes.

5.4.4.2 Discussion

Tests have shown that, under the operating conditions of different classes of BIPV products tested in the project, deformation due to static loads in the range of the typical displacement admitted for construction works, whether uniformly distributed or concentrated, does not lead to changes in electrical safety. Within the limits of the deformation imposed by the limit states of construction, at laboratory temperatures around $25^{\circ}\text{C} \pm 5^{\circ}\text{C}$, the PV cells and electrical circuits, being encapsulated in polymeric materials that provide flexible conditions, do not suffer breakage detectable by the electroluminescence method and no loss of electrical insulation occurs. Furthermore, even tests performed at different temperatures with low and high-temperature values of -30°C and 90°C , resulted in neither changes in the electrical insulation nor in the integrity of the PV components. Therefore, it is expected that under most of the recurring deformation conditions of a BIPV product, due to static actions resulting from its use in construction works, the conventional c-Si solar cells should not be at risk of breakage under static loads. For such deformation limits, the viscoelastic mechanical properties of the interlayer materials as described in EN 16613 (55) under temperature and load duration conditions help to preserve the integrity of the PV components. However, this observation is limited to the configurations observed and tested and cannot be extended to other types of solar cells or PV modules for which no tests have been performed.

The results obtained, therefore, show that the initially planned procedure achieves no relevant purpose or real benefit for the product classes considered in the project. Implementing a new testing procedure for PV modules is deemed unnecessary, leading to increased qualification costs without providing real benefits. For the qualification of BIPV products and building materials, the manufacturer can refer to the testing procedures according to the standards reported under the Construction Products Regulation. However, electrical safety will have to be verified as a result of testing since the BIPV product must meet the safety requirements expressed in the Low Voltage Directive and the rules for PV products.

However, it is important to consider that the test on the glass-glass module at a high temperature (90°C) showed high deflections compared to the same test at a low temperature (-30°C) and the test at 40°C . In this case, as a result of deformation, as expressed above, the tested glass underwent permanent deformation that did not allow it to return to its initial flatness. This fact must be considered when designing BIPV components because BIPV modules operating at higher temperatures may have different behaviors. EN 16613 (55), which aims to specify a test method for determining the mechanical properties of interlayer materials, identifies interlayer stiffness families and compares the behavior with temperature. However, the temperatures considered lying in the operable range of standard glass from -20°C to $+60^{\circ}\text{C}$ lower temperatures than the actual operation of BIPV modules.

A final observation regards the methodology of load application. The tests described involved load application without any pressure and vacuum cycling with high application times. BIPV products containing photovoltaic parts, according to IEC 61215-2 (3) must be evaluated according to the Cyclic (dynamic)

mechanical load test (MQT 20). As the same standard quotes "*The most likely reason for extreme susceptibility to low levels of mechanical stress is a module assembly process that compromises the integrity of module components (for example tabbing that puts too much pressure on the cell and creates micro cracks). Components that may be evaluated by the cyclic dynamic mechanical load test (DML) include solar cells, interconnect ribbons, electrical bonds, and edge seals.*" This needs to be explored further in the future, and procedures could be developed to qualify construction products by considering the need for verification of the dynamic cycles of the PV part.

5.5 Conclusions and next steps

The general procedure developed for impact resistance tests on BIPV products provided satisfactory results. This procedure is the first step toward the unification of combined testing for the electrical and mechanical requirements for multifunctional construction products.

Thanks to the performance-based approach, the developed methodology is consistent with the requirements for building materials, it introduces the possibility of evaluating electric and construction limit states and considering temperature effects due to operating conditions. By avoiding the repetition of duplicate testing, costs associated with the double product qualification process can also be reduced. Given the early stage of test development, it will still be necessary to carry out further tests on BIPV products so that they can validate and find the necessary adjustments. In the future, efforts will be made to better fine tune the procedure as required for some families of construction products.

In fact, due to their type and purpose, BIPV products consist of different materials that are affected differently by impact energy and temperatures. In some cases, just the variation of the interlayer polymer used can change the test result, so it is necessary to expand the case study to cover the countless products placed on the market. The procedure for mechanical loading did not achieve significant outcomes concerning the behaviour of BIPV modules, so that further research will be done in the future e.g. in relation to the effects of temperatures and dynamic cycles on the integrity and performance of the products.

6 FIRE SAFETY

6.1 Introduction

Even if glass and polymeric components are currently well assessed for building applications (roof and façade) with a specific standard framework, all the building requirements don't consider the active parts under the scope of fire safety in building directive, and electric standards can't handle appropriately this typology of new building components on the other hand. Among all the innovation for building efficiency improvement, multifunctional elements are always at a crossing point for a full standard management.

Despite active works are in progress on fire standards (PR NF EN 13823/A1:2022), with many new standard versions in the last couple years (XP CEN/TS 16459:2019, EN 13823:2020, EN ISO 11925-2:2020), all active elements are still considered as passive elements without any additive constraints on building and role on fire classification or results. Real operating conditions or more realistic operating conditions aren't applied or considered during the fire tests and to provide results for photovoltaic components is not relevant. Currently, photovoltaic elements and even more Building integrated photovoltaic elements aren't considered as active element with moving properties (thermal and electrical) according to the weather conditions and thermal situation. Among the set of properties that can be modified, above mentioned could have a significant contribution on fire tests results by modifying the fire kinetics, energy generation and variation in the fire spread. The main effect is likely a fire acceleration, which leads to a deterioration of the results.

To bring more confidence in the use of BIPV, in construction sector as a traditional element of building skin, the definition of the most appropriate fire requirements and test is needed for the BIPV development.

Strengthening or hardening of test condition is generally the common solution applied to assess innovative elements or elements not clearly identified in a specific building category what are the BIPV components. This results in a rise of tests parameters without connection with specific physical phenomena to fit the most demanding conditions. The test combination methodology promoted in this work, aims to introduce realistic operating conditions not only to adapt current standards to PV, but also, to define a more appropriate test conditions dedicated to building integrated photovoltaic element assessment. We move from the most demanding to the most realistic test condition considering the specific part of photovoltaic field, the generation of electricity – an active part. Based on this approach we have defined a pathway to combine as best as possible current standards to assess both the building and the electrical generation requirements. This approach leads to a demanding standard combination under the scope of realistic requirements, in order to determine if under highly unfavourable conditions (the worst conditions) a BIPV component can achieve results equivalent to passive components of the building.

In the presented procedures the combination of fire test and active electric part is the main goal, although many other stress factors could play a significant role in terms of fire results variation, specifically for complex sandwich layers with many compounds or polymers. Indeed, ageing effects aren't considered, and polymers can be massively affected by mechanical stress or fatigue, UV, thermal constraints or even by electrical stress.

The procedure could be extended with different combinations of stress factors e.g., on elements aged in accelerated conditions. However, we have focused the definition of the NTP on the most relevant and manageable combination, of Fire test procedure with the addition of the electricity sources in active layers in the basic realistic operating conditions.

6.2 Objectives

In order to conduct these new tests procedures, the most demanding tests condition have two aims. Firstly, to demonstrate that BIPV elements do not present additional risks or hazards compared to the traditional building components, namely that the active parts do not reduce the characteristics and properties of the component. Secondly, to demonstrate, as the expected lower performance level, that BIPV can reach at least the same performance threshold as reference equivalent traditional building components and does not reduce the initial classification. As an example, a passive roof element (tiles, and slates) with a Broof classification does not have to be downgraded if active parts are integrated within.

The definition of the most demanding test combination must present the worst test condition that can happen in a building with BIPV component applied on façade or on roof. To carry out this work we have based our work on existing fire standards, relating to products for building application. On the other hand, the existing IEC standards handle a part of fire tests for photovoltaic classification but concerning exclusively the fire reaction and fire resistance as any passive elements.

As a common work base in the NTP methodology definition, to take into account the contribution of an active layer we have considered that the electricity generation was at highest level during the fire test (according to the test configuration), current and voltage are managed to fit as best as possible with reality. Indeed, during the tests ultimate current value cannot exceed I_{sc} of the module and the Ultimate voltage value is fixed by the maximal voltage value from the current IEC maximum level, 1000 V. With this approach we can consider of the effect on fire results from the photovoltaic cell technology. UI combination for CIGS cells is quite different as UI combination for Si cells, and the connection between modules is not similar.

Based on this specific approach to integer the electric generation during the fire test, we can apply a voltage (U) and current (I) values specifically to the manufacturer specifications and adapt the effect of electrical part accordingly. As an example, the use of a micro inverter can limit the maximum voltage value on DC part to the module U_{oc} .

Considering that we have neither assembly specifications from manufacturers (available area of the construction site, disposition, energy yield) nor module numbers and serial or parallel connections, we apply the most severe electrical conditions during these tests both for façade and roof elements based on LVD (2014/35/EU) requirements and harmonized standard based on IEC 60364 (French versions is NF C 15-100:2022 with the additional support of the practical guide UTE C 15-712-1:2013). Module and system standards as IEC 61215-1 are also used to define de maximum voltage value to apply during the NTP U value is fixed by the maximum voltage value allowed for photovoltaic installation ($U=1000V$, up to 1500V for DC grid) and the corresponding I value is correlated to the module specificities and the maximum I_{sc} value of corresponding modules. The data pair selected to carry out the NTP is the combination of the whole.

When the correct electrical load is defined, it's applied on the field terminals (connectors) and fire tests are carried out. Piori this stage, an initial test is carried out without electrical load in order to determine the deviation of the fire results, resulting from the action of the electrical load. If a deviation is observed the active part has a negative effect on the building functions, if no deviation is observed we can conclude that the active part doesn't play a significant role on the fire test results and that these components are as efficient as conventional construction components. The deviation ratio R expresses the ratio between the value of the results in severe conditions on the value of the reference results. A value greater than 1 means that the performance from a fire point of view is improved, less than 1 underlines a decrease in performance due to the active part and that this presents a possible reduction in the possibilities of use as building categories. Equal to 1 expresses a neutral influence on fire behaviour within the framework of current normative tests.

The ratio R, relative to fire sensitivity with an active layer inside is applied for all the NTP explained here after, and annotated R_{fr} to underline the specific approach of this work.

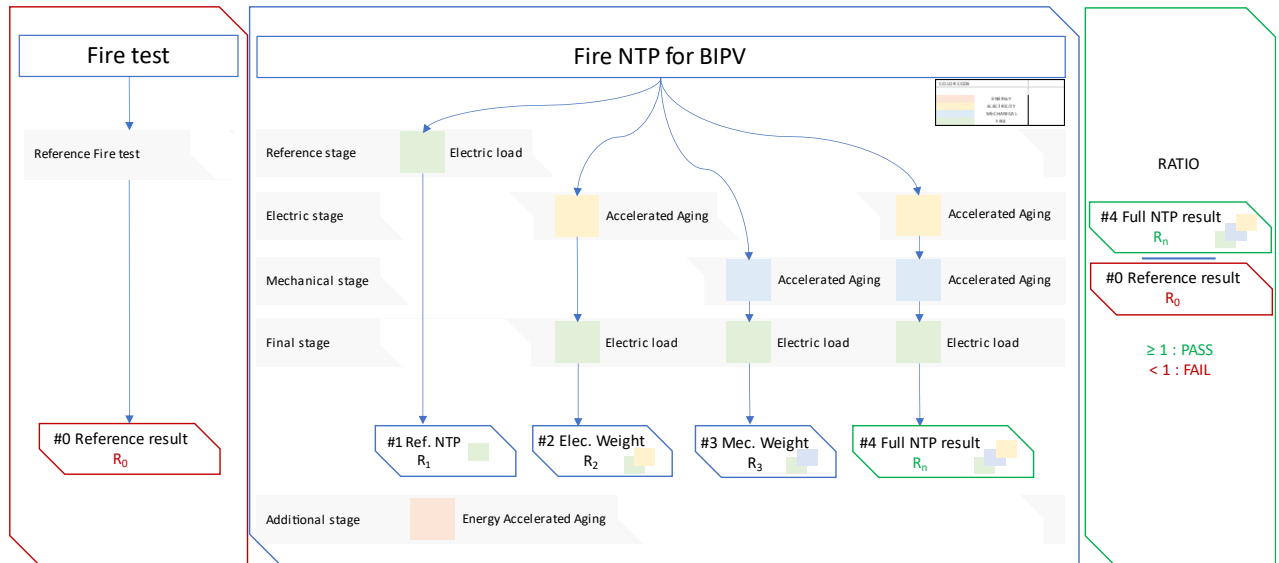


Figure 11 : Initial ratio determination stages to assess BIPV systems according the full NTP process

R_{fr} is a calculated ratio that can be applied on any test procedure and can be expressed with any formal results as a duration ratio, temperature ratio. For test results where a mean value or grade/aggregated value is expressed (like the SBI classification obtained from EN 13501), the initial R_0 value obtained with reference fire test is a normalized reference value equal to 1. The R_n value corresponding to the NTP application can be higher or lower than R_0 and affect the R_{fr} final corresponding value.

According to the definition of the NTP (normalized or not), if R_{fr} is higher than 1 the test is passed and the BIPV solution does not bring negative impact even if electric load or any others additional NTP are applied. Somehow, we could hypothesize that the NTP procedure have a positive effect on final ratio. Conversely, if R_{fr} value is lower than 1, that means that the NTP affect significantly BIPV test results and are very sensitive to an electrical load. As an example, for roof BIPV solution, if initial test reaches CroofT3 for conventional roof solution, the roof BIPV solution should reach a similar or better test result as Croof or Broof value. Under these conditions the BIPV solution passes the test and it can be concluded that it does not bring any negative contribution under the fire reaction test point of view. In the framework of BIPVBOOST project BIPV, all the aging effect procedures identified in the preliminary work have not been investigated due to the grant and time constraints. We have therefore only focused on the combination of fire test under electrical load as priority work. The R_{fr} ratio express exclusively the contribution of the electric load in a possible deviation in the fire test results.

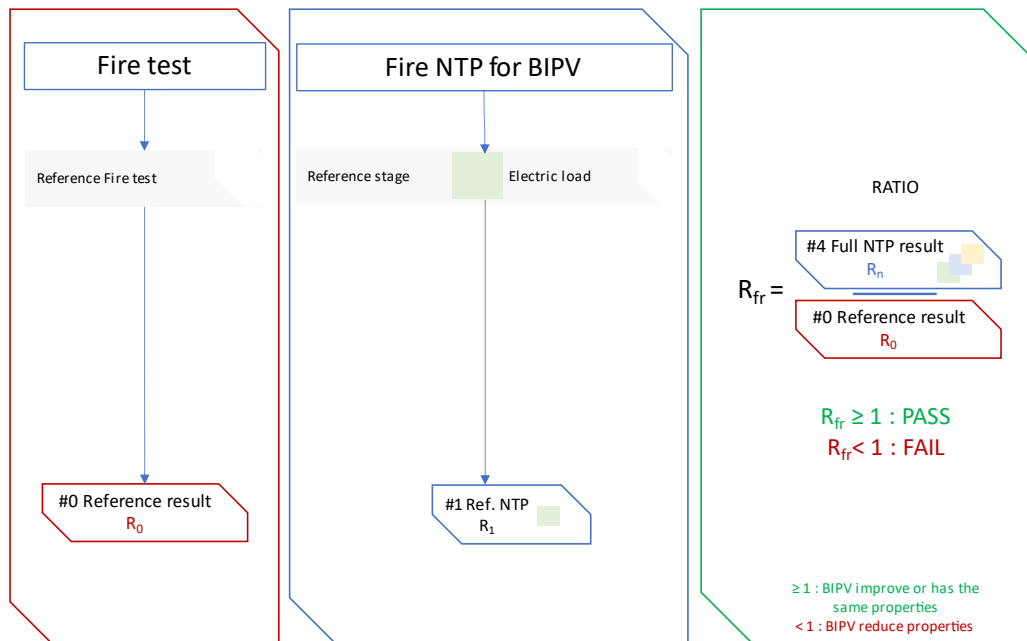


Figure 12 : Ratio determination to assess BIPV exclusively with electrical load under NTP

In both cases, the effect of the electric active layer is implemented in order to assess improvements or damages related the most real operating condition. Hereafter are explained implementation of the NTP according to integration categories detailed in EN 50583.

6.3 NTP FR01: Roof fire reaction for BIPV products with electric load in ultimate LS

6.3.1 Goal

The procedure is basically intended to introduce a testing approach to combine the fire performance limit states with the limit states related to the electric part for BIPV technology assessment in the building environment. This procedure is based to address requirements of EN 50583 category A and EN 50583 category B. The NTP FR01 aims to evaluate the intrinsic fire reaction of the product including additional stresses due to the electric load generated from the inner active layer impact, not only in terms of electrical properties related to the requirements of fire safety, but also of the consequences that the electric load could generate on the fire risks propagation. Thus, effects of actions are not only in terms of electrical properties related to the construction of the roof elements but also considering the consequences that an additional electric load could affect the PV part (electric generation) and final fire classification. By combining fire test setup with an electric load reflecting realistic operating conditions, the effect of the additional load on final fire test is assessed in order to define if current limit state levels are correct or must be adapted to BIPV configuration and address correctly BIPV solutions. Even if laminated glass components do not seem to be drastically affected, at first sight, the rise of complex bounding solutions (polymers and complex compounds) and thin layers cells used on roof elements, requires validating an effective influence on fire performance.

6.3.2 Problem

Currently fire tests are executed both in PV and building product certification, by performing different test procedures. Concerning the PV Side, for modification outside of the scope of IEC 61215 and IEC 61730-2 any modifications must use the retesting guideline described in IEC TS 62915 and to follow MST 23 (fire test) and MST 24 (ignitability test). Concerning the building side test requirements for roof systems follow CPR recommendation (CPR 305/2011) as a main procedure without no harmonized technical specification. Complementary approaches are used with as a key reference standard the test method exposed under the CEN TS 1187-2014 standard.

The purpose of the test is to identify a possible negative effect under adverse test conditions or to apply the most realistic test conditions considering effect of electric generation under fire attack taking part of LVD advises. The criterion for passing the test is defined by the initial (reference) performance result compared with the combined effect results according to the worth test conditions, regarding the operating conditions and setup in accordance with the procedure explained in Figure 12

The expected result, in the present form, is to assess the influence of electric load on fire kinetic in order to bring more confident in BIPV application in the roof environment.

6.3.3 Proposal

In the BIPVBOOST project framework, the test to qualify the BIPV product will be performed starting with the basic test integration mode and layout evaluated also in relation with electrical safety performance. The methodology is to describe a general test method, defining equipment and the configuration used in order to assess the fire classification under electric load of the BIPV roof systems.

The method aims at evaluating product's integrity after an additional stress due to an application of an additional load which can generate electric hazards, mainly electrical arcs, promoting additional fire ignition, bringing an additive ignitability source with possible negative effects on fire propagation, resulting in a performance downgrade in terms of fire resistance and fire reaction.

Electrical arcs impact from the inside part of the BIPV module could promote unexpected behavior of BIPV elements in front of fire hazard and the methodology adopted aims to develop a more realistic test setup and procedure to assess in conditions close to operating conditions, taking into account of integration mode and layout of the system.

The well-known approach for Roof test is detailed in current standards mainly used in Europe to characterize building components with a set of three pivot elements, namely: the EN 13501-2 :2016 - Fire classification of construction products and building elements, the EN 1364-1: 2012 – Fire resistance tests (general requirements) allowing to validate the fire classification on small samples and then, the standard CEN TS 1187: 2014 Test methods for external fire exposure to roofs. Based on these standards as a reference approach, we have developed an additive methodology to improve the test conditions to not only test the fire configuration from an external fire attack but including an additional effect of an electrical arc from inner element, generated by a malfunction, or aggravated by fire.

The test allows the assessment by behavior comparison of the reference test methods for external fire exposure to roofs applied on BIPV component with regard to its reference mounting scenario (Broof T3 : c. test 3 – with burning brands, wind and supplementary radiant heat) and by reproducing the similar test procedure by applying relevant electrical conditions occurring in operative conditions (Voltage and current). The fire test will be equipped with an energy generator (electric load) and with a monitoring system in order

to detect any electrical issues on the system. To detect an Arc default would be an ideal equipment to develop and to implement.

To carry out this NTP, a dynamic DC load is used to force current to flow through cables as if the BIPV system was running in operating conditions. A REGATRON TopCon Quadro device, a programmable DC power supply, is used with the TC LIN 10 kW Solar array simulation testing tool embedded. The full 4 quadrant grid simulator allows to combine a Current/Power or Voltage/Power supply with additional load limit. In the NTP the set Current/Power is supply, and the power value is fixed according to the maximum voltage value (Current/Power($f(U=1000V)$)).

The power is supplied in reverse mode. The REGATRON device allows to fix power value in combination with current or voltage, in this NTP, the current maximum value is imposed to detect any default during the fire test by the detection of a possible breakdown. A rapid current shutdown (from $I=I_{scA}$ to $I=0A$) is the result of a circuit break due to fire attack. We can assume that in case of rapid shutdown, an electric arc could bring additional energy to accelerate the spread of fire and reduce the overall performance of the BIPV system. The operating diagram is shown below.

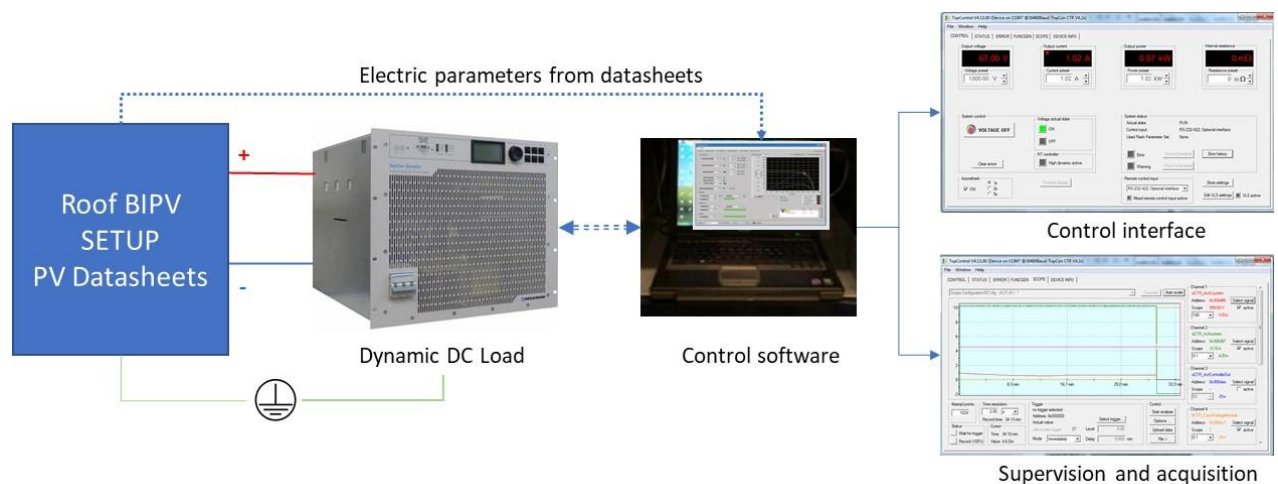


Figure 13: Electric load setup applied during the fire test to stress electrically the BIPV solution.

The electrical test conditions are defined from the framework of current standard procedure (IEC 61853 / IEC TS 63128 / ...) and are applied in the framework of CEN TS 1187.

The following standards are considered in the fire procedure in non-conventional scenarios:

- CPR 305/2011 : no harmonized technical specifications are mandatory for Fire resistance
- EN 13501-2 :2016 - Fire classification of construction products and building elements
- EN 1364-1: 2012 – Fire resistance tests (general requirements)
- CEN TS 1187: 2014 Test methods for external fire exposure to roofs
- IEC 61853 / IEC TS 63128 / ... adaptations to be the most demanding standards (SUPSI/CSTB)

- **Expected impact for product certification according to CPR and/or LVD**

Promotion of a NTP based on a combined approach (combination of CPR requirements and LVD requirements), allows to assess BIPV component under CPR requirement with additional requirements from LVD, specifics to photovoltaic standards requirements. It's a step forward to support current standard development on BIPV elements to have an adapted implementation. Currently EN 50583 standard is strongly

based on CPR for building integration assessment, and the active layer is not considered as a possible active part during these tests.

This work carried out on standard combination can lead to the implementation of a new certification or an enhancement of current certification to consider the combination of CPR test with LVD test. This improved qualification, specifically developed for BIPV components is perfectly suited for, allows to be applied in accordance with the specificities of the products to be tested rather than having adaptations of the current standards.

Dedicated certification, improved with more realistic operating conditions and considering the worst test conditions, would increase confidence in these building active components, greater insurability, and durability, supporting the development of the BIPV sector.

- **Expected impact on cost reduction**

To reduce cost of fire tests, the best way is to perform all tests during the same session, in order to reduce drastically time spent in mock-up preparation and maximize laboratory downtime by performing standard test and NTP in the same test session. On the other hand, to perform a set of tests during the same session reduce time and cost of logistic and component management. The same laboratory, at the same place can carry out all the tests. An additional effect is the drastic transportation cost reduction, all samples are tested in the same laboratory during the same period allowing also to save time in the certification process. An indirect cost reduction is also to minimize workforce and human resources. Implementation of the NTP requires having equipment suitable for the tests to be carried out and compatible with intense thermal conditions.

From the CPR part, CEN TS 1187 is the main standard used to support the definition of new test procedure, with the test setup, element layout, and results format.

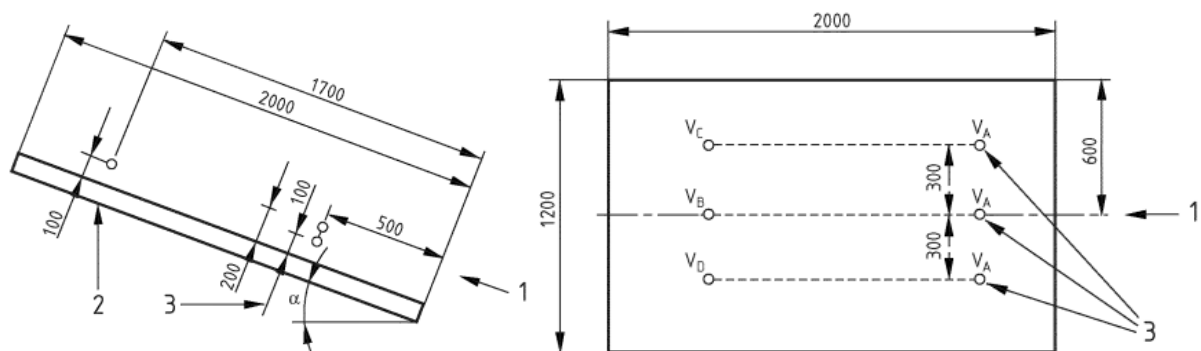


Figure 14: Side view and top view of test bench with location of the firebrands according to the CEN TS 1187 requirements.

The implementation of the BIPV components on the roof mock-up is presented on the Figure 15 to test the BIPV configuration according to the singular points, where are located the joints, or material layers division as ridges, eaves, and hips. Both configurations are tested to assess as best as possible the BIPV components behaviour under fire attack.

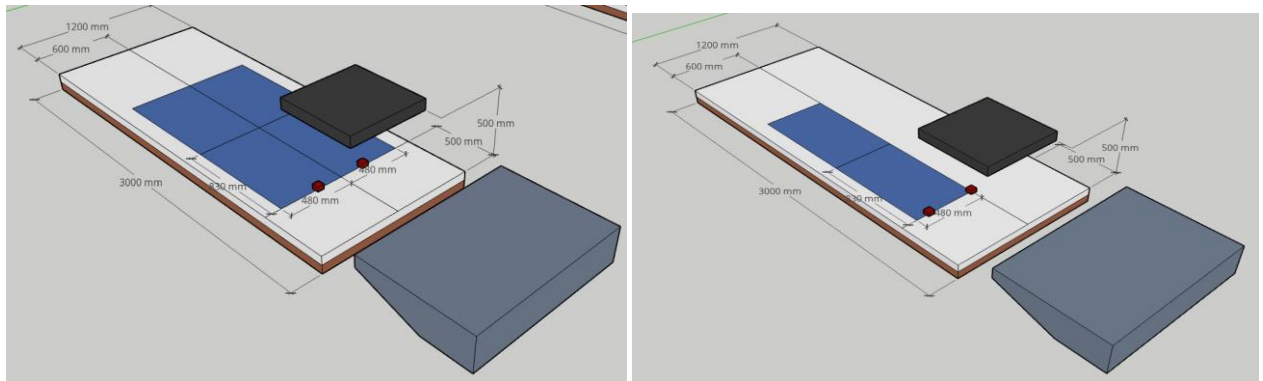


Figure 15: Configuration according to standard CEN TS 1187 recommendations

Note that glowing firebrands are located on joints to further experience the mounting singularities, in the case of vertical joints, its recommended to perform specific roof test by locate firebrands on singular points. The roof shingleBIPV solution used as sample product shows horizontal and vertical joints and have to be tested according to the most demanding configuration. As the gutter elements (lower than the bottom part of BIPV solution) is often a butyl element characterize by a low fire resistance.

On specific demand from the producer, the tested mounting system is installed according to the provisions shown below.

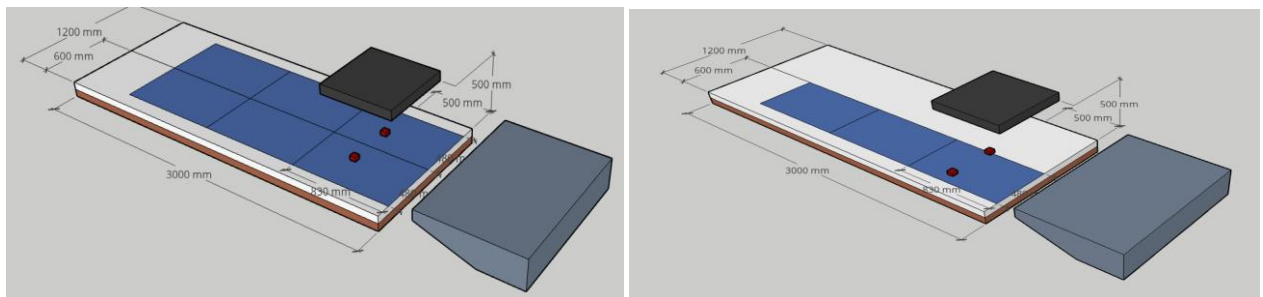


Figure 16 : configuration chosen according to the manufacturer's recommendations

The following schematic summary of the procedure developed is reported.

Activity 5.2.4: Fire reaction (FR) of BIPV components/systems	
Leading partner: CSTB	
Specific technical requirement covered by the new procedure (TR):	
1_ To assess fire reaction of BIPV components taking into account of technical surrounding, integration mode and interaction with other materials >> Fire Rating respective to BIPV solution	
2_ Evaluate the gap/difference from standard products (without active layer)	
Product family (PF):	
4-Roof	

New procedure code:
FR_CSTB_PR_1_PF_4
Specific reference standards in force in PV and building domain for product qualification/markings:
<p><i>CPR 305/2011 : no harmonized technical specification are mandatory for Fire resistance</i></p> <p><i>EN 13501-2 :2016 - Fire classification of construction products and building elements</i></p> <p><i>EN 1364-1: 2012 – Fire resistance tests (general requirements)</i></p> <p><i>CEN TS 1187: 2014 Test methods for external fire exposure to roofs</i></p> <p><i>+ specific standards dedicated to BIPV component to assess (floor or wall or roof ...)</i></p> <p><i>+ all relevant standards according to product family (CF; contribution matrix)</i></p> <p>In the matrix contribution standard tests are identified according of king of integration case (demo site specification and BIPV products). New standard or standard evolution is not targeted, but new testing procedure is expected with other field implementation > combination of several test approach</p>
Innovation of the new procedure with reference to existing standards:
<p>Perform FR tests with active elements (with/without electrical load) with combination with mechanical test procedures and electrical load (load stress before fire test and fire test under load) according IEC 61215 retesting guidelines and 5.2.2 and 5.2.3 work</p>
Methodology
<p>Test fire resistance and reaction of BIPV components with and without electrical load to assess effect of electrical on possible hazard expansion / perform same tests after mechanical stress tests and assess modification on fire resistance</p> <p>1 – Identified necessary roof fire test according to BIPV components = reference results (Gutter and pitch)</p> <p>2 – Aging preconditioning + electric load according to BIPV implementation cases (Gutter and pitch)</p> <p>3 – similar fire tests as 1) after 2) assessment = bias identification (risk identification rate)</p>
Equipment development
<p>Indoor devices for roof fire test (Burning brand, radiative heater and wind turbine, ...) with all building elements and integration components. All additional parts have to be included during test procedure (JBoxes, cables, connectors, sublayers elements). All modules/samples are electrically connected. An electric load is applied at terminals.</p>
Relation with other WPs innovation/development:
<p><i>WP3/4 – product families: all necessary specific inputs that could affect/change level of requirement including shape, characterization of any components, sketches, blueprint, electrical diagram...</i></p> <p><i>WP8 – democase: Final dimension of samples and nature of all elements used</i></p> <p><i>WP5.2 other activities linked with Fire test procedure including electrical and mechanical NTP for pre-aging (aging or age conditioning)</i></p>

Table 15 NTP FR01: Roof fire reaction for BIPV products with electric load in ultimate LS

6.3.4 Results

6.3.4.1 Test procedure

As a first step, a reference test is performed in order to harvest initial values according to building requirements. This first test is used as a reference value and will be used as denominator value in the ratio factor to overcome or to reach for the BIPV components with electrical load applied.

Then the similar test is performed again with significant changes to consider the electric configuration. All PV plugs are interconnected by taking a specific attention on the place of junction boxes, located close to the fire ignition location (the worst configuration). Aim of this approach is to expose the largest combustible mass close to the fire ignition or location of burning elements. All connections follow the manufacturer notice and/or standard rules for PV field connection or LVD recommendation.

The electric load used is a PV field GENERATOR (REGATRON PV SERIES) allowing to set the electric conditions according to two operating modes, switching from I and P to U and P mode imposed. The starting mode used is I and P values imposed according to PV datasheets to define the maximum current value to be applied during the fire test.

The I value is equal to the maximum current in short circuit according to the manufacturer prescription. The maximum power value is fixed according to the maximum voltage allowed according to IEC 61730 , 1000 V DC. According to this operating mode, Pmax is fixed by the value of I_{sc} multiplied by the maximum voltage value.

Considering an open circuit due to destruction of bus bars by the fire attack or due to an electric arc, the maximum voltage value remains the same, 1000V.

Afterwards, the DC generator is connected to the PV field plugs in reverse mode (++) and (--) to overdrive the bypass diodes. Before starting the fire test, an initial electric test is performed in order to validate the electric connection and check the perfect operating conditions. The set current value must be displayed on the DC generator, and Power mode have to be switched on. A multimeter is used to check that the current value imposed is correct.

Note : no additional sensors and monitoring system can be installed in the test room due to the increase of temperature during the test phase and extreme operating conditions (smoke, dust, soil and high temperature) a specific cabinet with fire protection and HVAC system will be developed for the next tests allowing more simple setup and installation of sensors as close as possible from the test bench. REGTRON measuring system is used to supervise and store the electric results during the NTP test.

If any issues are found during this first check, an overall electrical check is performed to fix this issue and replace damaged element. Please note that every PV module is checked with a multimeter prior the installation on the bench test.

6.3.4.2 Equipment

As described prior, a DC PV generator is used to generate a I(P) or U(P) power function image of a PV field. The DC PV GENERATOR is an industrial machine used to test inverters, storage and loading solution for PV application, only in DC mode. This element is used to apply an equivalent electrical load as one generated by the PV field under the sun radiation.

In order to impose the requirement as it higher point, the maximum power conditions are fixed according to the STC conditions (IEC 61215 – IEC 61648) and all electrical values are used according to these parameters.

In generator mode we selected to impose the current value (I_{sc}) and depending maximum power to have a more effective representation of operating conditions.

All these parameters are set on the REGATRON display board and the embedded storage solution allows to follow the evolution of Current and Voltage throughout the duration of the test.



Figure 16: DC PV GENERATOR (10 kW DC) used in electric load NTP

6.3.4.3 Test execution and main results

The main objective is to detect a possible current failure, that express bus bar destruction through combustion of combustible part, or electrical arc generation in the electrical circuit. In case of appearance of current default, that reach a null value, a nominal voltage value is imposed by the DC PV Generator equivalent to the global Voc values of modules.

The DC PV GENERATOR is preliminary connected to a BIPV module in order to test the connection quality and to validate the setup. We run a first load test to validate the process. After validation of this step, the DC PV Generator is then connected to the BIPV field to be fire tested with the application of the electrical load. Only BIPV elements and cables are located in the room test, only cables pass-through room wall. DC PV GENERATOR is located outside the test room, on a movable bench to be closed as possible of the tested mockup.

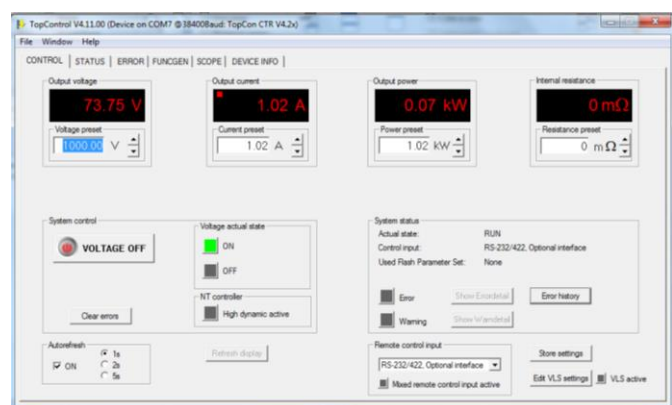


Figure 17. DC PV GENERATOR (10 kW DC) – preliminary settings before mockup connection Load device and remote control to test load on CIGS module (left) / User interface with load level (right)

The DC PV generator is preliminary tuned to deliver I_{sc} and the equivalent power to reach $U=1000V$ (the dataset is collected from module manufacturers or from tests characterization).

The corresponding electric load is applied on PV array 1 mn before to start the fire test to stabilize the voltage value according to the room temperature and to check possible current leakages.

Following the validation of this step (no current defaults), the test is carried out over a period defined by the test standard (Broof T3 = 30mn)



Figure 18. Before/during/after the fire test with DC PV GENERATOR load applied. During the test, current and voltage values are checked to identify possible breaks in the electrical circuit.

- If no electric breaks are observed, the electric part is safe (continuity is preserved) and do not bring additional fire contribution as firebrands and radiant part.
- If electric breaks are observed, the time is noted to identify later possible effect

Finally, roof test results are then checked to observe any deviation.

- Without electric breaks appearance, only the fire tests are selected for results and compared with initial results without electric load
- In case of electric break appearance, in depth analysis are conducted specifically at the time noted during the test where breaks are observed. Comparison results are performed to observe specific deviation with electric load contribution

Before to stop the load, another 1 mn stabilization is observed prior to force the switch off.

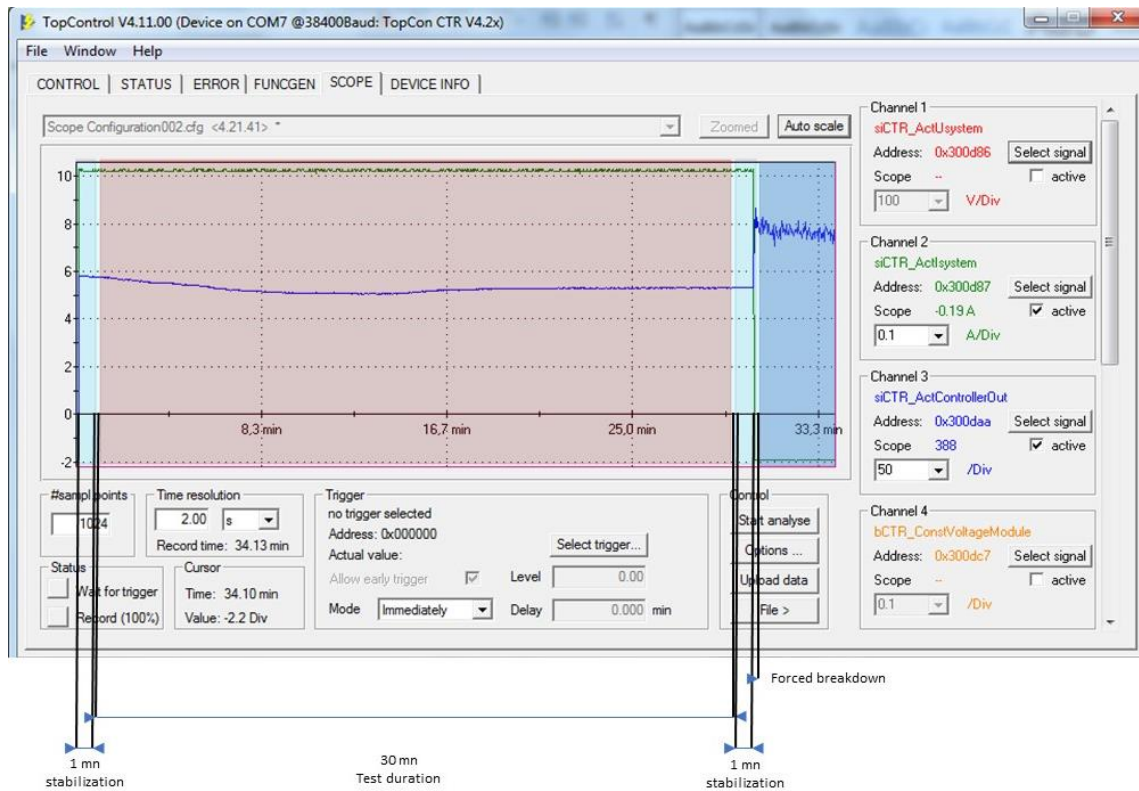


Figure 19. Example of electric load carried out during Broof test (roof shingle product)

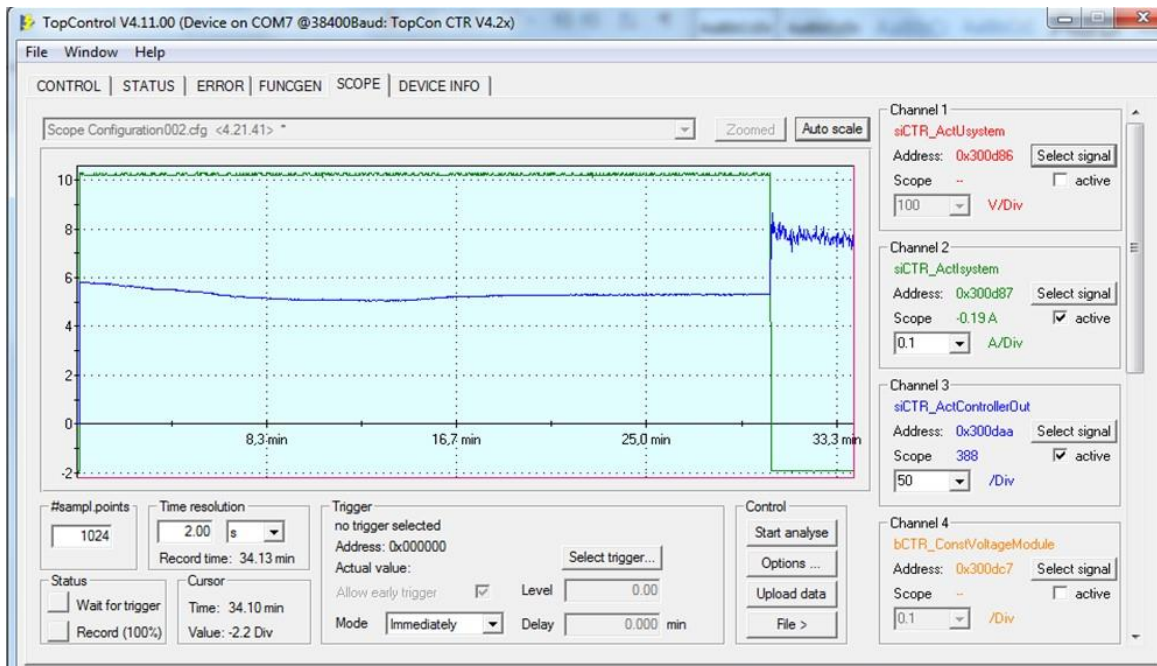


Figure 20. No electrical breakage observed – no negative effects due to electric load

- **Discussion**

All tests performed according to the Broof expectation are carried out with appropriate electric load. Results are compared with initial test in normal conditions in order to identify possible deviation due to additional constraints provided by the stress of the electric load. On any tests we haven't observed any current leakages or breakout, which emphasizes the absence of a break in the electrical circuit. The implementation of an electric charge does not degrade the fire properties (fire classification) of the BIPV components.

An active breakdown/breakout is correctly observed on the on the monitoring system, which highlights the absence of an electric defect during the tests.

On the other hand, this equipment is not initially developed to carry out this test in complete safety conditions (not for users but for the equipment as the active or rapid cut off may damage the fuse of the equipment. An intermediate load or an intermediate converter will have to be studied in order to limit the damage to the equipment afterwards. In the same way, arc detection is not implemented in this setup, thus the energy generated, and arc duration are not measured to assess the possible contribution on the fire propagation in case of default.

Specific equipment is under development to take into account of specific values to measure and also specific surrounding conditions tests with a dedicated cabinet installed in the test room. An additional monitoring system with subsection measurement per module to detect the place of default will be also to develop in order to detect the place of default in order to provide specific upgrade in case of failed test. Temperature measurement is still under study to assess the temperature gradient in the BIPV element but also in the entire mockup for possible fire penetration.

Next STEPS are to implement several test combinations to assess under fire test the worst test conditions not at initial time but on a full lifetime to ensure that a BIPV components is fire resistant regardless of its lifetime.

6.4 NTP FR02: Facade fire reaction for BIPV products with electric load in ultimate LS

6.4.1 Goal

The procedure is basically intended to introduce a testing approach to combine the photovoltaic limit states with the limit states related to the electric part for BIPV technology assessment in the building environment. This procedure is based to address requirements of EN 50583 category C and EN 50583 category D. The NTP FR02 aims to evaluate the intrinsic fire reaction of the product including additional stresses due to the electric load generated from the inner active layer impact, not only in terms of electrical properties related to the requirements of fire safety, but also of the consequences that the electric load could generate on the fire risks propagation. Thus, effects of actions are not only in terms of electrical properties related to the construction of the façade elements but also considering the consequences that additional electric load could affect the PV part (electric generation) and final fire classification. By combining fire test setup with an electric load reflecting realistic operating conditions, the effect of the additional load on final fire test is assessed in order to define if current limit state levels are correct or must be adapted to BIPV configuration and address correctly BIPV solutions. Even if laminated glass components seem not drastically affected, at first sight, the rise of complex bounding solutions (polymers and complex compounds) and thin layers cells used on façade elements, this requires validating an effective influence on fire performance.

6.4.2 Problem

Currently fire tests are executed both in PV and building product certification, by performing different test procedures. Concerning the PV Side, for modification outside of the scope of IEC 61215 and IEC 61730-2 any modifications must use the retesting guideline described in IEC TS 62915 and to follow MST 23 (fire test) and MST 24 (ignitability test). Concerning the building side test requirements for roof systems follow CPR recommendation (CPR 305/2011) as a main procedure without no harmonized technical specification. Complementary approaches are used with as a key reference standard the test method exposed under the EN 13823 -2020 standard.

The purpose of the test is to identify a possible negative effect under adverse test conditions or to apply the most realistic test conditions considering effect of electric generation under fire attack taking part of LVD advises. The criterion for passing the test is defined by the initial (reference) performance result compared with the combined effect results according to the worth test conditions, regarding the operating conditions and setup in accordance with the procedure explained in Figure 12

The expected result, in the present form, is to assess the influence of electric load on fire kinetic in order to bring more confident in BIPV application in the façade environment.

6.4.3 Proposal

In the BIPVBoost project framework, the test to qualify the BIPV product will be performed starting with the basic test integration mode and layout evaluated also in relation with electrical safety performance. The methodology is to describe a general test method, defining equipment and the configuration used in order to assess the fire classification under electric load of the BIPV façade systems. For the detailed description, refer to **Annexes**.

The method aims at evaluating product's integrity after an additional stress due to an application of an additional load which can generate electric hazards, mainly electrical arcs, promoting additional fire ignition, bringing an additive ignitability source with possible negative effects on fire propagation, resulting in a performance downgrade in terms of fire resistance and fire reaction.

Electrical arcs impact from the inside part of the BIPV module could promote unexpected behavior of BIPV elements in front of fire hazard and the methodology adopted aims to develop a more realistic test setup and procedure in order to assess in conditions close to operating conditions, taking into account of integration mode and layout of the system.

The well-known approach for façade test is detailed in current standards mainly used in Europe to characterize building components with a set of four pivot elements, namely: the EN 13501-2 :2016 - Fire classification of construction products and building elements, the EN 1364-1: 2012 – Fire resistance tests (general requirements) allowing to validate the fire classification on small samples and then, the standards EN ISO 11925-2:2020 and the EN 13823 -2020 are test methods to assess Reaction to fire tests for building products - Building products excluding floorings exposed to the thermal attack by a single burning item specifically applied for façade elements. Based on these standards as a reference approach, we have developed an additive methodology to improve the test conditions to not only test the fire configuration from an external fire attack but including an additional effect of an electrical arc from inner element, generated by a malfunction, or aggravated by fire.

The test allows the assessment by behavior comparison of the reference test methods for external fire exposure to roofs applied on BIPV component with regard to its reference mounting scenario (SBI test report and classification) and by reproducing the similar test procedure by applying relevant electrical conditions occurring in operative conditions (Voltage and current). The fire test will be equipped with an energy generator (electric load) and with a monitoring system in order to detect any electrical issues on the system. To detect an Arc default would be an ideal equipment to develop and to implement.

To carry out this NTP, a dynamic DC load is used to force current to flow through cables as if the BIPV system was running in operating conditions. A REGATRON TopCon Quadro device, a programmable DC power supply, is used with the TC LIN 10 kW Solar array simulation testing tool embedded. The full 4 quadrant grid simulator allows to combine a Current/Power or Voltage/Power supply with additional load limit.

In the NTP the set Current/Power is supply, and the power value is fixed according to the maximum voltage value (Current/Power($f(U=1000V)$)).

The power is supplied in reverse mode. The REGATRON device allows to fix power value in combination with current or voltage, in this NTP, the current maximum value is imposed to detect any default during the fire test by the detection of a possible breakdown. A rapid current shutdown (from $I=I_{sc}A$ to $I = 0A$) is the result of a circuit break due to fire attack. We can assume that in case of rapid shutdown, an electric arc could bring additional energy to accelerate the spread of fire and reduce the overall performance of the BIPV system. The operating diagram is shown below.

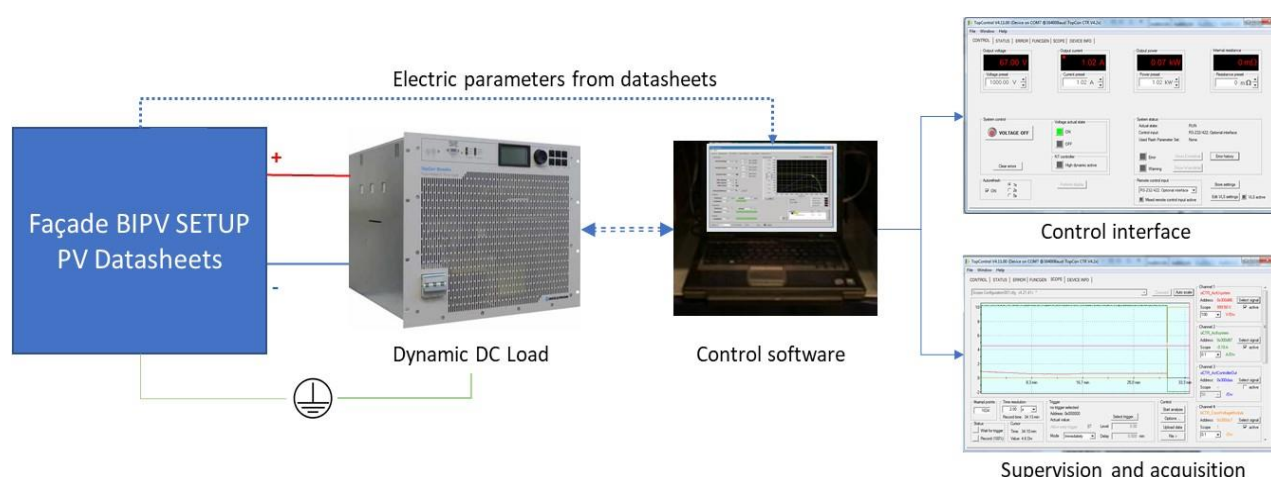


Figure 21 Electric load setup applied during the fire test to stress electrically the BIPV solution

The electrical test conditions are defined from the framework of current standard procedure (IEC 61853 / IEC TS 63128 / ...) and are applied in the framework of EN 13823 -2020.

The following standards are considered in the fire procedure in non-conventional scenarios:

- *CPR 305/2011 : no harmonized technical specifications are mandatory for Fire resistance*
- *EN 13501-2 :2016 - Fire classification of construction products and building elements*
- *EN 1364-1: 2012 – Fire resistance tests (general requirements)*
- *ISO 11925-2 Single flame test or ignitability*
- *EN 13823: 2020: Reaction to fire tests for building products - Building products excluding floorings exposed to the thermal attack by a single burning item*
- *IEC 61853 / IEC TS 63128 / ... adaptations to be the most demanding standards (SUPSI/CSTB)*

- Expected impact for product certification according to CPR and/or LVD

Promotion of a NTP based on a combined approach (combination of CPR requirements and LVD requirements), allows to assess BIPV component under CPR requirement with additional requirements from LVD, specifics to photovoltaic standards requirements. It's a step forward to support current standard development on BIPV elements to have an adapted implementation. Currently EN 50583 standard is strongly based on CPR for building integration assessment, and the active layer is not considered as a possible active part during these tests.

This work carried out on standard combination can lead to the implementation of a new certification or an enhancement of current certification to consider the combination of CPR test with LVD test. This improved procedure, specifically developed for BIPV components is perfectly suited for, and allows to be applied in accordance with the specificities of the products to be tested rather than having adaptations of the current standards.

Dedicated qualification, improved with more realistic operating conditions, considering of the worst test conditions will increase confidence in these building active components, greater insurability, and durability, supporting the development of the BIPV sector.

- Expected impact for cost-reduction

To reduce cost of fire tests, the best way is to perform all tests during the same session, to reduce drastically time spent in mock-up preparation and maximize laboratory downtime by performing standard test and NTP in the same test session. On the other hand, to perform a set of tests during the same session reduce time and cost of logistic and component management. The same laboratory, at the same place can carry out all the tests. An additional effect is the drastic transportation cost reduction, all samples are tested in the same laboratory during the same period allowing also to save time in the certification process. An indirect cost reduction is also to minimize workforce and human resources. Implementation of the NTP requires having equipment suitable for the tests to be carried out and compatible with intense thermal conditions.

- The test procedure combination

From the CPR part, *EN 13823: 2020* is the main standard used to support the definition of new test procedure, with the test setup, element layout, and results format.

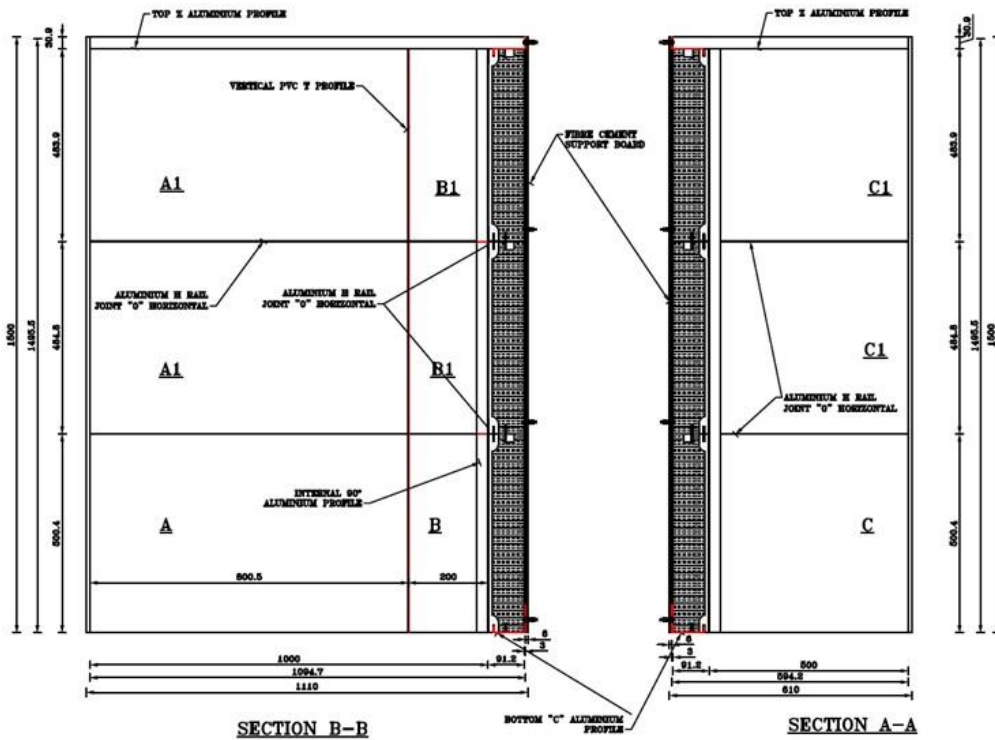


Figure 22 : Left side view (long wing/wall) and right side view (short wing/wall) of test bench with module size details according to the EN 13823: 2020 requirements.

The implementation of the BIPV components on the façade mock-up is presented on the Figure 22 to test the BIPV configuration according to the singular points, where are located the vertical and horizontal joints, or material layers division.

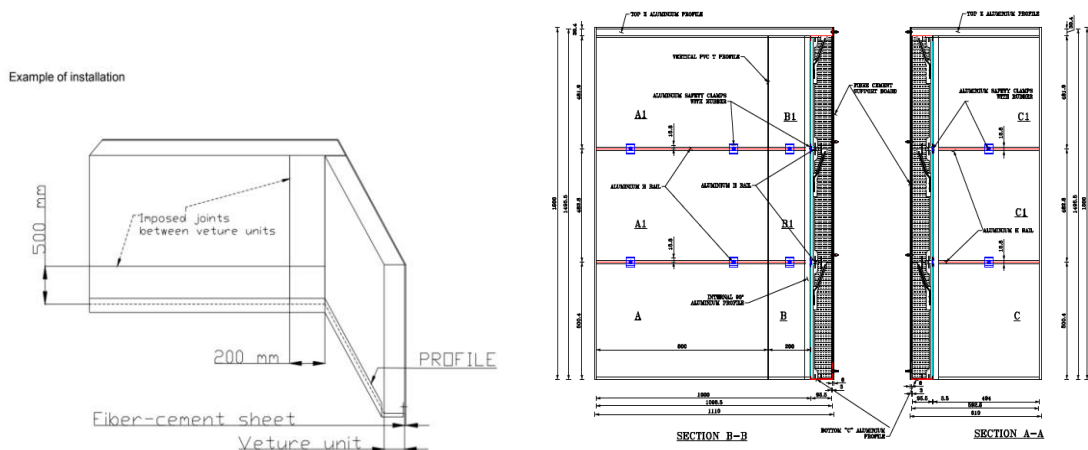


Figure 23 : Configuration according to standard EN 13823: 2020 recommendations, example of veture kit layout

Note that for flexible module (CIGS) on veture kit and CIGS standard size modules all the left wall is no active due to the half cut of the modules to fit with the mock-up size. glowing firebrands are located on joints to further experience the mounting singularities, in the case of vertical joints, its recommended to perform specific roof test by locate firebrands on singular points. The roof tile with a CIGS module based shows horizontal and vertical joints and have to be tested according to the most demanding configuration. As the gutter elements (lower than the bottom part of BIPV solution) is often a butyl element characterize by a low fire resistance.

On specific demand from the produced, the tested mounting system is installed according to the provisions shown on the

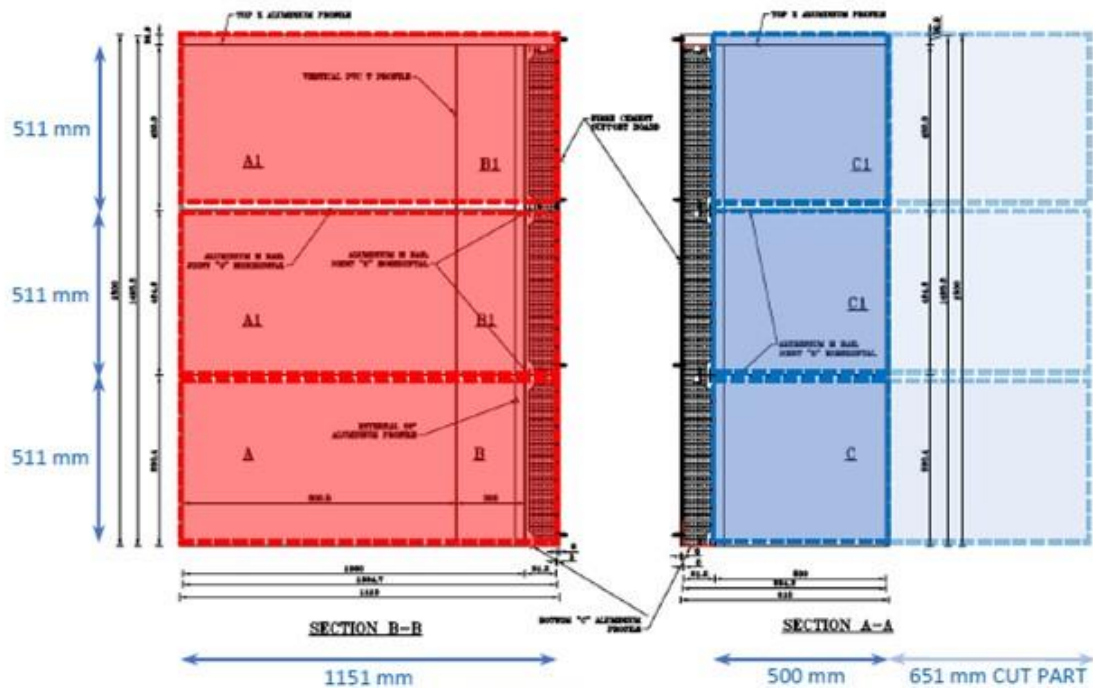


Figure 24 : Configuration CIGS flexible module on a veture kit façade cladding system according to the manufacturer's module size (red area). Blue area are halves cut modules (not operating)

The following schematic summary of the procedure developed is reported.

Activity 5.2.4: Fire reaction (FR) of BIPV components/systems		CSTB <small>le futur en construction</small>
Leading partner: CSTB		
Specific technical requirement covered by the new procedure (TR):		
1_ To assess fire reaction of BIPV components taking into account of technical surrounding, integration mode and interaction with other materials >> Fire Rating respective to BIPV solution		
2_ Evaluate the gap/difference from standard products (without active layer)		
Product family (PF):		
Wall / ventilated façade / cladding;		
New procedure code:		

FR_CSTB_PR_1_PF_3
Specific reference standards in force in PV and building domain for product qualification/markings:
<p><i>CPR 305/2011 : no harmonized technical specification are mandatory for Fire resistance</i></p> <p><i>EN 13501-2 :2016 - Fire classification of construction products and building elements</i></p> <p><i>EN 1364-1: 2012 – Fire resistance tests (general requirements)</i></p> <p><i>ISO 11925-2 Single flame test or ignitability</i></p> <p><i>If previous test fails > EN 13823: 2020 : Reaction to fire tests for building products - Building products excluding floorings exposed to the thermal attack by a single burning item</i></p> <p><i>+ specific standards dedicated to BIPV component to assess (floor or wall or roof...)</i></p> <p><i>+ all relevant standards according to product family (CF; contribution matrix)</i></p> <p>In the matrix contribution standard tests are identified according of king of integration case (demo site specification and BIPV products). New standard or standard evolution is not targeted, but new testing procedure is expected with other field implementation > combination of several test approach</p>
Innovation of the new procedure with reference to existing standards:
<p>Perform FR tests with active elements (with/without electrical load) with combination with mechanical test procedures and electrical load (load stress before fire test and fire test under load) according IEC 61215 retesting guidelines and 5.2.2 and 5.2.3 work</p>
Methodology
<p>Test fire resistance and reaction of BIPV components with and without electrical load to assess effect of electrical on possible hazard expansion / perform same tests after mechanical stress tests and assess modification on fire resistance</p> <p>1 – Identified necessary Façade fire test according to BIPV components = reference results</p> <p>2 - Aging preconditioning + electric load according to BIPV implementation cases</p> <p>3 – similar fire tests as 1) after 2) assessment = bias identification (risk identification rate)</p>
Equipment development
<p>Indoor devices for fire test (Burning brand, horizontal and vertical Furnace, fire spread façade, SBI ...) with all building elements and integration components. All additional parts have to be included durint test procedure (JBoxes, cables, connectors). All modules/samples are electrically connected. An electric load is applied at terminals</p>
Relation with other WPs innovation/development:
<p><i>WP3/4 – product families: all necessary specific inputs that could affect/change level of requirement including shape, characterization of any components, sketches, blueprint, electrical diagram...</i></p> <p><i>WP8 – democase: Final dimension of samples and nature of all elements used</i></p> <p><i>WP5.2 other activities linked with Fire test procedure including electrical and mechanical NTP for pre-aging (aging or age conditioning)</i></p>

6.4.4 Results

6.4.4.1 Test procedure

As a first step, a reference test is performed in order to harvest initial values according to building requirements. This first test is used as a reference value and will be used as denominator value in the ratio factor to overcome or to reach for the BIPV components with electrical load applied.

Then the similar test is performed again with significant changes to consider the electric configuration. All PV plugs are interconnected by taking a specific attention on the place of junction boxes, located close to the fire ignition location (the worst configuration). Aim of this approach is to expose the largest combustible mass close to the fire ignition or location of burning elements. All connections follow the manufacturer notice and/or standard rules for PV field connection or LVD recommendation.

The electric load used is a PV field GENERATOR (REGATRON PV SERIES) allowing to set the electric conditions according to two operating modes, switching from I and P to U and P mode imposed. The starting mode used is I and P values imposed according to PV datasheets to define the maximum current value to be applied during the fire test.

The I value is equal to the maximum current in short circuit according to the manufacturer prescription. The maximum power value is fixed according to the maximum voltage allowed according to IEC 61730 , 1000 V DC. According to this operating mode, Pmax is fixed by the value of I_{sc} multiplied by the maximum voltage value.

Considering an open circuit due to destruction of bus bars by the fire attack or due to an electric arc, the maximum voltage value remains the same, 1000V.

Afterwards, the DC generator is connected to the PV field plugs in reverse mode (++) and (--) to overdrive the bypass diodes. Before starting the fire test, an initial electric test is performed in order to validate the electric connection and check the perfect operating conditions. The set current value must be displayed on the DC generator, and Power mode have to be switched on. A multimeter is used to check that the current value imposed is correct.

Note: no additional sensors and monitoring system can be installed in the test room due to the increase of temperature during the test phase and extreme operating conditions (smoke, dust, soil and high temperature) a specific cabinet with fire protection and HVAC system will be developed for the next tests allowing more simple setup and installation of sensors as close as possible from the test bench. REGATRON measuring system is used to supervise and store the electric results during the NTP test.

If any issues are found during this first check, an overall electrical check is performed to fix this issue and replace damaged element. Please note that every PV module is checked with a multimeter prior the installation on the bench test.

6.4.4.2 Equipment

As described prior, a DC PV generator is used to generate a I(P) or U(P) power function image of a PV field. The DC PV GENERATOR is an industrial machine used to test inverters, storage and loading solution for PV application, only in DC mode. This element is used to apply an equivalent electrical load as one generated by the PV field under the sun radiation.

In order to impose the requirement as it higher point, the maximum power conditions are fixed according to the STC conditions (IEC 61215 – IEC 61648) and all electrical values are used according to these parameters.

In generator mode we selected to impose the current value (I_{sc}) and depending maximum power to have a more effective representation of operating conditions.

All these parameters are set on the DC PV GENERATOR display board and the embedded storage solution allows to follow the evolution of Current and Voltage throughout the duration of the test.



Figure 25. DC PV GENERATOR (10 kW DC) used in electric load NTP

6.4.4.3 Test execution and main results

The main aim is to detect a possible current failure, that express bus bar destruction through combustion of combustible part, or electrical arc generation in the electrical circuit. In case of appearance of current default, that reach a null value, a nominal voltage value is imposed by the DC PV Generator equivalent to the global Voc values of modules.

The DC PV GENERATOR is preliminary connected to a BIPV module in order to test the connection quality and to validate the setup (during this test session, veture kit cladding system with glass-based and polymeric-based PV module) are tested). We run a first load test to validate the process This first procedure is illustrated on Figure 26, then the load is switch off. After validation of this step, the DC PV Generator is then connected to the BIPV field to be fire tested with the application of the electrical load. Only BIPV elements and cables are located in the room test, only cables pass-through room wall. DC PV GENERATOR is located outside the test room, on a movable bench to be closed as possible of the tested mockup.



Figure 26. DC PV GENERATOR (10 kW DC) – SBI preliminary settings before mockup connection Load device and remote control to test load on CIGS module (left) / User interface with load level (right) – Same procedure is used for crystalline modules

The DC PV generator is preliminary tuned to deliver I_{sc} and the equivalent power to reach $U=1000V$ (the dataset is collected from module manufacturers or from tests characterization).

The corresponding electric load is applied on PV array 1 mn before to start the fire test to stabilize the voltage value according to the room temperature and to check possible current leakages.

Following the validation of this step (no current defaults), the test is carried out over a period defined by the test standard (SBI test = 20 mn)



Figure 27. Before/during/after the fire test with DC PV GENERATOR load applied on veture kit cladding system with a front glass-glass module



Figure 28. Before/during/after the fire test with DC PV GENERATOR load applied on veture kit cladding system with a front CIGS-based flexible module

During the test, current and voltage values are checked to identify possible breaks in the electrical circuit.

- If no electric breaks are observed, the electric part is safe (continuity is preserved) and do not bring additional fire contribution as firebrands and radiant part.
- If electric breaks are observed, the is noted to identify later possible effect

Finally, roof test results are then checked to observe any deviation.

- Without electric breaks appearance, only the fire tests are selected for results and compared with initial results without electric load
- In case of electric break appearance, in depth analysis are conducted specifically at the time noted during the test where breaks are observed. Comparison results are performed to observe specific deviation with electric load contribution

Before to stop the load, another 1 mn stabilization is observed prior to force the switch off.

As a general meaning we observed exactly the same procedure, with an observation session during the test period in order to detect arc generation or rapid breakage, and a switch off after a waiting period of 1 mn.

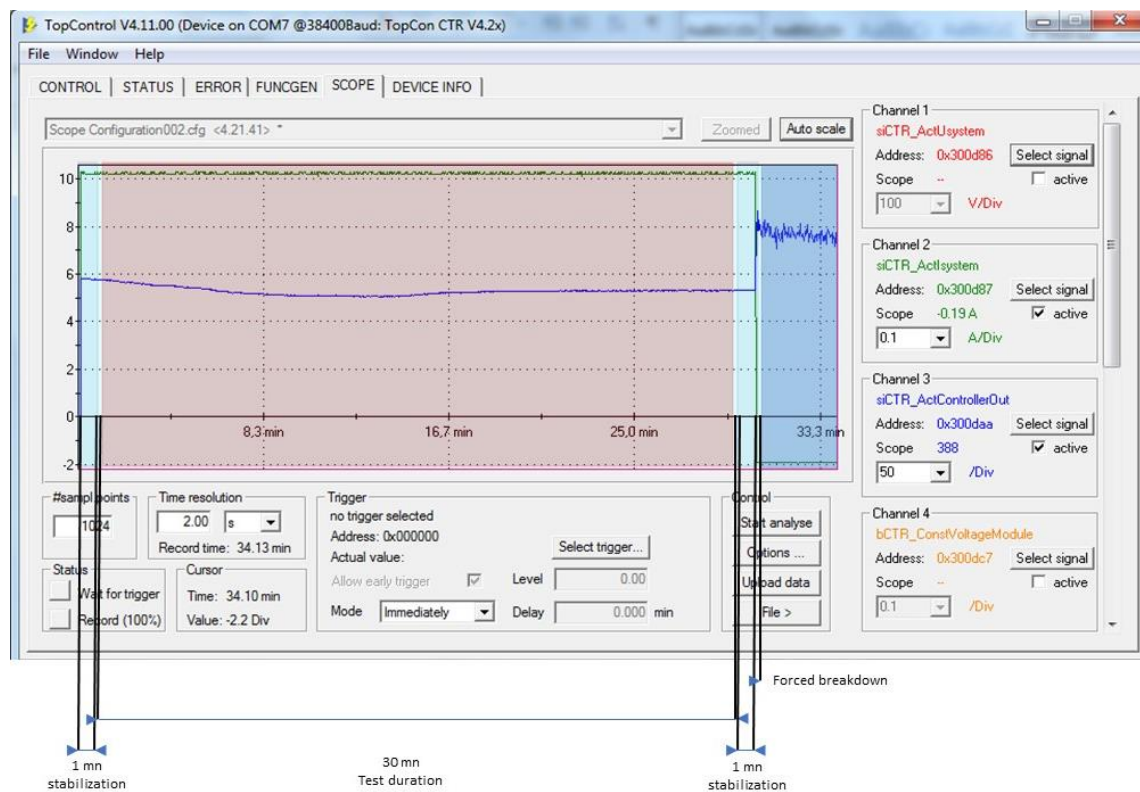


Figure 29. Example of electric load carried out during SBI test (façade product)



Figure 30. No electrical breakage observed – no negative effects due to electric load during all SBI tests. (picture as an example)

All tests performed according the SBI expectation are carried out with appropriate electric load. Results are compared with initial test in normal conditions in order to identify possible deviation due to additional constraints provided by the stress of the electric load. On any tests we haven't observed any current leakages or breakout, which emphasizes the absence of a break in the electrical circuit. The implementation of an electric charge does not degrade the fire properties of the BIPV components.

An active breakdown/breakout is correctly observed on the on the monitoring system, which highlights the absence of an electric defect during the tests.

On the other hand, this equipment is not initially developed to carry out this test in complete safety conditions (not for users but for the equipment as the active or rapid cut off may damage the fuse of the equipment. An intermediate load or an intermediate converter will have to be studied in order to limit the damage to the equipment afterwards. In the same way, arc detection is not implemented in this setup, thus the energy generated, and arc duration are not measured to assess the possible contribution on the fire propagation in case of default.

Specific equipment is under development to take into account of specific values to measure and also specific surrounding conditions tests with a dedicated cabinet installed in the test room. An additional monitoring system with subsection measurement per module to detect the place of default will be also to develop in order to detect the place of default in order to provide specific upgrade in case of failed test. Temperature measurement is still under study to assess the temperature gradient int the BIPV element but also in the entire mockup for possible fire penetration.

Next STEPS are to implement several test combinations to assess under fire test the worst test conditions not at initial time but on a full lifetime to ensure that a BIPV components is fire resistant regardless of its lifetime. Samples are currently under natural exposition for a minimal duration of one year and a half, it is expected to perform again the same tests in order to detect possible deviation due to aging effect.

6.5 NTP FR03: Fire reaction for other BIPV products with electric load in ultimate LS

As demonstrated in previous chapters, the NTP procedure is an application of an electrical load level adapted to BIPV cells technologies and taking into account the maximum power of any BIPV array. The NTP FR 03, is defined as “OTHER” according to EN 50583 E categories. That could be expected as a roof or a façade element with specific integration mode. As it’s a case-by-case approach, a preliminary assessment is necessary to identify which NTP and standard test is the most relevant. A walkable floor can be considered as a roof (according to its tilt angle) but have to fulfill fire regulation as a glass façade element.

NTP FR3 could be a copy of NTP FR 01 or NTP FR02 or a mash-up or combination of both. The most demanding must be retained.

6.6 Conclusions and next steps

To apply an electric load is quite challenging due to demanding test conditions. The technical solution has been defined and applied with the CSTB Fire lab and teams involved in this work. Even if devices used aren’t specifically developed for these investigations, the NTP procedures have been validated and results obtained determine the level of influence of the electrical charge on the results of the fire tests. As a first investigation step procedure of load determination suit the current standards and is relevant of real operating conditions.

For all tests performed, we haven’t observed negative deviation due to applying a load during the fire test, somehow, electricity load is not the main factor of degradation on the integration solutions we tested.

We observed that in the case of a failure or validation of the fire tests (with time limit of maximum energy generation according to standard requirements) we have never observed any destruction of the electrical circuits, even in the case of major failure. Electric connections are still working.



Figure 31. Busbar status after fire test, continuity test are performed, and module are still working / glass-glass module on veture kit cladding (Left) – thin film module polymeric-based on veture kit cladding (Right)

As a first conclusion, we can pretend that the NTP with most demanding electric condition have not a significant effect on tested configurations. For façade systems, glass/glass modules results seem not affected by electric load and BIPV pass the test without and without load. No classification deviation/bias are observed. With CIGS-based polymeric modules the result is a failure due to the generated energy rate during the test. The present combustible mass is too large and does not allow to highlight the impact of the electric charge. the result demonstrates the integrity of the electrical circuit, but if the test had been observed until the end of complete combustion, the possible impact of the electrical charge could have been observed.

For Roof BIPV solution, tests results are quite good even if the final result does not pass the test due to the fall of burning elements on the bottom part of the mockup. Beyond the self-extinguishing of the flames, the tests have been carried out until the end and do not show any electrical problems.

Beyond the first positive conclusions, we draw attention to the fact that these tests are carried out on specific configurations and that it will be necessary to extend the number of investigations in order to have statistically representative results. even if we carried out three tests per configuration, the sensitivity to the components used and their proportions remains to be determined in order to conclude definitively on an effect on the results obtained.

A positive aspect is the integrity of the electrical circuits which demonstrates that the current assembly techniques make it possible to ensure an electrical connection even under strong thermal stresses, which makes it possible to provide a high level of confidence in the use of this type components in the building

On the other hand, further investigations will have to be carried out in order to determine which equipment will be the most relevant in order to detect the slightest electrical problems such as arc detection or increases in resistive effects in operation. Specific equipment will have to be used or even be upgraded in order to be used specifically for these applications. Cooperation with manufacturers specializing in specific measures will be put in place to achieve this goal.

Finally, as part of this work, it will remain to determine the influences of other aging effects that could affect the fire performance of BIPV components. Mechanical stress, outdoor exposition, components aging could have additive effect with electrical stress and lead to poorer results.

These first results demonstrate that the current BIPV products are developed with a high level of performance and are able to meet a large part of the normative requirements of construction even when applying severe evaluation conditions. Conditions much more trying than those used for traditional building components

7 ANNEXES

7.1 Energy Economy

The aim of this work is to clarify whether the specific factors related to BIPV products can impact the current construction energy economy standards and, if required, propose adaptations in the assumptions and boundary conditions to correctly evaluate the thermal performance of the BIPV systems.

The new features and elements associated to the PV technology that may impact on the procedures and methodologies have been presented and assessed, with special attention on glazing thermal transmittance (U value) and glazing solar factor (G value) calculations. The potential impact of these characteristics has been investigated by means of state-of-the-art review, analytical studies, FEM simulation and optical measurements.

7.1.1 Standards review and its conclusions

In order to detect the discrepancies between the BIPV systems and current methodologies described in the energy economy standards, the last have been deeply analysed. The analysed standards are related to three main fields: determination of thermal transmittance (U value), energy performance of buildings, and determination of solar factor (G value or SHGC). The analysed standards and the conclusions are described in the Table 17,

Table 18, Table 19, Table 20, Table 21, Table 22. This work has been published in (56).

Table 17. List of analyzed standards related to glazing thermal transmittance (U value)

ANALYZED STANDARDS – THERMAL TRANSMITTANCE	
EN 673	Glass in building - Determination of thermal transmittance (U value) - Calculation method
EN 674	Glass in building - Determination of thermal transmittance (U value) - Guarded hot plate method
EN 675	Glass in building - Determination of thermal transmittance (U value) - Heat flow meter method
ISO 10292	Glass in building -- Calculation of steady-state U values (thermal transmittance) of multiple glazing
EN 12898	Glass in building - Determination of the emissivity
EN ISO 10077-1	Thermal performance of windows, doors and shutters - Calculation of thermal transmittance
EN ISO 10077-2	Thermal performance of windows, doors and shutters - Calculation of thermal transmittance - Part 2: Numerical method for frames
EN 12412-2	Thermal performance of windows, doors and shutters - Determination of thermal transmittance by hot box method - Part 2: Frames
EN ISO 12567-1	Thermal performance of windows and doors - Determination of thermal transmittance by the hot-box method - Part 1: Complete windows and doors
EN ISO 6946	Building components and building elements - Thermal resistance and thermal transmittance - Calculation method
EN ISO 12631	Thermal performance of curtain walling - Calculation of thermal transmittance
EN 1279-2	Glass in building - Insulating glass units - Part 2: Long term test method and requirements for moisture penetration
EN 1279-3	Glass in building - Insulating glass units - Part 3: Long term test method and requirements for gas leakage rate and for gas concentration tolerances
EN 1279-4	Glass in Building - Insulating Glass Units - Part 4: Methods of test for the physical attributes of edge seal components and inserts

Table 18. List of conclusions from the analysis of the standards related to glazing thermal transmittance (U value)

CONCLUSIONS – THERMAL TRANSMITTANCE	
<p>The operative temperature of the PV glass is usually higher than that of the common glass due to the higher absorption of the radiation, inherent to any PV application. In this sense, the values of some temperature dependent parameters considered for the calculation may be different than the ones proposed in the standard, like the average temperature of cavity gas and the average temperature difference between glass bounding surfaces of the insulation gap. For instance, in EN 673 and ISO 10292, the gas properties for 10°C are proposed to be taken for calculations. Further investigations have been done to clarify the potential temperature behaviour differences between BIPV and common glazing systems.</p>	
<p>The heat transfer coefficients of the internal and external surfaces depend on glazing position, wind velocity, external and internal temperatures, and surface temperatures of outer glass layers. The temperature of BIPV glass outer layers will be higher under radiation conditions.</p>	
<p>The heat flux can change from inner to outer glass even in winter due to radiation heat in the PV layer. Thus, the dynamic U-value might be different for a skylight in these conditions. Calculations with dynamic U-value including the effect of glass layers temperatures has been done.</p>	
<p>The junction boxes may impact on the thermal transmittance of the occupied area. Thus, whether the junction boxes should be included in the experimental measurements should be specified.</p>	
<p>The thermal transmittance of the framing might be affected by the cables within the frame chambers and the holes required for the cables that can communicate different chambers of the frame.</p>	
<p>The maximum temperature for ageing, moisture penetration or gas leakage tests has been studied because BIPV Insulated Glass Unit (IGU) could reach higher temperatures than common IGU.</p>	

Table 19. List of analyzed standards related to glazing solar factor (G value)

ANALYZED STANDARDS – SOLAR FACTOR	
EN 410	Glass in building - Determination of luminous and solar characteristics of glazing
ISO 9050	Glass in building - Determination of light transmittance, solar direct transmittance, total solar energy transmittance, ultraviolet transmittance and related glazing factors
ISO 15099	Thermal performance of windows, doors and shading devices - Detailed calculations
EN ISO 52022-1	Energy performance of buildings - Thermal, solar and daylight properties of building components and elements - Part 1: Simplified calculation method of the solar and daylight characteristics for solar protection devices combined with glazing
EN ISO 52022-3	Energy performance of buildings - Thermal, solar and daylight properties of building components and elements - Part 3: Detailed calculation method of the solar and daylight characteristics for solar protection devices combined with glazing
ISO 19467	Thermal performance of windows and doors - Determination of solar heat gain coefficient using solar simulator

Table 20. List of conclusions from the analysis of the standards related to glazing solar factor (G value)

CONCLUSIONS – SOLAR FACTOR	
<p>Heat reduction due to PV conversion. The efficiency of the PV technology should be removed from the system. If thermal dependence of PV efficiency is considered, the incident radiation and boundary temperatures should be known. Under this work,</p>	

the dynamic g-value is being studied including the effect of PV efficiency considering its temperature dependency. An additional effect not studied here is the PV efficiency dependency with the radiation level.

The **spectral transmittance of the solar cell** is normally considered as zero. However, the optical properties of several solar cell technologies have been measured and show significant transmittance in the NIR region that should be considered for the G-value calculations.

The presence of the **junction box** on the rear side of the BIPV module will **affect the optical properties** in this area. The optical and thermal properties of the junction box should be quantified to assess its impact on the final optical and thermal properties. Its contribution might not be included in the calculation of the center-of-glass properties (EN 410 and EN 673) but its effect can be included in the calculation of the system (window, curtain wall, skylight, etc) properties together with other elements like frames.

The **final G value is a weighted average between opaque (with PV) and transparent (without PV) parts**. This final calculation has been proposed to be proportional to the area and independently of solar cells position/ distribution in the glass. According to Baenas et al. (57) previous experimental works suggest that this approximation can be done (58). Also, ISO 15099 proposes this approximation for the total solar energy transmittance with frame area and glass area. However, this behavior **has not been sufficiently proven** and further investigations has been done.

Table 21. List of analyzed standards related to energy performance of buildings

ANALYZED STANDARDS – ENERGY PERFORMANCE OF BUILDINGS	
EN ISO 52000-1	Energy performance of buildings - Overarching EPB assessment - Part 1: General framework and procedures
EN ISO 52016-1	Energy performance of buildings - Energy needs for heating and cooling, internal temperatures and sensible and latent heat loads - Part 1: Calculation procedures
EN ISO 10456	Building materials and products - Hygrothermal properties -Tabulated design values and procedures for determining declared and design thermal values
EN 15316-4-3	Energy performance of buildings - Method for calculation of system energy requirements and system efficiencies - Part 4-3: Heat generation systems, thermal solar and photovoltaic systems, Module M3-8-3, M8-8-3, M11-8-3
EN ISO 13789	Thermal performance of buildings - Transmission and ventilation heat transfer coefficients - Calculation method

Table 22. List of conclusions from the analysis of the standards related to energy performance of buildings

CONCLUSIONS – ENERGY PERFORMANCE OF BUILDINGS
Some data provided to common windows for the calculation of the overall energy performance could be extended to BIPV systems as well. For instance, the G-value corrections provided for non-perpendicular incidence of light by EN ISO 52016-1 could be extended for BIPV systems. In this sense, the dynamic G-value of BIPV elements has been studied considering angular reflection losses.

7.1.2 New studies performed related to new BIPV effects

After reviewing the standards and comparing them with the characteristics of BIPV modules, a set of actions and studies were proposed to clarify the discrepancy points between the current standards descriptions and the requirements of BIPV.

For this purpose, a PV glazing thermal model (PVGTM) has been developed for the study of the different temperature characteristics under real meteorological conditions. Besides, several simulations based on finite-element-method (FEM) has been performed to validate and complement the PV glazing thermal model and study how the distribution of the opaque areas (areas covered with solar cells) may impact on the

thermal performance. Also, it has been performed an analytical calculation to assess the impact of the junction box (JB) on U and G values. Finally, optical measurements of different solar cell technologies have been performed to clarify when they should be considered in the optical calculations of PV glass, that will affect the G value. These activities are described in Table 23.

Table 23. Technical gaps and how they are studied in this work

Studies	By means of...
Average temperature of cavity IGU	Glass thermal model + FEM
Average temperature difference between glass surfaces of cavity in IGU	Glass thermal model + FEM
Dynamic U-value	Glass thermal model
Dynamic G value	Glass thermal model
Junction box effect on U-value and G-value	Analytical calculations
Thermal dependence of efficiency	Implemented in the glass thermal model
Same PV occupancy but different distribution of the solar cells, is the same?	FEM
Light transmittance of different solar cells technologies	Optical transmittance measurements of solar cells

7.1.3 Operating temperatures, dynamic U value and dynamic G value of double IGU PV glass

The operating temperature of the PV glazing can impact on different properties, so that to different energy economy and general glazing standards. In this sense, the steady-state U and G values of IGU glazing depends on the gas temperature in the cavity and on the temperature difference between the cavity surfaces. However, the operating temperature also impacts the mechanical performance, the materials ageing or the cavity pressure variations that must be considered in mechanical calculations (EN 16612). This has been mainly studied by means of a developed PV glazing thermal model, but also supported by the FEM simulations. For reference, it has been calculated the U value as function of gas temperature and temperature differences between the cavity surfaces (ΔT). The results for air, argon, and argon with LowE coating (low-emissivity) are shown in Table 24, Table 25 and

Table 26 respectively. The U value with EN 673 conditions is highlighted.

Table 24. U value as function of IGU gas temperature and ΔT . Air case. [4mm + 4mm / 16 mm Air / 4mm]

Air IGU		ΔT [°C]						
		3	6	9	12	15	18	21
Gas Temp [°C]	1	2,56	2,56	2,56	2,56	2,60	2,63	2,66
	4	2,60	2,60	2,60	2,60	2,63	2,66	2,69
	7	2,63	2,63	2,63	2,63	2,65	2,68	2,71
	10	2,67	2,67	2,67	2,67	2,68	2,71	2,73
	13	2,70	2,70	2,70	2,70	2,71	2,73	2,76
	16	2,73	2,73	2,73	2,73	2,73	2,76	2,78
	19	2,77	2,77	2,77	2,77	2,77	2,78	2,81
	22	2,80	2,80	2,80	2,80	2,80	2,81	2,83
	25	2,83	2,83	2,83	2,83	2,83	2,84	2,86
	28	2,87	2,87	2,87	2,87	2,87	2,87	2,88
	31	2,90	2,90	2,90	2,90	2,90	2,90	2,91

Table 25. U value as function of IGU gas temperature and ΔT . Argon case. [4mm + 4mm / 16 mm Argon / 4mm]

U value [W/m ² K] Argon IGU		ΔT [°C]						
		3	6	9	12	15	18	21
Gas Temp [°C]	1	2,42	2,42	2,42	2,44	2,47	2,50	2,52
	4	2,46	2,46	2,46	2,47	2,50	2,52	2,55
	7	2,49	2,49	2,49	2,50	2,53	2,55	2,57
	10	2,53	2,53	2,53	2,53	2,56	2,58	2,60
	13	2,56	2,56	2,56	2,56	2,59	2,61	2,63
	16	2,60	2,60	2,60	2,60	2,62	2,64	2,66
	19	2,64	2,64	2,64	2,64	2,65	2,67	2,69
	22	2,67	2,67	2,67	2,67	2,68	2,70	2,72
	25	2,71	2,71	2,71	2,71	2,71	2,73	2,74
	28	2,74	2,74	2,74	2,74	2,74	2,76	2,77
	31	2,77	2,77	2,77	2,77	2,77	2,78	2,80

Table 26. U value as function of IGU gas temperature and ΔT . Argon with LowE glass case. [4mm + 4mm / 16 mm Argon / LowE - 4mm]

Argon LowE IGU		Delta_T [°C]						
		3	6	9	12	15	18	21
Gas Temp [°C]	1	0,98	0,98	0,98	1,03	1,09	1,14	1,19
	4	0,99	0,99	0,99	1,02	1,09	1,14	1,19
	7	1,00	1,00	1,00	1,02	1,08	1,14	1,18
	10	1,01	1,01	1,01	1,02	1,08	1,13	1,18
	13	1,02	1,02	1,02	1,02	1,08	1,13	1,17
	16	1,03	1,03	1,03	1,03	1,07	1,12	1,17
	19	1,04	1,04	1,04	1,04	1,07	1,12	1,17
	22	1,05	1,05	1,05	1,05	1,07	1,12	1,16
	25	1,06	1,06	1,06	1,06	1,06	1,11	1,16
	28	1,07	1,07	1,07	1,07	1,07	1,11	1,15
	31	1,08	1,08	1,08	1,08	1,08	1,11	1,15

7.1.3.1 PV glazing thermal model - description

The purpose is to calculate the temperature of the different parts of a PV-IGU under real meteorological conditions for different locations and orientations. As the development is focused on a European context, the European standards EN 410, EN 673 and EN ISO 6946 has been used as reference for the calculations and initial boundary conditions assumptions.

The PV glazing system considered for the study is depicted in Figure 32. The system is an IGU (Insulated Glass Unit) whose first layer is a laminated glass containing the PV cells (referred as PV glass or PV laminated glass). The first glass layer before the PV cells is a low iron high transmittance glass, while the others are common glass layers. The thermal properties of the 16 mm thick cavity are calculated for Argon, as it widely used nowadays. Both normal emissivity and low emissivity (LowE) systems have been studied, with the low-emissivity coating in the outer surface of the inner glass (surface #5). Inner temperature of 22 °C has been assumed as an intermediate temperature for winter and summer conditions, while the external temperature is hourly determined by the meteorological conditions.

The surface external resistance (R_{se}) is 0,04 m²K/W while the internal (R_{si}) is 0,13 m²K/W, which are the standardized values of EN 673. When the glazing is not vertical, the R_{si} varies according to the indications of EN ISO 6946 for horizontal, upwards, and downwards heat fluxes. The calculation of R_{si} for intermediate angles is done by using equations showed in Figure 33, based on vectorial decomposition, using either upwards or downwards R_{si} depending on the temperatures of outer and inner glass layers. If the PV-IGU glazing inclination is lower than 45° (more horizontal than vertical) and the outer glass temperature is higher

than the temperature of the inner glass, the heat transfer due to convection is negligible, so the Nusselt number is fixed to 1.

Based on current PV efficiencies, a PV cell efficiency of 20% is assumed. It should be noted that this efficiency is for the PV cell but not for the module. This means that the efficiency is applied to the radiation absorbed by the solar cell, already considering the reflectance losses. The reduction of the PV efficiency due to temperature is also considered with $-0,4\%/^{\circ}\text{C}$. The PV occupancy or PV ratio is a variable of the model where the values of 0% (without PV cells), 50%, 80% and 100% (fully covered with PV cells) have been analyzed.

A sketch of the thermal circuit is depicted at the top of Figure 32. There are 4 temperatures: outdoor temperature; temperature at the middle point of PV laminated glass; temperature at the middle point of inner glass layer; and indoor temperature. Between these points, there are thermal resistances that are composed by the different thermal resistances of the different elements. In addition, there are two heat fluxes corresponding to the radiation absorbed by the two glass layers. According to this model, the temperatures T_1 and T_2 indicates the temperature at the middle point of the glass layers and can be calculated with the following equations. The temperatures of the glass surfaces, when needed, are not assumed to be T_1 and T_2 but they are calculated according to the intermediate heat fluxes and thermal resistances.

$$T_1 = \frac{T_{ext}(R_g + R_i) + T_{int}R_e + Q_1R_e(R_g + R_i) + Q_2R_iR_e}{R_e + R_g + R_i}$$

$$T_2 = \frac{T_{int}R_g + Q_2R_iR_g + T_1R_i}{R_g + R_i}$$

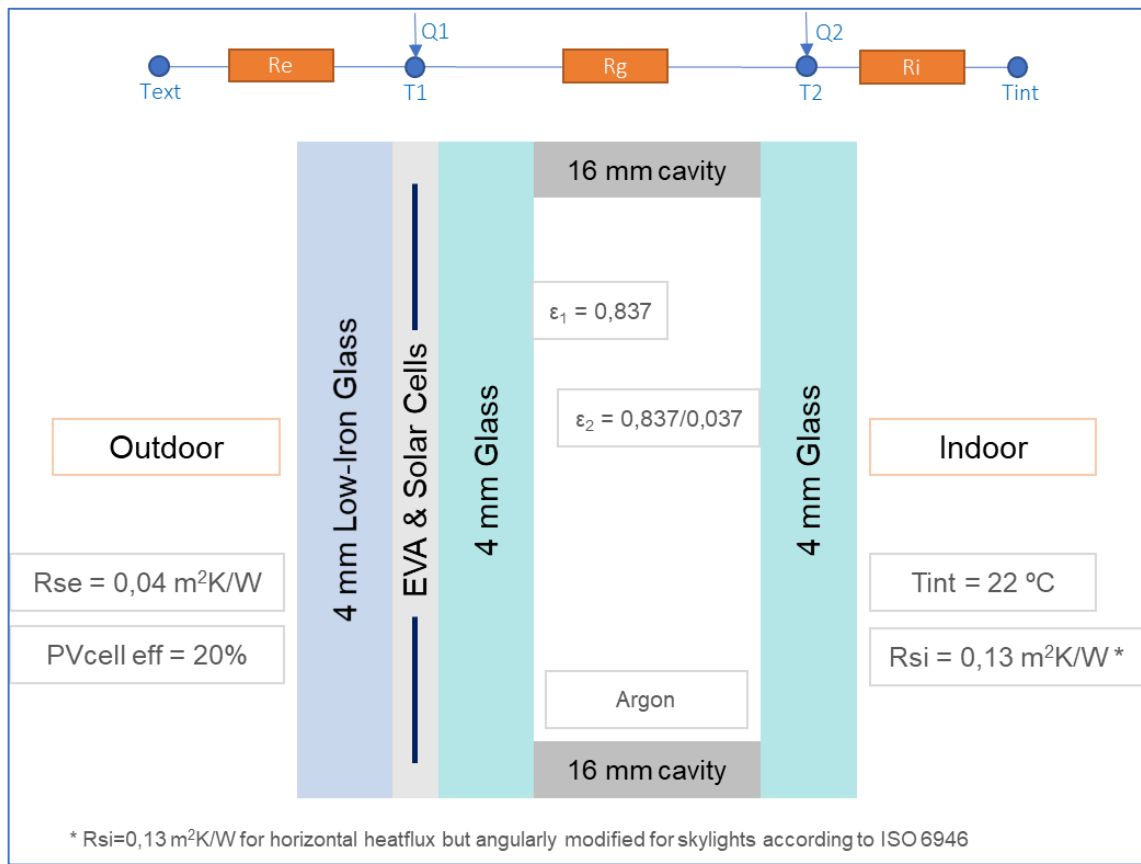


Figure 32. Sketch of PV-IGU system and the thermal circuit defined for the model.

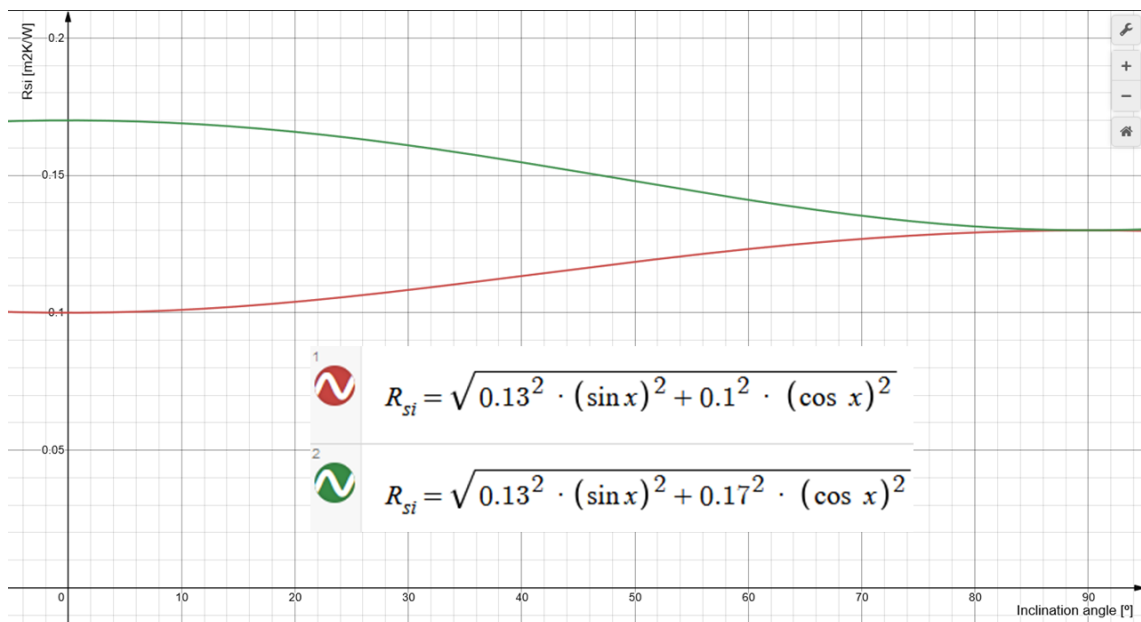


Figure 33. Model of internal surface resistance (R_{si}) as function of glass inclination (90° is vertical). Red: Outer glass is colder than inner glass. Green: Outer glass is hotter than inner glass.

Figure 34 shows the model information flux diagram. The first inputs are the hourly meteorological conditions including the different components of the radiation, the optical data of the independent glass layers and the other system parameters. Hourly meteorological data from 4 years (2013-2016) has been taken from PVGIS-

SARAH. Then, intermediate optical calculations are performed to get the angular optical properties of the glazing system. Also, the Sun position is calculated hourly to get the angle of incidence of the light on the PV-IGU and apply the angular optical properties accordingly.

Once the intermediate calculations are done, the temperature of the PV-IGU is hourly calculated at different points. This process is iterated three times to adjust the thermal equilibrium of the system. Note that, for instance, the PV efficiency depends on the temperature and vice versa. Also, the thermal resistance of the cavity depends on the gas temperature, but the gas temperature depends on this resistance. So that, starting with the EN 673 conditions and after three iterations, it has been found the differences in system temperatures are negligible.

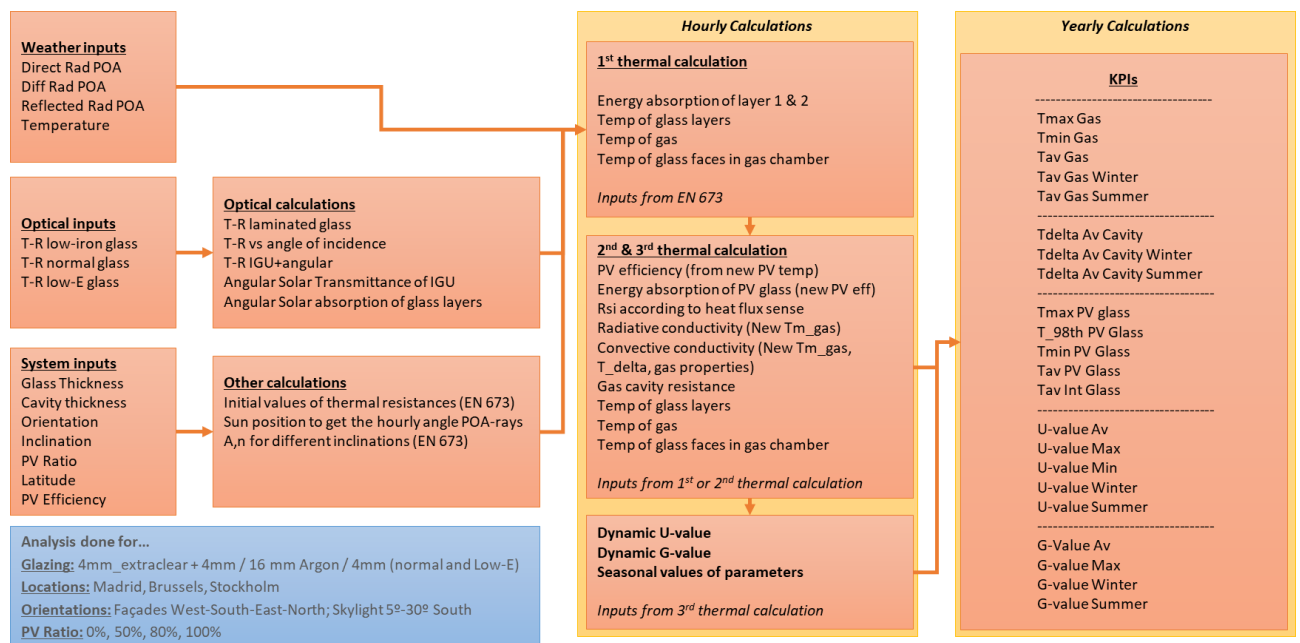


Figure 34. Information flux of PV glazing thermal model

Finally, the hourly U and G values are obtained according to the meteorological conditions. From this hourly data of 4 years, different KPIs are obtained that are directly related with the technological gaps described in section 7.1.1.

7.1.3.2 PV glazing thermal model - results

The temperature results and the yearly average dynamic U and G values are depicted in Table 32 for the PV-IGU without LowE, and in Table 33 for the PV-IGU with LowE.

PV-IGU temperature - Argon without LowE (Table 32)

The temperature results and the yearly average dynamic U and G values of individual cases can be seen in Table 32. The following comments are focused on analysing the maximum and average values among the different set of cases. The aim is to provide general values for the PV-IGU glazing when the final location and orientation is still unknown.

The temperature of the gas in the IGU cavity

Regarding the system without Low-E, the **maximum observed gas temperature is 56,1 °C**, corresponding to a PV skylight in Madrid with 100% PV occupancy (or PV Ratio), tilted 30° and oriented to South. Without considering the PV conversion (open-circuit state), the gas would reach 60,9 °C. The maximum gas

temperature of no-PV glazing would be 39,3 °C, for the same skylight system, which means that **the Argon in a PV-IGU could be about 21 °C higher than equivalent NO-PV-IGU**. The maximum temperatures are further analyzed in the next section because they could be even higher for higher values of R_{se} , that strongly depends on wind conditions (see Table 36). The minimum temperature of the gas is for Stockholm case with -2,7 °C. This temperature could be slightly lower if the indoor temperature is lower than 22 °C.

The yearly average temperature of the gas in the cavity among all PV glazing cases is 17,2 °C, and they are between 13,5 °C and 22,8 °C depending on the case. The same average gas temperature for a NO-PV glass is 16,0 °C. This means that, **in average, the PV-IGU cavity gas temperature is 1,2 °C higher than NO-PV-IGU**. The average temperature in winter is 13,1 °C for PV-IGU and 12,5 °C for NO-PV-IGU. This means that **the PV-IGU cavity gas temperature in winter is, in average, 0,6 °C higher than NO-PV-IGU**. The average temperature in summer is 21,3 °C for PV-IGU and 19,5 °C for NO-PV-IGU, which means that **the PV-IGU cavity gas temperature in the summer is, in average, 0,8 °C higher than NO-PV-IGU**. As a reference, the gas temperature proposed by EN 673 for U calculation is 10 °C, which is quite low, as it would correspond to average gas temperature in winter in Stockholm.

The temperature difference between cavity surfaces

Besides, the temperature difference between cavity surfaces (ΔT) is another parameter used for steady-state U calculation. In this case, the average ΔT among all PV-IGU cases is **6,3 °C, which is the same than for NO-PV-IGU**. The average ΔT for PV-IGU in winter is **8,2 °C, while for NO-PV-IGU is 8,7 °C**, this is 0,5 °C lower. The average ΔT for PV-IGU in summer is **4,4 °C, while for NO-PV-IGU is 4,0 °C**, this is 0,4 °C higher. As reference, the ΔT defined by EN 673 is 15°C, which is quite high as it is not reached by any yearly average in any of the simulated cases.

The temperature of the PV laminated glass

The maximum temperature of the PV laminated glass i.e. the first glass layer of the PV-IGU has been analysed. Among the simulated cases, the maximum temperature corresponds to a skylight in Madrid, tilted 30°, South oriented and covered 100% with PV. In this case, the **maximum temperature that the PV glass can reach according to the model conditions is 66,9 °C and could reach 72,9 °C in open-circuit conditions**. However, these temperatures could be significantly higher as they strongly depend on wind velocity (see Table 36). The **minimum temperature of the PV laminated glass is -14,1 °C**, reached for a façade in Stockholm. This could be slightly lower if indoor temperature is lower than 22°C. The yearly average temperatures of the PV glass are between 9,2 °C and 22,5 °C depending on the cases, with an average value of 14,4 °C. It should be considered that, despite the irradiation in maximum temperature conditions is between 1000-1100 W/m², only about 700 W/m² are absorbed by the glass+solar_cell area, because it absorbs 86% of direct and 82% of diffuse, and about 16-20% is PV converted.

Dynamic U value

Regarding the yearly average U values of the façades, it is observed that the differences among the different locations and orientations are relatively small (<0,08 W/m²K), and the average value is 2,61 W/m²K, with slightly higher values in Madrid and slightly lower values in Stockholm. It is also observed that **the differences of the dynamic U value of PV-IGU and NO-PV-IGU are very small in this glazing system**, which is reasonable considering the small differences in T_{gas} and ΔT . This average in winter is 2,56 W/m²K while in summer is 2,65 W/m²K. As reference, the steady-state U value according to EN 673 for a vertical façade is 2,56 W/m²K. This means that **the yearly average dynamic U value of a vertical PV-IGU is 0,05 W/m²K higher than the steady-state calculated with the EN 673 code**. The steady-state U value calculated with the EN 673 for this glazing system is the same as for the average dynamic U value in winter, but this is probably a coincidence as the assumptions of gas temperature and ΔT are not the appropriate.

Regarding the yearly average U values of the skylights, it is observed that the differences among the cases with PV are higher than for façades ($<0,2 \text{ W/m}^2\text{K}$), and the average value is $2,83 \text{ W/m}^2\text{K}$. The U value for skylights is higher than for façades because of the higher convection effects within the cavity and the lower internal surface thermal resistance (Rsi). In this case, there is a clear **reduction of the U value when including the PV in the glazing system compared to NO-PV-IGU**, probably because the outer glass is heated by the higher absorption received, and the heat flux changes from upwards to downwards, thus reducing the convection effects. This average in winter is $2,90 \text{ W/m}^2\text{K}$ while in summer is $2,76 \text{ W/m}^2\text{K}$. As reference, the steady-state U value according to EN 673 for a 5° tilted skylight is $2,80 \text{ W/m}^2\text{K}$. This means that **the yearly average dynamic U value of a PV-skylight is $0,03 \text{ W/m}^2\text{K}$ higher than the steady-state calculated with the EN 673 standard.**

Dynamic solar factor

Finally, the Table 27 shows the average dynamic solar factors as function of PV occupancy (PV ratio) together with steady-state solar factor calculated according to EN 410. The **steady-state solar factor is calculated with normal incidence of light while the dynamic considers the angle of incidence with higher reflection**. Thus, the average dynamic G is lower than the steady-state G, being the steady-state quite similar to the maximum dynamic G observed in every case except North orientations. Therefore, reduction coefficients of the steady-state G have been defined. These coefficients are also proposed for normal glass (no-PV) in EN ISO 52016-1 Table B.22, in order to use more realistic G value in combination with incident irradiation when calculating the heat fluxes in a building. It is observed that **the reduction coefficients from the steady-state to dynamic G of a façade with PV-IGU are between 0,81-0,86, while for an equivalent skylight are between 0,75-0,81.**

Table 27. Average dynamic solar factor compared to normal incidence steady-state solar factor of PV-IGU WITHOUT LowE

	Average Dynamic G	Steady-state G (EN 410)	Reduction coefficient
Façade - 100% PV	8%	10%	0,86
Façade - 80% PV	19%	23%	0,83
Façade - 50% PV	35%	42%	0,82
Façade - 0% PV	61%	75%	0,81
Skylight - 100% PV	8%	11%	0,75
Skylight - 80% PV	19%	24%	0,79
Skylight - 50% PV	35%	43%	0,80
Skylight - 0% PV	61%	75%	0,81

Finally, the G-value has been studied as function of the PV occupancy ratio and the PV efficiency, taking the example of a façade facing south and located in Madrid (Table 28). The PV effect remove a part of the energy from the system, reducing the heat generation in the PV glass, and thus the heat into the building. It should be noted that 0% efficiency correspond to the open-circuit state of the PV circuit. The results show that **the average dynamic solar factor can decrease up to 1,7 percentage points between open-circuit and MPP state**, being the PV effect impact higher as higher is the PV ratio. Similar reduction values were obtained by H. Ishii (33) even though his analysis were not based on meteorological real conditions but on the standardized radiation and temperature conditions described in JSTM K 6101.

Table 28. Solar factor as function of PV ratio and PV efficiency. PV-IGU WITHOUT LowE.

		G-value Rad Weighted (PV-IGU)				
		PV Ratio				
		0%	25%	50%	75%	100%
PV efficiency	0%	61,8%	48,6%	35,5%	22,3%	9,3%
	5%	61,8%	48,5%	35,3%	22,1%	8,9%
	10%	61,8%	48,5%	35,1%	21,8%	8,6%
	15%	61,8%	48,4%	35,0%	21,6%	8,3%
	20%	61,8%	48,3%	34,8%	21,3%	7,9%
	25%	61,8%	48,2%	34,6%	21,1%	7,6%
South Façade, Madrid						

PV-IGU temperatures – Argon with LowE (Table 33)

As the **temperature results and the yearly average dynamic U and G values of individual cases can be seen in Table 33**, the following comments are focused on analysing the maximum and average values among the different set of cases. The aim is to provide general values for the PV-IGU glazing when the final location and orientation is still unknown.

The temperature of the gas in the IGU cavity

Regarding the system **with Low-E, the maximum observed gas temperature is 51,2 °C**, corresponding to a PV skylight in Madrid with 100% PV occupancy (or PV Ratio), tilted 30° and oriented towards South. Without considering the PV conversion (open-circuit state), the gas would reach 55,2 °C. The maximum gas temperature of no-PV glazing would be 39,1 °C, for the same skylight system, which means that **the Argon in a PV-IGU-LowE could be about 16 °C higher than equivalent NO-PV-IGU-LowE**. These temperatures could be higher for higher values of Rse that depends on wind conditions (see Table 37). The minimum temperature of the gas is for Stockholm case with -0,7 °C. This temperature could be slightly lower if the indoor temperature is lower than 22 °C.

The yearly average temperature of the gas in the cavity among all PV glazing configurations is 17,7 °C, and they are between 14,3 °C and 22,4 °C. The same average gas temperature for a no-PV glass is 16,7 °C. This means that, **in average, the PV-IGU-LowE gas temperature is 1,0 °C higher than NO-PV-IGU-LowE**. The average gas temperature in winter is 13,9 °C for PV-IGU-LowE and 13,4 °C for NO-PV-IGU-LowE. This means that **the PV-IGU-LowE gas temperature in the winter is, in average, 0,5 °C higher than NO-PV-IGU-LowE**. The average temperature in summer is 21,4 °C for PV-IGU-LowE and 19,9 °C for NO-PV-IGU-LowE. This means that **the PV-IGU-LowE gas temperature in the summer is, in average, 0,5 °C higher than NO-PV-IGU-LowE**. As a reference, the gas temperature proposed by EN 673 for U calculation is 10 °C, which is even lower than the average gas temperature in winter in Stockholm.

The temperature difference between cavity surfaces

Besides, the temperature difference between cavity surfaces (ΔT) is another parameter used for steady-state U calculation. In this case, the average ΔT among all PV-IGU-LowE cases is **9,5 °C, which is the same than for NO-PV-IGU-LowE**. The average ΔT for PV-IGU-LowE in winter is **12,2 °C, while for NO-PV-IGU-LowE is 12,9 °C**, this is 0,7 °C lower. The average ΔT for PV-IGU-LowE in summer is **7,0 °C, while for NO-PV-IGU-LowE is 6,1 °C**, this is 0,9 °C higher. As reference, the ΔT defined by EN 673 is 15°C, which is only reached by winter averages in Stockholm.

The temperature of the PV laminated glass

The maximum temperature of the PV laminated glass i.e. the first glass layer of the PV-IGU has been analysed. Among the simulated cases, the maximum temperature corresponds to a skylight in Madrid, tilted 30°, South oriented and covered 100% with PV. In this case, **the maximum temperature that the PV glass can reach according to the model conditions is 71,1°C**, but could be 77,6 °C in open-circuit conditions. However, this temperature could be significantly higher as it strongly depends on wind velocity (see Table 37). The minimum temperature of the PV laminated glass is -16,3 °C, reached for a façade in Stockholm. This could be slightly lower if the indoor temperature is lower than 22°C. The yearly average temperatures of the PV glass are between 8,2 °C and 23,6 °C depending on the cases, with an average value of 13,8 °C. It should be considered that, despite the irradiation in maximum temperature conditions is between 1000-1100 W/m², only about 700 W/m² is absorbed by the glass+solar_cell area, because it absorbs 86% of direct and 82% of diffuse and about 15-20% is PV converted.

Dynamic U value

Regarding the yearly average U values of the façades, it is observed that the differences among the cases are relatively small (<0,02 W/m²K), and the average value is 1,06 W/m²K. It is also observed that **the differences of the dynamic U value of PV-IGU-LowE and NO-PV-IGU-LowE are negligible in this glazing system**. In Winter, this average is 1,07 W/m²K, while in summer is 1,05 W/m²K. As reference, the steady-state U value according to EN 673 for a vertical façade is 1,08 W/m²K. This means that **the yearly average dynamic U value of a vertical PV-IGU is 0,02 W/m²K lower than the steady-state calculated with the EN 673 standard**.

Regarding the yearly average U values of the skylights, it is observed that the differences among the cases are higher than for façades (<0,3 W/m²K), and the average value is 1,36 W/m²K. This is because of the higher convection effects within the cavity and the lower surface thermal resistances. In this case, there is a clear **reduction of the U value when including the PV in the glazing system compared to NO-PV-IGU-LowE**, probably because the outer glass is heated due to high radiation received, and the heat flux changes from upwards to downwards. This average in winter is 1,50 W/m²K while in summer is 1,23 W/m²K. As reference, the steady-state U value according to EN 673 for a 5° tilted skylight is 1,60 W/m²K. This means that **the yearly average dynamic U value of a PV-skylight is 0,24 W/m²K lower than the steady-state calculated with the EN 673 standard**.

Dynamic solar factor

Finally, the Table 27 shows the average dynamic solar factors as function of PV occupancy (PV ratio) together with steady-state solar factor calculated according to EN 410. The **steady-state solar factor is calculated with normal incidence of light while the dynamic considers the real incidence angle with higher reflection**. Thus, the average dynamic G is lower than the steady-state G, being the steady-state quite similar to the maximum dynamic G observed in every case except North orientations. Therefore, reduction coefficients of the steady-state G are defined. These coefficients are also proposed for normal glass (no-PV) in EN ISO 52016-1 Table B.22, in order to use more realistic G value in combination with incident irradiation when calculating the heat fluxes in a building. It is observed that **the reduction coefficients from the steady-state to dynamic G of a façade with PV-IGU-LowE are between 0,84-0,86, while for an equivalent skylight are between 0,59-0,84**.

Table 29. Average dynamic solar factor compared to normal incidence steady-state solar factor of PV-IGU WITH LowE

	Average Dynamic G	Steady-state G (EN 410)	Reduction coefficient
Façade - 100% PV	3%	4%	0,86
Façade - 80% PV	13%	16%	0,84
Façade - 50% PV	28%	33%	0,84
Façade - 0% PV	52%	62%	0,84

Skylight - 100% PV	4%	6%	0,59
Skylight - 80% PV	13%	17%	0,77
Skylight - 50% PV	28%	34%	0,82
Skylight - 0% PV	52%	62%	0,84

The G-value has been studied as function of the PV occupancy ratio and the PV efficiency, taking the example of a façade facing south and located in Madrid (Table 30). The PV effect remove a part of the energy from the system, reducing the heat generation in the PV glass, and thus the heat into the building. It should be noted that 0% efficiency correspond to the open-circuit state of the PV circuit. The results show that **the solar factor can decrease up to 0,7 percentage points between open-circuit and MPP state**, being the PV effect impact higher as higher is the PV ratio. Moreover, the Table 31 analyses the impact of the PV efficiency dependency with the temperature, which is define with the Pmpp temperature coefficient. The common value of this coefficient for c-Si is about -0,4 %/°C, and a value of 0 means that the PV efficiency is not reduced when the temperature is increased (or vice versa). **The results show that the impact of the PV efficiency variation with temperature on the solar factor is negligible.** Note that the results are based on the analysis of the average dynamic (or operational) G value. Equivalent analysis using the steady-state calculations of the EN 410 have not been made in this study, but they might be slightly different.

Table 30. Solar factor as function of PV ratio and PV efficiency. PV-IGU WITH LowE.

		G-value Rad Weighted (PV-IGU-LowE)				
		PV Ratio				
		0%	25%	50%	75%	100%
PV efficiency	0%	52,7%	40,4%	28,1%	15,9%	3,7%
	5%	52,7%	40,4%	28,1%	15,8%	3,5%
	10%	52,7%	40,4%	28,0%	15,7%	3,4%
	15%	52,7%	40,3%	28,0%	15,6%	3,2%
	20%	52,7%	40,3%	27,9%	15,5%	3,1%
	25%	52,7%	40,3%	27,8%	15,4%	3,0%
South Façade, Madrid						

Table 31. Solar factor as function of PV ratio and temperature coefficient of PV efficiency. PV-IGU WITH LowE.

		PV Ratio				
		0%	25%	50%	75%	100%
Temp Coef Pmpp	0,0 %/°C	52,74%	40,31%	27,89%	15,47%	3,08%
	-0,2 %/°C	52,74%	40,31%	27,89%	15,48%	3,09%
	-0,4 %/°C	52,74%	40,31%	27,89%	15,48%	3,11%
	-0,6 %/°C	52,74%	40,31%	27,89%	15,49%	3,12%
Radiation Weighted dynamic G. South façade in Madrid, 20% PV efficiency						

The impact of the PV efficiency on the operating temperature parameters and U has been also studied and the results are shown in Table 34 and Table 35. The results show that the PV conversion, so that the **PV-IGU-LowE in MPP state, can significantly reduce the maximum temperatures of the PV glass and the gas cavity**

(about 3-6 °C in the analyzed example). However, its impact on long period averages is very low. In the analyzed example, the reduction of PV glass average temperature is less than 1 °C, the reduction of solar factor is less than 1 percentage point and the U value is not significantly affected.

7.1.3.3 PV glazing thermal model – maximum temperatures with worse boundary conditions

The previous results are based on the standard external surface resistance (Rse) value of 0,04 m²K/W and assuming indoor temperature of 22 °C. However, these conditions could be different, so that the maximum temperatures could be higher.

The Rse depends strongly on the wind velocity near the glass surface. According to EN ISO 6946, the external convective coefficient can be calculated as

$$h_{ce} = 4 + 4v$$

Where v is the wind velocity near the external surface of the glazing.

Following this criterion, the Rse has been recalculated for lower wind velocity conditions, and the maximum temperatures have been recalculated for the new Rse values, including higher indoor temperatures as a second variable.

The results for the system without LowE and with LowE are shown in Table 36 and Table 37 respectively. They show that **the increase of Rse (lower wind speed and lower heat evacuation) significantly increase the temperature of PV-IGU especially with high PV occupancy ratio, while the temperature increase of NO-PV-IGU is significantly lower**. An analysis of the real value of Rse based on meteorological conditions was done following the procedure of ISO 15099 - 8.3.3.4. For a South oriented glazing in Madrid, using four years of hourly wind data (2013-2016), the **calculated minimum and maximum Rse are 0,039 and 0,091 m²K/W, with an average value of 0,077 m²K/W and 98th-percentil of 0,087 m²K/W**. Therefore, **Rse values above 0,09 m²K/W are extremely rare** and that is why the corresponding lines in Table 36 and Table 37 are in grey. However, they are shown up to 0,13 m²K/W because is the limit value used for indoor conditions (standard Rsi).

The maximum temperatures of the PV glass have been observed for the PV-IGU-LowE system; thus, it has been deeply analysed. The Table 38 shows the maximum temperatures of the system with Low-E with even worse conditions i.e. assuming 29 °C as indoor temperature and open-circuit conditions. The open-circuit state means that there is not PV conversion, so there is no energy transformed into electricity and the whole absorbed radiation in the solar cell is transformed into heat. The results show that, **in these particular conditions, the gas in the cavity could reach up to 83 °C, while the PV glass could reach up to 118 °C**, both under very low wind speed conditions and a glass fully covered with PV. It should be noted that the impact of external convection (so that Rse) is higher as higher is the PV occupancy ratio.

Table 32. Operating temperature, dynamic U and dynamic G of PV-IGU WITHOUT LowE [4mm_lowIron + 4mm / 16 mm Argon / 4mm]

Location	Integration	PV Ratio	Tmax	Tmin	Tav	Tav Gas	Tav Gas	ΔT Av	ΔT Av	ΔT Av	Tmax	T_98th	Tmin	Tav	Tav	U-	U-	U-	U-value	U-value	G-	G-	G-value	G-value
			Gas	Gas	Gas	Winter	Summer		Cavity	Cavity	Cavity	PV	98th	PV	PV									
Madrid	East Façade	100%	44,9	5,9	19,9	15,1	24,6	5,5	6,5	4,8	53,7	45,4	-1,5	18,9	20,9	2,64	2,93	2,51	2,59	2,70	8%	10%	8%	9%
Madrid	East Façade	80%	42,6	5,9	19,5	14,9	24,1	5,3	6,5	4,4	50,2	42,2	-1,5	18,3	20,8	2,64	2,90	2,51	2,59	2,69	19%	21%	19%	19%
Madrid	East Façade	50%	39,2	5,9	19,0	14,6	23,4	5,1	6,7	3,7	44,9	37,4	-1,5	17,5	20,6	2,63	2,87	2,51	2,58	2,69	35%	40%	35%	36%
Madrid	East Façade	0%	33,8	5,9	18,2	14,1	22,2	5,2	7,2	3,3	37,3	32,7	-1,5	16,1	20,3	2,62	2,81	2,51	2,58	2,67	62%	73%	61%	62%
Madrid	South Façade	100%	50,8	5,9	20,7	17,3	23,8	5,7	7,0	4,5	61,5	44,9	-1,5	19,9	21,4	2,65	2,99	2,51	2,61	2,69	8%	9%	8%	8%
Madrid	South Façade	80%	45,5	5,9	20,2	16,8	23,5	5,4	6,6	4,2	53,6	42,2	-1,5	19,2	21,2	2,65	2,94	2,51	2,61	2,69	18%	21%	19%	18%
Madrid	South Façade	50%	41,2	5,9	19,5	16,0	22,9	5,0	6,3	3,7	47,6	38,6	-1,5	18,1	20,9	2,64	2,89	2,51	2,60	2,68	34%	40%	37%	32%
Madrid	South Façade	0%	36,2	5,9	18,4	14,8	22,0	5,2	7,3	3,3	39,9	33,9	-1,5	16,3	20,5	2,63	2,83	2,51	2,58	2,67	60%	73%	66%	56%
Madrid	West Façade	100%	49,7	5,9	19,9	15,2	24,4	5,8	6,8	5,1	60,1	51,4	-1,5	18,8	20,9	2,64	2,98	2,51	2,59	2,70	9%	9%	8%	9%
Madrid	West Façade	80%	46,9	5,9	19,5	15,0	24,0	5,6	6,8	4,6	55,9	48,0	-1,5	18,2	20,8	2,64	2,95	2,51	2,59	2,69	19%	21%	19%	20%
Madrid	West Façade	50%	43,1	5,9	19,0	14,7	23,2	5,3	6,8	4,0	50,1	43,0	-1,5	17,4	20,6	2,63	2,91	2,51	2,58	2,68	35%	41%	35%	36%
Madrid	West Façade	0%	37,1	5,9	18,2	14,1	22,1	5,1	7,2	3,2	41,1	35,1	-1,5	16,1	20,3	2,62	2,84	2,51	2,58	2,67	62%	75%	61%	63%
Madrid	North Façade	100%	35,8	5,9	18,3	14,1	22,3	5,1	6,9	3,5	41,4	34,7	-1,5	16,5	20,0	2,63	2,83	2,51	2,58	2,67	9%	10%	9%	9%
Madrid	North Façade	80%	35,2	5,9	18,1	14,1	22,1	5,1	6,9	3,4	40,4	34,2	-1,5	16,4	19,9	2,62	2,82	2,51	2,58	2,67	19%	20%	19%	18%
Madrid	North Façade	50%	34,3	5,9	18,0	14,0	21,9	5,1	7,0	3,4	39,0	33,5	-1,5	16,1	19,8	2,62	2,81	2,51	2,58	2,67	34%	36%	35%	33%
Madrid	North Façade	0%	33,1	5,9	17,7	13,8	21,5	5,1	7,2	3,3	37,3	32,3	-1,5	15,6	19,7	2,62	2,80	2,51	2,57	2,66	60%	62%	62%	58%
Madrid	Skylight 5º South	100%	56,1	6,5	22,3	16,5	28,0	6,3	6,5	6,3	66,5	57,7	-0,9	21,8	22,8	2,78	3,00	2,41	2,88	2,68	8%	10%	8%	8%
Madrid	Skylight 5º South	80%	52,5	6,5	21,6	16,2	27,1	5,9	6,5	5,5	61,4	53,2	-0,9	20,8	22,5	2,79	3,00	2,41	2,91	2,68	18%	21%	18%	19%
Madrid	Skylight 5º South	50%	47,4	6,5	20,7	15,6	25,6	5,3	6,6	4,3	54,0	46,6	-0,9	19,3	22,0	2,81	3,00	2,41	2,94	2,69	34%	40%	33%	35%
Madrid	Skylight 5º South	0%	39,3	6,5	19,0	14,8	23,3	5,0	7,3	3,0	42,1	36,4	-0,9	16,8	21,3	2,87	3,04	2,41	2,98	2,75	61%	75%	58%	63%
Madrid	Skylight 30º South	100%	56,1	6,3	22,8	17,5	27,9	6,6	6,9	6,4	66,9	58,9	-1,1	22,5	23,0	2,73	2,87	2,47	2,78	2,68	8%	10%	8%	8%
Madrid	Skylight 30º South	80%	52,6	6,3	22,0	17,0	26,9	6,0	6,6	5,6	61,8	54,1	-1,1	21,4	22,6	2,73	2,87	2,47	2,79	2,68	19%	21%	19%	19%
Madrid	Skylight 30º South	50%	47,4	6,3	20,9	16,2	25,5	5,3	6,4	4,4	54,3	47,3	-1,1	19,7	22,1	2,75	2,89	2,47	2,82	2,68	36%	41%	36%	35%
Madrid	Skylight 30º South	0%	39,1	6,3	19,1	15,0	23,2	5,1	7,3	3,0	42,0	36,4	-1,1	16,9	21,3	2,79	2,96	2,47	2,86	2,71	64%	75%	65%	63%
Brussels	East Façade	100%	42,5	2,8	16,8	13,3	20,3	5,7	7,6	3,9	50,4	35,7	-6,0	14,4	19,1	2,61	2,90	2,50	2,57	2,65	9%	9%	8%	9%
Brussels	East Façade	80%	40,1	2,8	16,5	13,2	19,9	5,7	7,7	3,7	46,8	32,9	-6,0	14,0	19,0	2,61	2,88	2,50	2,57	2,65	19%	21%	19%	19%
Brussels	East Façade	50%	36,6	2,8	16,2	13,0	19,4	5,7	7,8	3,5	41,4	29,5	-6,0	13,5	18,9	2,60	2,84	2,50	2,57	2,64	35%	41%	35%	35%
Brussels	East Façade	0%	31,0	2,8	15,6	12,8	18,5	6,1	8,1	3,9	32,7	25,4	-6,0	12,5	18,7	2,60	2,77	2,50	2,56	2,63	62%	74%	62%	62%
Brussels	South Façade	100%	42,9	2,8	17,4	14,2	20,5	5,8	7,4	4,2	51,0	38,7	-6,0	15,3	19,5	2,62	2,91	2,50	2,58	2,65	8%	9%	8%	8%
Brussels	South Façade	80%	40,7	2,8	17,1	14,0	20,1	5,7	7,4	4,0	47,6	35,9	-6,0	14,8	19,4	2,61	2,88	2,50	2,58	2,65	19%	21%	19%	19%
Brussels	South Façade	50%	37,5	2,8	16,6	13,6	19,5	5,6	7,5	3,7	42,5	31,9	-6,0	14,0	19,2	2,61	2,85	2,50	2,57	2,64	35%	40%	36%	34%
Brussels	South Façade	0%	32,2	2,8	15,8	13,1	18,6	6,1	8,1	3,9	34,5	26,3	-6,0	12,7	18,9	2,60	2,79	2,50	2,57	2,63	61%	73%	65%	60%
Brussels	West Façade	100%	45,2	2,8	16,8	13,3	20,3	5,9	7,7	4,2	54,1	38,9	-6,0	14,4	19,1	2,61	2,93	2,50	2,57	2,65	8%	9%	8%	9%
Brussels	West Façade	80%	42,9	2,8	16,5	13,2	20,0	5,9	7,7	4,0	50,5	35,9	-6,0	14,0	19,0	2,61	2,91	2,50	2,57	2,65	19%	21%	19%	19%
Brussels	West Façade	50%	39,5	2,8	16,2	13,0	19,4	5,8	7,8	3,8	45,2	32,0	-6,0	13,5	18,9	2,60	2,87	2,50	2,57	2,64	35%	41%	34%	35%
Brussels	West Façade	0%	33,9	2,8	15,6	12,8	18,5	6,0	8,1	3,9	36,5	26,4	-6,0	12,5	18,7	2,60	2,81	2,50	2,56	2,63	61%	75%	60%	62%
Brussels	North Façade	100%	32,1	2,8	15,9	12,9	19,0	5,6	7,8	3,4	36,3	27,4	-6,0	13,2	18,6	2,60	2,79	2,50	2,56	2,63	9%	9%	9%	9%
Brussels	North Façade	80%	31,6	2,8	15,8	12,9	18,8	5,7	7,9	3,5	35,4	26,9	-6,0	13,0	18,6	2,60	2,78	2,50	2,56	2,63	19%	20%	19%	19%
Brussels	North Façade	50%	30,8	2,8	15,6	12,8	18,6	5,8	8,0	3,6	34,0	26,0	-6,0	12,7	18,5	2,60	2,77	2,50	2,56	2,63	35%	37%	35%	34%
Brussels	North Façade	0%	29,4	2,8	15,4	12,7	18,1	6,0	8,1	3,9	32,2	24,7	-6,0	12,3	18,4	2,59	2,76	2,50	2,56	2,62	61%	66%	62%	60%
Brussels	Skylight 5º South	100%	50,2	3,5	18,3	14,0	22,6	6,1	7,5	4,9	59,1	44,7	-5,3	16,3	20,3	2,86	3,01	2,41	2,96	2,76	8%	10%	9%	8%
Brussels	Skylight 5º South	80%	47,0	3,5	17,9	13,9	21,9	5,9	7,6	4,4	54,5	41,0	-5,3	15,6	20,1	2,87	3,01	2,41	2,96	2,77	19%	21%	19%	19%
Brussels	Skylight 5º South	50%	42,4	3,5	17,3	13,7	20,9	5,7	7,8	3,8	47,6	35,7	-5,3	14,7	19,9	2,89	3,01	2,41	2,97	2,80	34%	41%	34%	35%
Brussels	Skylight 5º South	0%	35,1	3,5	16,2	13,3	19,2	6,1	8,2	4,0	36,6	27,4	-5,3	13,1	19,4	2,95	3,04	2,41	2,99	2,91	61%	74%	58%	62%
Brussels	Skylight 30º South	100%	52,0	3,3	18,6	14,4	22,7	6,2	7,4	5,1	61,7	47,5	-5,5	16,7	20,4	2,77	2,87	2,47	2,83	2,72	8%	10%	9%	8%
Brussels	Skylight 30º South	80%	48,5	3,3	18,1	14,2	22,0	5,9	7,4	4,5	56,6	43,2	-5,5	16,0	20,2	2,78	2,87	2,47	2,84	2,73	19%	21%	20%	19%
Brussels	Skylight 30º South	50%	43,4	3,3	17,4	13,9	21,0	5,7	7,6	3,9	49,1	37,1	-5,5	14,9	19,9	2,80	2,89	2,47	2,85	2,74	36%	41%	36%	36%

Brussels	Skylight 30° South	0%	35,3	3,3	16,2	13,3	19,2	6,1	8,2	4,0	36,9	27,7	-5,5	13,1	19,4	2,84	2,95	2,47	2,86	2,82	63%	74%	63%	63%
Stockholm	East Façade	100%	40,7	-2,7	14,5	10,0	19,1	7,5	10,4	4,6	48,0	35,7	-14,1	11,1	17,9	2,59	2,88	2,49	2,54	2,64	8%	9%	8%	8%
Stockholm	East Façade	80%	38,3	-2,7	14,3	10,0	18,7	7,4	10,5	4,4	44,3	32,7	-14,1	10,8	17,8	2,58	2,86	2,49	2,54	2,63	19%	21%	18%	19%
Stockholm	East Façade	50%	34,8	-2,7	14,0	9,9	18,2	7,4	10,6	4,3	38,8	28,4	-14,1	10,3	17,7	2,58	2,82	2,49	2,54	2,62	35%	40%	33%	35%
Stockholm	East Façade	0%	29,2	-2,7	13,5	9,8	17,2	7,8	10,7	4,9	30,3	23,0	-14,1	9,4	17,5	2,57	2,75	2,49	2,53	2,61	61%	73%	58%	62%
Stockholm	South Façade	100%	41,5	-2,7	15,1	10,6	19,4	7,5	10,2	4,9	49,1	38,1	-14,1	12,0	18,3	2,59	2,89	2,49	2,54	2,64	8%	9%	8%	8%
Stockholm	South Façade	80%	39,2	-2,7	14,8	10,5	19,0	7,4	10,2	4,6	45,6	35,1	-14,1	11,5	18,1	2,59	2,87	2,49	2,54	2,63	18%	21%	18%	18%
Stockholm	South Façade	50%	36,0	-2,7	14,4	10,3	18,4	7,3	10,3	4,4	40,4	30,8	-14,1	10,8	18,0	2,58	2,83	2,49	2,54	2,63	34%	41%	34%	34%
Stockholm	South Façade	0%	30,7	-2,7	13,7	10,0	17,4	7,8	10,7	4,9	31,9	24,3	-14,1	9,6	17,7	2,58	2,77	2,49	2,54	2,62	60%	74%	61%	59%
Stockholm	West Façade	100%	42,9	-2,7	14,5	10,0	19,0	7,6	10,5	4,8	50,9	36,6	-14,1	11,0	17,9	2,58	2,91	2,49	2,54	2,63	8%	9%	8%	8%
Stockholm	West Façade	80%	40,3	-2,7	14,3	10,0	18,6	7,5	10,5	4,6	47,0	33,7	-14,1	10,7	17,8	2,58	2,88	2,49	2,54	2,63	18%	21%	18%	19%
Stockholm	West Façade	50%	36,5	-2,7	14,0	9,9	18,1	7,5	10,6	4,4	41,0	29,7	-14,1	10,2	17,7	2,58	2,84	2,49	2,54	2,62	34%	41%	33%	34%
Stockholm	West Façade	0%	30,4	-2,7	13,5	9,8	17,2	7,8	10,7	4,9	31,2	23,8	-14,1	9,4	17,5	2,57	2,77	2,49	2,53	2,61	60%	75%	58%	61%
Stockholm	North Façade	100%	28,4	-2,7	13,7	9,9	17,6	7,4	10,6	4,1	31,1	24,9	-14,1	9,9	17,4	2,58	2,74	2,49	2,54	2,62	8%	9%	9%	8%
Stockholm	North Façade	80%	27,9	-2,7	13,6	9,9	17,5	7,4	10,6	4,2	30,2	24,3	-14,1	9,8	17,4	2,57	2,74	2,49	2,53	2,62	19%	20%	19%	18%
Stockholm	North Façade	50%	27,0	-2,7	13,5	9,8	17,2	7,6	10,6	4,4	28,8	23,4	-14,1	9,6	17,3	2,57	2,73	2,49	2,53	2,61	34%	37%	35%	33%
Stockholm	North Façade	0%	25,9	-2,7	13,2	9,8	16,8	7,8	10,7	4,8	27,3	22,1	-14,1	9,2	17,3	2,57	2,71	2,49	2,53	2,61	60%	66%	62%	58%
Stockholm	Skylight 5° South	100%	44,4	-1,8	15,8	10,7	21,1	7,6	10,3	5,2	51,7	41,0	-13,1	12,7	19,0	2,89	3,01	2,41	2,99	2,78	8%	10%	9%	8%
Stockholm	Skylight 5° South	80%	41,6	-1,8	15,5	10,6	20,5	7,5	10,4	4,7	47,5	37,6	-13,1	12,2	18,8	2,90	3,01	2,41	2,99	2,80	18%	21%	18%	19%
Stockholm	Skylight 5° South	50%	37,8	-1,8	15,0	10,5	19,5	7,4	10,5	4,3	41,8	32,7	-13,1	11,4	18,6	2,92	3,01	2,41	2,99	2,83	34%	40%	32%	34%
Stockholm	Skylight 5° South	0%	31,7	-1,8	14,1	10,4	17,9	7,8	10,7	4,9	32,3	24,8	-13,1	10,0	18,2	2,97	3,04	2,41	3,00	2,95	59%	73%	56%	61%
Stockholm	Skylight 30° South	100%	48,6	-2,1	16,1	10,8	21,4	7,7	10,1	5,5	57,3	44,7	-13,3	13,2	19,0	2,79	2,87	2,47	2,85	2,73	8%	10%	8%	8%
Stockholm	Skylight 30° South	80%	45,3	-2,1	15,7	10,7	20,7	7,5	10,2	5,0	52,4	40,7	-13,3	12,5	18,9	2,80	2,87	2,47	2,86	2,74	19%	21%	19%	19%
Stockholm	Skylight 30° South	50%	40,4	-2,1	15,1	10,6	19,7	7,4	10,4	4,4	45,1	34,8	-13,3	11,6	18,6	2,81	2,89	2,47	2,86	2,76	35%	41%	34%	35%
Stockholm	Skylight 30° South	0%	32,7	-2,1	14,1	10,3	17,9	7,8	10,7	4,9	33,2	25,3	-13,3	10,0	18,2	2,85	2,95	2,47	2,87	2,84	61%	74%	60%	62%

Table 33. Operating temperature, dynamic U and dynamic G of PV-IGU WITH LowE [4mm_lowiron + 4mm / 16 mm Argon / LowE - 4mm]

Location	Integration	PVRatio	Tmax Gas	Tmin Gas	Tav Gas	Tav Gas Winter	Tav Gas Summer	ΔT Av Cavity	ΔT Av Cavity Winter	ΔT Av Cavity Summer	Tmax PV glass	T_98th PV Glass	Tmin PV Glass	Tav PV Glass	Tav Int Glass	U-value Av	U-value Max	U-value Min	U-value Winter	U-value Summer	G-Value Av	G-value Max	G-value rad weighed	G-value Winter	G-value Summer
Madrid	East Façade	100%	42,3	7,4	20,1	15,8	24,3	8,7	9,9	7,9	56,7	47,7	-3,2	18,6	21,5	1,06	1,23	1,02	1,05	1,06	3%	4%	3%	3%	3%
Madrid	East Façade	80%	40,5	7,4	19,8	15,7	23,9	8,3	10,0	7,1	52,9	44,1	-3,2	18,0	21,6	1,05	1,18	1,02	1,05	1,06	13%	15%	13%	13%	13%
Madrid	East Façade	50%	37,8	7,4	19,4	15,4	23,3	8,0	10,3	6,0	47,2	38,9	-3,2	17,1	21,7	1,05	1,18	1,02	1,05	1,06	28%	32%	29%	28%	28%
Madrid	East Façade	0%	33,6	7,4	18,7	15,0	22,4	8,0	11,1	5,2	38,7	33,7	-3,2	15,6	21,9	1,05	1,18	1,02	1,05	1,05	53%	61%	54%	52%	53%
Madrid	South Façade	100%	47,5	7,4	20,8	17,7	23,6	9,1	10,8	7,4	65,3	47,1	-3,2	19,8	21,7	1,06	1,28	1,02	1,06	1,06	3%	4%	3%	3%	3%
Madrid	South Façade	80%	43,3	7,4	20,4	17,3	23,3	8,5	10,2	6,8	56,7	44,1	-3,2	19,0	21,8	1,06	1,20	1,02	1,06	1,06	13%	15%	13%	14%	12%
Madrid	South Façade	50%	39,5	7,4	19,9	16,8	22,9	7,8	9,8	6,0	50,2	40,2	-3,2	17,9	21,9	1,05	1,18	1,02	1,05	1,05	27%	32%	28%	29%	26%
Madrid	South Façade	0%	35,7	7,4	19,0	15,8	22,2	8,0	11,2	5,2	41,7	35,0	-3,2	15,9	22,2	1,05	1,18	1,02	1,05	1,05	51%	61%	53%	56%	48%
Madrid	West Façade	100%	46,6	7,4	20,1	15,9	24,1	9,2	10,5	8,3	63,7	54,1	-3,2	18,6	21,5	1,06	1,27	1,02	1,05	1,07	3%	4%	3%	3%	3%
Madrid	West Façade	80%	44,4	7,4	19,8	15,7	23,8	8,8	10,4	7,6	59,2	50,4	-3,2	18,0	21,6	1,06	1,23	1,02	1,05	1,06	13%	15%	14%	13%	13%
Madrid	West Façade	50%	41,3	7,4	19,4	15,5	23,2	8,3	10,5	6,5	52,9	45,0	-3,2	17,1	21,7	1,05	1,18	1,02	1,05	1,06	28%	32%	29%	28%	29%
Madrid	West Façade	0%	36,6	7,4	18,7	15,1	22,3	8,0	11,1	5,2	43,0	36,4	-3,2	15,6	21,8	1,05	1,18	1,02	1,05	1,05	53%	62%	55%	52%	54%
Madrid	North Façade	100%	34,2	7,4	18,6	15,0	22,3	7,9	10,5	5,7	43,2	35,9	-3,2	16,1	21,1	1,05	1,18	1,02	1,05	1,05	3%	4%	3%	3%	3%
Madrid	North Façade	80%	33,7	7,4	18,5	14,9	22,1	7,9	10,6	5,5	42,2	35,3	-3,2	15,9	21,2	1,05	1,18	1,02	1,05	1,05	13%	14%	13%	13%	13%
Madrid	North Façade	50%	33,0	7,4	18,4	14,8	21,9	7,9	10,8	5,3	40,6	34,5	-3,2	15,6	21,2	1,05	1,18	1,02	1,05	1,05	27%	28%	27%	28%	27%
Madrid	North Façade	0%	31,9	7,4	18,2	14,7	21,6	8,0	11,1	5,2	38,7	33,2	-3,2	15,1	21,2	1,05	1,18	1,02	1,05	1,05	51%	53%	50%	53%	50%
Madrid	Skylight 5° South	100%	51,1	7,4	21,9	16,8	27,0	10,0	9,4	11,0	70,5	60,8	-2,4	21,8	22,1	1,30	1,77	1,01	1,44	1,16	3%	6%	3%	3%	3%
Madrid	Skylight 5° South	80%	48,6	7,4	21,5	16,5	26,4	9,1	9,2	9,4	64,9	55,9	-2,4	20,7	22,2	1,30	1,77	1,01	1,45	1,16	13%	15%	14%	13%	13%
Madrid	Skylight 5° South	50%	44,9	7,4	20,8	16,1	25,3	8,0	9,3	7,1	56,8	48,8	-2,4	19,1	22,4	1,32	1,77	1,01	1,48	1,17	28%	32%	29%	27%	28%
Madrid	Skylight 5° South	0%	39,1	7,4	19,5	15,4	23,5	7,3	10,2	4,5	43,9	37,7	-2,4	16,5	22,4	1,37	1,77	1,01	1,54	1,21	52%	62%	56%	50%	53%
Madrid	Skylight 30° South	100%	51,2	7,3	22,4	17,8	26,9	10,6	10,3	11,1	71,1	62,3	-2,6	22,6	22,2	1,22	1,63	1,02	1,32	1,13	3%	5%	3%	3%	3%
Madrid	Skylight 30° South	80%	48,7	7,3	21,9	17,4	26,3	9,5	9,7	9,5	65,5	57,0	-2,6	21,4	22,3	1,23	1,63	1,02	1,33	1,13	13%	15%	14%	14%	13%



Madrid	Skylight 30° South	50%	44,9	7,3	21,1	16,8	25,2	8,1	9,2	7,2	57,2	49,5	-2,6	19,6	22,5	1,24	1,63	1,02	1,35	1,13	29%	33%	30%	29%	28%
Madrid	Skylight 30° South	0%	38,9	7,3	19,6	15,7	23,5	7,4	10,4	4,7	43,9	37,8	-2,6	16,6	22,6	1,28	1,63	1,02	1,41	1,15	54%	62%	57%	55%	53%
Brussels	East Façade	100%	40,2	4,5	17,3	14,2	20,5	8,9	11,6	6,2	53,1	37,0	-7,9	13,8	20,8	1,05	1,23	1,02	1,05	1,05	3%	4%	3%	3%	3%
Brussels	East Façade	80%	38,3	4,5	17,1	14,1	20,2	8,8	11,8	5,9	49,2	34,0	-7,9	13,4	20,8	1,05	1,23	1,02	1,05	1,05	13%	15%	14%	13%	13%
Brussels	East Façade	50%	35,6	4,5	16,9	14,0	19,8	8,7	12,0	5,5	43,3	30,2	-7,9	12,8	20,9	1,05	1,23	1,02	1,05	1,05	28%	32%	29%	28%	28%
Brussels	East Façade	0%	31,2	4,5	16,4	13,8	19,0	9,3	12,4	6,1	33,9	25,7	-7,9	11,8	21,0	1,05	1,23	1,02	1,06	1,04	53%	62%	55%	53%	53%
Brussels	South Façade	100%	40,6	4,5	17,9	15,0	20,6	9,1	11,4	6,7	53,8	40,3	-7,9	14,8	20,9	1,05	1,23	1,02	1,06	1,05	3%	4%	3%	3%	3%
Brussels	South Façade	80%	38,8	4,5	17,6	14,8	20,3	8,8	11,3	6,3	50,1	37,3	-7,9	14,2	21,0	1,05	1,23	1,02	1,05	1,05	13%	15%	13%	14%	13%
Brussels	South Façade	50%	36,3	4,5	17,2	14,6	19,9	8,7	11,5	5,8	44,6	32,9	-7,9	13,4	21,1	1,05	1,23	1,02	1,05	1,05	28%	32%	28%	29%	27%
Brussels	South Façade	0%	32,2	4,5	16,6	14,1	19,1	9,3	12,4	6,1	35,7	26,8	-7,9	12,0	21,2	1,05	1,23	1,02	1,06	1,04	52%	61%	54%	55%	51%
Brussels	West Façade	100%	42,6	4,5	17,3	14,2	20,5	9,2	11,7	6,7	57,1	40,5	-7,9	13,8	20,8	1,05	1,23	1,02	1,05	1,05	3%	4%	3%	3%	3%
Brussels	West Façade	80%	40,7	4,5	17,1	14,1	20,2	9,0	11,8	6,3	53,3	37,3	-7,9	13,4	20,8	1,05	1,23	1,02	1,05	1,05	13%	15%	13%	13%	13%
Brussels	West Façade	50%	38,0	4,5	16,9	14,0	19,8	8,9	12,0	5,9	47,6	33,0	-7,9	12,8	20,9	1,05	1,23	1,02	1,05	1,05	28%	32%	28%	28%	28%
Brussels	West Façade	0%	33,8	4,5	16,4	13,8	19,1	9,3	12,4	6,1	38,0	26,9	-7,9	11,8	21,0	1,05	1,23	1,02	1,06	1,04	53%	62%	53%	52%	53%
Brussels	North Façade	100%	31,0	4,5	16,6	13,9	19,3	8,7	12,0	5,4	37,6	27,9	-7,9	12,5	20,6	1,05	1,23	1,02	1,05	1,04	3%	4%	3%	4%	3%
Brussels	North Façade	80%	30,5	4,5	16,5	13,8	19,2	8,8	12,0	5,4	36,6	27,3	-7,9	12,3	20,6	1,05	1,23	1,02	1,05	1,04	13%	14%	13%	13%	13%
Brussels	North Façade	50%	29,9	4,5	16,3	13,8	19,0	8,9	12,2	5,6	35,1	26,4	-7,9	12,0	20,6	1,05	1,23	1,02	1,05	1,04	28%	29%	27%	28%	27%
Brussels	North Façade	0%	28,9	4,5	16,1	13,7	18,6	9,3	12,4	6,1	33,2	25,0	-7,9	11,5	20,7	1,05	1,23	1,02	1,06	1,04	52%	56%	51%	53%	51%
Brussels	Skylight 5° South	100%	46,1	4,5	18,4	14,6	22,3	9,0	10,6	7,8	62,3	46,5	-7,0	15,9	21,0	1,39	1,83	1,01	1,54	1,24	4%	6%	3%	4%	3%
Brussels	Skylight 5° South	80%	43,9	4,5	18,1	14,4	21,8	8,6	10,7	6,8	57,3	42,6	-7,0	15,2	21,0	1,40	1,83	1,01	1,55	1,25	13%	16%	13%	14%	13%
Brussels	Skylight 5° South	50%	40,6	4,5	17,6	14,2	21,1	8,2	10,9	5,7	49,9	36,9	-7,0	14,1	21,1	1,42	1,83	1,01	1,56	1,27	28%	32%	29%	27%	28%
Brussels	Skylight 5° South	0%	35,3	4,5	16,8	13,9	19,7	8,6	11,5	5,7	38,0	28,1	-7,0	12,5	21,1	1,47	1,83	1,01	1,59	1,35	52%	61%	54%	50%	53%
Brussels	Skylight 30° South	100%	47,7	4,5	18,7	14,9	22,4	9,3	10,6	8,2	65,3	49,7	-7,2	16,3	21,1	1,29	1,68	1,02	1,40	1,18	4%	6%	3%	4%	3%
Brussels	Skylight 30° South	80%	45,2	4,5	18,3	14,8	21,9	8,9	10,6	7,2	59,8	45,1	-7,2	15,5	21,1	1,29	1,68	1,02	1,41	1,18	14%	15%	14%	14%	13%
Brussels	Skylight 30° South	50%	41,5	4,5	17,8	14,5	21,1	8,3	10,9	5,9	51,6	38,4	-7,2	14,4	21,2	1,31	1,68	1,02	1,42	1,19	29%	33%	30%	29%	28%
Brussels	Skylight 30° South	0%	35,7	4,5	16,9	14,0	19,7	8,8	11,7	5,8	38,4	28,4	-7,2	12,5	21,2	1,35	1,68	1,02	1,45	1,24	53%	62%	56%	54%	53%
Stockholm	East Façade	100%	38,5	-0,7	15,3	11,2	19,4	11,4	15,6	7,3	50,4	36,9	-16,3	10,3	20,2	1,07	1,32	1,02	1,10	1,05	3%	4%	3%	3%	3%
Stockholm	East Façade	80%	36,6	-0,7	15,1	11,2	19,1	11,3	15,7	6,9	46,4	33,7	-16,3	9,9	20,3	1,07	1,32	1,02	1,10	1,05	13%	15%	13%	13%	13%
Stockholm	East Façade	50%	33,9	-0,7	14,9	11,1	18,7	11,2	15,8	6,7	40,5	29,0	-16,3	9,4	20,3	1,07	1,32	1,02	1,10	1,05	28%	32%	28%	27%	28%
Stockholm	East Façade	0%	29,5	-0,7	14,4	11,1	17,9	11,8	16,0	7,5	31,1	23,1	-16,3	8,5	20,4	1,07	1,32	1,02	1,10	1,05	52%	61%	53%	50%	53%
Stockholm	South Façade	100%	39,3	-0,7	15,8	11,7	19,7	11,4	15,2	7,7	51,6	39,6	-16,3	11,2	20,4	1,07	1,32	1,02	1,10	1,05	3%	4%	3%	3%	3%
Stockholm	South Façade	80%	37,5	-0,7	15,6	11,6	19,3	11,2	15,3	7,3	47,9	36,3	-16,3	10,7	20,4	1,07	1,32	1,02	1,10	1,05	13%	15%	13%	13%	13%
Stockholm	South Façade	50%	35,0	-0,7	15,2	11,5	18,9	11,1	15,5	6,9	42,2	31,6	-16,3	10,0	20,5	1,07	1,32	1,02	1,10	1,05	27%	32%	27%	27%	27%
Stockholm	South Façade	0%	30,9	-0,7	14,7	11,3	18,1	11,8	16,0	7,5	33,0	24,6	-16,3	8,7	20,6	1,07	1,32	1,02	1,10	1,05	51%	62%	52%	51%	51%
Stockholm	West Façade	100%	40,5	-0,7	15,2	11,2	19,3	11,5	15,7	7,5	53,7	38,0	-16,3	10,2	20,2	1,07	1,32	1,02	1,10	1,05	3%	4%	3%	3%	3%
Stockholm	West Façade	80%	38,5	-0,7	15,1	11,2	19,0	11,4	15,7	7,2	49,4	34,8	-16,3	9,9	20,2	1,07	1,32	1,02	1,10	1,05	13%	15%	12%	13%	13%
Stockholm	West Façade	50%	35,5	-0,7	14,8	11,1	18,6	11,4	15,8	6,9	42,9	30,4	-16,3	9,3	20,3	1,07	1,32	1,02	1,10	1,05	27%	32%	26%	26%	28%
Stockholm	West Façade	0%	30,9	-0,7	14,4	11,1	17,9	11,8	16,0	7,5	32,3	24,1	-16,3	8,5	20,4	1,07	1,32	1,02	1,10	1,05	51%	62%	50%	49%	52%
Stockholm	North Façade	100%	27,7	-0,7	14,5	11,1	18,1	11,2	15,8	6,4	31,9	25,2	-16,3	9,0	20,0	1,07	1,32	1,02	1,10	1,05	3%	4%	3%	4%	3%
Stockholm	North Façade	80%	27,2	-0,7	14,4	11,1	18,0	11,3	15,8	6,6	30,9	24,5	-16,3	8,9	20,0	1,07	1,32	1,02	1,10	1,04	13%	14%	12%	13%	13%
Stockholm	North Façade	50%	26,5	-0,7	14,3	11,0	17,8	11,4	15,9	6,8	29,4	23,6	-16,3	8,6	20,1	1,07	1,32	1,02	1,10	1,04	27%	29%	26%	28%	27%
Stockholm	North Façade	0%	25,5	-0,7	14,1	11,0	17,4	11,8	16,0	7,5	27,8	22,1	-16,3	8,2	20,1	1,07	1,32	1,02	1,10	1,04	51%	56%	49%	53%	50%
Stockholm	Skylight 5° South	100%	41,2	-0,6	16,1	11,4	21,0	11,0	14,3	8,0	54,2	42,5	-15,2	12,1	20,2	1,47	1,92	1,01	1,65	1,28	4%	6%	3%	5%	4%
Stockholm	Skylight 5° South	80%	39,2	-0,6	15,9	11,3	20,5	10,7	14,4	7,2	49,7	38,9	-15,2	11,5	20,3	1,48	1,92	1,01	1,66	1,30	13%	16%	13%	13%	13%
Stockholm	Skylight 5° South	50%	36,6	-0,6	15,5	11,3	19,8	10,4	14,5	6,3	43,5	33,6	-15,2	10,6	20,3	1,49	1,92	1,01	1,66	1,32	27%	32%	28%	26%	28%
Stockholm	Skylight 5° South	0%	32,3	-0,6	14,7	11,1	18,4	10,9	14,8	6,9	33,3	25,3	-15,2	9,2	20,3	1,54	1,92	1,01	1,67	1,40	50%	61%	52%	48%	52%
Stockholm	Skylight 30° South	100%	44,8	-0,7	16,4	11,6	21,2	11,3	14,3	8,6	60,5	46,7	-15,4	12,6	20,3	1,36	1,77	1,02	1,51	1,22	4%	6%	3%	4%	3%
Stockholm	Skylight 30° South	80%	42,5	-0,7	16,1	11,5	20,7	10,9	14,4	7,7	55,1	42,3	-15,4	11,9	20,4	1,36	1,77	1,02	1,51	1,22	13%	15%	13%	14%	13%
Stockholm	Skylight 30° South	50%	39,0	-0,7	15,7	11,4	20,0	10,5	14,6	6,6	47,2	35,9	-15,4	10,9	20,5	1,38	1,77	1,02	1,52	1,23	28%	32%	29%	28%	28%
Stockholm	Skylight 30° South	0%	33,4	-0																					

Table 34. Operating temperature as function of PV efficiency of PV-IGU WITH LowE [4mm_lowIron + 4mm / 16 mm Argon / LowE - 4mm]

Location	Integration	PVRatio	PV Efficiency	Tmax Gas	Tmin Gas	Tav Gas	Tav Gas Winter	Tav Gas Summer	Tdelta Av Cavity Winter	Tdelta Av Cavity Summer	Tmax PV glass	T_98th PV Glass	Tmin PV Glass	Tav PV Glass	Tav Int Glass	
Madrid	South Façade	80%	0%	46,3	7,4	20,8	17,8	23,6	8,9	10,7	7,1	61,7	46,7	-3,2	19,7	21,9
Madrid	South Façade	80%	5%	45,6	7,4	20,7	17,7	23,5	8,8	10,6	7,0	60,4	46,1	-3,2	19,5	21,9
Madrid	South Façade	80%	10%	44,8	7,4	20,6	17,6	23,4	8,7	10,5	7,0	59,2	45,4	-3,2	19,4	21,8
Madrid	South Façade	80%	15%	44,1	7,4	20,5	17,5	23,4	8,6	10,3	6,9	58,0	44,7	-3,2	19,2	21,8
Madrid	South Façade	80%	20%	43,3	7,4	20,4	17,3	23,3	8,5	10,2	6,8	56,7	44,1	-3,2	19,0	21,8
Madrid	South Façade	80%	25%	42,5	7,4	20,3	17,2	23,3	8,4	10,1	6,7	55,4	43,5	-3,2	18,9	21,8

Table 35. Dynamic U and dynamic G as function of PV efficiency of PV-IGU WITH LowE [4mm_lowIron + 4mm / 16 mm Argon / LowE - 4mm]

Location	Integration	PVRatio	PV Efficiency	U-value Av	U-value Max	U-value Min	U-value Winter	U-value Summer	G-Value Av	G-value rad weigthed	G-value Max	G-value Winter	G-value Summer
Madrid	South Façade	80%	0%	1,06	1,24	1,02	1,06	1,06	13,0%	13,4%	15,3%	14,0%	12,4%
Madrid	South Façade	80%	5%	1,06	1,23	1,02	1,06	1,06	12,9%	13,3%	15,1%	13,9%	12,3%
Madrid	South Façade	80%	10%	1,06	1,22	1,02	1,06	1,06	12,9%	13,2%	15,0%	13,8%	12,3%
Madrid	South Façade	80%	15%	1,06	1,21	1,02	1,06	1,06	12,8%	13,1%	14,8%	13,7%	12,2%
Madrid	South Façade	80%	20%	1,06	1,20	1,02	1,06	1,06	12,7%	13,0%	14,6%	13,6%	12,2%
Madrid	South Façade	80%	25%	1,06	1,20	1,02	1,06	1,06	12,7%	12,9%	14,5%	13,5%	12,1%

Table 36. Temperatures as function of Rse/Wind velocity and indoor temperature of PV-IGU WITHOUT LowE (MPP).

		Indoor Temperature [°C]										
		22	23	24	25	26	27	28			29	
External surface heat resistance [m ² K/W]	0,04	56,1	56,5	56,8	57,2	57,5	57,9	58,2	58,6	5,3	Wind velocity adjacent to glass surface [m/s]	
	0,05	60,3	60,7	61,1	61,4	61,8	62,2	62,5	62,9	4,0		
	0,06	64,4	64,8	65,1	65,5	65,9	66,3	66,7	67,1	3,2		
	0,07	68,2	68,6	69,0	69,4	69,8	70,2	70,6	71,0	2,6		
	0,08	73,1	73,5	73,9	74,4	74,8	75,2	75,6	76,0	2,1		
	0,09	78,5	79,0	79,4	79,8	80,3	80,7	81,1	81,6	1,8		
	0,10	83,7	84,2	84,6	85,1	85,5	86,0	86,4	86,8	1,5		
	0,11	88,7	89,1	89,6	90,0	90,5	91,0	91,4	91,9	1,3		
	0,12	93,3	93,8	94,3	94,8	95,2	95,7	96,2	96,7	1,1		
	0,13	97,8	98,3	98,8	99,3	99,8	100,2	100,7	101,2	0,9		
	Maximum temperature of Gas for a PV Skylight in Madrid (30° tilt, PVR=100%)											
	0,04	39,1	39,5	39,8	40,2	40,5	40,9	41,2	41,6	5,3		Wind velocity adjacent to glass surface [m/s]
	0,05	39,7	40,1	40,4	40,8	41,2	41,5	41,9	42,3	4,0		
0,06	40,2	40,6	41,0	41,4	41,7	42,1	42,5	42,9	3,2			
0,07	40,7	41,1	41,5	41,9	42,3	42,7	43,1	43,5	2,6			
0,08	41,2	41,6	42,0	42,4	42,8	43,2	43,6	44,0	2,1			
0,09	41,6	42,0	42,5	42,9	43,3	43,7	44,2	44,6	1,8			
0,10	42,0	42,5	42,9	43,4	43,8	44,2	44,7	45,1	1,5			
0,11	42,5	42,9	43,4	43,8	44,3	44,7	45,2	45,6	1,3			
0,12	42,9	43,3	43,8	44,3	44,7	45,2	45,6	46,1	1,1			
0,13	43,2	43,7	44,2	44,7	45,1	45,6	46,1	46,6	0,9			
Maximum temperature of Gas for a NO-PV Skylight in Madrid (30° tilt, PVR=0%)												
0,04	66,9	67,0	67,2	67,3	67,4	67,5	67,7	67,8	5,3	Wind velocity adjacent to glass surface [m/s]		
0,05	72,2	72,4	72,5	72,7	72,8	73,0	73,1	73,3	4,0			
0,06	77,2	77,4	77,6	77,7	77,9	78,1	78,3	78,4	3,2			
0,07	82,0	82,2	82,3	82,5	82,7	82,9	83,1	83,3	2,6			
0,08	87,9	88,1	88,3	88,6	88,8	89,0	89,2	89,4	2,1			
0,09	94,5	94,7	95,0	95,2	95,4	95,7	95,9	96,1	1,8			
0,10	100,7	100,9	101,2	101,4	101,7	101,9	102,2	102,5	1,5			
0,11	106,5	106,8	107,0	107,3	107,6	107,9	108,1	108,4	1,3			
0,12	112,0	112,3	112,6	112,9	113,2	113,4	113,7	114,0	1,1			
0,13	117,2	117,5	117,8	118,1	118,4	118,7	119,0	119,3	0,9			
Maximum temperature of outer PV Glass for a PV Skylight in Madrid (30° tilt, PVR=100%)												
0,04	58,9	59,1	59,2	59,3	59,4	59,6	59,7	59,8	5,3		Wind velocity adjacent to glass surface [m/s]	
0,05	64,1	64,3	64,4	64,6	64,7	64,9	65,0	65,2	4,0			
0,06	69,1	69,3	69,4	69,6	69,8	69,9	70,1	70,3	3,2			
0,07	73,8	74,0	74,2	74,4	74,6	74,8	75,0	75,2	2,6			
0,08	78,3	78,5	78,7	78,9	79,2	79,4	79,6	79,8	2,1			
0,09	82,5	82,8	83,0	83,2	83,5	83,7	83,9	84,2	1,8			
0,10	86,6	86,8	87,1	87,4	87,6	87,9	88,1	88,4	1,5			
0,11	90,5	90,7	91,0	91,3	91,5	91,8	92,1	92,4	1,3			
0,12	94,2	94,4	94,7	95,0	95,3	95,6	95,9	96,2	1,1			
0,13	97,7	98,0	98,3	98,6	98,9	99,2	99,5	99,9	0,9			
Percentil_98 temperature of outer PV Glass for a PV Skylight in Madrid (30° tilt, PVR=100%)												
0,04	42,0	42,1	42,2	42,3	42,5	42,6	42,7	42,8	5,3	Wind velocity adjacent to glass surface [m/s]		
0,05	42,7	42,8	43,0	43,1	43,3	43,4	43,6	43,7	4,0			
0,06	43,4	43,6	43,7	43,9	44,1	44,2	44,4	44,6	3,2			
0,07	44,0	44,2	44,4	44,6	44,8	45,0	45,2	45,3	2,6			
0,08	44,7	44,9	45,1	45,3	45,5	45,7	45,9	46,1	2,1			
0,09	45,3	45,5	45,7	45,9	46,1	46,4	46,6	46,8	1,8			
0,10	45,8	46,1	46,3	46,5	46,8	47,0	47,3	47,5	1,5			
0,11	46,4	46,6	46,9	47,1	47,4	47,6	47,9	48,2	1,3			
0,12	46,9	47,1	47,4	47,7	48,0	48,2	48,5	48,8	1,1			
0,13	47,4	47,6	47,9	48,2	48,5	48,8	49,1	49,4	0,9			
Maximum temperature of outer glass for a NO-PV Skylight in Madrid (30° tilt, PVR=0%)												
		22	23	24	25	26	27	28	29			
		Indoor Temperature [°C]										

Table 37. Temperatures as function of Rse/Wind velocity and indoor temperature of PV-IGU WITH LowE (MPP).

		Indoor Temperature [°C]										
		22	23	24	25	26	27	28	29			
External surface heat resistance [m ² K/W]	0,04	51,2	51,7	52,1	52,5	53,0	53,4	53,9	54,3	5,3	Wind velocity adjacent to glass surface [m/s]	
	0,05	55,4	55,8	56,3	56,7	57,2	57,6	58,0	58,5	4,0		
	0,06	59,5	59,9	60,4	60,8	61,3	61,7	62,2	62,6	3,2		
	0,07	63,6	64,0	64,5	65,0	65,4	65,9	66,3	66,8	2,6		
	0,08	68,6	69,1	69,5	70,0	70,5	70,9	71,4	71,8	2,1		
	0,09	74,4	74,8	75,3	75,8	76,2	76,7	77,2	77,6	1,8		
	0,10	80,0	80,5	81,0	81,5	81,9	82,4	82,9	83,4	1,5		
	0,11	85,6	86,1	86,6	87,1	87,6	88,0	88,5	89,0	1,3		
	0,12	91,1	91,6	92,1	92,6	93,1	93,6	94,1	94,5	1,1		
	0,13	96,5	97,0	97,5	98,0	98,5	99,0	99,5	100,0	0,9		
	Maximum temperature of Gas for a PV Skylight in Madrid (30° tilt, PVR=100%)											
	0,04	38,9	39,4	39,8	40,3	40,7	41,1	41,6	42,0	5,3		Wind velocity adjacent to glass surface [m/s]
	0,05	39,7	40,1	40,5	41,0	41,4	41,9	42,3	42,8	4,0		
0,06	40,4	40,8	41,3	41,7	42,2	42,6	43,1	43,5	3,2			
0,07	41,0	41,5	41,9	42,4	42,9	43,3	43,8	44,2	2,6			
0,08	41,7	42,2	42,6	43,1	43,6	44,0	44,5	44,9	2,1			
0,09	42,4	42,8	43,3	43,8	44,2	44,7	45,2	45,6	1,8			
0,10	43,0	43,5	44,0	44,4	44,9	45,4	45,8	46,3	1,5			
0,11	43,6	44,1	44,6	45,1	45,5	46,0	46,5	47,0	1,3			
0,12	44,3	44,7	45,2	45,7	46,2	46,7	47,1	47,6	1,1			
0,13	44,9	45,3	45,8	46,3	46,8	47,3	47,8	48,3	0,9			
Maximum temperature of Gas for a NO-PV Skylight in Madrid (30° tilt, PVR=0%)												
0,04	71,1	71,1	71,2	71,2	71,3	71,3	71,4	71,4	5,3	Wind velocity adjacent to glass surface [m/s]		
0,05	77,9	78,0	78,0	78,1	78,2	78,2	78,3	78,4	4,0			
0,06	84,7	84,7	84,8	84,9	85,0	85,0	85,1	85,2	3,2			
0,07	91,4	91,5	91,6	91,6	91,7	91,8	91,9	92,0	2,6			
0,08	99,6	99,7	99,8	99,8	99,9	100,0	100,1	100,2	2,1			
0,09	108,9	109,0	109,1	109,2	109,3	109,4	109,5	109,6	1,8			
0,10	118,0	118,2	118,3	118,4	118,5	118,6	118,7	118,8	1,5			
0,11	127,0	127,1	127,3	127,4	127,5	127,6	127,7	127,9	1,3			
0,12	135,8	135,9	136,0	136,2	136,3	136,4	136,6	136,7	1,1			
0,13	144,3	144,5	144,6	144,8	144,9	145,0	145,2	145,3	0,9			
Maximum temperature of outer PV Glass for a PV Skylight in Madrid (30° tilt, PVR=100%)												
0,04	62,3	62,3	62,4	62,4	62,5	62,5	62,6	62,6	5,3		Wind velocity adjacent to glass surface [m/s]	
0,05	68,8	68,8	68,9	68,9	69,0	69,1	69,1	69,2	4,0			
0,06	75,3	75,3	75,4	75,5	75,6	75,6	75,7	75,8	3,2			
0,07	81,7	81,8	81,9	81,9	82,0	82,1	82,2	82,3	2,6			
0,08	88,0	88,1	88,2	88,3	88,4	88,5	88,6	88,6	2,1			
0,09	94,3	94,4	94,5	94,6	94,7	94,8	94,9	95,0	1,8			
0,10	100,4	100,6	100,7	100,8	100,9	101,0	101,1	101,2	1,5			
0,11	106,6	106,7	106,8	107,0	107,1	107,2	107,3	107,4	1,3			
0,12	112,6	112,8	112,9	113,0	113,2	113,3	113,4	113,6	1,1			
0,13	118,6	118,8	118,9	119,0	119,2	119,3	119,4	119,6	0,9			
Percentil_98 temperature of outer PV Glass for a PV Skylight in Madrid (30° tilt, PVR=100%)												
0,04	43,9	43,9	44,0	44,0	44,1	44,1	44,2	44,2	5,3	Wind velocity adjacent to glass surface [m/s]		
0,05	45,1	45,1	45,2	45,2	45,3	45,4	45,4	45,5	4,0			
0,06	46,2	46,3	46,3	46,4	46,5	46,6	46,6	46,7	3,2			
0,07	47,3	47,4	47,5	47,6	47,7	47,7	47,8	47,9	2,6			
0,08	48,4	48,5	48,6	48,7	48,8	48,9	49,0	49,1	2,1			
0,09	49,5	49,6	49,7	49,8	49,9	50,0	50,1	50,2	1,8			
0,10	50,6	50,7	50,8	50,9	51,0	51,1	51,2	51,3	1,5			
0,11	51,6	51,7	51,8	52,0	52,1	52,2	52,3	52,4	1,3			
0,12	52,6	52,8	52,9	53,0	53,1	53,3	53,4	53,5	1,1			
0,13	53,6	53,8	53,9	54,0	54,2	54,3	54,4	54,6	0,9			
Maximum temperature of outer glass for a NO-PV Skylight in Madrid (30° tilt, PVR=0%)												
		22	23	24	25	26	27	28	29			
		Indoor Temperature [°C]										

Table 38. Maximum temperatures as function of Rse and PV occupancy ratio of PV-IGU WITH LowE. Indoor temperature 29 °C. Open-circuit state.

		PV Ratio			
		0%	50%	80%	100%
Rse [m ² K/W]	0,04	42,0	50,0	54,9	58,2
	0,05	42,8	52,8	59,0	63,3
	0,06	43,5	55,5	63,1	68,3
	0,07	44,2	58,2	67,1	73,1
	0,08	44,9	61,0	71,1	77,8
	0,09	45,6	63,7	74,9	82,9
<i>Maximum temperature of Gas for a PV Skylight in Madrid (30° tilt)</i>					
		0%	50%	80%	100%
Rse [m ² K/W]	0,04	44,2	60,9	71,0	77,9
	0,05	45,5	65,5	77,8	86,3
	0,06	46,7	70,0	84,6	94,4
	0,07	47,9	74,4	91,1	102,3
	0,08	49,1	78,9	97,6	109,9
	0,09	50,2	83,3	103,8	118,1
<i>Maximum temperature of PV Glass for a PV Skylight in Madrid (30° tilt)</i>					
		0%	50%	80%	100%
Rse [m ² K/W]	0,04	38,1	53,0	62,3	68,6
	0,05	39,2	57,2	68,6	76,3
	0,06	40,4	61,6	74,8	83,7
	0,07	41,5	65,8	80,9	91,1
	0,08	42,6	70,0	86,9	98,2
	0,09	43,7	74,0	92,7	105,2
<i>Percentil_98 temperature of PV Glass for a PV Skylight in Madrid (30° tilt)</i>					

7.1.4 Finite-Element-Method thermal simulations

The finite element method simulation is a powerful tool to simulate many physical events. In this case, the simulations have included the thermal analysis in stationary and transient conditions linked with the CFD (computational fluid dynamics) analysis of the air movement. The air is always present in the cavity of the IGU and, in some cases, in contact with the internal and external surface of the PV IGU unit.

7.1.4.1 The purposes

The FEM simulation tool have been used for different purposes:

First, to perform thermal simulations that validate the results from the PV glazing thermal model (PVGTM). The FEM calculates the temperature in the different glass layers, and these temperatures are compared with the ones obtained from PVGTM. It should be considered that FEM requires as inputs the calculated radiation absorption, so it only validates the thermal behaviour but not the optical calculations.

At the same time, the cases that have been chosen for the validation are the ones that have shown the highest solar cell temperature in the PV glass model calculations, so the temperature differences between FEM and PVGTM are enhanced due to the higher temperature reached by the chosen cases. Thus, these FEM simulations will provide information about the maximum temperatures that the different parts of the PV glazing can reach, and how this temperature is distributed.

The PV optical-thermal model (PVGTM) is based on stationary calculations. This means that the impact of thermal inertia of glass is assumed to be very low, and the temperature reaches the equilibrium state in less than 30-60 minutes. This hypothesis is analysed with the comparison of stationary and transient thermal FEM analysis.

Finally, several FEM simulations have been used to assess how the different distribution of the solar cells, with same PV occupancy, impacts on the total irradiated energy of the external surface. In other words, PV glazing with the same PV occupancy but different distribution of this occupancy may have different temperature profiles at their external surfaces. As the total thermal irradiance depends on T^4 (Stephan-Boltzmann equation), thermal boundary conditions could be different depending on the PV distribution. This could impact the solar factor, that could not be linear with the PV occupancy as it is normally assumed.

7.1.4.2 The cases

To fulfil the different purposes, 94 FEM simulations cases have been selected, modelled, and executed. All the cases are detailed in Table 39. All these cases differ from each other in their geometric model and/or in their boundary conditions.

Table 39. List of thermal FEM simulations cases

Case number	Purpose	PV glass system	Shape of solar cells	Dimensions	Tout [°C]	Tint [°C]	Absorption in PV area glass 1 [W/m ²]	Absorption in transparent area glass 1 [W/m ²]	Absorption in glass 2 (behind cells interstice) [W/m ²]	Absorption in glass 2 (homogeneously) [W/m ²]	Rse [m ² K/W]	Rsi [m ² K/W]	PV ratio	Inclination [°]
1	Maximum temperature and validation	Ext -- 4mm+EVA+PV+4mm / 16mm airgap / 4mm -- Int	156x156	1x2m	40	29	900	-	-	-	0,040	0,130	100%	90
2							750	-	-	-			100%	
3							750	120	55	-			80%	
4							620	-	-	11			80%	
5							900	-	-	-			100%	
6							750	-	-	-			100%	
7							750	120	55	-			80%	
8							620	-	-	11			80%	
9							900	-	-	-			100%	
10							750	-	-	-			100%	
11							750	120	55	-			80%	
12							620	-	-	11			80%	
13							900	-	-	-			100%	
14							750	-	-	-			100%	
15							750	120	55	-			80%	
16							620	-	-	11			80%	
17							900	-	-	-			100%	
18							750	-	-	-			100%	
19							750	120	55	-			80%	
20							620	-	-	11			80%	
21							900	-	-	-			100%	
22							750	-	-	-			100%	
23							750	120	55	-			80%	
24							620	-	-	11			80%	
25	Stationary vs transient	Ext -- 4mm+EVA+PV+4mm / 16mm airgap / 4mm -- Int	Homogeneous	1x2m	4,9	22	0,0	-	-	0,0	0,040	0,130	50%	90
26					5,2	22	51,2	-	-	3,6				
27					5,5	22	44,2	-	-	3,1				
28					6,5	22	23,9	-	-	1,7				
29					7,5	22	31,6	-	-	2,2				
30					8,6	22	53,2	-	-	3,7				
31					9,5	22	29,4	-	-	2,0				

32				10,3	22	38,8	-	-	2,7						
33				11,2	22	29,2	-	-	2,0						
34				10,0	22	42,2	-	-	2,9						
35				8,8	22	0,0	-	-	0,0						
36	Stationary vs transient	Ext -- 4mm+EVA+PV+4mm / 16mm airgap / 4mm -- Int	Homogeneous	1x2m	23,0	22	0,0	-	-	0,0	0,040	0,130	50%	90	
37					22,3	22	2,9	-	-	0,2					
38					25,6	22	31,2	-	-	2,1					
39					28,9	22	96,6	-	-	6,4					
40					32,2	22	169,2	-	-	11,4					
41					34,0	22	227,8	-	-	15,5					
42					35,9	22	268,0	-	-	18,2					
43					37,7	22	280,1	-	-	19,0					
44					37,8	22	268,4	-	-	18,2					
45					37,9	22	233,7	-	-	15,8					
46					38,0	22	173,1	-	-	11,6					
47					36,7	22	105,3	-	-	6,9					
48					35,4	22	39,7	-	-	2,6					
49					34,1	22	4,8	-	-	0,3					
50	32,3	22	0,0	-	-	0,0									
51	Stationary vs transient	Ext -- 4mm+EVA+PV+4mm / 16mm airgap / 4mm -- Int	Homogeneous	1x2m	4,94	22	0,0	-	-	0,0	0,040	0,108	50%	30	
52					5,2	22	35,4	-	-	2,4					
53					5,46	22	55,3	-	-	3,9					
54					6,5	22	37,0	-	-	2,6					
55					7,54	22	48,0	-	-	3,3					
56					8,58	22	75,1	-	-	5,2					
57					9,45	22	46,4	-	-	3,2					
58					10,32	22	59,2	-	-	4,1					
59					11,19	22	41,6	-	-	2,9					
60					10	22	42,9	-	-	3,0					
61					8,8	22	0,0	-	-	0,0					
62	Stationary vs transient	Ext -- 4mm+EVA+PV+4mm / 16mm airgap / 4mm -- Int	Homogeneous	1x2m	22,95	22	0,0	-	-	0,0	0,040	0,161	50%	30	
63					22,32	22	5,8	-	-	0,4					
64					25,62	22	66,9	-	-	4,5					
65					28,93	22	175,0	-	-	12,0					
66					32,23	22	283,7	-	-	19,1					
67					34,04	22	362,8	-	-	23,6					
68					35,85	22	419,1	-	-	26,5					
69					37,67	22	433,5	-	-	27,2					
70					37,78	22	417,1	-	-	26,4					
71					37,89	22	371,1	-	-	24,1					
72					38	22	284,4	-	-	19,1					
73					36,69	22	188,6	-	-	12,8					
74					35,37	22	89,0	-	-	5,8					
75					34,05	22	7,7	-	-	0,5					
76	32,34	22	0,0	-	-	0,0									
77	SHGC linearity with PV ratio	Ext -- 4mm+EVA+PV+4mm / 16mm airgap / 4mm -- Int	Concentrated cells	89,6 x 173,8 cm	15	22	600,0	135	65	-	Simulated	Simulated	50%	90	
78			Distributed cells				600,0	135	65	-					
79			Homogeneous				367,5	-	-	32,5					
80			Ext -- 6mm+EVA+PV+6mm -- Int				Concentrated cells	600,0	135	65					-
81			Distributed cells				600,0	135	65	-					
82			Homogeneous				367,5	-	-	-					
83		Ext -- 12mm+EVA+PV+12mm -- Int	Concentrated cells	600,0	135	65	-								
84			Distributed cells	600,0	135	65	-								
85			Homogeneous	367,5	-	-	-								
86			Ext -- 4mm+EVA+PV+4mm / 16mm airgap / 4mm -- Int	Concentrated cells	600,0	135	65	-							
87			Distributed cells	600,0	135	65	-								
88			Homogeneous	367,5	-	-	32,5								
89		Ext -- 6mm+EVA+PV+6mm -- Int	Concentrated cells	89,6 x 173,8 cm	15	22	600,0	135	65	-	Simulated	Simulated	50%	0	
90			Distributed cells				600,0	135	65	-					
91	Homogeneous		367,5				-	-	-						
92	Ext -- 12mm+EVA+PV+12mm -- Int		Concentrated cells				600,0	135	65	-					
93	Distributed cells		600,0				135	65	-						
94	Homogeneous		367,5				-	-	-						

The first set correspond to the maximum temperature cases, and the ones used to validate to PV glazing thermal model (PVGTM). They include the PV-IGU system with an assumed outdoor and indoor high temperatures of 40 °C and 29 °C respectively. The variable parameters among the cases include the

irradiation absorbed at the opaque (solar cell) area, at the transparent area of PV glass, and at the transparent inner glass layer. High PV occupancy ratios have been included with values of 100% (fully opaque) and 80%. For the 80% case, it has been considered both homogeneous and heterogeneous light absorptance, corresponding to transparent thin film and c-Si solar cells respectively. In homogeneous case (Figure 35), the irradiation is absorbed homogeneously in the glass area according to the PV occupancy, while in the heterogeneous case (Figure 36) the irradiation is absorbed mainly by the area with solar cells and only a small part is absorbed in the transparent area. The fully opaque case is included as an extreme case that will show the maximum temperature due to high light absorptance. It should be noted that light absorption is normally lower than the real incident radiation. For instance, 750 W/m^2 of absorption correspond to 885 W/m^2 of direct radiation plus 137 W/m^2 of diffuse radiation. Also, different inclinations have been considered with corresponding standardized R_{se} and R_{si} coefficients.

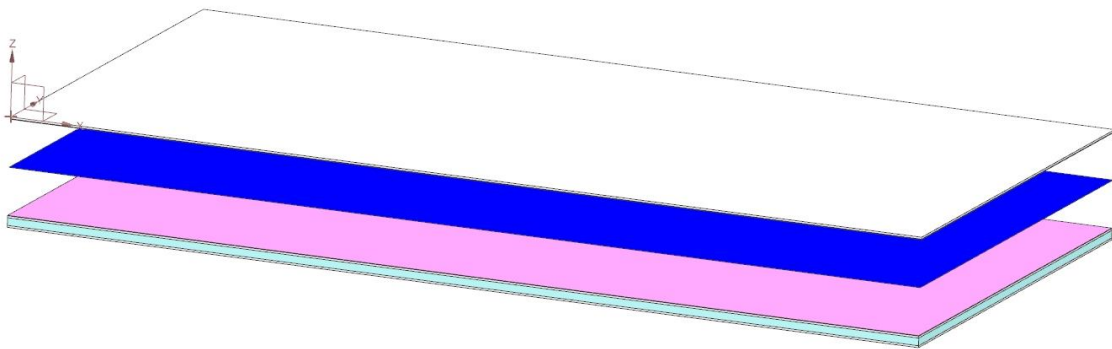


Figure 35. Example of 100% PV occupancy or lower with homogeneous absorption of sun radiation (e.g. transparent thin film)

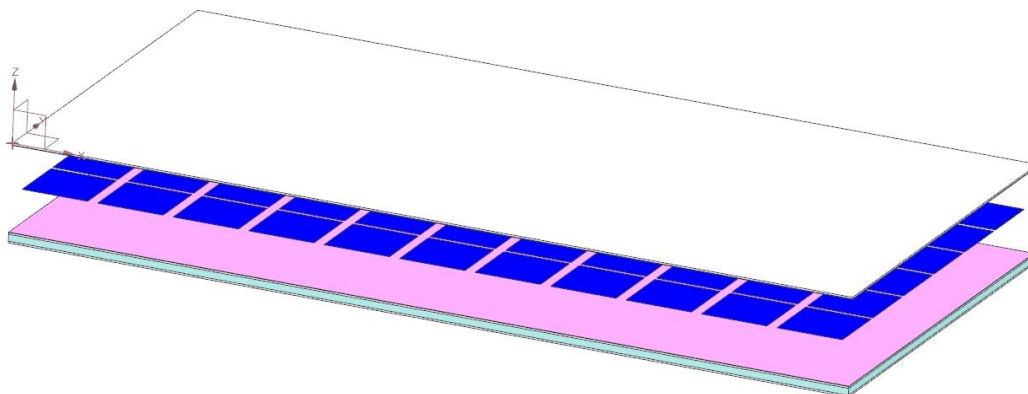


Figure 36. Example of 80% PV occupancy with heterogeneous absorption of sun radiation in 156x156 mm solar cells.

The second set of cases correspond to the daylight hours of two complete days in Madrid, one of them is the 21/01/2016 and the other is the 07/09/2016. This analysis is done for the PV-IGU in vertical and with an inclination of 30° (skylight). These cases have been simulated in stationary and transient conditions to compare the results and evaluate the thermal inertia of the system. All of them are done with homogeneous absorption of radiation (like Figure 35) corresponding to 50% PV occupancy.

Finally, the third set of cases correspond to intermediate PV occupancy (50%) in different configurations: 1) in a concentrated way (half of the module opaque and the other half transparent), 2) with the c-Si cells distributed (like Figure 36 but 50% PV occupancy) and 3) an absorptance fully homogenous of the radiation (like Figure 35). The PV concentrated vertical cases have been analysed with the cells at the top and bottom

of the module (Figure 37). The 600 W/m² heat absorptance correspond to a real situation of 692 W/m² direct plus 180 W/m² diffuse radiation. The main difference of these cases is that no thermal resistances have been applied on either the outer surface or the inner surface. Instead, a control volume of air has been defined on both sides, so that the convection and radiation effects are not imposed but they are calculated by the simulation tool. The internal radiative flux is defined as a flux to an environment at the defined internal temperature of 22°C, while the external radiative flux is defined to an environment at 15 °C with corresponding sky temperature calculated with Swinbank formula. These have been simulated for glazing systems with and without gas cavity and different glass thicknesses. Also, the whole set of combinations have been simulated in vertical (90°) and horizontal (0°).

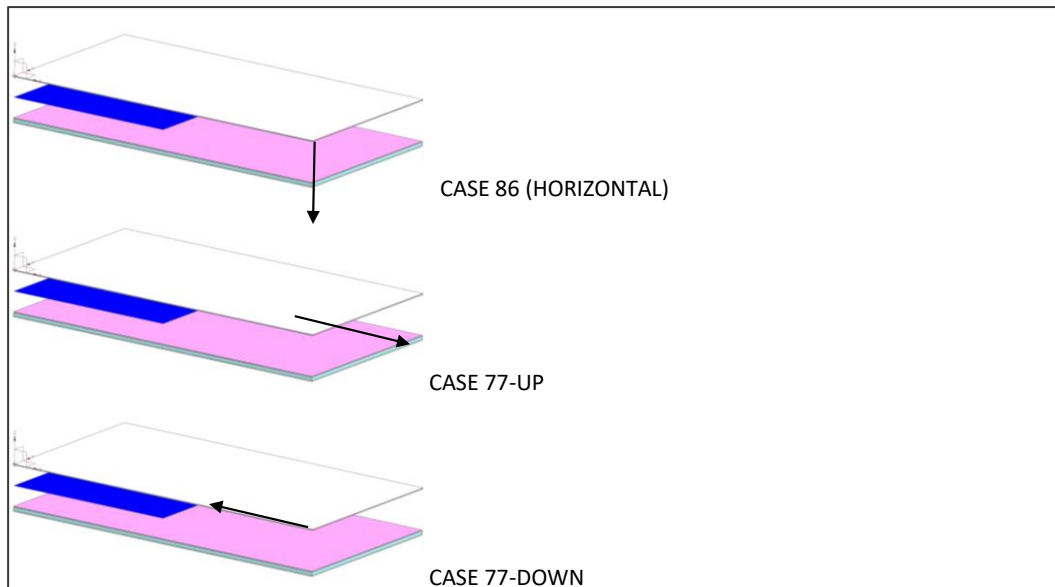


Figure 37. Different positions of the concentrated solar cells (blue). The arrow is the gravity vector. Examples for PV-IGU configuration.

A diagram of the different material layers and material properties are shown in Table 40 and Table 41 respectively.

Table 40. Diagram of material layers of PV-IGU in FEM simulations

	Layer	Thickness (mm)
EXT	PV module glass (top)	4
	EVA	0,9
	PV cells (homogeneous or heterogeneous)	0,2
	EVA	0,9
	PV module glass (bottom)	4
INT	Air chamber	16
	Inner glass layer	4

Table 41. Material properties considered in FEM simulations

Material	Thermal conductivity [W/m·K]	Density [Kg/m ³]	Specific Heat [J/Kg·K]
Glass	1	2550	720
EVA	0,23	950	2480
PV cells	148	2330	700
Air	T dependant (25,1 at 20°C)	T dependant (1,2 at 20°C)	T dependant (1007 at 20°C)

7.1.4.3 The results

Maximum temperatures and comparison between FEM and PV Glazing Thermal model (PVGTM)

The simulation cases from 1 to 24 of Table 39 describe the situations when the maximum temperatures of PV glazing have been observed. Their purposes are to evaluate the maximum temperature that the PV-IGU can reach and to validate the PV Glazing Thermal model (described in 7.1.3.1) by comparing the results.

The outdoor temperature conditions and radiation absorbed correspond approximately with the real conditions when the maximum temperatures have been observed for a 30° tilted PV skylight in Madrid. For clarifying, the FEM model do not calculate the optical behaviour of the glass; thus, it requires the irradiation absorbed by the different parts as inputs, which are described as heat generation sources in the FEM simulations. The irradiation absorbed is not the total incident radiation, as the reflected and transmitted part has been already calculated and removed.

All the cases assume outdoor temperature of 40 °C and indoor temperature of 29 °C. The simulations are done with PV-IGU module dimensions of 1x2 m in portrait, with PV occupancy (PV ratio) of 100% and 80%. With 80% there are two cases, one with 156x156 mm c-Si solar cells combined with 20% of transparent area, this means that the absorption of radiation is heterogeneous and there are different absorption levels for opaque and transparent areas in first PV glass, but also in the second glass layer; and a second case assuming homogeneous absorption corresponding to transparent thin film PV technologies. The 100% PV ratio cases assume homogeneous absorption of radiation as the whole PV glass is covered with opaque solar cells. There are two 100% cases, first assumes 900 W/m² of heat generation (due to irradiation absorption) and correspond to PV glass in open circuit conditions (Voc), i.e. without production of electricity due to PV effect; while in the second the heat generation is 750 W/m² because 16,7% (i.e. PV efficiency at 66 °C with 20% at STC and -0,4%/°C) of the absorbed radiation is transformed to electricity, this is the called MPP (Maximum Power Point) state. Even though 100% PV ratio is unlikely to be used in real conditions because it would be fully opaque, it has been included in the study to represent the worst-case scenario. All the previously described cases are simulated with different inclinations of 90° (vertical), 30°, and 0° (horizontal), corresponding to PV curtain walls of skylights. The inner surface thermal resistance (R_{si}) is varied according to the inclination as described in Figure 33 for upwards heat flux. The outer surface resistance (R_{se}) of 0,04 m²K/W described in EN 673 has been considered for cases 1 to 12, while the minimum limit value of 0,13 m²K/W is considered for cases 13 to 24, representing an extremely low heat removal across the outer surface of the PV glass (more info in 7.1.3.3).

The temperature of the different parts of the PV-IGU are shown in Table 42. The first four columns show the results obtained with the FEM simulations, including the average temperature of the PV cells, average temperature of the air in the cavity, average temperature of inner glass layer and the temperature difference between cavity surfaces (ΔT). Then, the equivalent results are shown but calculated with the PV glazing model instead of FEM simulations, and finally the absolute difference between both are shown. There is a clear difference between the results with R_{se} 0,04 m²K/W (1 to 12) and 0,13 m²K/W (13 to 24). As the second set represent an extreme case with very low heat removal of the outer surface, they are shown in grey.

Regarding the difference between FEM and PVGTM calculations (Table 42), it is observed that FEM predicts slightly lower temperatures of the PV cells (differences <1 °C), while the temperatures of inner glass layer are higher (1,5-2,3 °C). This implies very similar temperature of the air in the cavity (differences <0,5 °C), but differences of several degrees in ΔT (2,2-3,1 °C). This is probably because the FEM simulations predict slightly lower thermal resistance of the air cavity than the method used in PVGTM which is the one from EN 673, also affected by the edge effects. The heatflux across the air cavity depends on fluid modelling and may have slight deviations from one approach to another leading to a few degrees impact on the temperature results. The FEM simulations uses *Boussinesq* as buoyancy model and *Mixing Length* as turbulence model. In addition, it should be considered that the cases with highest temperatures have been chosen to enhance the

deviations, which are relatively low compared to the high temperature of the glass layers. The “Mean T PV Cells” predicted by the PVGTM is slightly higher for the cases 3, 7, 11, 15, 19, 23 because in this case, the FEM considers only the PV cells area, while the PVGTM cannot distinguish between cell and transparent area, so it considers the average of the whole surface. In summary, **despite there are some temperature differences between FEM and PVGTM, they are reasonably low considering the high impact of small deviations in the thermal resistance of the air cavity, the edge effects of the FEM model, and the high temperatures reached with the selected boundary conditions.**

The **highest temperature of the PV cells assuming $R_{se}=0,04 \text{ m}^2\text{K/W}$ in a PV-IGU with air cavity (instead of Argon) is about $74,4 \text{ }^\circ\text{C}$ for 100% PV occupied glazing in open circuit (Figure 38) but decreases about $6 \text{ }^\circ\text{C}$ in MPP conditions.** These results are very similar to the ones obtained for Argon described in section 7.1.3.2. Here (case 1), the temperature at the top of the cavity is about $73,5 \text{ }^\circ\text{C}$ and about $53 \text{ }^\circ\text{C}$ at the bottom, with an air velocity of 94 mm/s (Figure 39). This means that, **in a vertical 2 m height module, temperature difference between bottom-top gas cavity can reach about $8\text{-}10 \text{ }^\circ\text{C}$.** On the other hand, the temperature of the air in the cavity could reach about $63 \text{ }^\circ\text{C}$ for open circuit state but it is reduced about $4\text{-}5 \text{ }^\circ\text{C}$ in MPP state.

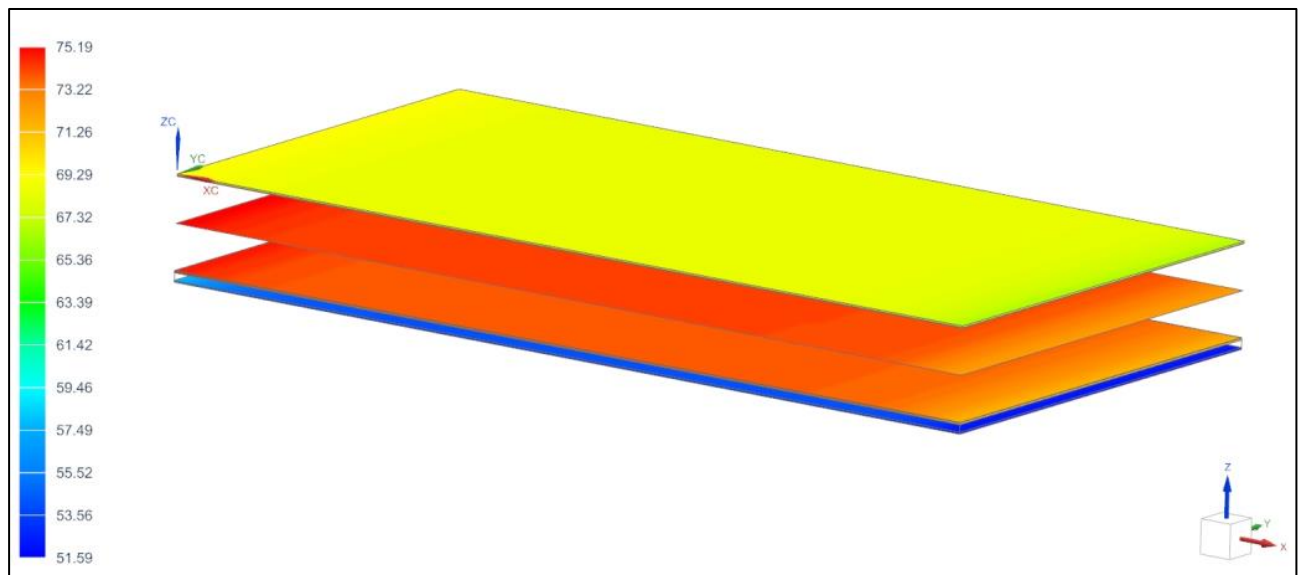


Figure 38. Temperature results of case 1 in FEM simulations

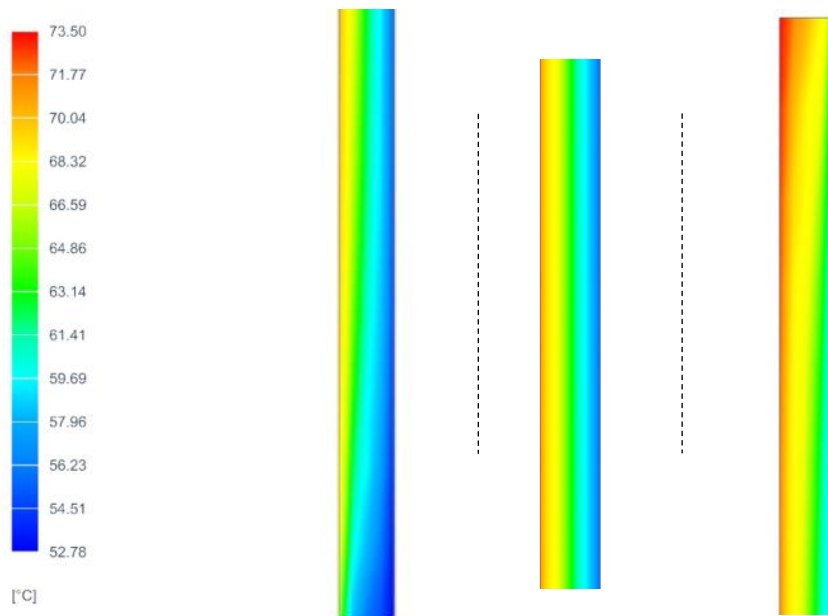


Figure 39. Temperature of the air in the PV-IGU cavity. Case 1. From left to right: Bottom, middle and top of the cavity.

The 80% PV occupied glass in MPP (case 3) shows about 3-5 °C lower temperature than equivalent 100% PV occupied. The temperature distribution in all the elements of case 3 (heterogeneous absorption of radiation) can be seen in Figure 40, while the detailed temperature distribution for the solar cells and the intermediate EVA layers is in Figure 41. For clarifying, the elements are separated for a better view of the results, but the thermal model is described assuming that the elements are in direct contact. Here, it is observed that **the temperature difference between the transparent area and the central area of the solar cells is about 8 °C, while the temperature difference between the centre and the edge of a solar cell can reach 5-6 °C.** The highest temperature of the solar cells also affects the outer surface of the PV glass, and can slightly impact the inner glass (Figure 42). At the inner glass can be also observed slightly hotter lines between the cells, corresponding to the radiance absorption in these areas because they are behind the transparent area of the first PV glass layer. Regarding the **air cavity temperature for PV ratio of 80%, this is reduced to 53-56 °C, which is 3 °C lower than for 100% PV occupancy, and is very similar in both homogeneous and heterogeneous absorption of radiation.**

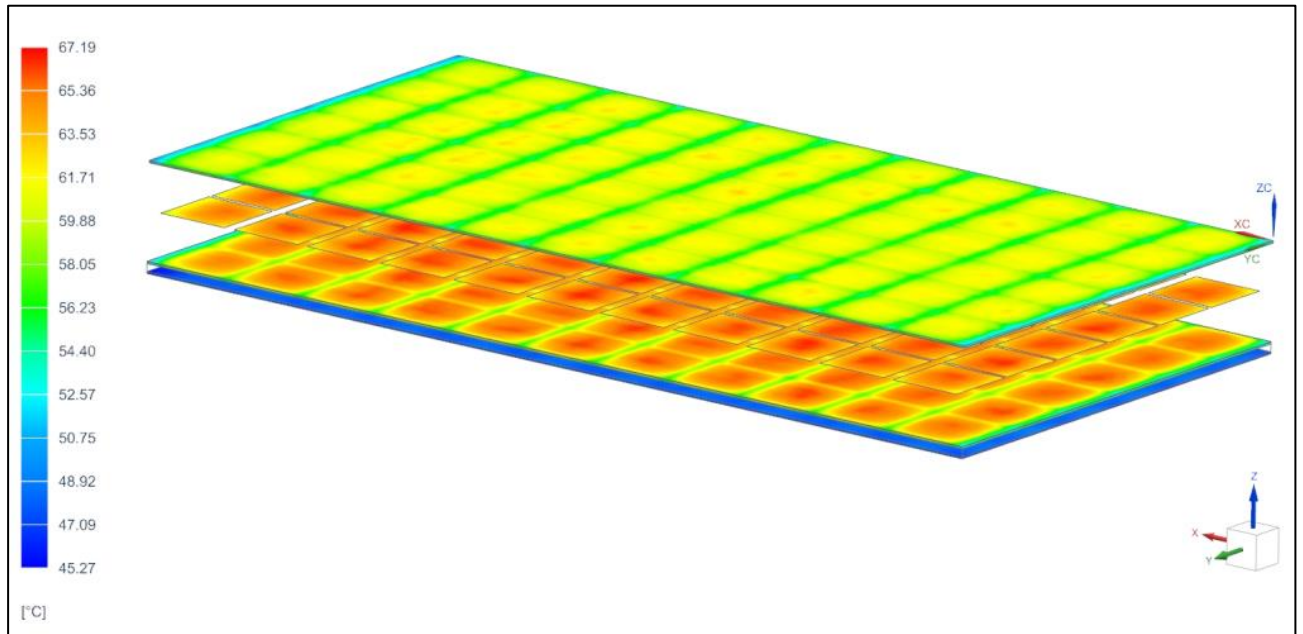


Figure 40. Temperature results of case 3 in FEM simulations. All elements.

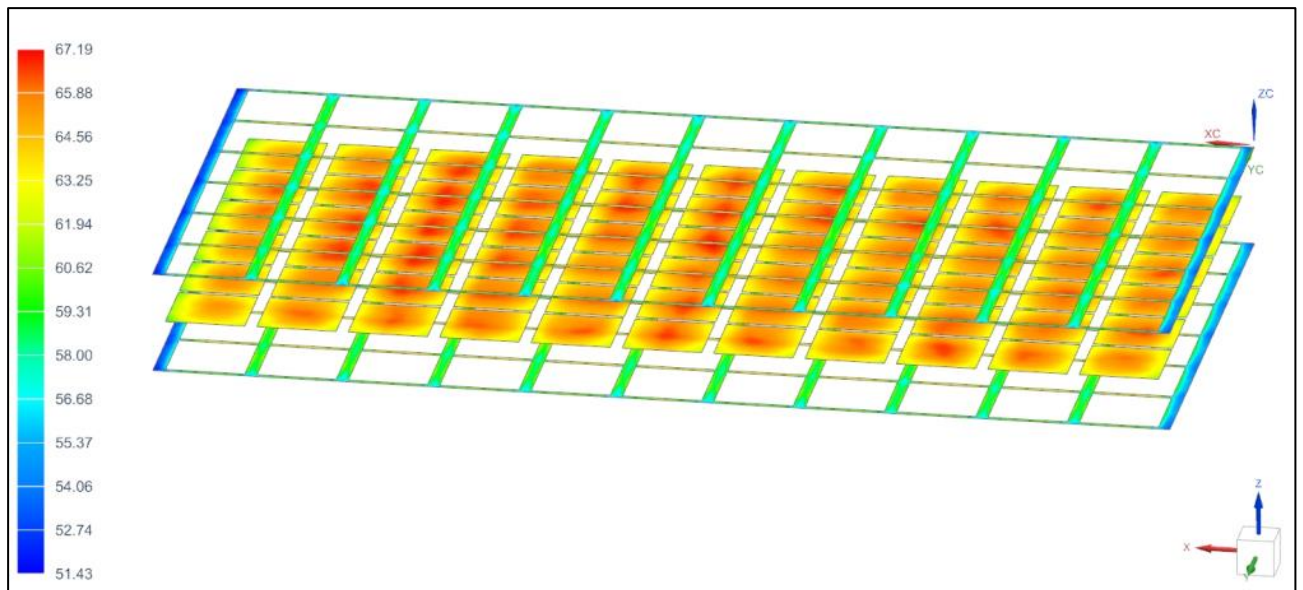


Figure 41. Temperature results of case 3 in FEM simulations. Solar cells and intermediate EVA.

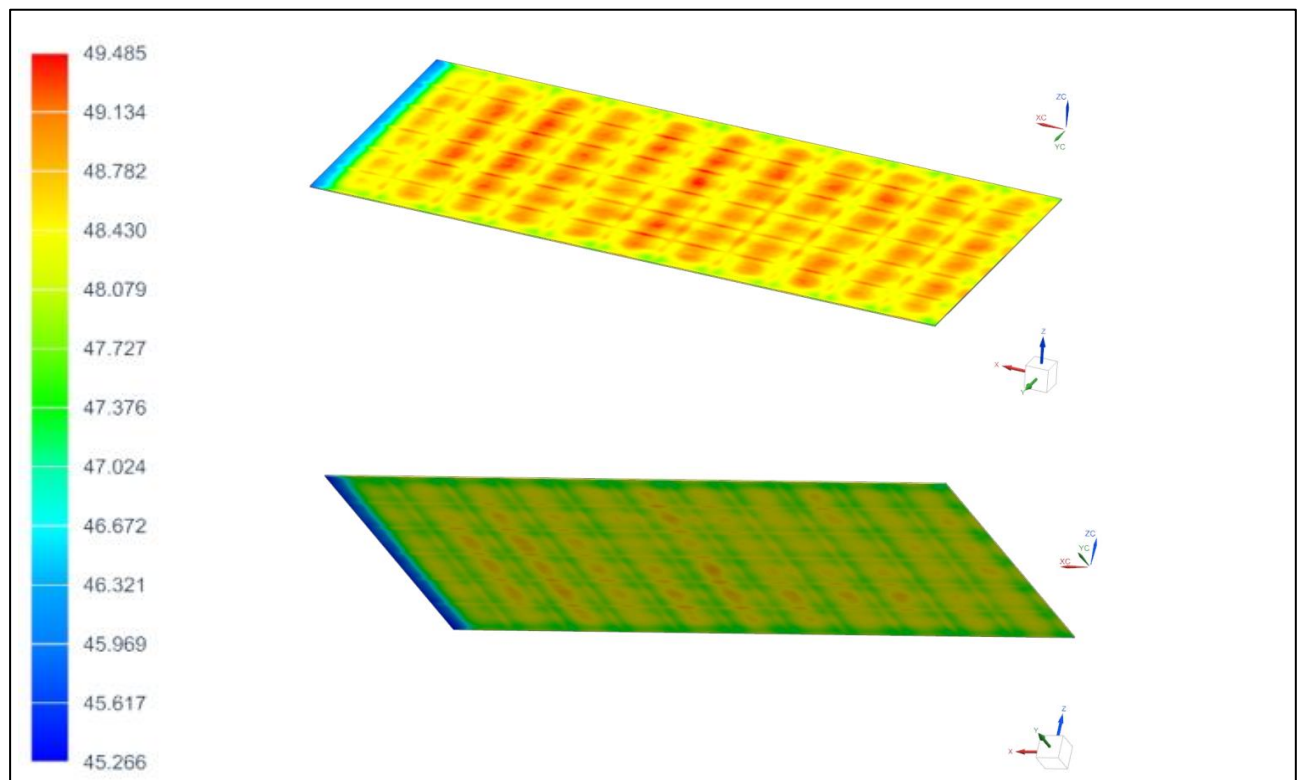


Figure 42. Temperature results of case 3 in FEM simulations. Internal (2nd) glass layer. Outer face (top) and inner face (bottom)

Going to the extreme cases represented by $R_{se}=0,13 \text{ m}^2\text{K/W}$, the temperatures of the PV cells could be as high as 112-114 °C in open circuit conditions for a 100% covered PV-IGU, and is strongly reduced (10-12 °C) if the PV glazing is in MPP conditions. If the PV coverage ratio is 80%, the temperature of PV cells is reduced about 10 °C compared to equivalent 100%. Regarding the air temperature in the cavity, it could reach about 95 °C for Voc conditions, but it decreases about 9-10 °C for MPP state. Like the temperature of PV glass, the temperature of the air cavity is also significantly reduced 8-9 °C for 80% PV occupancy compared to 100%. Therefore, **small reduction of the PV ratio and the PV conversion (MPP state) can significantly decrease the operating temperature of the PV glass in high temperature conditions, these are high outdoor temperature, high radiation and low heat evacuation.**

It is interesting to analyse the PV cells temperature of 80% with c-Si cells and 100%, both in MPP state. As the dimensions of c-Si cells are 156x156 mm, it could be thought that their temperature does not depend on the PV ratio (or occupancy) as they are big enough to have proper thermal characteristics. The results show that the average temperature of PV cells in 80% with c-Si cells in MPP are 3-4 °C lower than equivalent 100% case, and its difference with 80%-homogeneous radiation absorption is between 1-2 °C. **This means that the temperature of c-Si PV cells in an IGU glazing are affected by the PV occupancy and cannot be considered as thermally independent.** This result is linked to the glazing configuration described in Figure 32, and could be different for non-IGU PV laminated glass.

Table 42. Temperatures results of PV-IGU for FEM cases, both from FEM simulations and PV glazing thermal model. In grey, extreme cases with Rse = 0,13 m²K/W.

Case number	FEM simulations				PV GLAZING THERMAL MODEL (PVGTM)				DIFFERENCE FEM- PVGTM			
	Mean T PV cells	Mean T air	Mean T 2nd glass	ΔT airgap faces	Mean T PV cells	Mean T air	Mean T 2nd glass	ΔT airgap faces	Mean T PV cells	Mean T air	Mean T 2nd glass	ΔT airgap faces
1	74,1	63,5	53,9	18,3	74,4	63,0	51,6	21,4	-0,3	0,5	2,3	-3,1
2	68,2	58,8	50,4	16,2	68,5	58,4	48,4	18,9	-0,3	0,4	2,0	-2,7
3	64,7	55,6	48,3	13,7	63,7	55,1	46,6	16,2	1,0	0,4	1,7	-2,4
4	63,3	55,4	48,1	13,8	63,5	55,0	46,5	16,1	-0,2	0,4	1,6	-2,2
5	73,4	61,9	51,4	20,0	73,8	61,5	49,2	23,1	-0,4	0,3	2,1	-3,1
6	67,6	57,4	48,1	17,7	68,0	57,1	46,3	20,5	-0,4	0,3	1,8	-2,7
7	64,1	54,3	46,3	15,1	63,3	54,0	44,7	17,5	0,9	0,3	1,6	-2,4
8	62,8	54,1	46,1	15,2	63,1	53,9	44,6	17,5	-0,3	0,2	1,5	-2,3
9	73,1	61,2	50,3	20,8	73,6	60,9	48,2	23,9	-0,4	0,3	2,1	-3,1
10	67,4	56,8	47,2	18,4	67,8	56,6	45,4	21,1	-0,4	0,2	1,8	-2,7
11	63,9	53,8	45,5	15,7	63,1	53,5	43,9	18,1	0,8	0,3	1,6	-2,4
12	62,6	53,6	45,3	15,8	62,9	53,4	43,8	18,0	-0,3	0,2	1,5	-2,3
13	111,7	94,4	79,1	28,9	114,4	95,3	76,2	35,3	-2,7	-0,9	2,8	-6,4
14	99,8	84,4	70,7	25,9	102,1	85,2	68,2	31,5	-2,4	-0,8	2,5	-5,6
15	91,4	76,9	64,9	22,4	92,1	77,4	62,7	27,4	-0,6	-0,5	2,2	-5,0
16	89,8	76,5	64,6	22,5	91,7	77,1	62,5	27,3	-2,0	-0,6	2,1	-4,7
17	108,8	89,9	73,1	31,7	111,8	91,2	70,5	38,2	-3,0	-1,2	2,6	-6,6
18	97,3	80,7	65,7	28,3	100,0	81,7	63,5	34,0	-2,6	-1,0	2,2	-5,7
19	89,4	73,7	60,6	24,5	90,2	74,4	58,6	29,5	-0,9	-0,7	2,0	-5,0
20	87,7	73,3	60,4	24,6	89,9	74,2	58,5	29,4	-2,2	-0,9	1,9	-4,8
21	107,7	88,2	70,7	33,0	110,8	89,5	68,2	39,5	-3,0	-1,3	2,5	-6,5
22	96,5	79,3	63,7	29,4	99,1	80,3	61,5	35,0	-2,6	-1,1	2,2	-5,6
23	88,6	72,5	58,9	25,5	89,5	73,2	57,0	30,4	-0,9	-0,7	1,9	-5,0
24	87,0	72,1	58,6	25,5	89,2	73,0	56,8	30,3	-2,2	-0,9	1,8	-4,8

Stationary vs Transient thermal behaviour of PV-IGU

The temperature of the PV laminated glass layer, within the PV-IGU, has been analysed with stationary and transient thermal FEM simulations. The purpose is to assess how the thermal inertia of the glass elements impacts on the temperature of the PV glass. This corresponds to FEM cases 25 to 76 in Table 39.

The simulated system is the PV glazing configuration showed in Figure 32 but with air instead of argon, 50% PV occupancy and homogeneous absorption of irradiation (equivalent to transparent thin film PV technology). Its thermal behaviour has been analysed during two different days in Madrid, one in January (21/01/2016), and a sunny day in September (07/09/2016), so that the irradiation and external temperature vary hourly as described in Table 39. The energy absorption of the glazing layers is the calculated optical absorption without the energy converted to electricity due to PV effect. Two system inclinations have been considered, a vertical façade (FC) and a 30° tilted skylight (SK).

The results are shown in Figure 43. The stationary results (dots) are slightly different than the transient results (line) specially when the irradiance is higher, so that the temperature variations of the glass are higher as well. However, the maximum temperature difference observed is 0,9 °C, with average absolute value deviations up to 0,22 °C, which is assumed to be reasonably low. Thus, **the stationary calculations can be considered accurate enough, with deviations lower than 1 °C compared to transient calculations.** In addition, it should be considered that in yearly, monthly, or even daily averages the temperature delay caused by the thermal inertia will be offset due to cumulative effect of data.

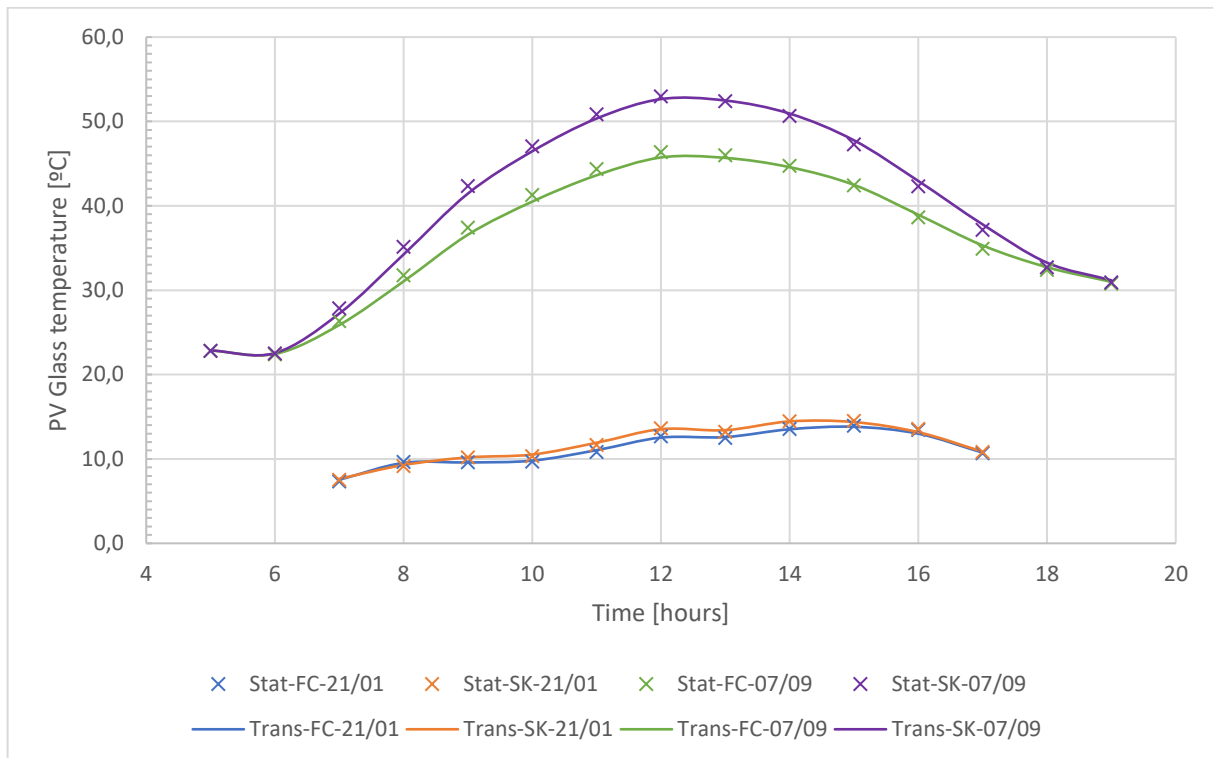


Figure 43. Outer PV glass temperature of PV-IGU calculated with stationary and transient conditions. Façade (FC) and 30° tilted skylight (SK). Meteorological data from 21st January and 7th September in Madrid.

Radiative effects vs PV cells distribution – potential impact on G value

The cases 77 to 94 of Table 39 are focused on analysing the potential thermal differences of PV glazing with same PV occupancy (50%) but different distribution of this occupancy. In the cases where the PV cells are concentrated, the temperatures reached in this area is higher while the temperature at the transparent area is lower. Even if the average temperature could be the same, the radiative thermal effects are not linear with temperature as they depend on T^4 , so the thermal irradiance may differ depending on whether the cells are concentrated or distributed.

In previous simulations, the outer surface resistance (R_{se}) was a fixed value, including both convective and radiative effects. However, in this case the R_{se} is calculated by the FEM simulation, including free convective effects calculated with CFD. Regarding the external radiative flux, it is defined as a heat flux to an environment at 15°C, which corresponding sky temperature is calculated by using the Swinbank formula:

$$T_{sky} = 0,0552 (T_{ambient} + 273,15)^{1,5}, \text{ with } T_{ambient} \text{ in Celsius scale.}$$

The boundary conditions of these cases are not the ones corresponding to evaluate the maximum temperatures but intermediate-high conditions. The outdoor temperature is 15 °C, indoor temperature of 22 °C and relatively high incident radiation of 692 W/m² direct and 180 W/m² diffuse to enhance the temperature differences between opaque and transparent areas. Then, the radiation absorption at the different layers is calculated according to incident radiation and optical properties of glass layers.

The results are shown in Table 43, where the first column indicates the maximum temperature in the PV laminated glass (1st glass layer for IGU cases), then the average temperature of the same PV laminated glass and, finally, the mean radiative flux from the external surface to the sky. As for the concentrated cell cases the half of the PV module is opaque and the other half is transparent, the outwards radiative flux of each part is also indicated for reference. Also, for these cases, the half module covered with solar cells could be at the top (-Up) or at the bottom (-Down) of the vertical module.

Regarding the punctual maximum temperature of the PV laminated glass, the highest are reached for the concentrated cells at the upper part of the module. This is because the surrounding air is hotter in these areas. The difference between Up/Down cases regarding maximum temperature is quite low for the NO-IGU PV glass but is significant in the PV-IGU case (case 77) because the hot air at the top of the cavity affects the result. In particular, **the maximum temperatures are shown by the PV-IGU with concentrated solar cells at the top**. There is an important maximum temperature difference between the concentrated and distributed, as **the concentrated PV solar cells could reach temperatures 12-14 °C higher than the distributed ones, even though the PV module has the same PV occupancy**. In addition, it is observed that in all the configurations the **maximum temperature reached in the distributed solar cell case is almost the same as the PV glass with completely homogeneous absorption**.

The mean temperature of PV laminated glass has a different behaviour. **Most cases show similar average temperatures of PV glass except the PV cells concentrated at the top, that shows about 1-2 °C lower temperature**. It seems that, in many cases, as higher is the maximum temperature reached somewhere in the module, the lower is its average temperature. However, this is not truth in every case, as the concentrated at the bottom shows similar average temperatures as distributed cells, despite their maximum temperatures are different.

The highest radiative heat fluxes of the external surface are shown by the PV-IGU, as expected due to higher insulation to the interior. The highest value is shown by the concentrated cells at the bottom while the lowest is for the homogeneous radiation absorption. However, the concentrated cells at the top shows also low average radiative heat flux. In any case, **the differences of radiative flux among the different distribution of solar cells are relatively low and do not show significant differences (<5%)**. Therefore, **it seems that the different distribution of the solar cells does not impact significantly on the radiative heat flux of the outer PV glass surface**. The Figure 44 shows the radiative heat fluxes of the external surface of 77-Up and 77-Down cases. As expected, the radiative flux is significantly higher in the area with solar cells, as its temperature is significantly higher. It is remarkable that the air movement in the cavity has an impact on the radiation flux profile of 77-Down, and thus in the temperature profile as well. This is because the high temperature at the bottom increases the air movement in the cavity.

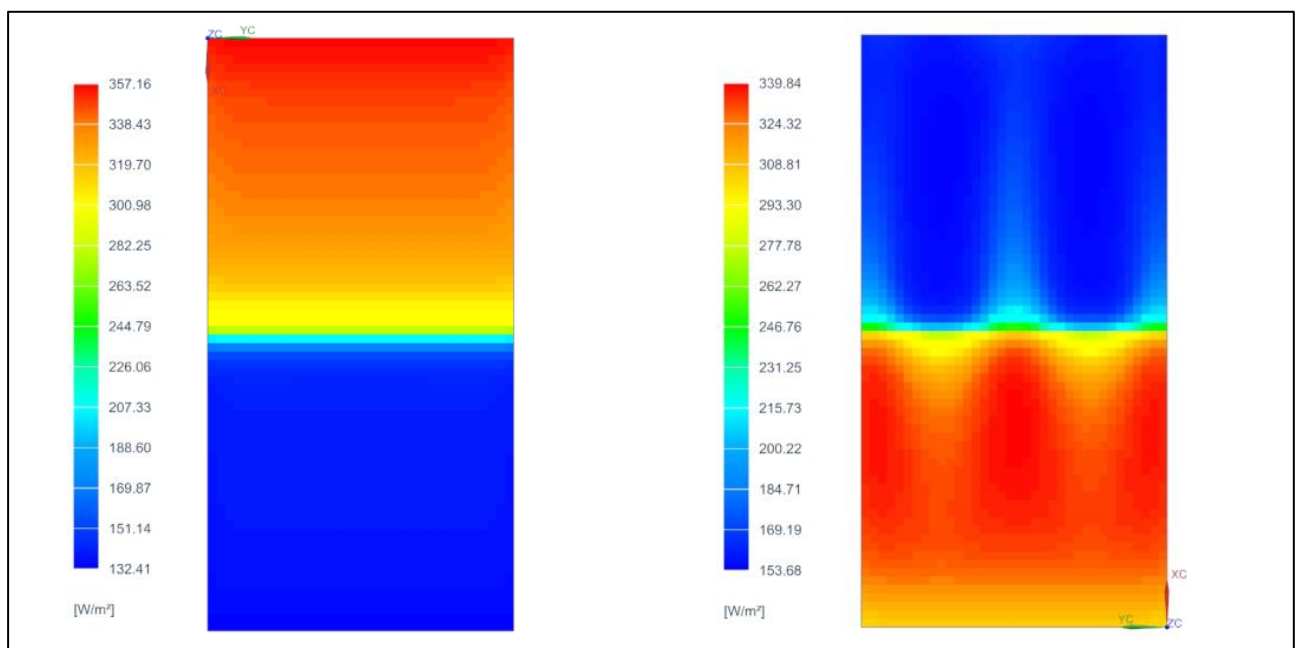


Figure 44. Radiative heat fluxes of outer surface of PV glass with 50% PV occupancy. Left: PV cells concentrated at the top. Right: PV cells concentrated at the bottom

Table 43. Temperatures and outwards radiation flux of different PV glass configurations

Case	Max T PV glass	Mean T PV glass	Mean Outwards Radiative flux [W/m ²]	Outwards Rad flux Cell area [W/m ²]	Outwards Rad flux Transp area [W/m ²]
77-Up	57,0	38,9	239	338	139
77-Down	54,7	40,3	247	328	165
78	41,3	40,3	242	-	-
79	41,4	39,7	238	-	-
80-Up	48,4	33,9	203	281	125
80-Down	48,1	35,2	211	280	141
81	36,2	35,1	205	-	-
82	36,2	34,6	202	-	-
83-Up	50,2	34,3	201	278	124
83-Down	49,9	35,6	208	277	139
84	37,3	35,5	203	-	-
85	37,3	35,0	200	-	-
86	56,8	39,4	246	350	142
87	41,4	40,5	243	-	-
88	40,9	39,7	238	-	-
89	50,1	34,9	210	291	129
90	36,7	35,7	209	-	-
91	36,8	35,2	206	-	-
92	51,8	35,3	208	287	128
93	37,8	36,0	207	-	-
94	37,8	35,5	203	-	-

7.1.5 Junction box effect on U-value and G-value

The aim of this study is to evaluate the impact of the junction box (JB) on the U and G value of the overall glazing system. The Figure 45 shows the cases studied for the analysis of the U value while the Figure 46 shows the cases for the G value. Although the thicknesses and characteristics of the objects are only indicated in PV-IGU case, they can be extrapolated to the other cases.

The simplest case is a double laminated glass, where the front glass layer is a 4 mm low iron (high transmittance) glass, then a 0,4 mm EVA with embedded solar cells and a back normal glass layer of 4 mm. The junction box (JB) is attached to the backside with default dimensions of 80 x 69 x 18 mm, composed by PPO/PPE plastic thickness of 2 mm. Between the JB and the glass, there is a black silicone layer of 2 mm thick. This is one of the most common PV glazing configurations in the market.

The second case is an IGU unit whose front side is the laminated glass previously described. Then, there is a 16 mm thick air cavity and a 4 mm normal glass layer at the back. This configuration is difficult to be found in real projects due to the difficulty to pass the electrical connections across the cavity, but its assessment is useful for reference, for potential future developments and for the more realistic PV-IGU offset case.

In the case of PV-IGU with offset, the glazing is occupied mostly by an IGU area (with or without low-e), but the cavity ends before the front laminated PV glass, so a small area has the U value corresponding to the laminated glass. The purpose of this glasses is to attach the JB easier to the backside, as normally the electrical connections from PV cells to JB cannot go through the gas cavity.

The fourth case is like the PV-IGU but including a low emissivity (LowE) coating on the inner cavity surface. Because the hemispherical emissivity of the glass normally is 0,837 and the emissivity of this coated surface is 0,04, the heat flux due to radiation between cavity surfaces is strongly reduced so that the U value as well.

Again, this configuration is difficult to be done in real projects, but its assessment is useful for reference, for potential future developments and for the more realistic PV-IGU offset case.

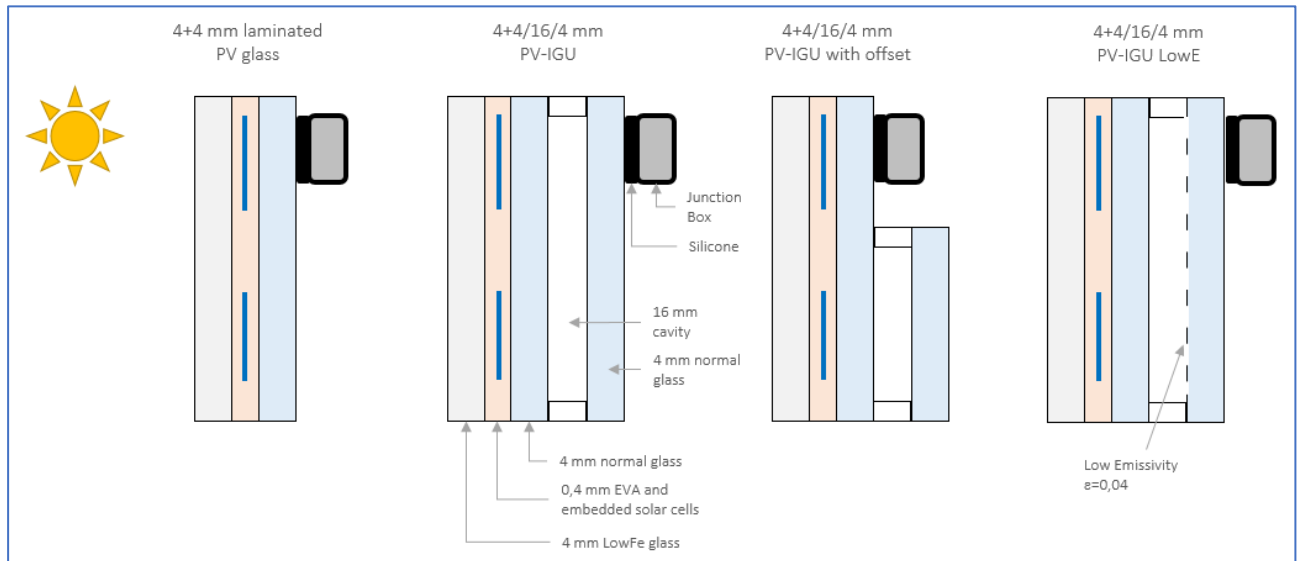


Figure 45. Sketches of the four cases where the impact of the JB on the U value has been studied. The sun represents the external side.

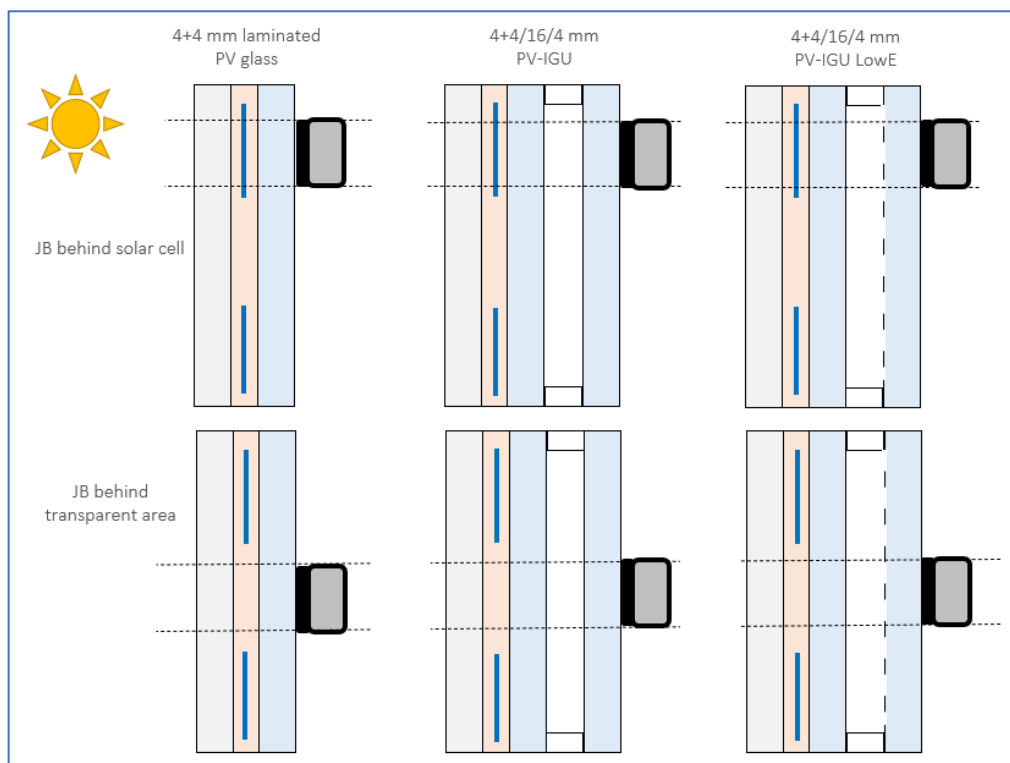


Figure 46. Sketches of the six cases where the impact of the JB on the G value has been studied. The sun represents the external side.

The standards focused on the calculation of U and G for overall windows has been used instead of centre-of-glass calculations. In these standards, it is considered the impact of additional elements others than glass like

the frames, so the JB is considered as an additional element that impacts on the overall energy properties of the system.

The junction boxes are assumed to be empty air chambers surrounded by 2 millimetres of plastic. Thus, the metallic parts and other elements inside the JB are not considered, and the box is assumed to be airtight. Possible heating due to joule effect on the electrical parts is not considered as it strongly depends on specific radiation and electrical conditions. The effect of JB cables is negligible and is not considered.

Only cases with the junction box on the back side have been considered. The junction box located at the edges of the PV glass and normally hidden in the structure/framing is not expected to affect significantly to the U or G values, except for the slight effect on the thermal transmittance of the frames in the small volume occupied.

Besides, the modules with the JB in the front side normally are not based on glass and their integration do not require to know the U and G values. Nevertheless, due to the summatory laws behind the thermal transmittance, the U value can be calculated analogously both for front and backside position of the JB. This cannot be extended to G value calculation due to different optical behaviour.

7.1.5.1 U value calculation method

From the U value viewpoint, the JB adds an extra thermal resistance to the area that occupies. This thermal resistance is calculated according to EN ISO 10077-2, which describes a numerical method to calculate the thermal resistance of windows, doors, and shutters. The method considers the limited area of the surfaces and the different view factors, so it is more appropriate than other similar standards like EN 673 or ISO 10292 that considers infinite surfaces. The convective heat fluxes have been calculated with section 6.4.2.3.2 and the radiative fluxes with section 6.4.3.4.3 of the standard. The view factors of a parallelepiped have been calculated with the formula described in (59).



Figure 47. Picture of the reference junction box and the surfaces for view factors calculation

Table 44. Data for the calculation of the thermal resistance of the JB cavity. Example for 18 mm JB thickness and $\Delta T=7,5$ K (on IGU)

Total JB resistance	0,2367	m2K/W	Air cavity + 2 mm silicone + 2 mm PPO/PPE
Air cavity JB resistance	0,2207	m2K/W	ISO 10077-2
Radiation conductance	3,101	W/m2K	ISO 10077-2 6.4.3.4.3
Emissivity	0,9	-	Common for polymers
Average gas temp	283	K	EN 673 / ISO 10292
F1 → 2	0,6398	-	(59) View factor
F1 → 3-4	0,0973	-	(59) View factor
F1 → 5-6	0,0828	-	(59) View factor
Gas conductance	1,429	W/m2K	ISO 10077-2 6.4.2.3.2
JB Height	0,080	m	Fixed
JB Thickness	0,018	m	Variable
JB Width	0,069	m	Fixed
C	0,73	W/(m ² K ^{4/3})	ISO 10077-2 6.4.2.3.2
ΔT	7,5	K	EN 673 / ISO 10292
Air conductivity	0,025	W/mK	ISO 10077-2 6.4.2.3.2
Nusselt	1,03	-	ISO 10077-2 6.4.2.3.2
Equivalent air conductivity	0,0257	W/mK	ISO 10077-2 6.4.2.3.2

The Figure 47 shows the picture of the junction box that have been used for reference. Its dimensions and other data for the calculations are described in

Table 44. This table shows, in blue, the parameters used for the calculation of thermal conductance due to convection and, in yellow, the ones for radiation among surfaces.

The total JB cavity resistance is 0,2207 m²K/W for this example. However, there are some inputs that have been parametrized to perform different studies that are shown in italics and bold. The studies include the thickness variation from 10 to 26 mm, their impact in the view factors, and the final thermal resistance of the cavity.

According to EN 673 and ISO 10292, the temperature difference between the cavity surfaces (ΔT) is 15 K when a glazing system only has one cavity, so 15 K has been used for a PV laminated glass with JB. However, when the JB is placed on a IGU unit with already one cavity, the JB cavity is the second one in the system, Thus, for these cases, the 15 K temperature difference among faces is assumed to be equally distributed between cavities so that the first has $\Delta T = 7,5$ K and the second one also has $\Delta T = 7,5$ K. As already seen in Table 24, the ΔT parameter impacts on the final thermal resistance. Besides, the ISO 10077-2 proposes 10 K instead of 15 K but, as most of the area involves a glazing system according to EN 673 and the ISO 10077-2 is applied only to the small area that represents the JB, the EN 673 and ISO 10292 boundary conditions are considered a better option.

The thickness of the silicone between the JB and the backside of the glass is assumed to be 2 mm. The thermal conductivity of the polymeric materials like the silicone, the PPO/PPE used for the JB case, and the EVA, are assumed to be 0,25 W/mK. The internal surface resistance of the JB area is 0,125 W/m²K (instead of 0,13) according to the higher emissivity of PPO/PPE compared to the glass (0,9 instead of 0,837).

Other parameters for the calculation of the thermal resistances of the glazing are as detailed in EN 673 and ISO 10292 for vertical glazing.

The final U value of the whole glazing is assumed to be proportional to the area occupied by the JB and the area without the JB according to the following formula:

$$U' = \frac{A_{JB}}{A_T} * U_{G \& JB} + \frac{A_T - A_{JB}}{A_T} * U_0$$

Where A_{JB} is the area occupied by the junction box, A_T is the total PV glass area, $U_{G \& JB}$ is the thermal transmittance of the glass with JB system, and U_0 is the thermal transmittance of the glass system without the effect of JB. This formula follows the criteria described in EN ISO 6946 section 6.7.2.

Similarly, for the PV-IGU with offset case, the U value is calculated according to the area occupied by the three different systems: PV-IGU, PV laminated without JB, and PV laminated with JB.

7.1.5.2 G value calculation method

The G value is the sum of the solar transmittance (T_{solar}) and the heat absorbed by the glass system elements and reemitted to the interior (q_i). The thermal resistances are needed for the calculation of the second term, so the previous calculations explained for the U value are also inputs of the G value calculation.

$$g = T_{solar} + q_i$$

The solar transmittance, reflectance and absorption have been calculated for the different glazing cases described in Figure 46, i.e. transparent area of the laminated glass, the PV-IGU and PV-IGU with LowE, and the opaque area of the solar cell. The transmittance of the solar cell is assumed to be 0, which means that is a common monofacial solar cell. The calculations are based on EN 410 so, the solar spectrum used is the AM1.0 (instead of AM1.5 used in other standards) among other characteristics described in this standard. The G value has been calculated at normal incidence of light i.e. no angular effects have been considered. The absorbed radiation in the PV area do not consider the photovoltaic energy conversion, so the data is calculated for open-circuit conditions and not MPP conditions.

The optical data of the laminated unit has been calculated from the data of independent layers and their characteristics are shown in Figure 48. The data from the low iron (LowFe) high transmittance glass, the normal glass and the LowE glass (NFRC ID 4375) were taken from Optics software database, while the tau of encapsulant was calculated from the experimental data of a laminated unit. The optical properties of the glass with black silicon, required for the JB on transparent area, were measured experimentally.

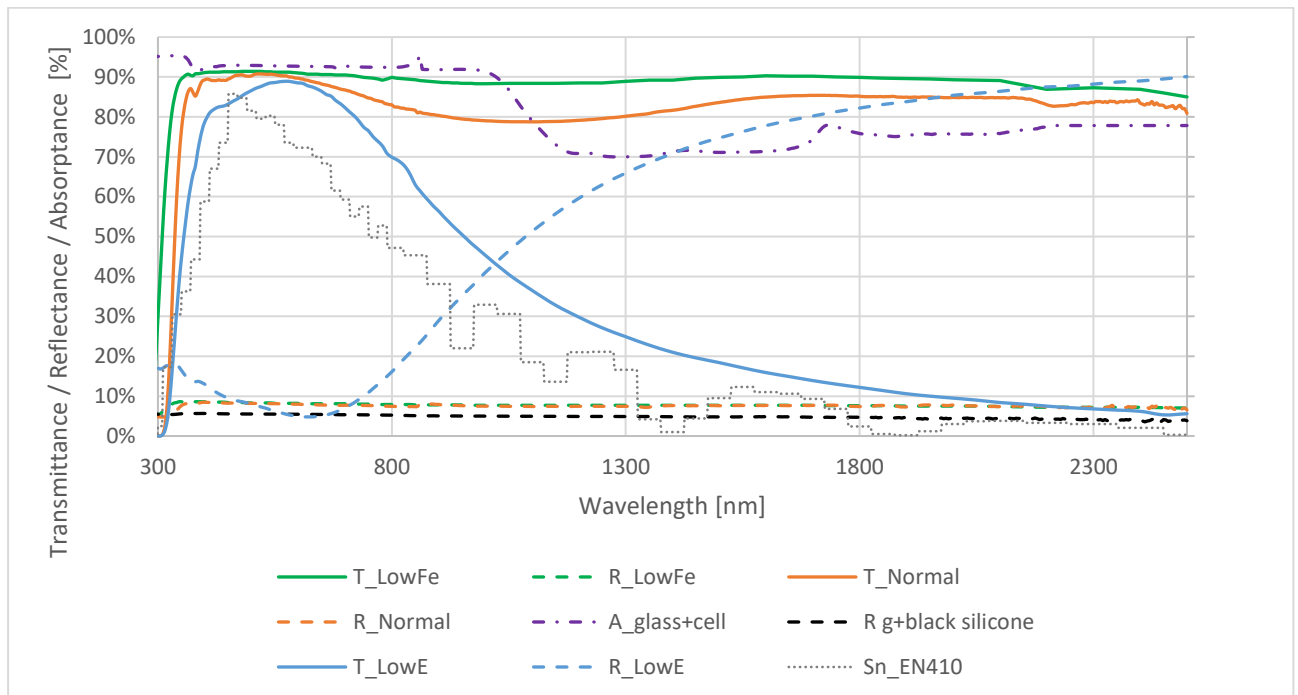


Figure 48. Optical data of glass layers used for the calculation of the optical properties of the laminated PV glass, PV-IGU and PV-IGU Low E.

The obtained optical data of the transparent areas of laminated glass, IGU and IGU Low E are shown in Figure 49.

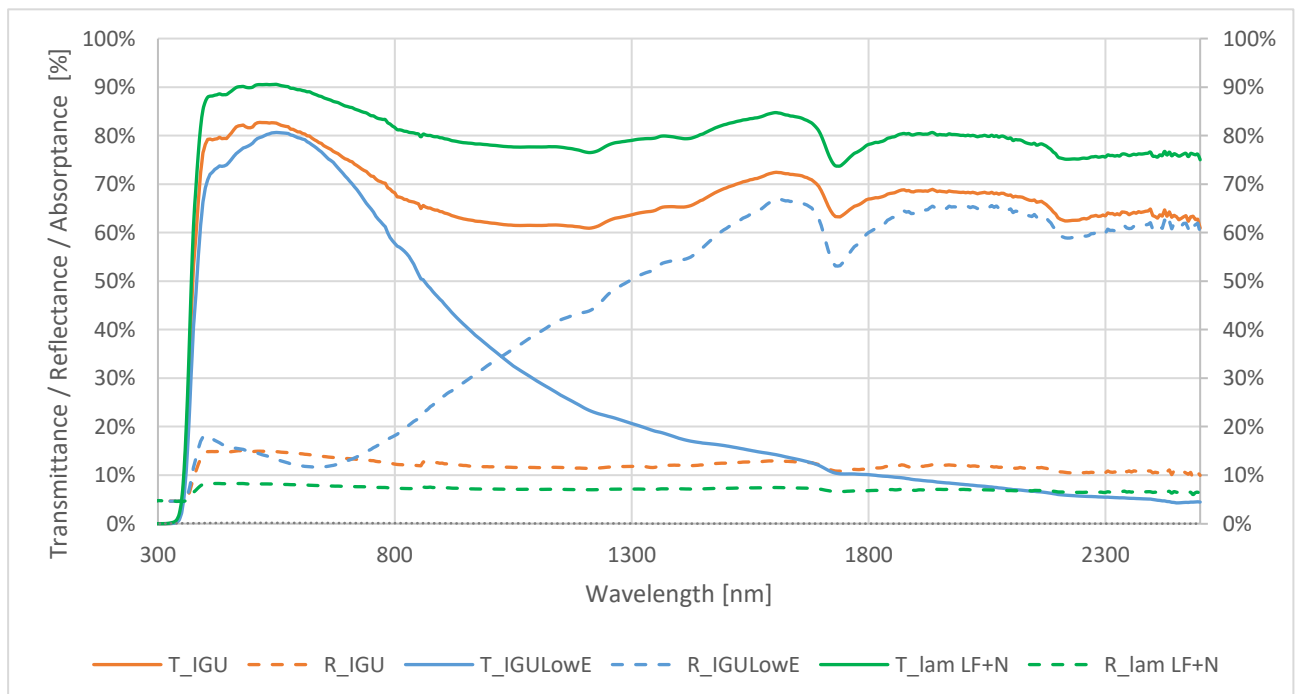


Figure 49. Optical data of the transparent areas of laminated glass, IGU and IGU Low E.

The general formula for the calculation of q_i for systems up to two cavities is:

$$q_i = \frac{\frac{\alpha_{e3}}{\Lambda_{23}} + \frac{\alpha_{e3} + \alpha_{e2}}{\Lambda_{12}} + \frac{\alpha_{e3} + \alpha_{e2} + \alpha_{e1}}{h_e}}{\frac{1}{h_i} + \frac{1}{h_e} + \frac{1}{\Lambda_{12}} + \frac{1}{\Lambda_{23}}}$$

Where α_{e1} , α_{e2} and α_{e3} is the solar absorption at the three layers that forms the two cavities; h_e and h_i are the external and internal heat transfer coefficients; Λ_{12} and Λ_{23} are the thermal conductance from the external glass surface to the middle point of the second glass, and from the middle point of second glass to the internal surface.

Similar to the calculation of the U value, the G value of the overall glass can be calculated as the area weighted G values of the different optical-thermal areas, as described in EN 410 Annex C, following this equation:

$$G = \frac{A_1}{A_T} * G_1 + \frac{A_2}{A_T} * G_2 + \dots$$

7.1.5.3 Results for specific JB dimensions

The Figure 50, Figure 51 and Figure 52 shows the U and G values of the different areas that can be found in a laminated PV, PV-IGU and PV-IGU LowE respectively. This is the U value of the area with and without the JB, and the G value of the area with and without the JB, both in the transparent and solar cell area. These results are specifically for the JB with dimensions of 80 mm height, 69 mm width and 18 mm depth (or thickness) and the glazing configurations described in Figure 45.

In terms of U value, the highest value corresponds to laminated glass only, with a value of 5,45 W/m²K. Then, the U value of the area with laminated glass and JB is like the IGU case (2,49 and 2,69 W/m²K respectively), which makes sense as in both cases there is an air cavity. Then, the area of IGU with JB has a very low U value, like the triple IGU glazing with two cavities. Finally, as expected, the IGU with LowE has a quite low U value (1,36 W/m²K) that is even lower in the area with a JB (1,02 W/m²K).

In terms of G, the highest values are for the transparent areas with 84%, 75% and 62% for laminated, IGU and IGU-LowE respectively. The transparent areas with JB have G values of 10%, 32% and 41% for laminated, IGU and IGU-LowE respectively, where the two last ones are relatively high because the heat absorbed by the JB area is insulated from the outside by the cavity. However, the JB is not normally in the transparent area as it is normally hidden behind solar cells. The solar cell areas without the JB have G values of 21%, 10% and 4% for laminated, IGU and IGU-LowE respectively. Finally, the solar cell areas with JB have G values of 9%, 6% and 4% for laminated, IGU and IGU-LowE, which are the lowest values.

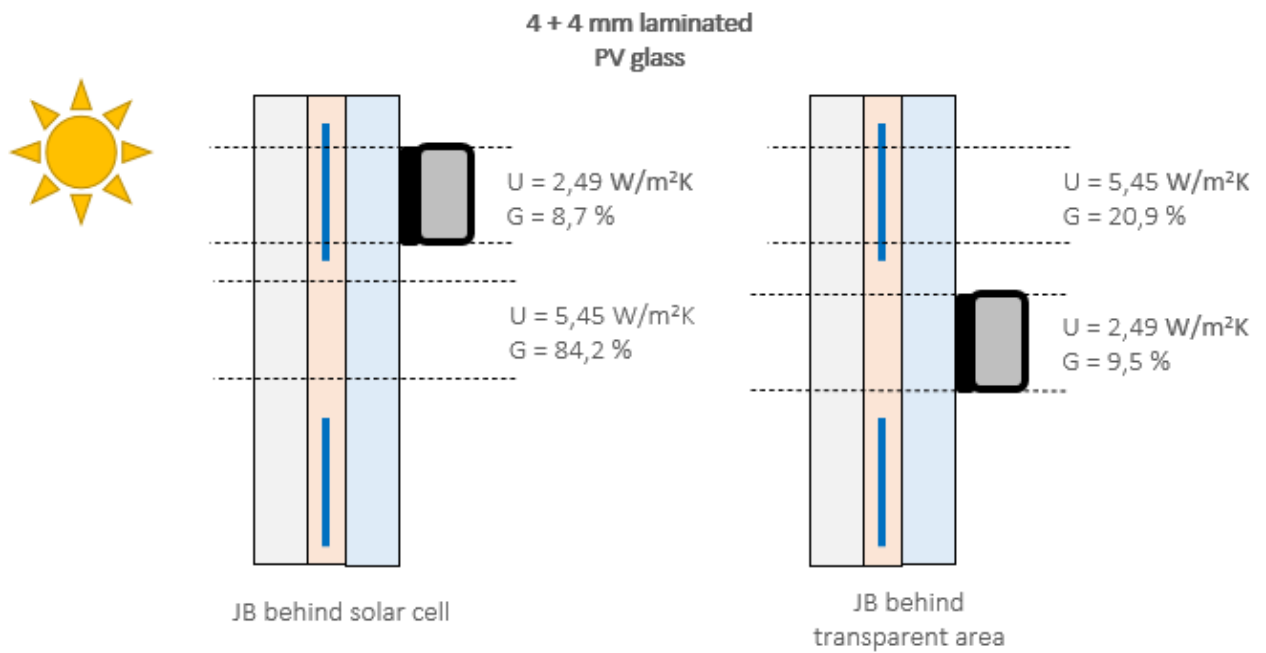


Figure 50. U and G value for PV double laminated glass with 4 mm Low iron and 4 mm normal glass. Results for JB with dimensions 80 x 69 x 18 mm (H x W x D)

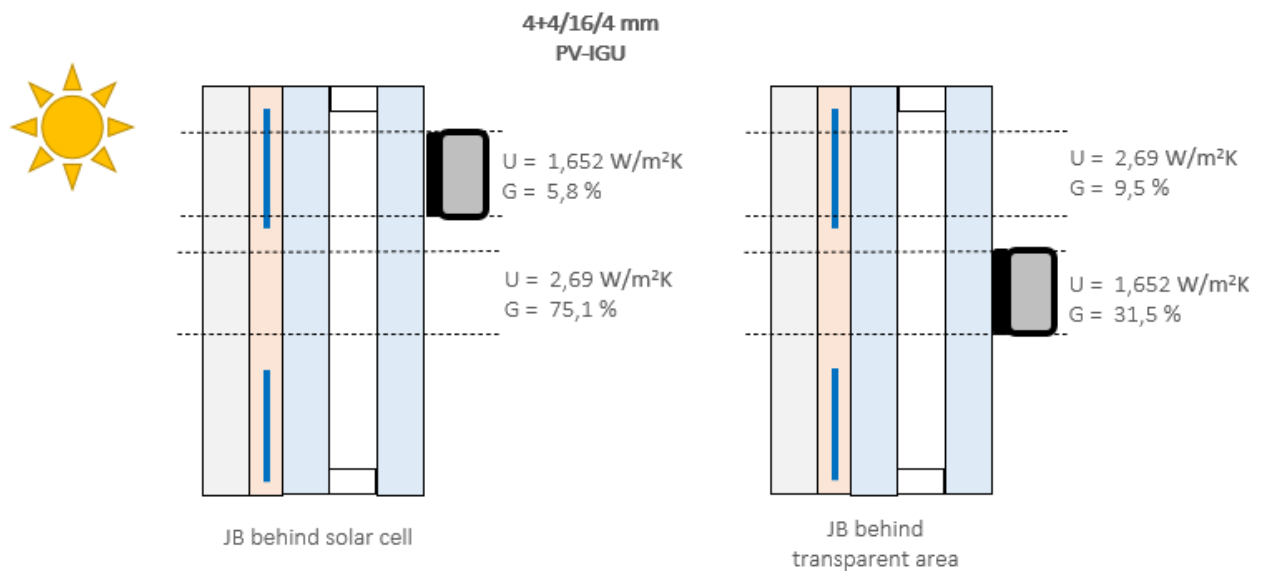


Figure 51. U and G value for PV-IGU with previously PV laminated glass plus 16 mm cavity and back normal glass. Results for JB with dimensions 80 x 69 x 18 mm (H x W x D)

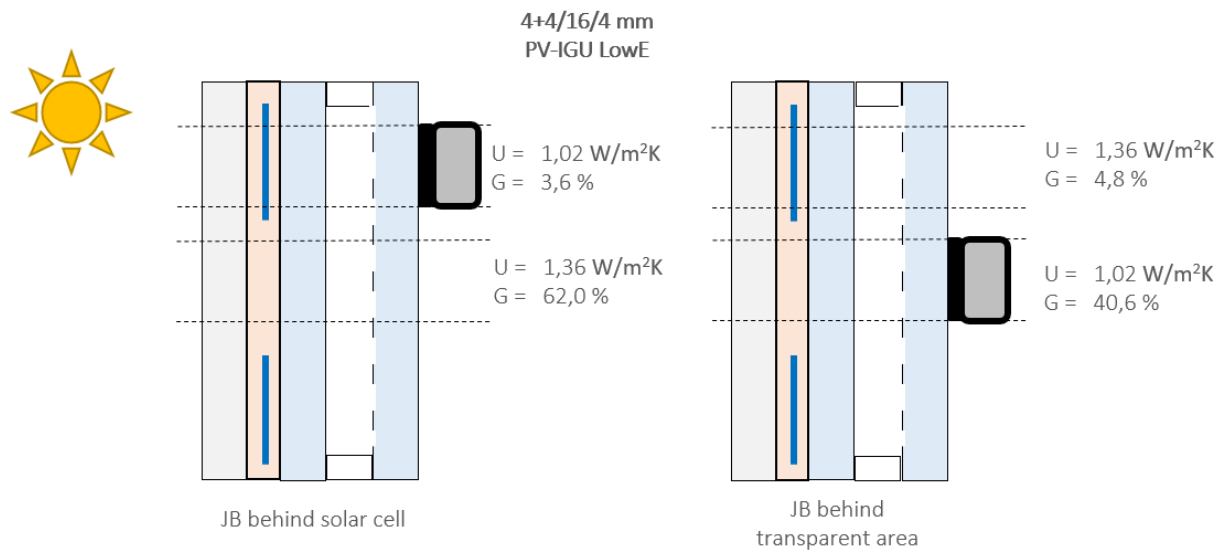


Figure 52. U and G value for PV-IGU LowE with previously PV laminated glass plus 16 mm cavity and back low emissivity glass. Results for JB with dimensions 80 x 69 x 18 mm (H x W x D)

7.1.5.4 Generalized U value results for different JB dimensions

As the dimensions of the JB could be different, the thermal resistance of the junction box has been analyzed for different dimensions and thicknesses, the results are shown in Table 45 and Table 46. The calculations assume that the JB has a squared shape with the same height and the width, while the thickness (or depth) of the JB is independent and goes from 10 mm to 26 mm.

The Table 45 shows the results when the temperature differences between cavity faces (ΔT) is 15 K, which means that the JB cavity is the only cavity in the system. In other words, Table 45 should be used with JB attached to PV laminated glass. The Table 46 shows the results when the temperature differences between cavity faces (ΔT) is 7,5 K, which means that the JB cavity is the second cavity in the system. Thus, Table 46 should be used with JB attached to PV-IGU units with one cavity.

Table 45. Thermal resistance of a squared shape JB (Height = Width) for different surfaces and thicknesses. 15 K as temperature difference between cavity faces, i.e. to be used with no-IGU PV glazing

		Thermal resistance of JB [m ² K/W] for different JB thicknesses and Height/Width [mm]; $\Delta T = 15$ K									
		10	12	14	16	18	20	22	24	26	
JB Surface [cm ²] / Height and Width [mm]	9 30	0,202	0,222	0,238	0,240	0,241	0,240	0,239	0,237	0,234	
	16 40	0,195	0,215	0,231	0,234	0,237	0,239	0,240	0,241	0,240	
	25 50	0,191	0,209	0,224	0,228	0,232	0,234	0,237	0,238	0,240	
	36 60	0,187	0,204	0,219	0,223	0,226	0,229	0,232	0,234	0,236	
	49 70	0,184	0,201	0,215	0,218	0,222	0,225	0,228	0,230	0,232	
	64 80	0,182	0,198	0,211	0,215	0,218	0,221	0,224	0,226	0,229	
	81 90	0,180	0,196	0,209	0,212	0,215	0,218	0,220	0,223	0,225	
	100 100	0,179	0,194	0,206	0,209	0,212	0,215	0,217	0,220	0,222	
	121 110	0,178	0,192	0,204	0,207	0,210	0,212	0,215	0,217	0,219	
	144 120	0,177	0,191	0,203	0,205	0,208	0,210	0,212	0,215	0,217	
	169 130	0,176	0,190	0,201	0,204	0,206	0,208	0,210	0,213	0,215	
	196 140	0,175	0,189	0,200	0,202	0,204	0,207	0,209	0,211	0,213	
	225 150	0,175	0,188	0,199	0,201	0,203	0,205	0,207	0,209	0,211	
	256 160	0,174	0,187	0,198	0,200	0,202	0,204	0,206	0,208	0,210	
289 170	0,174	0,187	0,197	0,199	0,201	0,203	0,205	0,206	0,208		

324	180	0,173	0,186	0,196	0,198	0,200	0,202	0,203	0,205	0,207
361	190	0,173	0,185	0,196	0,197	0,199	0,201	0,202	0,204	0,206
400	200	0,172	0,185	0,195	0,197	0,198	0,200	0,202	0,203	0,205

Table 46. Thermal resistance of a squared shape JB (Height = Width) for different surfaces and thicknesses. 7,5 K as temperature different between cavity faces, i.e. to be used with one cavity PV IGU glazing

		Thermal resistance of JB [m ² K/W] for different JB thicknesses and Height/Width [mm]; ΔT = 7,5 K								
		10	12	14	16	18	20	22	24	26
JB Surface [cm ²] / Height and Width [mm]	9 30	0,202	0,222	0,239	0,253	0,261	0,261	0,259	0,256	0,253
	16 40	0,195	0,215	0,232	0,246	0,257	0,259	0,261	0,261	0,261
	25 50	0,191	0,209	0,225	0,240	0,250	0,254	0,256	0,258	0,260
	36 60	0,187	0,204	0,220	0,234	0,244	0,248	0,251	0,254	0,256
	49 70	0,184	0,201	0,215	0,229	0,239	0,242	0,246	0,249	0,251
	64 80	0,182	0,198	0,212	0,225	0,234	0,238	0,241	0,244	0,247
	81 90	0,180	0,196	0,209	0,221	0,231	0,234	0,237	0,240	0,243
	100 100	0,179	0,194	0,207	0,219	0,227	0,231	0,234	0,236	0,239
	121 110	0,178	0,192	0,205	0,216	0,225	0,228	0,231	0,233	0,236
	144 120	0,177	0,191	0,203	0,214	0,222	0,225	0,228	0,231	0,233
	169 130	0,176	0,190	0,202	0,212	0,220	0,223	0,226	0,228	0,231
	196 140	0,175	0,189	0,201	0,211	0,219	0,221	0,224	0,226	0,228
	225 150	0,175	0,188	0,199	0,210	0,217	0,219	0,222	0,224	0,226
	256 160	0,174	0,187	0,199	0,208	0,216	0,218	0,220	0,222	0,224
	289 170	0,174	0,187	0,198	0,207	0,215	0,217	0,219	0,221	0,223
324 180	0,173	0,186	0,197	0,207	0,213	0,216	0,218	0,219	0,221	
361 190	0,173	0,185	0,196	0,206	0,212	0,214	0,216	0,218	0,220	
400 200	0,172	0,185	0,196	0,205	0,212	0,213	0,215	0,217	0,219	

The impact of the JB on the module's U value depends on the relative area occupied by the JB. In this sense, the Table 47, Table 48 and Table 49 shows the reduction of the U value for different ratios occupied by the JB, and different JB thicknesses. As these results are the reduction of the initial U without the JB, they should be deducted from the center-of-glass U value to get the U value of the system with the JB, according to:

$$U' = U_0 - \Delta U$$

The surface area consider for the JB is the area of the surface in direct contact with the glass, which normally is also the area of the outer surface (the cover). The other surfaces of the JB are not considered.

To assess the real impact, the following example is proposed. In the case of a laminated 4 mm + 4mm glass (Table 47) the U value is 5,45 W/m²K (Figure 50). If the glass surface is 1 m² and the JB is 10 x 10 x 2 cm, the JB occupies the 1% of the module area, so the U value of the overall PV glass is 5,45-0,03 = 5,42 W/m²K, which represents a reduction of 0,5%. This means that the impact of normal size JB is lower than 1% on double laminated modules bigger than 1 m². However, **if the 4+4 mm module is small and the JB occupies an important part of it (e.g. more than 2% of the surface) it can reduce the final U value more than 1%.**

Table 47. Reduction of overall PV module U value due (ΔU) to junction box [W/m²K] (4mm+4mm laminated)

		JB Thickness [mm]								
		10	12	14	16	18	20	22	24	26
Module area occupied by	0,20%	0,005	0,006	0,006	0,006	0,006	0,006	0,006	0,006	0,006
	0,40%	0,011	0,011	0,012	0,012	0,012	0,012	0,012	0,012	0,012
	0,60%	0,016	0,017	0,017	0,018	0,018	0,018	0,018	0,018	0,018
	0,80%	0,021	0,022	0,023	0,023	0,024	0,024	0,024	0,024	0,024

1,00%	0,027	0,028	0,029	0,029	0,029	0,030	0,030	0,030	0,030
1,20%	0,032	0,034	0,035	0,035	0,035	0,036	0,036	0,036	0,036
1,40%	0,038	0,039	0,041	0,041	0,041	0,041	0,042	0,042	0,042
1,60%	0,043	0,045	0,046	0,047	0,047	0,047	0,048	0,048	0,048
1,80%	0,048	0,050	0,052	0,053	0,053	0,053	0,054	0,054	0,054
2,00%	0,054	0,056	0,058	0,058	0,059	0,059	0,060	0,060	0,060
2,20%	0,059	0,062	0,064	0,064	0,065	0,065	0,066	0,066	0,066
2,40%	0,064	0,067	0,070	0,070	0,071	0,071	0,071	0,072	0,072
2,60%	0,070	0,073	0,075	0,076	0,076	0,077	0,077	0,078	0,078
2,80%	0,075	0,079	0,081	0,082	0,082	0,083	0,083	0,084	0,084
3,00%	0,081	0,084	0,087	0,088	0,088	0,089	0,089	0,090	0,090
3,20%	0,086	0,090	0,093	0,093	0,094	0,095	0,095	0,096	0,096
3,40%	0,091	0,095	0,099	0,099	0,100	0,101	0,101	0,102	0,102
3,60%	0,097	0,101	0,104	0,105	0,106	0,107	0,107	0,108	0,108
3,80%	0,102	0,107	0,110	0,111	0,112	0,112	0,113	0,114	0,114
4,00%	0,107	0,112	0,116	0,117	0,118	0,118	0,119	0,120	0,120
4,20%	0,113	0,118	0,122	0,123	0,124	0,124	0,125	0,126	0,126
4,40%	0,118	0,123	0,127	0,128	0,129	0,130	0,131	0,132	0,132
4,60%	0,124	0,129	0,133	0,134	0,135	0,136	0,137	0,138	0,138
4,80%	0,129	0,135	0,139	0,140	0,141	0,142	0,143	0,144	0,144
5,00%	0,134	0,140	0,145	0,146	0,147	0,148	0,149	0,150	0,150

In the case of PV-IGU without low-emissivity coating (Table 47) the center-of-glass U value is 2,69 W/m²K (Figure 51). For the previous example of 1 m² glass where the JB occupies the 1% of the area, the final U value would be 2,69 – 0,01 = 2,68 W/m²K, which represents a reduction of 0,3%. **For PV-IGU, a reduction in the U value higher than 0,01 W/m²K is expected for the cases where the JB represents more than 1% of the module area.**

Table 48. Reduction of overall PV module U value (ΔU) due to junction box [W/m²K] (4mm+4mm / 16mm / 4mm)

		JB Thickness [mm]								
		10	12	14	16	18	20	22	24	26
Module area occupied by JB [%]	0,20%	0,002	0,002	0,002	0,002	0,002	0,002	0,002	0,002	0,002
	0,40%	0,004	0,004	0,004	0,004	0,004	0,004	0,004	0,004	0,004
	0,60%	0,005	0,006	0,006	0,006	0,006	0,006	0,006	0,006	0,006
	0,80%	0,007	0,007	0,008	0,008	0,008	0,008	0,008	0,009	0,009
	1,00%	0,009	0,009	0,010	0,010	0,010	0,010	0,011	0,011	0,011
	1,20%	0,011	0,011	0,012	0,012	0,012	0,013	0,013	0,013	0,013
	1,40%	0,012	0,013	0,014	0,014	0,015	0,015	0,015	0,015	0,015
	1,60%	0,014	0,015	0,016	0,016	0,017	0,017	0,017	0,017	0,017
	1,80%	0,016	0,017	0,018	0,018	0,019	0,019	0,019	0,019	0,019
	2,00%	0,018	0,019	0,019	0,020	0,021	0,021	0,021	0,021	0,021
	2,20%	0,019	0,020	0,021	0,022	0,023	0,023	0,023	0,023	0,024
	2,40%	0,021	0,022	0,023	0,024	0,025	0,025	0,025	0,026	0,026
	2,60%	0,023	0,024	0,025	0,026	0,027	0,027	0,027	0,028	0,028
	2,80%	0,025	0,026	0,027	0,028	0,029	0,029	0,030	0,030	0,030
	3,00%	0,026	0,028	0,029	0,030	0,031	0,031	0,032	0,032	0,032
	3,20%	0,028	0,030	0,031	0,032	0,033	0,034	0,034	0,034	0,034
	3,40%	0,030	0,032	0,033	0,034	0,035	0,036	0,036	0,036	0,036
	3,60%	0,032	0,033	0,035	0,036	0,037	0,038	0,038	0,038	0,039
	3,80%	0,033	0,035	0,037	0,038	0,039	0,040	0,040	0,040	0,041
	4,00%	0,035	0,037	0,039	0,040	0,042	0,042	0,042	0,043	0,043
4,20%	0,037	0,039	0,041	0,042	0,044	0,044	0,044	0,045	0,045	

4,40%	0,039	0,041	0,043	0,044	0,046	0,046	0,047	0,047	0,047
4,60%	0,040	0,043	0,045	0,047	0,048	0,048	0,049	0,049	0,049
4,80%	0,042	0,045	0,047	0,049	0,050	0,050	0,051	0,051	0,051
5,00%	0,044	0,047	0,049	0,051	0,052	0,052	0,053	0,053	0,054

In the case of PV-IGU with low emissivity coating (Table 49), the center-of-glass U value is 1,36 W/m²K (Figure 52). Following the example of 1 m² glass with a JB that occupies the 1% of its area, the U value is reduced 0,003/1,36 = 0,2%. **For PV-IGU with LowE, a reduction in the U value higher than 0,01 W/m²K is expected for the cases where the JB represents more than 3% of the module area.**

Table 49. Reduction of overall PV module U value (ΔU) due to junction box [W/m²K] (4mm+4mm / 16mm / 4mm LowE)

		JB Thickness [mm]								
		10	12	14	16	18	20	22	24	26
Module area occupied by JB [%]	0,20%	0,001	0,001	0,001	0,001	0,001	0,001	0,001	0,001	0,001
	0,40%	0,001	0,001	0,001	0,001	0,001	0,001	0,001	0,001	0,001
	0,60%	0,002	0,002	0,002	0,002	0,002	0,002	0,002	0,002	0,002
	0,80%	0,002	0,002	0,003	0,003	0,003	0,003	0,003	0,003	0,003
	1,00%	0,003	0,003	0,003	0,003	0,003	0,003	0,004	0,004	0,004
	1,20%	0,003	0,004	0,004	0,004	0,004	0,004	0,004	0,004	0,004
	1,40%	0,004	0,004	0,004	0,005	0,005	0,005	0,005	0,005	0,005
	1,60%	0,005	0,005	0,005	0,005	0,006	0,006	0,006	0,006	0,006
	1,80%	0,005	0,005	0,006	0,006	0,006	0,006	0,006	0,006	0,006
	2,00%	0,006	0,006	0,006	0,007	0,007	0,007	0,007	0,007	0,007
	2,20%	0,006	0,007	0,007	0,007	0,008	0,008	0,008	0,008	0,008
	2,40%	0,007	0,007	0,008	0,008	0,008	0,008	0,008	0,009	0,009
	2,60%	0,007	0,008	0,008	0,009	0,009	0,009	0,009	0,009	0,009
	2,80%	0,008	0,009	0,009	0,009	0,010	0,010	0,010	0,010	0,010
	3,00%	0,009	0,009	0,010	0,010	0,010	0,010	0,011	0,011	0,011
	3,20%	0,009	0,010	0,010	0,011	0,011	0,011	0,011	0,011	0,011
	3,40%	0,010	0,010	0,011	0,011	0,012	0,012	0,012	0,012	0,012
	3,60%	0,010	0,011	0,012	0,012	0,012	0,013	0,013	0,013	0,013
	3,80%	0,011	0,012	0,012	0,013	0,013	0,013	0,013	0,013	0,014
	4,00%	0,011	0,012	0,013	0,013	0,014	0,014	0,014	0,014	0,014
4,20%	0,012	0,013	0,013	0,014	0,014	0,015	0,015	0,015	0,015	
4,40%	0,013	0,013	0,014	0,015	0,015	0,015	0,015	0,016	0,016	
4,60%	0,013	0,014	0,015	0,015	0,016	0,016	0,016	0,016	0,016	
4,80%	0,014	0,015	0,015	0,016	0,017	0,017	0,017	0,017	0,017	
5,00%	0,014	0,015	0,016	0,017	0,017	0,017	0,018	0,018	0,018	

Finally, the case of the **PV-IGU with offset** has been analyzed. In this case, it has been found that the **laminated glass reduction table** (¡Error! No se encuentra el origen de la referencia.) **can be directly subtracted from the U value of the equivalent glass without the JB**. It should be noted that the U value without JB should be calculated according to the areas of IGU and laminated glass. This has been mathematically checked.

7.1.5.5 Generalized G value results for different JB dimensions

The impact of the JB in the G value has also been analyzed for different glazing configurations as function of the module area occupied by the JB. Table 50 shows the G value reduction due to the junction box compared to the G value of the overall PV glazing without the JB. So that:

$$G_{JB} = G_0 - \Delta G$$

Being G_0 the G value of the PV glazing with any PV occupancy, calculated as the area weighted G value of transparent and solar cell areas, G_{JB} is the G value of the same PV glazing but calculated as the area weighted of the different areas including the area with JB. Note that Table 50 shows data for the JB fully behind the solar cell and JB fully in the transparent area. Nevertheless, in most of the BIPV modules the JB is located behind the solar cell for better aesthetics. This analysis was initially done for different PV occupancy from 10% to 100%, but it was found that the value of ΔG does not depend on this parameter.

The highest impact of the JB on the G value is found for the laminated PV glass configuration. Taking as reference the 1% module area occupied by JB, the G value is reduced up to 0,75 percentage points when the JB is in the transparent area, while is significantly lower (0,1) if it is located behind a solar cell. In this sense, considering **1 percentage point a significant variation of the G value, this is reached for 1,40% JB area occupancy when is fully located in the module transparent area of a PV laminated glass.**

However, in the glazing configurations with JB behind the solar cell, a 1 percentage point variation of G value is not reached for any reasonable case. Thus, it can be concluded that, **when the JB is located behind the solar cell, its impact on the G value is not significant.**

In the case of **PV-IGU** with the JB in the transparent area, the **reduction of 1 percentage point is reached when the JB occupies the 2,4% of the module area.** This case could correspond to a relatively small 0,4 m² PV glass with a normal 10x10 cm JB. In the case of **IGU-LowE** the **1 percentage difference is only reached for very small modules, where the JB occupies more than 4,8% of the surface.**

Table 50. Reduction of overall PV module G value (ΔG) due to junction box [%]

		JB fully behind solar cell			JB fully behind transparent area		
		IGU	IGU LowE	Laminated	IGU	IGU LowE	Laminated
Module area occupied by JB	0,20%	0,01%	0,00%	0,02%	0,09%	0,04%	0,15%
	0,40%	0,01%	0,00%	0,05%	0,17%	0,09%	0,30%
	0,60%	0,02%	0,01%	0,07%	0,26%	0,13%	0,45%
	0,80%	0,03%	0,01%	0,10%	0,35%	0,17%	0,60%
	1,00%	0,04%	0,01%	0,12%	0,44%	0,21%	0,75%
	1,20%	0,04%	0,01%	0,14%	0,52%	0,26%	0,90%
	1,40%	0,05%	0,02%	0,17%	0,61%	0,30%	1,05%
	1,60%	0,06%	0,02%	0,19%	0,70%	0,34%	1,20%
	1,80%	0,07%	0,02%	0,22%	0,79%	0,39%	1,34%
	2,00%	0,07%	0,02%	0,24%	0,87%	0,43%	1,49%
	2,20%	0,08%	0,03%	0,27%	0,96%	0,47%	1,64%
	2,40%	0,09%	0,03%	0,29%	1,05%	0,51%	1,79%
	2,60%	0,10%	0,03%	0,31%	1,13%	0,56%	1,94%
	2,80%	0,10%	0,03%	0,34%	1,22%	0,60%	2,09%
	3,00%	0,11%	0,04%	0,36%	1,31%	0,64%	2,24%
	3,20%	0,12%	0,04%	0,39%	1,40%	0,69%	2,39%
	3,40%	0,13%	0,04%	0,41%	1,48%	0,73%	2,54%
	3,60%	0,13%	0,04%	0,43%	1,57%	0,77%	2,69%
	3,80%	0,14%	0,05%	0,46%	1,66%	0,81%	2,84%
	4,00%	0,15%	0,05%	0,48%	1,74%	0,86%	2,99%
4,20%	0,16%	0,05%	0,51%	1,83%	0,90%	3,14%	

4,40%	0,16%	0,05%	0,53%	1,92%	0,94%	3,29%
4,60%	0,17%	0,06%	0,56%	2,01%	0,99%	3,44%
4,80%	0,18%	0,06%	0,58%	2,09%	1,03%	3,59%
5,00%	0,19%	0,06%	0,60%	2,18%	1,07%	3,74%

It can be concluded that **the JB only impacts the PV glazing G value if it is located behind the transparent area (instead of solar cell area) of laminated glass. For IGU and IGU-LowE the JB only impacts if the module is small and the JB represents more than 2,4% and 4,8% of the module surface respectively. If the JB is located behind the solar cells, its impact on the overall PV glazing G value is negligible.**

7.1.6 Light transmittance of different solar cells technologies

It is quite common to consider the area covered with solar cells as fully opaque for the calculation of the optical properties and the G value of a PV glazing. However, this is not completely truth for some solar cell technologies. To clarify this point, the optical properties of different solar cell technologies were measured with a spectrophotometer using an integrating sphere.

Figure 53 shows the optical transmittance of different solar cell technologies. It is observed that the bifacial and the back-contact solar cells have significant optical transmittance in the near infrared region, i.e. in the region where the silicon absorptance is lower. The poly-Si and mono-Si monofacial solar cells have nearly zero transmittance in the whole spectrum, probably due to backside coatings.

Therefore, when calculating the solar optical properties of PV glazing, the **optical transmittance of the solar cell area can only be considered as zero for conventional monofacial solar cells. For other technologies like bifacial solar cells and back-contact solar cells, the optical transmittance should be measured and considered.**

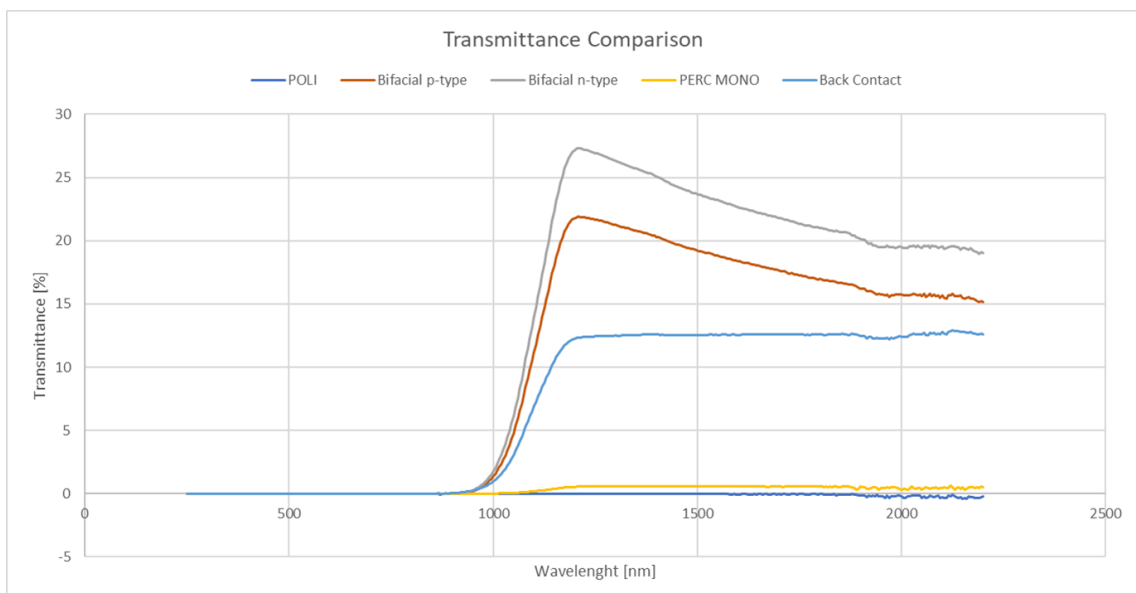


Figure 53. Transmittance of different solar cell technologies (bare cells, not laminated)

7.2 Mechanical Safety

7.2.1 NTP_ME01: general procedure for impact resistance test procedure for BIPV products

BIPV system and its construction parts should be designed, executed, and maintained in such a way that the product during its intended life, with appropriate degrees of reliability and in an economical way, will remain fit for the use for which it is required, will sustain all actions and influences likely to occur during execution and use, will not be damaged or will have controlled damage by pre-defined events, impact or consequences. The choice of the levels of reliability should take account of the relevant factors, including the possible cause and/or mode of attaining a limit state; the possible consequences of failure in terms of risk to life, injury, and potential economic losses; public aversion to failure, and social and environmental conditions in a particular location; the expense and procedures necessary to reduce the risk of failure. The levels of reliability that apply to a particular BIPV product may be specified by classifying the system as a whole (BIPV system) or by classifying its components (e.g. BIPV module). The system's "working life" represents the assumed period for which it has to be used for its intended purpose with anticipated maintenance but without major repairs necessary. The notion of design working life is useful for the selection of design actions (e.g. mechanical load, temperature, etc.), the consideration of material property deterioration (e.g. fatigue, ageing), evaluation of the life cycle cost and developing maintenance strategies. The procedure for BIPV qualification should assume that appropriate measures are taken in order to provide a component/system that corresponds to the requirements and to the assumptions made in the design. These measures comprise testing procedures with the definition of the reliability requirements, and they should be integrated with further organizational measures and controls for the stages of design, execution, and O&M.

At the present stage, this procedure does not lay down conditions for the placing or making of available on the market construction products and does not establish rules on how to express the performance of construction products in relation to their essential characteristics and on the use of CE marking. The procedure, only developed for a pre-qualification phase intended to orientate the product development and its TRL enhancement in the R&D framework, aims at introducing a testing approach to combine the photovoltaic limit states with the limit states related to the construction part for BIPV technology assessment.

7.2.1.1 Summary

1. Summary
2. Definitions
3. Scope
4. Applicability on use categories, product families and kits
5. Normative references
6. Limit states requirements
7. Equipment
8. Device under test – sample definition
9. Impact point determination and temperature control
10. Procedure workflow
11. Assessing and judging limit states thresholds and test results
12. Legal basis

7.2.1.2 Definitions

Below are the main definitions presented in the NTP_ME01: a general procedure for impact resistance test procedure for BIPV products:

'Construction product': is intended, according to CPR 305/2011, as any product or kit which is produced and placed on the market for incorporation in a permanent manner in construction works or parts thereof and the performance of which has an effect on the performance of the construction works with respect to the basic requirements for construction works.

- "BIPV product": photovoltaic module/systems used as a construction product as defined by EN50583: 2016 (all parts)
- 'Performance of a construction product' means the performance related to the relevant essential characteristics, expressed by level or class, or in a description;
- 'Level' means the result of the assessment of the performance of a construction product in relation to its essential characteristics, expressed as a numerical value;
- 'Class' means a range of levels, delimited by a minimum and a maximum value, of the performance of a construction product;
- 'Threshold level' means a minimum or maximum performance level of an essential characteristic of a construction product;
- 'Product-type' means the set of representative performance levels or classes of a construction product, in relation to its essential characteristics, produced using a given combination of raw materials or other elements in a specific production process;
- 'Limit state' (LS) is a condition beyond which the product no longer fulfils the relevant pre-defined criteria. The condition may refer to a degree of actions on the module/system, while the criteria refer to system integrity, fitness for use, durability, or other requirements. A system designed by LS is proportioned to sustain all actions likely to occur during its design life and to remain fit for use, with an appropriate level of reliability for each limit state.
- "Safety in use" (Annex I- CPR 305/2011- basic requirements for construction works) The construction works must be designed and built in such a way that they do not present unacceptable risks of accidents or damage in service or in operation such as slipping, falling, collision, burns, electrocution, injury:
- "PV safety" as safety criteria for photovoltaic modules as indicated by the IEC 61215: 2021 and the IEC 61730: 2016 series, namely intended as basic protection against electric shock according to IEC 61140.
- "Electrical Safety" Recognizing hazards associated with the use of electrical energy and taking precautions so that hazards do not cause injury or death applying a system of organizational measures and technical means to prevent harmful and dangerous effects from electric current, arcing, electromagnetic fields, and static electricity.
- "Electrical Hazard" is a dangerous condition such that contact or equipment failure can result in electric shock, arc-flash burn, thermal burn, or blast. Electrical hazards include those associated with direct contact and those associated with electromagnetic fields and induced currents in conductive objects immersed in RF fields.
- "Performance-based approach" as a matter of principle, performance-based procedures do not prescribe the value of the characteristics, nor the criteria for deciding on the suitability of a particular product but provide the means to assess them. Prescription and criteria are matters for regulations, usually set by national authorities, or the user e.g. architect, or building owner. A performance-based procedure is based on the reliability-based principles that have to be defined as a number of limit states to be explicitly checked. The performance-based approach usually relies on the use of design engineering principles, calculations, and/or appropriate software tools to substantiate the proposed solution and satisfy the limit state. When using the performance-based pathways to performance compliance, values

are entered into a model, allowing the building designer to optimize the various components, equipment and assemblies, saving money, time and operating expenses.

7.2.1.3 Scope

The purpose of this document is to describe a general test method, equipment, and configuration used to determine the limit state for impact resistance of a BIPV product.

The method aims at evaluating a product’s integrity after stresses due to an impact of an external body, not only in terms of mechanical proprieties related to “safety in use” requirements but also the consequences that impact could generate on “electrical safety”. Moreover, by ensuring the control of the device temperature simulating operating conditions, the limit state levels can be affected by the characteristics of the materials.

The method is valid for each type of BIPV and, as described in **¡Error! No se encuentra el origen de la referencia.**, on the basis of this general procedure, other specific test procedures are adopted to be applied to specific test types and requirements (TT) as well as to specific product-types or kit or parts thereof (PT) by referencing the harmonized EN standards (hEN) or ETAG/EAD in force.

In order to reproduce the effect of impacts on vertical construction elements from an external body (for example for cladding system kits), reference will be originated by harmonized standards (EAD 040914-00-0404) which describes the type of impact as specified in ISO 7892: 2012 - Vertical construction elements - Impact Resistance Test - Impact Bodies and General Test Procedures.

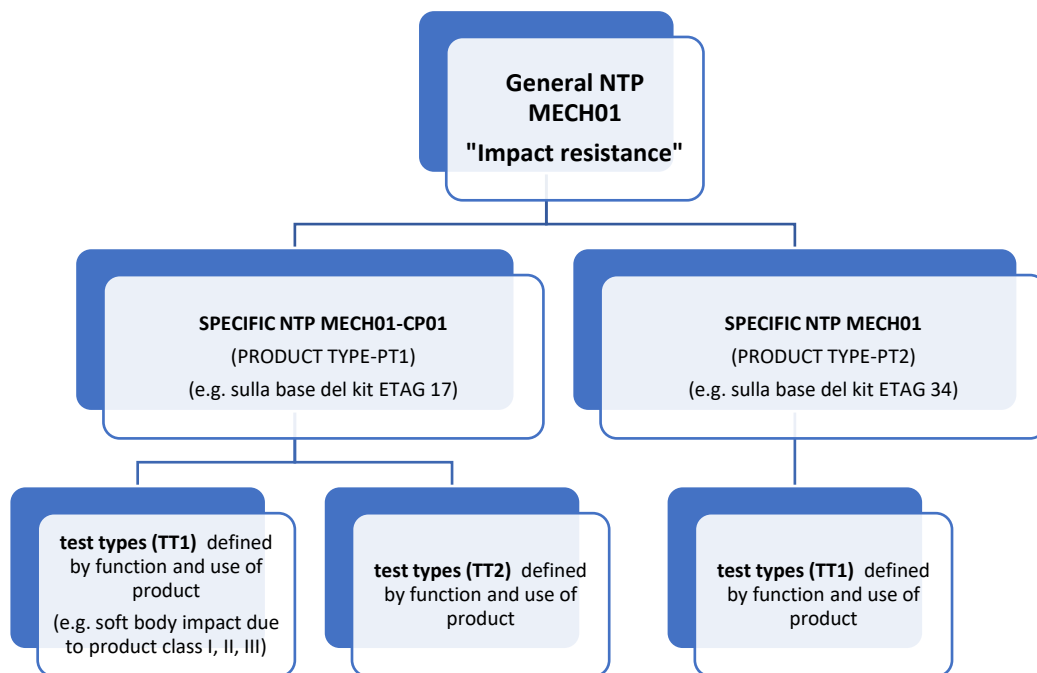


Figure 54. Hierarchical approach for NTP development. This procedure is related to “General NTP-MECH01”. Specific procedures “NTP MECH-01-CPXX” will be adopted for defined “product type”(PTX) and “test type” (TTX)

The procedure will take into account a product characterization based on “limit states” according to a “performance-based approach”. The testing procedure is developed with the perspective of supporting higher design flexibility based on performance objectives, to constitute a beneficial and competitive concept for BIPV engineering, ensuring a higher reliability level of a design choice, a simplification of the testing procedures, and a reduction of the needed time and costs. In defining the Limit States, starting from the

general definitions, specifications will be found in relation to the technical requirement investigated, to both the electrical and building aspects involved (e.g. the same LS can involve the definition of different electrical and construction safety/reliability levels) and also in relation to the product-type concerned.

7.2.1.4 Applicability on use categories, product families and kits

This procedure is applicable to all typologies of BIPV modules. The present document defines the general framework for determining the limit states for impact resistance of a BIPV product. In particular, the focus is on conventional impact bodies used in order to reproduce the effect of actual impacts on vertical building elements, as specified in ISO 7892:2012. Further specific procedures are developed for construction products (CP) and test types (TT).

7.2.1.5 Normative references

General references:

- EN 50583-1 Photovoltaics in buildings - Part 1: BIPV modules
- EN 50583-2 Photovoltaics in buildings - Part 2: BIPV systems
- IEC 63092-1:2020 Photovoltaics in buildings - Part 1: Requirements for building-integrated photovoltaic modules
- IEC 63092-2:2020 Photovoltaics in buildings - Part 2: Requirements for building-integrated photovoltaic systems
- IEC 61730-1 Photovoltaic (PV) module safety qualification – Part 1: Requirements for construction
- IEC 61730-2 Photovoltaic (PV) module safety qualification – Part 2: Requirements for testing
- Regulation (EU) No 305/2011 named as Construction Products Regulation (CPR) and related Harmonised standards or harmonised technical specifications in use as European Assessment Documents (EAD) originated by
- EAD 090062-00-0404 “Kits for external wall claddings mechanically fixed” chapter 2 “Essential characteristics and relevant assessment methods and criteria” paragraph 2.2.11 “Impact resistance” - Annex G “Impact resistance test”
- EAD 040914-00-0404 “Veture kits – prefabricated units for external wall insulation and their fixing devices” chapter 2 “Essential characteristics and relevant assessment methods and criteria” - paragraph 2.2.17 “Impact resistance” – Annex L “Impact resistance test”
- EAD 220010-01-0402 “Flat plastic roofing sheets made of recycled plastic for self-supporting and/or fully supported discontinuous roofing and/or external cladding”
- EOTA TR001 “Determination of impact resistance of panels and panel assemblies”
- ISO 7892:1988 “Vertical building elements — Impact resistance tests — Impact bodies and general test procedures”
- M.O.A.T. No 43:1987 UEAtc “Directives for Impact Testing - Opaque Vertical Building Components”
- Directive 2014/35/EU “Low voltage directive” (LVD) – relevant harmonised standards EN IEC 61730 series
- European Committee for Standardization, EN 1990:2002 - Basis of structural design, CEN, 2002

It should be noted that some products with glass cladding are excluded from above defined standards and do not have an explicit harmonized reference in the EOTA framework. A non-exhaustive list of references for glass parts is as follows:

- EN ISO 12543 Laminated glass and laminated safety glass
- EN 14449: 2005 Glass in building - Laminated glass and laminated safety glass - Evaluation of conformity / Product standard
- EN 356 Safety glass. Tests and classification against manual attack
- EN 12600 Pendulum test. Impact test method and classification for flat glass

For engineering design aspects, such as building construction products, BIPV modules and their mounting structure frame and fastenings have to be designed to comply with other requirements set out in the Eurocodes EN 1990, EN 1991 and, if relevant for glazing parts, with structural safety criteria according to EN 16612, CEN/TS 19100 (all parts) or their national equivalents.

7.2.1.6 Limit states requirements

Limit state design is a design methodology for structural elements, which considers both the effects of actions and the resistance of a material or component to the effects of actions. Limit state design forms the basis of Eurocodes, which now forms the basis of structural design throughout Europe. In the framework of this procedure, a product limit state qualification is adopted. The procedure defines different limit states for the BIPV product:

<p>BIPV-Serviceability Limit State (SLS)</p> <p><i>“BIPV product under a frequent use condition can change the behavior/condition, but it must remain reliable and functional for its intended use without damages”.</i></p>
<p>The SLS represents a condition where the BIPV building skin module/system is useable as originally intended and designed in a frequent use condition. The system, under SLS actions, must remain reliable and functional for its intended use (e.g. energy production, building functions ensured, etc.) after being subjected to routine/typical loading/agent and it is not compromised in any of its building and electrical performances.</p> <p><i>Example: A normal wind load is applied to the system in operation. It behaves in an elastic mechanical state, the energy production is not affected, and the action doesn't compromise the materials and building/electrical functions, safety, efficiency and reliability in any way. After the action, the construction comes back to its initial state.</i></p>
<p>BIPV- Safeguard limit state (SfLS)</p> <p><i>“BIPV under a rare event may suffer permanent damages, but it must ensure a safe user evacuation for people and things. It does not maintain the initial functionality”.</i></p>
<p>After a rare event that induces a certain input action (e.g. mechanical action, electrical load, etc.) the system may suffer permanent damages and performance reduction, being also economically unrecoverable, but it should ensure a safe user evacuation and a certain residual protection after possible shocks (e.g. avoiding collapses). The SfLS represents a condition in which the safety of a BIPV building skin system and its users is ensured. In terms of construction and electrical aspects, safety is safeguarded and it can be assumed as long as this state is fulfilled.</p> <p><i>Example: a rare and unexpected mechanical load, exceeding the design load, is applied to the system in operation. It suffers construction damage with breakage of parts, being unable to still function as a skin cladding (e.g. water-tightness, weather protection, and mechanical stability are lost), and with interruption of its energy production. However, the systems do not suffer a complete collapse (parts are still attached to frames and do not fall down, electrical shocks are avoided thanks to protection systems, etc.) so that people's safety is still safeguarded after the event as long as the system is replaced.</i></p>
<p>BIPV-Ultimate limit state (ULS)</p> <p><i>“BIPV collapses in a performance mechanism. Safety conditions are no longer guaranteed”.</i></p>
<p>In principle, collapse occurs when the first element in a system reaches collapse in a performance mechanism according to a limit value. The different definitions of collapse available in codes and the published literature can be used to define collapse predictions.</p>

Example: The same is used for SflS but with the difference that the systems suffer a complete collapse (parts are not attached anymore to frames and fell down, electrical shocks and other phenomena can seriously be a danger for people) so that people's safety is at risk after the event.

7.2.1.7 Equipment

The equipment already presents in the SUPSI PVLab was used to perform the tests. An impact using a hard body and a soft body with the use of pendulum is made. The equipment used for PV module impact tests is made according to the requirements of Module breakage test MST 32 of IEC 61730-2. For this new test procedure, the impactors, hard bodies and soft bodies, were defined as specified by the reference European Assessment Documents (EADs) derived from ISO 7892. (Figure 55)

An infrared camera with an electroluminescence technique was used to analyze on the integrity of solar cells and electrical circuits following impact.

A climate chamber was used to control the temperature and ensure that the tests were performed at certain temperature values, in which the modules were placed, and the test was performed inside the chamber. Temperature tests were performed with vertical drop.

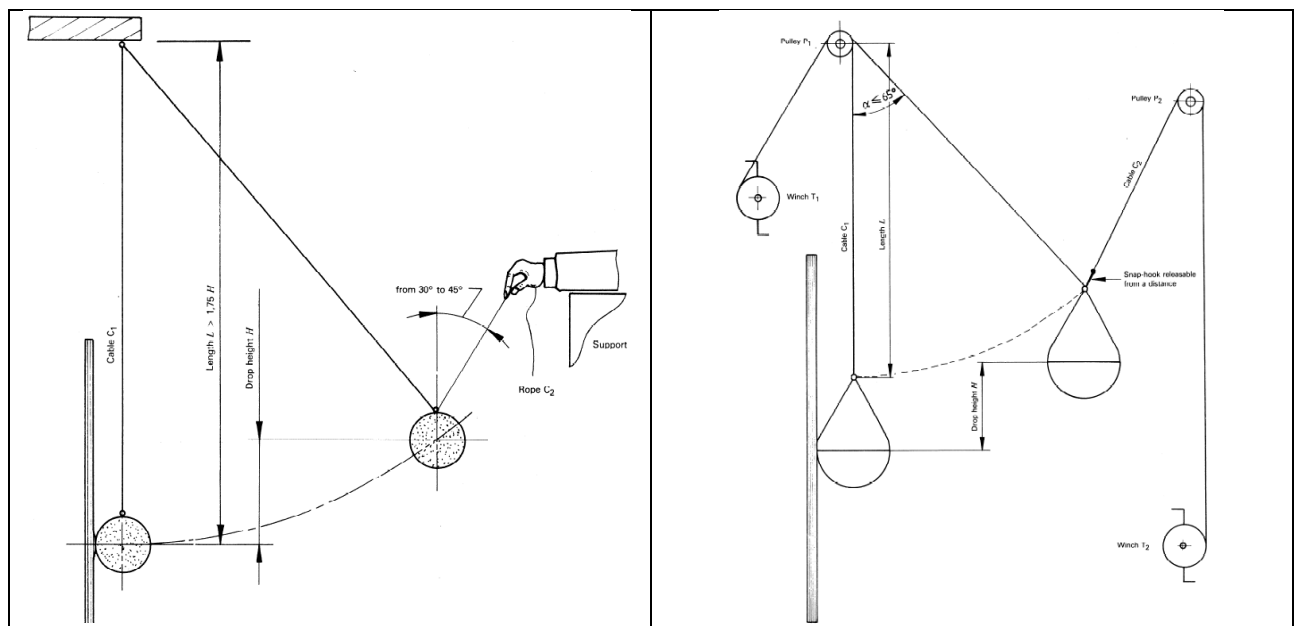


Figure 55. Hard bodies and soft bodies, as specified by the reference European Assessment Documents (EADs) derived from ISO 7892

7.2.1.8 Device under test – sample definition

This procedure contains assumptions taking account of state of the art and makes provisions for case-by-case approach within the general framework. The guidance remains valid for construction product cases to be used case by case in an appropriate way. This use is the responsibility of the lab, which receives the special application, and is subject to consensus with producers. Experience in this respect is collected after validation. In specific cases relevant to product development, the test lab can define, in accordance with the producer, small-scale representative samples (defining numbers, size, incorporation of critical parts such as j-box, etc.) in order to properly assess a certain performance aspect of the product by reproducing a certain impact condition, to be case by case established. However, this should be only considered as a test for product pre-qualification and not for assessing the construction kit's performance.

When only the products (without fixings) are placed on the market by the applicant (manufacturer), the procedure shall indicate the other components of the kit (e.g. fixings) used during the test, and specified by the description of dimensions, material and performances of components. The manufacturer and trading reference of fixings have to be indicated.

In the specific procedure, PT-TT for the construction product and test type further specification will apply. See **Annex 7.2.2** for the specification related to the Vecture KIT.

7.2.1.9 Impact point determination and temperature control

Impact point determination

The requirements expressed by the reference EADs for the specific products in addition to the requirements required by IEC61215-2 were taken into account in determining the impact points. In fact, an assessment was made on the photovoltaic part considering the weaknesses that the active part brings to the product. To consider the weaknesses generated by the active part, the Hail test (MQT 17) in IEC 61215-2 was taken as a reference, which aims to verify that the module is able to withstand the impact of hail and has already determined the weaknesses for photovoltaic products.

Therefore, for vecture kits, for example, both EAD 040914-00-0404 and the Hail test (MQT 17) in IEC 61215-2 were taken as references.

For impact points, the EAD mentions that impact must be made "at least in three positions," which means that three different points must be considered for hard-body impact H1/H2/H3 (0.5 to 1 kg ball) and small soft-body impact S1/S2 (3 kg ball). To determine the impact resistance from large soft body S3/S4 (50 kg ball), at least one impact is needed at the center point of the lining element (Table 51).

Table 51. Hard and soft body impact locations (Source EAD 040914-00-0404)

Hard body impact	H1-H2-H3	No. impact: 5 Position of impact: 3 different locations
Soft body impact	S1-S2	No. impact: 3 Position of impact: 3 different locations
	S3-S4	No. impact: 1 Position of impact: at least in the center point of a cladding element

In order to consider the weak points given by the electrical PV part, the starting point will be the IEC 61215-2 standard (3), in detail, what is reported in the hail test (MQT 17) (Table 52).

Table 52. Impact locations (Source IEC 61215-2 (3)).

Shot No.	Location
1	Any corner of the module window, not more than one radius from the module edge
2	Any edge of the module, not more than one radius of ice-ball from the module edge
3, 4	Over edges of the circuit (e.g. individual cells)
5, 6	Over the circuit near interconnects (e.g. cell interconnects and bus ribbons)
7, 8	On the module window, not more than half the diameter of the ice ball from one of the points at which the module is mounted to the supporting structure
9, 10	On the module window, at points farthest from the points selected above

11	Any points which may prove especially vulnerable to hail impact like over the junction box
----	--

Of all the points indicated, the impact points and the number of impacts defined by EAD040914-00-0404 will be taken into consideration as well as a selection of impact points defined by IEC 61215.

A selection of impact points is considered because the test should not be a repetition of the hail test but it shall consider the points, which in the event of an impact from an external body (hard or soft), could lead to a change in the electrical/mechanical state.

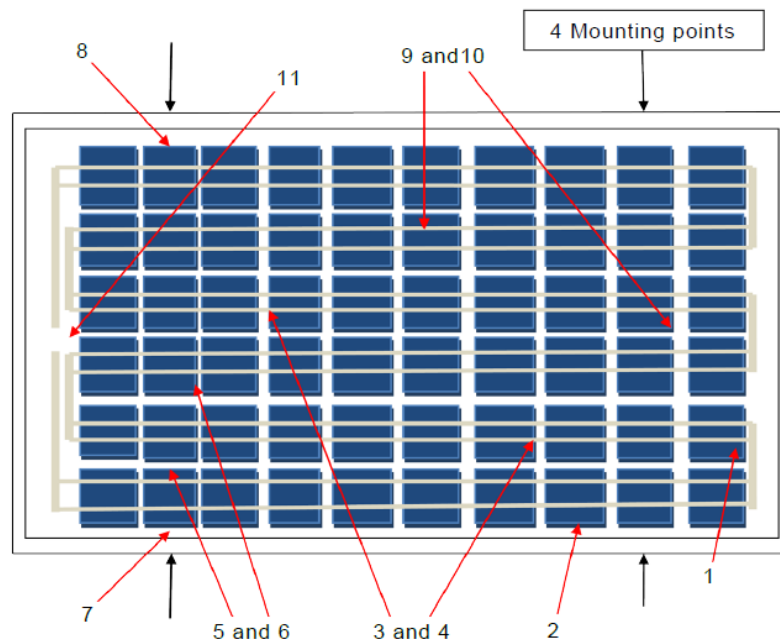


Figure 56. Hail test impact locations for wafer/cell based technologies (Source: IEC 61215-2 (3)).

Temperature control

The regulatory framework for construction products does not provide for active photovoltaic products or testing at different temperatures. EN 12600 for the classification of flat glass products used in construction requires that tests be performed following the conditioning of specimens to the calibration temperature of $(20 \pm 5^\circ\text{C})$. In many cases, the reference EADs for construction products do not state any temperature requirements for the impact test, which must be carried out at room temperature. In other cases such as for EAD 220010-01-0402 which applies to flat plastic roofing sheets due to material behavior at low-temperature values requires verification to be carried out. Specifically, "Resistance to low temperature - hard body impact resistance at the temperature $(-20 \pm 2)^\circ\text{C}$."

Since the procedure applies to BIPV products in which there is an active part, in order to consider the behavior of the polymer material used as solar cell encapsulant depending on temperature, the impact point will be stabilized in the controlled temperature scenarios, as valid for construction product cases to be defined case by case in an appropriate way, as following specified:

- **Scenario 0:** Laboratory ambient temperature. Normally this is a temperature of $(20 \pm 5^\circ\text{C})$ and complies with that defined by the standard test conditions expressed for photovoltaics with cell temperature of $25^\circ\text{C} \pm 1^\circ\text{C}$ (conditions under which the Performance at STC is performed (MQT 06.1) according to IEC 61215-2.
- **Scenario 1:** Low temperature. The cell temperature was set at -20°C considering both EN 16613:2019 for glass products and EAD 220010-01-0402 for products without glass with a plastic layer. In fact, for EN

16613 to determine the glass transition temperature T_g of the polymeric materials used for layering, in order to cover the whole temperature range, the lower limit is -20°C . On the other hand, as mentioned earlier for EAD, the temperature of -20°C is the verification temperature for low-temperature impact resistance.

- **Scenario 2:** High temperature. As reported in the previous chapter "Electrical safety" in the technical specification IEC IEC TS 63126 two categories of high-temperature operation have been defined for PV modules (Level 1 $> 70^{\circ}\text{C}$ to 80°C at the 98th percentile and Level 2 $> 80^{\circ}\text{C}$ to 90°C at the 98th percentile). Level 2 temperatures may result from products with insulated substrates when the ambient temperature is high. The high-temperature value should be defined by the specific product type under test and as a boundary condition of the test and should be indicated with the test results.

Glass products can be considered as an alternative the EN 50583-1:2015 (E) - Annex A- Further requirements on PV modules that containing glass can be adopted as a reference for determining temperature or valid simulation analysis based on ISO 15099 for glazing.

The specific procedures for each product construction type will encompass the temperature scenario.

7.2.1.10 Procedure workflow

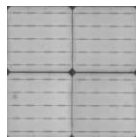
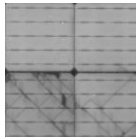
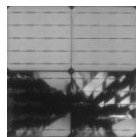
In order to define the reference NTP to be used for a BIPV construction product, it is necessary to follow the following steps:

- a) Consider which essential characteristic shall be assessed in relation to the basic requirements for construction works in relation to the BIPV module under investigation (e.g. impact resistance)
- b) Identify the BIPV-NTP developed for such a relevant essential characteristic (e.g. NTP-MECH 01 for Impact Resistance)
- c) Define the product type (**PT**) which originates the BIPV module as its basic part according to harmonized standards originated by CPR 305/2011 (e.g. veture kit according to ETAG017);
- d) Define the specific impact test type (**TT**) to execute as described in the CPR standard adopted for the product type (e.g. vertical drop, pendulum test, hard body, or soft body impact).
- e) Consider the specific BIPV-NTP developed for such a construction product and test type "**CP-TT**" and refer to the instruction reported within

7.2.1.11 Assessing and judging limit states thresholds and test results

For the building part, the general limit states are defined according to ETAG/EAD or harmonized EN standards depending on technology/material while for PV, the electrical limits are defined considering electrical insulation loss taking into account the IEC 62446-1:2016 "Photovoltaic (PV) systems - Requirements for testing, documentation, and maintenance - Part 1: Grid connected systems - Documentation, commissioning tests and inspection". Table 53 defines the following threshold criteria. The final product limit state, due to the multi functionality, is defined as soon as the first condition (electrical or mechanical) is achieved in the construction or electrical part, according to the previous table, for each type of limit state.

Table 53 . LS assessment criteria

Impact Safety - Limit state assessment for BIPV products			
	Serviceability SLS	Safeguard SfLS	Ultimate ULS
	ELECTRICAL LS		
Electrical Insulation*	> 40 M ohm*mq ± 5% (measurement uncertainty)	> 1 M ohm*mq	< 1 M ohm*mq
Energy loss**	5%	5-20%	>20%
Cell crack f(T)***	No circuits/solar cells breakage	Micro cracks or breaks in one or more cells may be present without involving most of the solar cell area	Breakage affecting the most area of one or more solar cells
i.e.			
Note	<p>* Electrical insulation is a quantitative parameter that provides a value of electrical safety that can be related to limit states by defining the condition of the BIPV product from the electrical point of view following impact.</p> <p>** ** Energy loss, a quantitative parameter, is not directly related to safety; however, an energy loss may be related to improper operation of the active part. Ref due to failure Energy loss is also related to economic loss related to investment. (60), (61), (62)</p> <p>*** Cell failure, although not directly related to electrical safety, leads to reduced performance and possible future problems. This qualitative parameter has been considered as it relates to energy production and possible future failures. The procedure to detect cracks is based on electroluminescence (EL) imaging, a non-destructive test that can also be performed on components installed with special procedures. (63), (64)</p>		
	MECHANICAL LS		
	More specific acceptance criteria are to be defined in specific NTP-PT-TT, according to ETAG/EAD or harmonized EN standards depending on technology/material, the applicable criteria, according to product category, and use. Below is an example according to EAD 040914-00-0404 for Veture KIT		
No deterioration, no penetration, no perforation	No cracking is considered as showing "no deterioration" for all the impacts.	The presence of any cracking penetrating is observed.	Destruction of the skin (perforation) is shown up

A partial factor method of verification approach, incorporating design values for actions, material properties, geometrical data, and resistance or combination of them in order to allow the design verification of ULS and SLS is not the object of this procedure.

7.2.1.12 Legal basis

Disclaimer. The procedure does not have the value of law, regulation, or technical specification but is designed for research purposes and in the form of a prototype of a procedure being tested and validated. SUSPI declines all responsibility for any choices resulting from the application of this. The procedure has the sole purpose of providing preliminary inputs of feasibility and product characterization as a basis to be developed and verified under the sole responsibility of the manufacturer (s) and the designer (s) of the building and electrical systems for the related mandates., on the basis of the project and product requirements in force and dictated by general and local regulations, the technical specifications and regulations in force in relation to safety, product quality, and convenience criteria.

7.2.2 NTP-ME01-VK- SC00: Impact resistance test and results for a Veture KIT” in Scenario ”0”.

7.2.2.1 Scope

The purpose of the test is to evaluate the integrity of the PV Veture KIT. It consists of a multifunctional BIPV facade cladding system with integrated insulation to withstand stresses due to the impact of an external body, not only in terms of mechanical properties related to the requirements of "safety in use", but also of the consequences that the impact could generate on the "electrical safety". The test also provides indications to support the performance evaluation of the product installed on the demonstration site of the BIVBOOST project of a multi-family residential home in Morbegno Italy. Within the following paragraphs the test executed on the PV Veture KIT and the procedure, the equipment, and the set-up used by the laboratory to assess the behavior are presented.

7.2.2.2 Applicability

This test concerns a PV Veture KIT that consists of a laminated PV (c-Si) glass, an 8-9 mm thick mortar outer skin combined with 80 mm thick mineral wool insulation. Polycrystalline colored PV cells have been encapsulated between the two glass panes. The junction box (JB) is placed on the back of the module, between the mortar and the mineral wool.

7.2.2.3 Normative references

- EAD 040914-00-0404 “Veture kits – prefabricated units for external wall insulation and their fixing devices” chapter 2 “Essential characteristics and relevant assessment methods and criteria” - paragraph 2.2.17 “Impact resistance” – Annex L “Impact resistance test”
- ISO 7892:2012 “Vertical building elements — Impact resistance tests — Impact bodies and general test procedures”
- IEC 61215-1. Terrestrial photovoltaic (PV) modules – Design qualification and type approval – Part 1: Test requirements. Edition 2.0 - 2021.
- EC 61215-2. Terrestrial photovoltaic (PV) modules – Design qualification and type approval – Part 2: Test procedures. Edition 2.0 - 2021.

7.2.2.4 Equipment

Instrument	Note
Impact test apparatus	Used existing laboratory equipment built according to IEC 61730-2 with impactors for impact testing derived from the reference EAD 040914-00-0404
Impactor	Hard body (0.5 -1 kg) steel ball, small soft body 3kg and large soft body 50kg spherical bag as defined by EAD 040914-00-0404
Infrared camera	To perform infrared photography with electroluminescence (EL) imaging.

7.2.2.5 Procedure

Below is presented the procedure defined to assess Veture KITs based on the EAD 040914-00-0404 for the construction part and the according to Insulation test MST 16 - IEC 61730-2 for those electrical:

- a) Execute an electroluminescence test on the PV Veture KIT following the specific procedure and note possible aberrations.
- b) Mount the substructure of the module according to the defined by IEC 61730-2 so that it is centered into the impact test apparatus, using the method described by the manufacturer. The front side of the module is oriented toward the impact ball.
- c) Choose and mount the impactor on the impact test apparatus, according to the specific test following the requirements of the EAD 040914-00-0404 (soft body or hard body).
- d) Sign the impact points selected (weakest points) considering both the requirements of the reference EAD and what is reported by IEC 61215-2 on the impact to hail. Impacts performed at the margin of the module should occur at less than 50 mm from the edge of the Veture KIT.
- e) Lift the ball to a predefined drop height according to the EAD 040914-00-0404¹ and ensure that the temperature of the cells is in the condition provided by scenario 0, ambient laboratory temperature of $(20 \pm 5 \text{ }^\circ\text{C})$.
- f) Allow the impactor to stabilize and then release the ball to strike the module.
- g) Note if the skin is penetrated, perforated, or if possible glass deterioration occurred. Take a picture or a video of the module tested.
- h) Execute an electroluminescence test following the specific procedure and note possible aberrations of the cells.
- i) Execute an Insulation (dielectric withstand) test (MST 16, IEC 61730) to determine whether or not the module is sufficiently well insulated between live parts and accessible parts.
- j) Execute a Wet leakage current test (MQT 15 IEC 61215-2) to evaluate the insulation of the module simulating wet operating conditions.
- k) Execute a flash test to measure the energy loss after the impact.
- l) Repeat steps e. to k. for each impact point identified. For the identified number/type of samples as described in NTP-ME01.

7.2.2.6 Uncertainty

Weight of the impactor: $\pm 5 \text{ g}$

Drop height: $\pm 5 \text{ mm}$

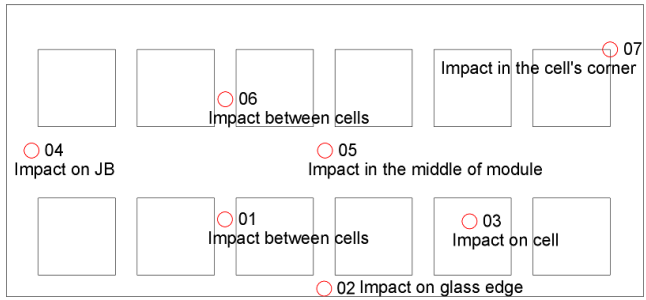
Impact point temperature during the impact: $\pm 5^\circ\text{C}$

7.2.2.7 Test results

The following presented results are referred as a test case considering the execution of BIPV Veture KIT samples. For more clear readability, the results are presented according to the specific category in use defined by the EAD 040914-00-0404 (category IV and III).

Category IV: defined as “a zone out of reach from ground level”. Below is a scheme of the tests performed on two samples of PV Veture KITs.

¹ Since the impact resistance is unknown, the specific EAD suggested to execute the test starting from the lowest impact energy (category IV) and continuing to higher values (up to category I).

Hard body impact Weight: 0.5 Kg Impact: 1 J (height 0.2 m)	Requirement after impact Not penetrated Not perforated	
Soft body impact Weight: 3 Kg Impact: 10 J (height 0.34 m)	Requirement after impact Not deteriorated	

The results show that the PV Veture KIT remained in the **serviceability limit state** and the mechanical performance of the module has not been compromised after the impacts were executed according to the EAD 040914-00-0404. The same results, no changes in the limit state, have been registered for the electrical performance. The integrity of solar cells, assessed through electroluminescence, has not been compromised. Indeed, no damages or fractures have been registered. Table 54 shows a summary of the results for the use of category IV.

Table 54. Test results NTP ME01-VK-SC00 – cat.IV

ID	Impact	Position*	Mechanical status	Electrical results
1, 2	Hard body	From 01 to 07	No glass breakage No glass penetration/perforation No cell breakage	Insulation test MST 16 - No electrical insulation loss Insulation resistance > 500 Mohm - Humidity 24 %
1, 2	Soft body	From 01 to 07	No glass breakage No glass deterioration No cell breakage	Insulation test MST 16 - No electrical insulation loss Insulation resistance > 500 Mohm - Humidity 24 %

* As defined by the EAD 040914-00-0404 and the IEC 61215

The results show that the Veture KIT assessed is suitable for installation, as a construction product, in the use category IV (e.g. high facade levels that cannot be hit by a thrown object. Cleaning gondolas should not be used on the façade).



Figure 57. Hard body impact test.



Figure 58. Hard body impact test, detail.



Figure 59. Soft body impact test.



Figure 60. Soft body impact test, detail.

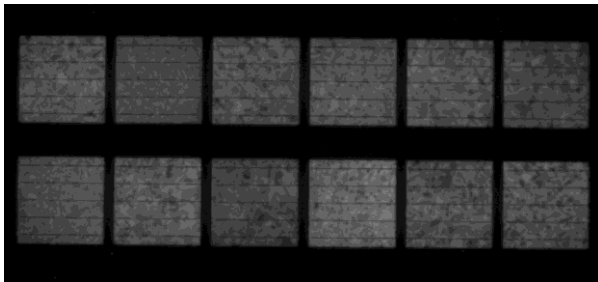


Figure 61. Electroluminescence before hard and soft body test.



Figure 62. Electroluminescence after a hard body impact. No damages on cells.

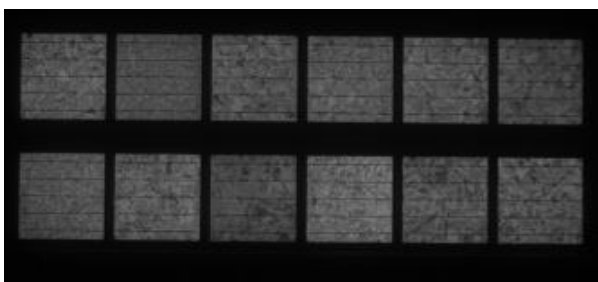
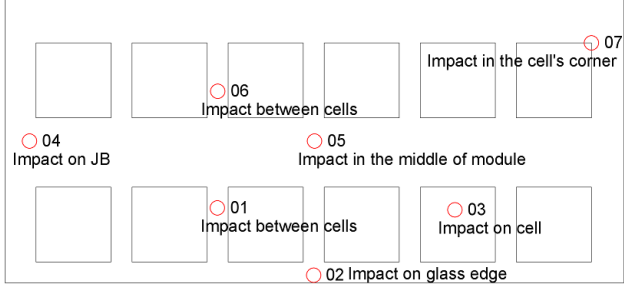


Figure 63. Electroluminescence after a soft body impact. No damages on cells.

Category III: defined as “a zone not likely to be damaged by normal impacts caused by people or by thrown or kicked objects”. Below is a resume of the tests performed on two samples of PV Veture KITs.

<p>Hard body impact Weight: 0.5 Kg Impact: 3 J (height 0.61 m)</p>	<p>Requirement after impact Not penetrated Not perforated</p>	
<p>Soft body impact Weight: 3 Kg Impact: 10 J (height 0.34 m)</p>	<p>Requirement after impact Not deteriorated</p>	

The test executed with the soft body impactor shown that the PV Veture KIT remained in the serviceability limit state, and the mechanical performance of the module has not been compromised after the impacts were executed according to the EAD 040914-00-0404. The same results have been registered for the electrical performance with no changes in the limit state. The integrity of solar cells, assessed through electroluminescence, has not been compromised. Indeed, no damages or fractures have been registered.

In the case of the test performed with the hard body impactor, the mechanical performance of the glass occurred. Test sample 1 (ID 1 in Table 55) reveals that in position 05, the rear glass breakage occurred after the impact. The reason for the breakage is due to the specific design of the PV Veture KIT. Indeed, the contact between the mortar and the glass during the impact, due to the deflection of the glass, caused the breakage of the rear glass. The weakest point of this BIPV product is given in the points where there are not any solar cells. That occurs because, for aesthetic reasons, silicone adhesive was placed only on the back of the solar cells during construction; silicone adhesive changes color under solar radiation and a yellowing emerges.. This thesis is also supported by tests made in WP4 where the preliminary tests pointed out the weakest point where there are no solar cells. After the same impact at the same energy, the PV Veture KIT module had the rear glass broken only when the impact hit a part without solar cells. This is a typical design effect on the BIPV module, according to the design choice could change the BIPV behavior. However, no electrical loss or damage to the PV cells has been registered for sample 1.

For sample 2 (ID 2 in Table 55) the breakage of the glass occurred after an impact on the edge of the module (position 02), a very fragile point of the glass module. However, even if the mechanical performance of the glass has been achieved, no penetration or perforation of the glass has been registered. Considering the electrical results, no electrical insulation loss has been observed on the PV cells. Only a dark response of a single cell, not at the same position of the impact point, is visible after the electroluminescence.

Table 55. Test results NTP ME01-VK-SC00 – cat.III

ID	Impact	Position*	Mechanical status	Electrical results
1	Hard body	05	Rear glass breakage No glass penetration/perforation No cell breakage	No electrical insulation loss Insulation test MST 16: Insulation resistance > 500 Mohm - Humidity 24 % Wet leakage current test MST 17: Insulation resistance > 500 Mohm Water temperature 20 °C Water conductivity 480 uS
2	Hard body	02	Rear/front glass breakage No glass penetration/perforation Single cell dark response	No electrical insulation loss Insulation test MST 16: Insulation resistance > 500 Mohm - Humidity 24 % Wet leakage current test MST 17: Insulation resistance > 500 Mohm Water temperature 20 °C Water conductivity 480 uS
1, 2	Soft body	From 01 to 07	No glass breakage No glass deterioration No cell breakage	Insulation test MST 16 - No electrical insulation loss Insulation resistance > 500 Mohm - Humidity 24 %

* As defined by the EAD 040914-00-0404 and the IEC 61215 (see **Annex 8.3.1**)



Figure 64. Hard body impact equipment.



Figure 65. Hard body impact breakage of the rear glass (ID 1, position 05).

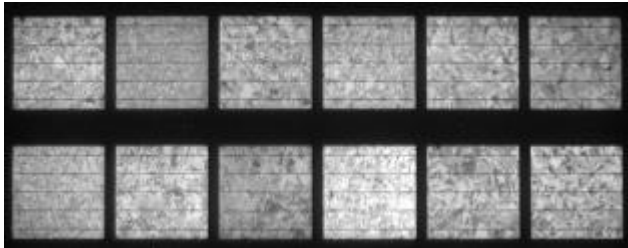


Figure 39. Electroluminescence before hard body test.

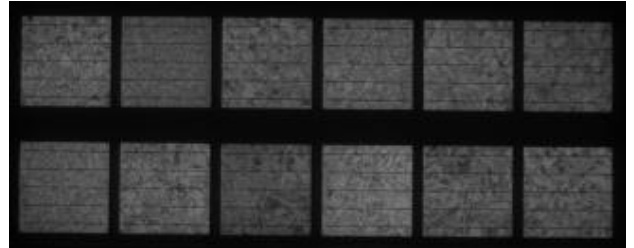


Figure 40. Electroluminescence after a hard body impact



Figure 66. Hard body impact test on the edge (ID 2, position 02).

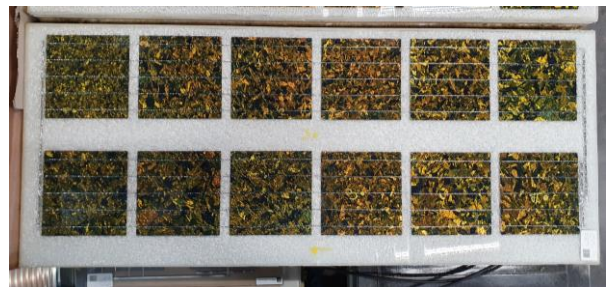


Figure 67. Glass breakage after hard body impact test (ID 2, position 02).

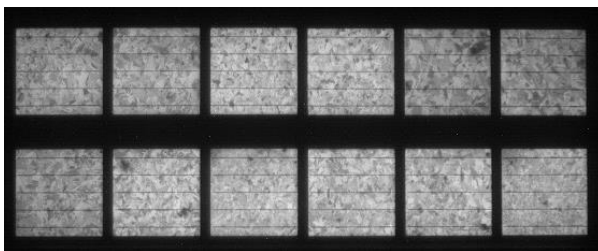


Figure 68. Electroluminescence before hard body test.

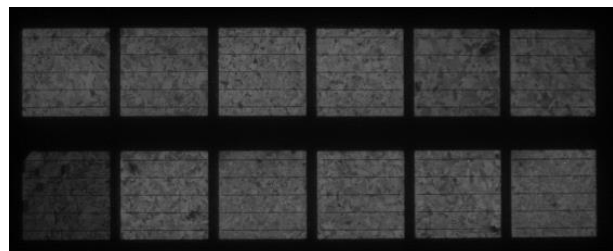


Figure 69. Electroluminescence after a hard body impact (ID 2, position 7). Dark response of a single cell.

7.2.3 NTP-ME01: results of impact resistance test with temperature effect on different product classes

7.2.3.1 Scope

This part's purpose is to apply procedure NTP ME-01 considering the effects of the variation in operating temperature during the impact test execution and the consequences on the limit states. In particular, the NTP-01 has been applied for each of the following product categories:

- PV laminated glass: to define the effect of the temperature at the module/cell breakage;
- PV Veture KIT: to define the effect of the temperature according to the category in use III and IV defined in the reference standard (EAD 040914-00-0404);
- PV roof tiles: to define the effect of the temperature at different drop heights according to the requirements defined by the EAD 220010-01-0402.

7.2.3.2 Applicability

The features of the products undergoing testing are listed below.

- i. The PV laminated glass consists of a 60 cells c-Si module (6x10) enclosed in front and rear tempered glass in the dimension of 1'004x1'680mm². The polymeric material is in EVA, commonly used for PV.
- ii. PV Veture KIT consists of a laminated PV (c-Si) glass, overlaid an 8-9 mm thick mortar layer combined with 80 mm thick mineral wool insulation. Polycrystalline colored PV cells have been encapsulated between the two glass panes. The junction box (JB) is placed on the back of the PV glass contained between the mortar and the mineral wool.
- iii. PV roof tiles equipped with CIGS PV cells and encapsulated in a polymeric material. The tile is presented with a dimension of 853mm in width and 487 mm in height with an area of about 0,42sqm.

7.2.3.3 Normative references

- i. PV laminated glass: EN356:1999 "Glass in building - Security glazing - Testing and classification of resistance against manual attack"
- ii. PV Veture KIT: EAD 040914-00-0404 "Veture kits – prefabricated units for external wall insulation and their fixing devices" chapter 2 "Essential characteristics and relevant assessment methods and criteria" - paragraph 2.2.17 "Impact resistance" – Annex L "Impact resistance test"
- iii. PV roof tiles: no specific regulatory references regarding the impact resistance of roofing shingles exist. However, two EADs were taken as a reference for test development.
 - a. EAD 220025-00-0401 deals with cantilever structural horizontal glazing.
 - b. EAD 220010-01-0402 deals with film plastic roofing sheets made of recycled plastic discontinuous roofing and/or external cladding. This standard specifies tests for plastic materials not containing the material glass and specifies the value of -20°C as the test temperature to consider the low-temperature resistance of plastic materials.

7.2.3.4 Equipment

Instrument	Note
Impact test apparatus	Equipment appositely developed in order to permit the drop of the steel ball
Impactor	Hard body 0.5 kg (in a specific case for PV roof tiles 1.0 kg)
Infrared camera	To perform infrared photography with the electroluminescence technique
Thermal chamber	Temperature for a low value is set at -30°C for glass and -20°C for tiles while it has been set at + 90 °C for the high value

7.2.3.5 Test procedure

The three procedures adopted from the general definition of NTP ME-01, are shown in the table below. To perform the test at the desired temperature, the impact test was performed by placing both the module and the equipment to perform the test in the climatic chamber. To verify that the module's temperature before impact is correct, PT100 thermocouples were placed on the module in addition to the temperature values taken from the climatic chamber. Compared with the impact test performed with the laboratory equipment for Module breakage test MST 32A and reported in the procedure, for reasons of space and simplicity of the test, special equipment was made to allow, by height adjustment, the steel ball to drop. In developing the test, EN 356 was taken as a reference. The impactors to be used in the test were then defined. The impact of a hard body was chosen for 3 main reasons. The first one is to follow what is stated in EN356, the impact test is made with a steel ball. The second is because the hard-body impact is harmful in that the ability of the polymer to absorb the impact energy through elastic and plastic deformations is partially canceled compared to the soft-body impact in which the impact time of the soft body is longer than the relaxation time of the polymer sheet. (65), (66). The third since at high temperatures of 90 degrees the soft-body impactor deforms and ruins itself at high temperatures. It should be highlighted, however, that high temperature leads to a deformation of the size of the steel balls by thermal expansion; however, this aspect is not considered in the test because it is considered not critical to the outcome of the result.

ID	PV laminated glass	PV Veture KIT	PV roof tiles
1	Execute an electroluminescence test on the module following the specific procedure and note possible aberrations.		
2	Mount the substructure of the module according to the method described by the manufacturer. Lay the module and the substructure horizontally under the impactor into the climatic chamber. The front side of the module is oriented towards the impact ball (Fig. X, Fig. Y, Fig. Z).		
3	Choose and mount on the impact test apparatus the hard body impactor		
4	Sign the impact points considering that the impact point for each product will be performed:		
5	In the middle of the module	Over the solar cells	In the middle of the module
6	Lift the ball to a drop height of:		
7	0.61 m	0.2 m for the use of category IV ² 0.6 m for the use of category III	1.02 m
8	Ensure that the temperature of the cells measures i) -20°C, ii) 25°C, iii) 90°C	Ensure that the temperature of the cells measures i) -30°C, ii) 90°C	Ensure that the temperature of the cells measures i) -20°C, ii) 25°C, iii) 90°C
9	Allow the impactor to stabilize and then release the ball to strike the module		
10	Note if the skin is penetrated, perforated or possible deterioration of the glass/polymer occurred. Take a picture or a video of the module tested		
11	Execute an electroluminescence test following the procedure and note possible aberrations		

² See **Annex 8.3.2** for more details regarding the categories in use and the tests on PV Veture KITs

12	Repeat the procedure from step 6 to step 11 by considering that:		
13	The drop height will be increased by 10% until the change of the mechanical state (breakage) of the module/cell	The impacts are made according to the hard body impact test of the category IV (0.2 m) and III (0.61 m)	Only two impact will be performed. The second impact is made with a hard body impact of 1 kg at 1.02 m.



Figure 70. Structure consisting of two rails that guarantee the attachment of the module on the long side



Figure 71. Structure consisting of two rails that are fixed in between the insulation layer and the mortar of the module



Figure 72. Temporary structure consisting of two railings on which four clamps are fixed to ensure the attachment of the module

7.2.3.6 Result

The impact tests performed on the products at different temperatures are shown in the next paragraphs.

Photovoltaic laminated glass

The tests carried out at different temperatures for the PV laminated glass have shown interesting results. However, the results cannot be considered exhaustive by considering the scarce number of samples and the observed behavior variability. The mechanical behavior of glazed elements at different temperatures will require further studies and in-depth analysis since it is subjected to many factors, including the treatment of the glass, the point of impact, and the lamination process. It should be noted that the glass modules tested are of the same type, all with the same size, number of solar cells, thickness, and composition.

Test A - Room temperature (scenario "0" NTP ME-01)

The following results show the tests carried out on the first three samples of PV laminate at room temperature. The glass breakage has been achieved at different impact energies, between 4.4 J and 6.2 J. When the breakage occurred, both the front and the rear glass were compromised. The breakage of the glass implied damage to solar cells in all three modules. The electroluminescence (Figure 75) shows that not only the cell corresponding to impact point or adjacent (in the image marked with a red arrow) were compromised but also non-adjacent cells. This behavior is probably due to the glass breakage energy propagating through the polymer. Further investigations on more samples are necessary to validate this assumption.

Table 56. Hard body impact made at room temperature

ID	Position	Impact energy [J]	Cell temp	Mechanical status	Electrical results
1	Middle	3.0	25 °C	No glass breakage	No cell breakage
		... ³		No glass breakage	No cell breakage
		4.4		Glass breakage (front/rear)	Cell breakage
2	Middle	3.0	25 °C	No glass breakage	No cell breakage
		... ²		No glass breakage	No cell breakage
		6.2		Glass breakage (front/rear)	Cell breakage
3	Middle	3.0	25 °C	No glass breakage	No cell breakage
		... ²		No glass breakage	No cell breakage
		5.3		Glass breakage (front/rear)	Cell breakage

Test B - High temperature (scenario "2" NTP ME-01)

Table 57 shows the tests carried out on three samples of PV laminate at high temperatures (90°C). The energy value that led to the breakage of the glass is slightly lower than the test at room temperature and is between 3.7 and 5.3 J. In the test "ID 4", only the breakage of the front glass occurred without damage or power reduction of the PV cell. The "ID5" and "ID6" test samples achieved the breakage of both the front and the rear glass and the PV cells, as observed on the tests at room temperature. The electroluminescence (Figure 74, Figure 79) reveals a different kind of cell breakage than the previous tests by showing diagonal cracks on cells adjacent and non-adjacent to the impact point. In Figure 77 two rows of cells are not operative after the impact.

Table 57. Hard body impact made at high temperature (90°C)

ID	Position	Impact energy [J]	Cell temp	Mechanical status	Electrical results
4	Middle	3.0	90 °C	No glass breakage	No cell breakage
		... ²		No glass breakage	No cell breakage
		3.7		Glass breakage (front)	No cell breakage
5	Middle	3.0	90 °C	No glass breakage	No cell breakage
		... ²		No glass breakage	No cell breakage
		4.4		Glass breakage (front/rear)	Cell breakage
6	Middle	3.0	90 °C	No glass breakage	No cell breakage
		... ²		No glass breakage	No cell breakage
		5.3		Glass breakage (front/rear)	Cell breakage

Test C - Low temperature (scenario "1" NTP ME-01)

³ Impact energy increased by 10% after each impact

Table 58 shows the tests carried out on three samples of PV laminate at the low temperatures (-30°C). All the tests at low temperature shown the breakage of the glass with a value of 5.3 J. In the test “ID9”, after the breakage of the front glass, no breakage occurred in the solar cells. On the PV laminated glass “ID7” and ID8”, (Figure 78, Figure 79) the electroluminescence reveals that the breakage of the solar cells is different from the behavior observed at room/high temperature.

Table 58. Hard body impact made at low temperature (-30°C)

ID	Position	Impact energy [J]	Cell temp	Mechanical status	Electrical results
7	Middle	3.0	-30 °C	No glass breakage	No cell breakage
		... ²		No glass breakage	No cell breakage
		5.3		Glass breakage (front)	Cell breakage
8	Middle	3.0	-30 °C	No glass breakage	No cell breakage
		... ²		No glass breakage	No cell breakage
		5.3		Glass breakage (front/rear)	Cell breakage
9	Middle	3.0	-30 °C	No glass breakage	No cell breakage
		... ²		No glass breakage	No cell breakage
		5.3		Glass breakage (front)	No cell breakage

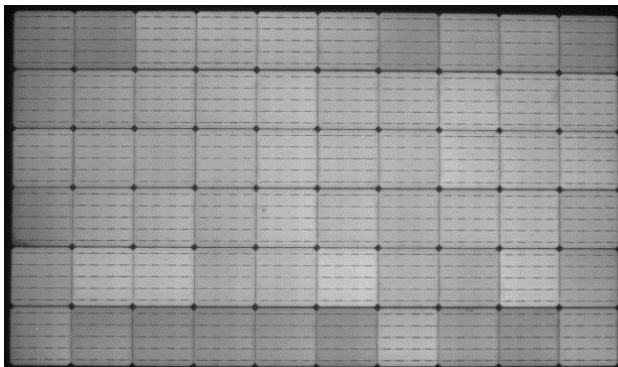


Figure 73. Aspect of the PV module before the impact.

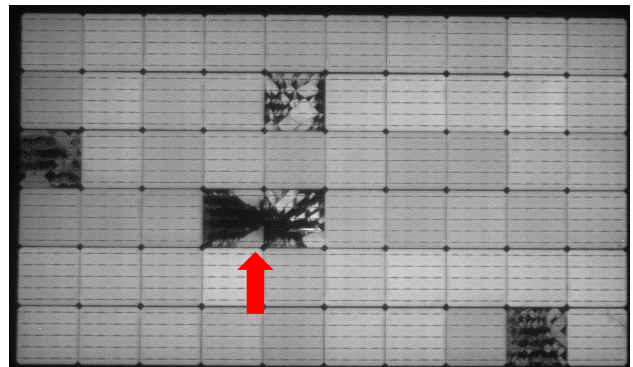


Figure 75. Electroluminescence made on the “ID3” at room temperature (25°C).

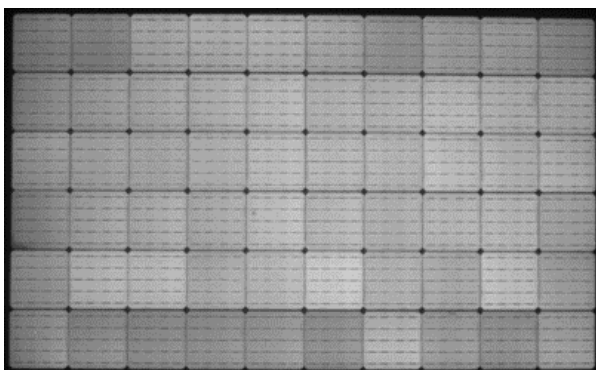


Figure 74. Electroluminescence made on the “ID4” at high temperature (90°C).

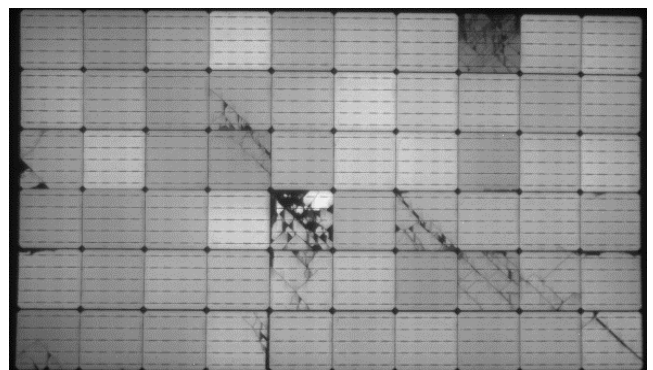


Figure 76. Electroluminescence made on the “ID5” at high temperature (90°C).

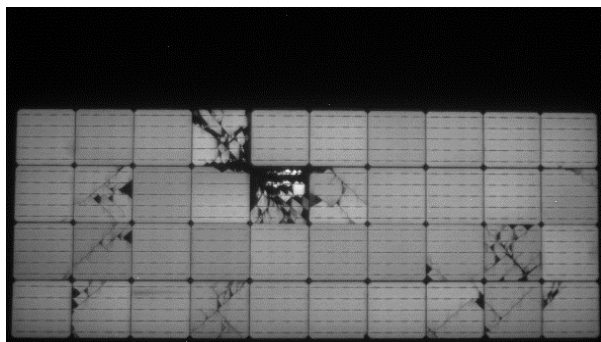


Figure 77. Electroluminescence made on the “ID6” at high temperature (90°C).

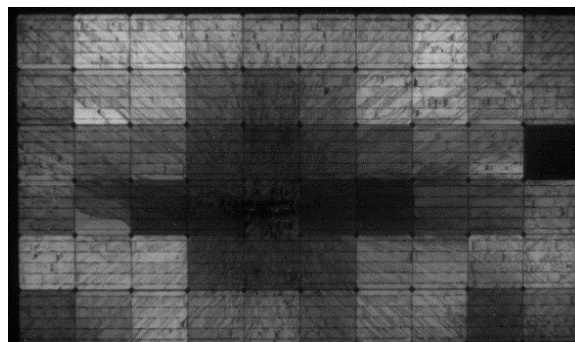


Figure 78. Electroluminescence made on the “ID7” at high temperature (-30°C).

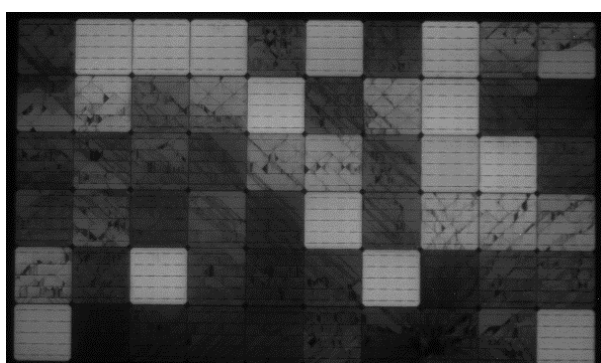


Figure 79. Electroluminescence made on the “ID8” at high temperature (-30°C).

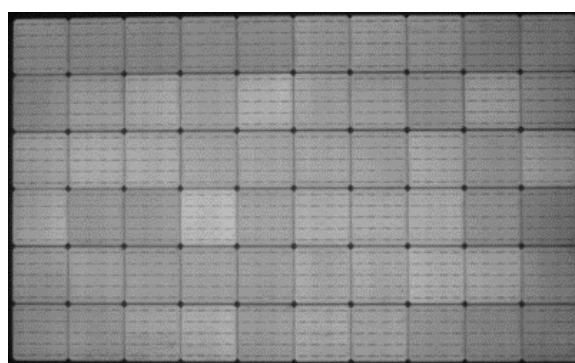


Figure 80. Electroluminescence made on the “ID9” at high temperature (-30°C).

PV Veture KIT

The impact test has been performed at different temperatures in order to assess the behavior of the PV Veture KIT. Considering the scarce number of samples tested, the results cannot be considered exhaustive and further analysis are necessary. However, the tests shown that different temperatures (90°C in the specific case) could lead to variation in behavior compared with standard non-PV products. In Table 59, the results of the tests performed on the PV Veture KIT at different temperatures are shown. In the next paragraphs, an analysis of the test has been presented.

Table 59. Hard body impact made at high and low temperatures for the PV Veture KIT

ID	Position	Impact energy [J]	Cell temp	Mechanical status	Electrical results
1	Over PV cell	1.0 (category IV)	90 °C	No glass breakage	No cell breakage
		3.0 (category III)		No glass breakage	Darken dot on the cell
2	Over PV cell	1.0 (category IV)	-30 °C	No glass breakage	No cell breakage
		3.0 (category III)		No glass breakage	No cell breakage

Test A - High temperature (90°C) (scenario “2” NTP ME-01)

As shown in Table 59, the impact performed in category IV did not change the material and electrical integrity. No fractures have been registered on the photovoltaic laminate or the solar cells. The module

tested in category III shown a small deterioration of the cell after the impact (Figure 82), consisting of a dark spot in correspondence with the impact point. This implied a small change in the electrical behavior of the Veture KIT, even though no breakage has been observed on the glass. The impact did not come in any change in respect of the KIT electrical insulation. However, further investigations are necessary to formulate more precise conclusions.

Test B - Low temperature (-30°C) (scenario "1" NTP ME-01)

At low temperatures, the test did not lead to any appreciable result. The PV laminate did not show any deterioration or insulation loss, and there was no change or breakage on the solar cells (Fig. Y).

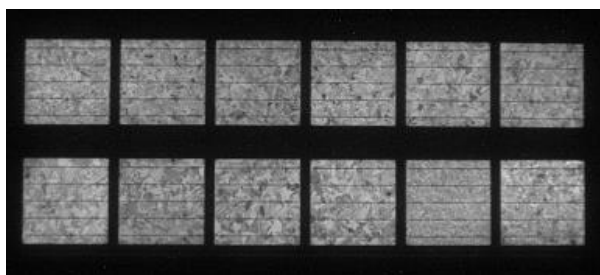


Figure 81. Aspect of the sample "ID1" module before the impact.

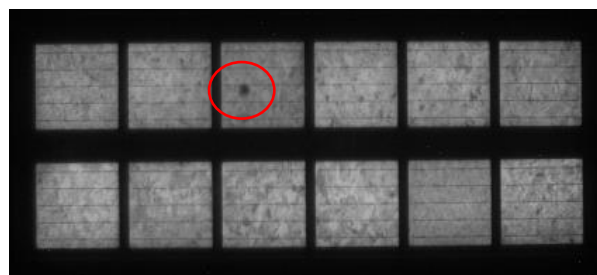


Figure 82. Electroluminescence made on the "ID1" at high temperature (90°C) for the category III.

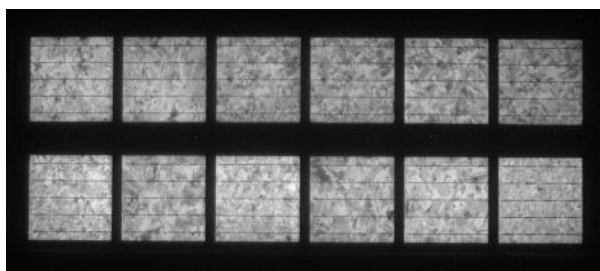


Figure 83. Aspect of the sample "ID2" module before the impact.

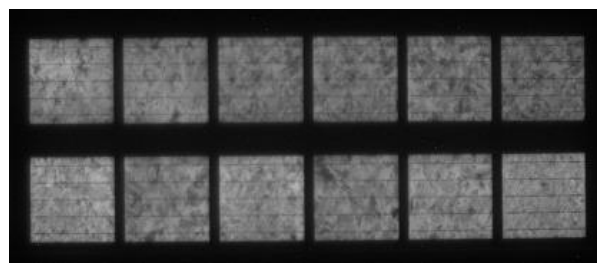


Figure 84. Electroluminescence made on the "ID2" at low temperature (-30°C) for the category III.

PV roof tiles

As for the PV laminated glass and the PV Veture KIT, also for PV roof tiles, the tests have been performed at high, low and room temperatures. Considering the scarce number of samples tested, the results cannot be considered exhaustive, and further analysis is necessary. Table 60 shows the test performed on the PV roof tiles.

Table 60. Hard body impact made at different temperature for the PV Roof tile

ID	Position	Impact energy [J]	Cell temp	Mechanical status	Electrical results
1	Middle	5.0	25 °C (SCENARIO 0)	Deformation (polymer/metal)	Darken dot on the cell
		10.0 ³		Deformation (polymer/metal)	Darken dot on the cell

2	Middle	5.0	54 °C (SCENARIO 2)	Deformation (polymer/metal)	Darken dot on the cell
		10.0 ⁴		Deformation (polymer/metal)	Darken dot on the cell
3	Middle	5.0	-20 °C (SCENARIO 1)	Deformation (polymer/metal)	No cell damages
		10.0 ³		Deformation (polymer/metal)	No cell damages

After impacts, the mechanical behavior of the PV roof tiles reveals permanent deformation of the polymer and the metal substrate. The electroluminescence reveals a different behavior at different temperatures. In particular, at room and high temperatures, dark spots in correspondence with the impact point have been observed (Figure 86). This does not imply a loss of insulation/performance at the moment, but further investigations to analyse these results are necessary for the future. The impact test performed at low temperatures did not reveal changes in the electrical behavior of the module, probably due to the greater rigidity of plastic materials at low temperatures. Finally, it should be noted that from the mechanical point of view, circles have emerged on the front sheet of the module as if there is an imprint of the sphere that made the impact (Figure 88).

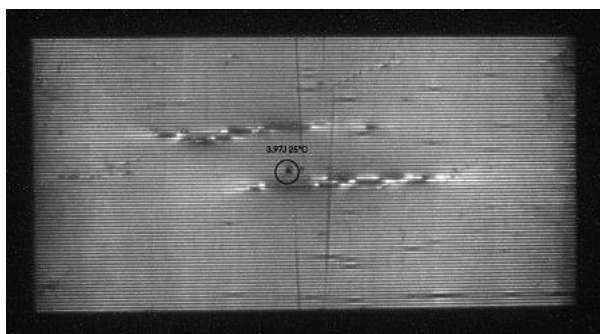


Figure 85. Electroluminescence made on the “ID1” at room temperature (25°C).

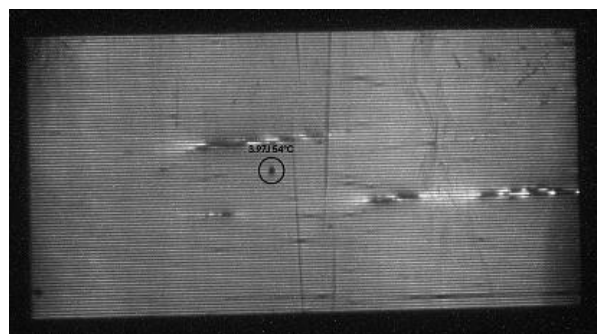


Figure 86. Electroluminescence made on the “ID2” at high temperature (54°C).

⁴ The impactor weights 1 kg

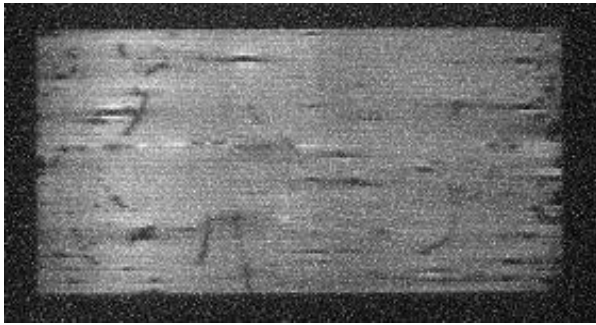


Figure 87. Electroluminescence made on the “ID3” at low temperature (-30°C).



Figure 88. Detail of the circle formed on the polymer after the impact

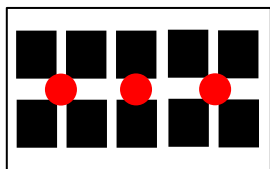
7.2.4 NTP_ME02: Static mechanical load test for BIPV products

7.2.4.1 Purpose

The tests aim to understand the reaction of PV cells and their electrical behavior (e.g. changing of limit state) after the deformation of the module due to a uniformly distributed or concentrated load. The scope of the test is not to assess the resistance of BIPV product/system.

7.2.4.2 Methodology

Tests were performed on a single component, and no samples representing portions of facades, roofs, or other systems were tested. The equipment complying with IEC 61215 (3) (MQT16) was used to perform the tests. In addition, purposely developed tests have been carried out to evaluate and correlate deformations to the integrity of the PV part under concentrated loads. The electrical limit states have been considered and tested in the form of electrical insulation (first safety requirement). The integrity of solar cells subjected to the load was verified through infrared photography with electroluminescence in order to determine any breakage on the cells and the electrical circuit. The electroluminescence was carried out in correspondence and simultaneously with the mechanical load test. Indeed, a darkroom has been reproduced by protecting the camera from light.

Product	Distributed load design	Test description
PV Veture KIT		i) Test according to IEC standard (up to 2500 Pa) ii) Increasing the pressure intervals until a failure or permanent deformation of the PV module (> 2500 Pa) (EAD 040914-00-0404 ⁵)

⁵ Wind suction and pressure load test for PV Veture KITS

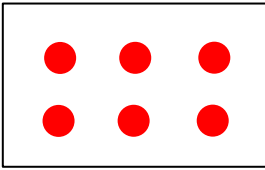
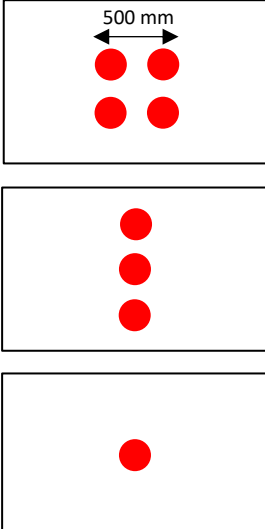
PV roof tile		i) Test according to IEC standard (up to 2500 Pa)
PV laminated glass		i) Deformation limited to 65 or 50 mm (EN 16612 (54)) "in absence of any specific requirement" (up to 2500 Pa) ii) Linear load concentrated and 10 alternating cycles of loading and traction (to verify positive/negative deformations) iii) Concentrated load tested at different temperatures in a climatic chamber (25°C, 85°C, and -40°C ⁶). The load is represented by 5 concrete cubes of 8 kg each. 2% module inclination to simulate the roof tilt angle.

Figure 89. Static mechanical load test for BIPV products. Test description

⁶ The maximum temperature indicated by EN 16612 (54), only in the case of the permanent load is 60°C, while the other temperatures considered for glass building products are a maximum of 40°C. These temperatures are much lower than the possible operation of BIPV products that work at much higher temperatures. Also, EN 16613 (55) defines the module of the interlayer EL. reports a range from -20°C to +60°C in order to determine a master curve for EL (Tref,f), not compatible with the operation of BIPV

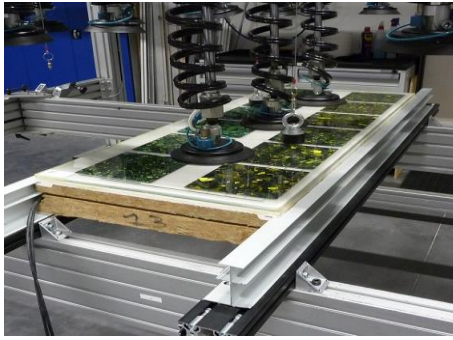


Figure 90. Equipment developed for the PV Veture KIT



Figure 91. Electroluminescence equipment developed

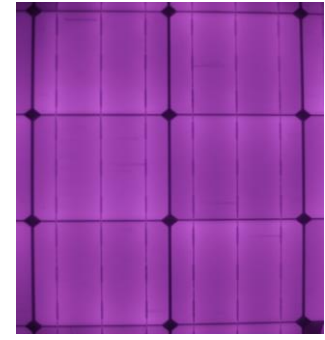


Figure 92. Electroluminescence of a PV laminated module

7.2.4.3 Results

Tests have been carried out to evaluate the behavior of the electrical part under load on different products. Below are shown the results obtained for different types of BIPV products.

PV Veture KIT

The test performed according to the IEC values (2500 Pa) revealed that no changes in terms of the mechanical and electrical behavior of the module were found during and after the test. By increasing the pressure according to the wind suction and pressure load test for PV Veture KIT presented by the EAD 040914-00-0404, the module led to deformations and cracks on the sealing mortar. However, the PV cells did not change their status in terms of insulation loss and integrity of the cells.

PV roof tile

The roofing tile is a product made without the use of glass with an active photovoltaic part in CIGS. This technology is used for flexible modules; therefore, under load, there are no particular deformation-related problems. The test carried out on a BIPV tile has shown that there are no consequences on the PV part even after important deformations.

The tests shown that for the type of product, there are no variations of the electrical part even with significant deformations that lead to the exceeding of the limit state for the construction product.

PV laminated glazing

Load tests have been performed on PV laminated glazing to assess the reaction of solar cells under a concentrated load, which would permit achieving a larger glass deformation leading to variation in the electrical limit state.

i) The first test was carried out with the arrangement of suction cups positioned in the center of the module to form a square-shaped load impression area measuring 500 x 500 mm². The maximum deformation executed on the glass is 50 mm, as expressed by EN 16612 (54). No changes in the electrical limit states of the module have been registered.

ii) A second test was performed with a linear load represented by suction cups positioned in the middle of the module, perpendicular to the long side. The maximum deformation observed was 80 mm. A further test to verify the module's positive deformation (thrust from the front glass) and negative deformation (traction from the front glass) was performed by interchanging 10 cycles of pressure and traction. The tests shown

that at deformations compatible with the building products requirements, consisting of laminated glass, there are no changes in the electrical state. The breakage of the solar cells or the alterations in the electrical insulation has been observed only with the breakage of the glass.

iii) Finally, three concentrated load tests were performed on the same type of PV laminated at different temperatures to evaluate whether temperature could contribute to a change in the electrical limit state. During the execution of the tests, no changes in the electrical state of the tested samples occurred. At the temperature of possible operation of the photovoltaic equal to 85°, a permanent deformation of 9 mm of the photovoltaic laminated glass was obtained (Table 61).

Table 61. General test indications and strain results

ID	Additional weight (kg)	Test temp. (°C)	Load (minutes)	Bend (mm)	Bend after test (mm)	Notes
1	40	+ 25	30	12	0,5	No isolation loss No cracks
2	40	- 40	30	3	0,2	No isolation loss No cracks
3	40	+ 85	30	14	9,0	No isolation loss No cracks but permanent deformation



Figure 93. Deformation on PV roof tile under mechanical load.

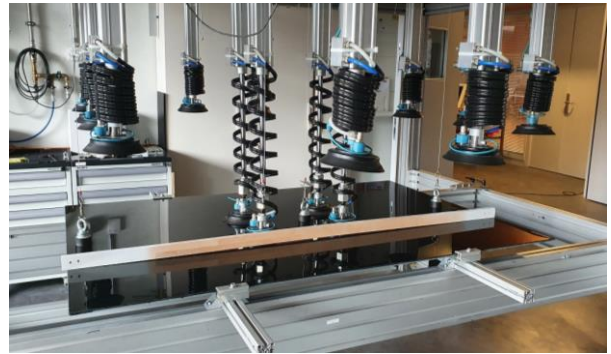


Figure 94. Test made on BIPV glass-glass module.

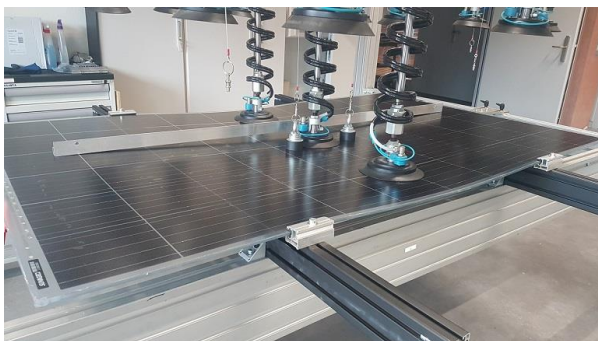


Figure 95. Test made with push load on PV laminated glass during the cycles.



Figure 96. Test made with pull load on PV laminated glass during the cycles.

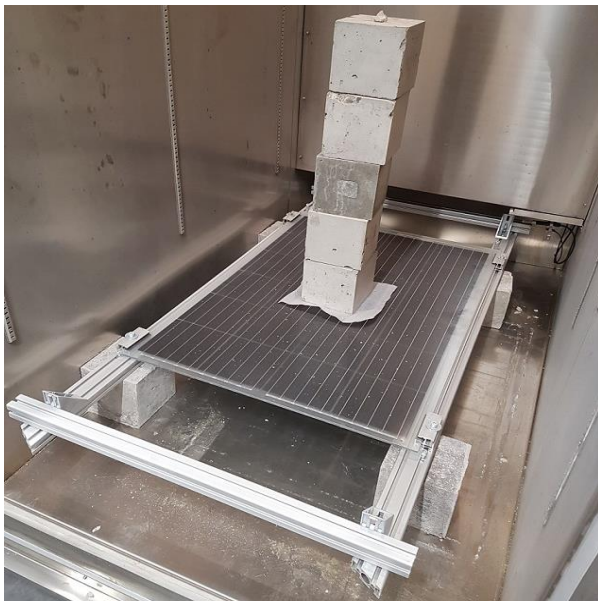


Figure 97. Concentrated load on PV laminate glass in the climatic room.

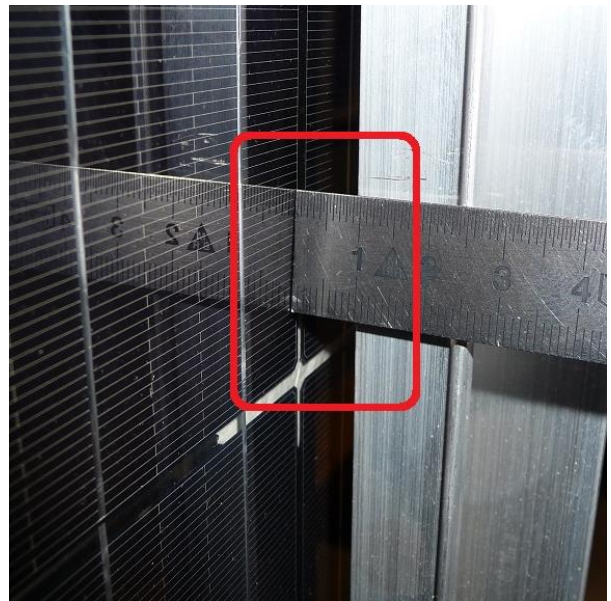


Figure 98. Permanent deformation due to concentrated load at high temperature on PV laminated glass.

7.2.4.4 Conclusions

The tests carried out to understand the reaction of PV cells and the electrical behavior due to a uniformly distributed or concentrated load shown up that no changes occurred in the electrical limit state during the tests. However, given the limited number of tests for each type of BIPV product, the results will need to be further investigated in the future.

Results have shown that the maximum deformation required by the building regulation does not compromise the electrical integrity of the modules. Within the limits of permissible deformation of construction products, no electrical insulation loss or alteration of the integrity of the solar cells occurred. Aligned with the final goal of the BIPVBOOST project, the PV qualification tests simplification would help to decrease the cost of the entire BIPV value chain.

Furthermore, for BIPV products the verification at low cyclic stresses for example through the Cyclic (dynamic) mechanical load test (MQT 20) reported in IEC 61215-2 is necessary. Components within BIPV products may be susceptible to low levels of mechanical stress that could compromise component integrity. Components that can be evaluated by the dynamic cyclic mechanical load (DML) test include solar cells, interconnect strips, electrical bonds, and onboard seals.

Finally, the tests shown that a design approach rather than a testing approach would need further investigations in order to test and assess the real behavior of BIPV products and materials. As instance, a design approach would allow to assess the behavior of the polymer at high/low temperatures, which is not considered in the current regulatory framework and causes a permanent deformation on the glass-glass PV module.

8 CONCLUSIONS

The construction of multifunctional BIPV products that can perform different functions, with electrically active and non-active parts assembled together lacks a performance relation at the state of art. Due to the interaction between PV and building parts, the quality assessment requires to go further than the application of test methodologies provided separately by the PV or by the building regulations. In BIPVBOOST project, a possible path is considered achievable by developing a new approach for the qualification of BIPV products, coherent with the principles of CPR 305/2001 considering BIPV as a construction product. Grounding on the analysis of the missing gaps at the state-of-art, the project targets to implement proposal for a unified and effective approach aimed at harmonizing or amending current standards, achieving the main quality requests by reducing the number of steps needed for the product qualification and saving time and cost.

Independently of the boundary conditions, it has been observed that the U value of the PV-IGU is similar to the equivalent glazing system without PV. Therefore, the current EN 410 and ISO 10292 standards can be used to calculate the U value of the vertical PV-IGU as it was a normal IGU. For horizontal glazing, the new thermal effects of PV-IGU can impact on the average dynamic U. Besides the mentioned standards, these results may impact on other standards like EN 674 and EN 675 for the experimental determination of U. The JB may reduce slightly the U value, but this reduction is significant only in PV laminated (not IGU) if the JB occupies a significant area of the glazing. The G value of PV-IGU seems to be slightly (but significantly) affected by the PV conversion effect, so it is recommended to perform the dynamic G value calculations considering this heat reduction due to the radiation energy transformed into electricity. The maximum temperatures found both for the cavity gas and PV glass layer of a PV-IGU unit are significantly higher than for NO-PV equivalent glazing. Also, the pressure in the cavity can be significantly higher, and thus the risk of gas leakages and mechanical loads. For instance, this fact should be considered in EN 1279 standard series.

The operating temperatures expected in normal serviceability conditions (SLS), can include potential temperature rise due to the non-conventional shading scenarios as reported in the development of NTP-

EL01. In SflS, the determination of the shade tolerance in terms of temperature rise, is linked to either abnormal operation of protective devices or severe mismatch among the parts connected in series within a product string. The consequent classification of the BIPV, can imply different severity levels for all the subsequent accelerated ageing tests (see NTP – EL 02) and bypass diodes thermal test (see NTP – EL 03), which are designed to verify the suitability of materials, components and protective devices in the BIPV product's construction over time, according to the IEC TS 63126. The NTP-EL02 makes available of a new highly accelerated ageing test sequence tailored for the assessment of the durability of BIPV products, with regard to the ageing of polymeric materials and to the reliability over time of all the adhesion interfaces of the product, in the framework of a performance-based approach. The new test procedure introduces a combined recipe of thermal, electrical, and environmental stresses, yet covering and exceeding the overall IEC ageing procedures and including the modifications on the test levels as laid down in IEC TS 61326. Preliminary tests that the total time needed to complete the ageing sequence is significantly reduced, since a complete ageing test can be performed in only one thermal chamber, and using only 2 identical samples instead of 6. Moreover, any potential insulation failure or excessive degradation of the performances can be detected at an earlier stage, so avoiding expensive and time-consuming re-testing procedures. The main innovative outcome from this NTP EL 03 is the evaluation of the suitability of the thermal design of the junction boxes (which embeds one or more bypass diodes), used in BIPV products, by means of a strongly simplified test set-up and a significant reduction of the test duration. The proposed test method allows TJ to be measured at full current under actual operating conditions.

NTP ME-01 aims at evaluating a product's integrity after stresses due to an impact of an external body, focused on adopting a performance-based approach and considering the real temperature conditions of the product. As an outcome, a series of new BIPV-specific testing methodologies were defined as the basis to be adopted in current CPR-related test procedures and for verifying the Fracture Limit State by testing in glass design. From preliminary test at high temperatures (90°C) for glass-glass modules with crystalline solar cells, the value of the energy that led to the breakage of the glass resulted slightly lower than the test at room temperature. At low temperatures (-30°C), all the tests have shown the breakage of the glass with the highest energy registered in all tested samples, and the electroluminescence revealed a very diffuse propagation of the cell's fracture throughout the surface in this condition, differently by other cases. II NTP ME-02, preliminary tests have shown that, under the operating conditions of different classes of BIPV products tested in the project, deformation due to static loads in the range of the typical displacement admitted for construction works, whether uniformly distributed or concentrated, does not lead to changes in electrical safety or in cells' fracture.

In NTP-FR01 and NTP FR-02, the tests for Roof fire reaction according to Broof and for Facade fire reaction according the SBI respectively, are carried out with appropriate electric load. Results are compared with initial test in normal conditions in order to identify possible deviation due to additional constraints provided by the stress of the electric load. It's not been observed any current leakages or breakout, which emphasizes the absence of a break in the electrical circuit. Beyond the first positive conclusions, we draw attention to the fact that these tests are carried out on specific configurations and that it will be necessary to extend the number of investigations in order to have statistically representative results. As part of this work, it will remain to determine the influences of other aging effects that could affect the fire performance of BIPV components.

The implementation and adoption of the procedural outcomes are expected to provide a pre-normative reference to support international joint actions (e.g. IEA PVPS Task 15) as well as to revamp the procedures of EU standards.

9 REFERENCES

1. (CENELEC), European Committee for Electrotechnical Standardization. CENELEC - EN 50583 part. 1-2. *Photovoltaics in buildings - Part 1: BIPV modules / Part 2: BIPV systems*.
2. International Electrotechnical Commission. IEC 61215-1. *Terrestrial photovoltaic (PV) modules – Design qualification and type approval – Part 1: Test requirements*. Edition 2.0 - 2021.
3. —. IEC 61215-2. *Terrestrial photovoltaic (PV) modules – Design qualification and type approval – Part 2: Test procedures*. Edition 2.0 - 2021.
4. —. IEC 61730-1. *Photovoltaic (PV) module safety qualification – Part 1: Requirements for construction*. 2016.
5. —. IEC 61730-2. *Photovoltaic (PV) module safety qualification – Part 2: Requirements for testing*. 2016.
6. EUROPEAN COMMISSION. Regulation (EU) N° 305/2011 of the European Parliament and of the Council of March 9th 2011 - Construction Products Regulation, CPR 305/2011. 2011.
7. BIPVBOOST - Horizon 2020. *D5.1 Report on standardization, performance risks and identification of related gaps for a performance-based qualification in BIPV*.
8. INTERNATIONAL, ENERGY AGENCY (IEA) - Task 15 - Subtask C – International framework for BIPV specifications. *Analysis of requirements, specifications and regulation of BIPV*. 2019.
9. International Energy Agency. Subtask E. *Pre-normative international research on BIPV characterisation methods*. 2020-2023.
10. Construct PV. [Online] European Union's Seventh Framework Programme. <http://www.constructpv.eu/>.
11. European Union's Horizon 2020 research and innovation programme. *PVSITES*. [Online] grant agreement No 691768. www.pvsites.eu.
12. International Electrotechnical Commission. IEC TS 62915:2018. *Photovoltaic (PV) modules - Type approval, design and safety qualification - Retesting*.
13. International Energy Agency. Multifunctional Characterisation of BIPV. *Proposed Topics for Future International Standardisation Activities*. 2020.
14. International Organization for Standardization. ISO 12543 Series. *Glass in building — Laminated glass and laminated safety glass*.
15. European Committee for Standardization. EN 12600. *Glass in building - Pendulum test - Impact test method and classification for flat glass*. 2002.
16. Regulation (EU) N° 305/2011 of the European Parliament and of the Council of March 9th 2011 - Construction Products Regulation, CPR 305/2011.
17. European Committee for Electrotechnical Standardiz. EN 50583-1:2016. *Photovoltaics in buildings - Part 1: BIPV modules*. 2016.
18. —. EN 50583-2: 2016. *Photovoltaics in buildings - Part 2: BIPV systems*. 2016.
19. EUROPEAN PARLIAMENT AND OF THE COUNCIL. DIRECTIVE 2014/35/EU (LVD). *Harmonisation of the laws of the Member States relating to the making available on the market of electrical equipment designed for use within certain voltage limits*. 2014.
20. —. DIRECTIVE 2006/95/EC . *Harmonisation of the laws of Member States relating to electrical equipment designed for use within certain voltage limits*. 2006.

21. International Electrotechnical Commission. IEC 63092-1. *Photovoltaics in buildings - Part 1: Requirements for building-integrated photovoltaic modules*. 2020.
22. —. IEC 63092-2. *Photovoltaics in buildings - Part 2: Requirements for building-integrated photovoltaic systems*. 2020.
23. *Thermal Behaviours of BIPV-Modules (U-Value and g-Value)*. Misara, S, Henze, N and Sidelev, A. 2011.
24. *Building-Integrated Photovoltaic (BIPV) products and systems: A review of energy-related behavior*. Martín-Chivelet, Nuria, et al. 2022, *Energy & Buildings*, Vol. 262.
25. *Modeling temperature and thermal transmittance of building integrated photovoltaic modules*. Sánchez-Palencia, P, Martín-Chivelet, N and Chenlob, F. 2019, *Solar Energy*, Vol. 184, pp. 153-161.
26. *Spectral effects on the transmittance, solar heat gain, and performance rating of glazing systems*. Gueymard, Christian A. and duPont, William C. 2009, *Solar Energy*, Vol. 83.
27. *Thermal analysis of a BIPV system by various modelling approaches*. Assoa, Ya-Brigitte and al., et. 2017, *Solar Energy*, Vol. 155.
28. *Assessment of energy performance of semi-transparent PV insulating glass units using a validated simulation model*. Wang, Meng and al., et. 2016, *Energy*, Vol. 112.
29. *Performance of building integrated photovoltaic facades: Impact of exterior convective heat transfer*. Gonçalves, Juliana E. and al., et. *Applied Energy*, Vol. 287.
30. *Study on the overall energy performance of a novel c-Si based semitransparent solar photovoltaic window*. Peng, Jinqing and al., et. 2019, *Applied Energy*, Vol. 242.
31. *Integral energy performance characterization of semi-transparent photovoltaic elements for building integration under real operation conditions*. Olivieri, Lorenzo and al., et. *Energy and Buildings*, Vol. 68.
32. *On the analytical calculation of the solar heat gain coefficient of a BIPV module*. Baenas, Tomas and Machado, Maider. *Energy and Buildings*, Vol. 151.
33. *Thermal Performance (G-value and U-value) - Evaluation of BIPV Applied to Glass Facade*. Ishii, Hisashi. EUPVSEC.
34. Pierluigi Bonomo, Fabio Parolini, Francesco Frontini. Safety of laminated BIPV glasses: progresses towards product qualification. *Engineered Transparency 2021 - Glass in Architecture and Structural Engineering*. 2021, pp. 541-557.
35. *Laminated BIPV glass: approaches for the integration in the building skin*. Erika Saretta, Pierluigi Bonomo, Francesco Frontini. s.l.: *Engineered Transparency: Glass in Architecture and Structural Engineering* Engineered Transparency., 2016.
36. Hemmerle, Claudia. 29th European Photovoltaic Solar Energy Conference and Exhibition. *GLASS-GLASS BIPV MODULES AS CONSTRUCTION PRODUCT: MECHANICAL RESISTANCE AND POST-BREAKAGE BEHAVIOUR*.
37. Bernhard Weller, Claudia Hemmerle, Michael Kothe. 24th European Photovoltaic Solar Energy Conference. *TESTING PROCEDURES FOR BUILDING INTEGRATED PHOTOVOLTAICS*. Hamburg, Germany : s.n., 2009.
38. Bernhard Weller, Claudia Hemmerle, Sven Jakubetz, Stefan Unnewehr. Photovoltaics Technology Architecture Installation - Edition detail. *Detail Practice: Photovoltaics: Technology, Architecture, Installation*. 2010.

39. Hyun-Il Kim, Jin-Ho Ahn, Seung-Min Shin, Myung-Ick Hwang and Eun-Chel Cho. 27th European Photovoltaic Solar Energy Conference and Exhibition. *CHARACTERISTICS OF GLASS TO GLASS BIPV MODULE UNDER MECHANICAL PROPERTIES AND OPERATING TEMPERATURE*.
40. Siwanand Misara, Maria Roos, Norbert Henze, Martin Sander. 27th European Photovoltaic Solar Energy Conference and Exhibition. *POST-BREAKAGE-INTEGRITY OF BIPV MODULE IN BUILDING REGULATION (MULTIELEMENT PROJECT RESULTS)*.
41. *Experimental operating cell temperature assessment of BIPV with different installation configurations on roofs under Mediterranean climate*. M. D’Orazio, C. Di Perna, E. Di Giuseppe. August 2014 - Renewable Energy 68:378–396, Vol. Renewable Energy.
42. *Monitoring the Operating Temperatures of Modules in Open-Rack and Typical BIPV Configurations*. Ebrar Özkalay, Gabi Friesen, Andrew Fairbrother, Christophe Ballif, Alessandro Virtuani,. 2021 IEEE 48th Photovoltaic Specialists Conference (PVSC).
43. European Committee for Standardization. EN 12600:2002. *Glass in building - Pendulum test - Impact test method and classification for flat glass*.
44. EN 14019. *Curtain Walling - Impact resistance - Performance requirements*. 2016.
45. EN 13049. *Windows - Soft and heavy body impact - Test method, safety requirements and classification*. 2003.
46. UNI, Ente nazionale italiano di unificazione -. UNI 11678. *Vetro per edilizia - Elementi di tamponamento in vetro aventi funzione anticaduta - Resistenza al carico statico lineare ed al carico dinamico - Metodi di Prova*. 2017.
47. European Assessment Document. EAD 090062-00-0404. *Kits for external wall claddings mechanically fixed*. 2018.
48. European Organization for Technical Assessment. EOTA TR-001. *Determination of impact resistance of panels and panel assemblies*. 2003.
49. European Assessment Document. EAD 040914-00-0404. *Veture kits - Prefabricated units for external wall insulation and their fixing devices*. 2018.
50. International Organization for Standardization. ISO 7892:1988. *Vertical building elements — Impact resistance tests — Impact bodies and general test procedures*. 1998.
51. European Committee for Standardization. EN 13830:2015+A1:2020. *Curtain walling - Product standard*. 2015+A1:2020.
52. G. Menges, E. Haberstroh, W.R. Michaeli, E. Schmachtenberg. *Plastics Materials Science*. s.l. : Hanser Verlag ISBN 3-446-21257-4, 2002.
53. Marc Martín, Xavier Centelles, Aran Solé, Camila Barreneche, A. Inés Fernández, Luisa F. Cabeza. *Polymeric interlayer materials for laminated glass: A review*. 2020.
54. European Committee for Standardization. EN 16612. *Glass in building - Determination of the lateral load resistance of glass panes by calculation*. 2019.
55. —. EN 16613. *Glass in building - Laminated glass and laminated safety glass - Determination of interlayer viscoelastic properties*. 2019.
56. *Analysis and Evaluation of Energy Economy Related BIPV Standardization Needs*. Valencia-Caballero, D., et al. s.l. : 38th European Photovoltaic Solar Energy Conference and Exhibition, 2021.

-
57. *On the analytical calculation of the solar heat gain coefficient of a BIPV module*. Baenas, T. and M.Machado. 2017, *Energy and Buildings*, Vol. 151, pp. 146-156.
58. *G-value indoor characterization of semi-transparent photovoltaic elements for building integration: new equipment and methodology*. Olivieri, L., et al. 2015, *Energy and Buildings*, Vol. 101, pp. 84-94.
59. *Fundamental Shape Factors in Radiative Heat Transfer With Numerical Integration*. Yeh, P.S. 2000. ASEE Southeast Section Conference.
60. *Impact of Cracks in Multicrystalline Silicon Solar Cells on PV Module Power—A Simulation Study Based on Field Data*. Arnaud Morlier, Felix Haase, and Marc Köntges. 6, November 2015, *IEEE JOURNAL OF PHOTOVOLTAICS*, Vol. 5.
61. Isidoro Lillo-Bravo, Pablo González-Martínez, Miguel Larrañeta and José Guasumba-Codena. *Impact of Energy Losses Due to Failures on Photovoltaic Plant Energy Balance*. 2018.
62. Mahmoud Dhimish. *Renewable Energy. Micro cracks distribution and power degradation of polycrystalline solar cells wafer: Observations constructed from the analysis of 4000 samples*. 2020.
63. *Modelling and experimental investigations of microcracks in crystalline silicon photovoltaics: A review*. Lamprini Papargyri, Marios Theristis, Bernhard Kubicek, Thomas Krametz, Christoph Mayr, Panos Papanastasiou, George E. Georghiou. s.l. : Elsevier, 2020, *Renewable energy*.
64. Felix Haase, Jörg Käsewieder, Seyed Roozbeh Nabavi, Eelco Jansen, Raimund Rolfes, and Marc Köntges. *IEEE JOURNAL OF PHOTOVOLTAICS. Fracture Probability, Crack Patterns, and Crack Widths of Multicrystalline Silicon Solar Cells in PV Modules During Mechanical Loading*. 2018. Vol. 8, 6.
65. Tonella, Elisabetta. master thesis. *Il vetro strutturale: risposta di elementi stratificati inflssi e prove di identazione*. 2010.
66. *Laminated Glass Cantilevered Plates under Static and Impact Loading*. Luigi Biolzi, Antonio Bonati, and Sara Cattaneo. 2018, *ADVANCES IN CIVIL ENGINEERING*.
67. International Electrotechnical Commission. IEC 61215:2005 Withdrawn. *Crystalline silicon terrestrial photovoltaic (PV) modules - Design qualification and type approval*. 2005.
68. —. IEC 61646:2008 Withdrawn. *Thin-film terrestrial photovoltaic (PV) modules - Design qualification and type approval*. 2008.
69. *Degradation in PV Encapsulant Strength of Attachment : An Interlaboratory Study Towards a Climate-Specific Test Preprint*. Miller, David C., et al. Portland, Oregon : s.n., 2016-07-01. Presented at the 43rd IEEE Photovoltaic Specialists Conference, 5-10 June 2016.
70. International Electrotechnical Commission. IEC 61853-1. *Photovoltaic (PV) module performance testing and energy rating - Part 1: Irradiance and temperature performance measurements and power rating*. 2011.
71. —. IEC 61853-2. *Photovoltaic (PV) module performance testing and energy rating - Part 2: Spectral responsivity, incidence angle and module operating temperature measurements*. 2016.
72. —. IEC 61853-3. *Photovoltaic (PV) module performance testing and energy rating - Part 3: Energy rating of PV modules*. 2018.
73. —. IEC 61853-4. *Photovoltaic (PV) module performance testing and energy rating - Part 4: Standard reference climatic profiles*. 2018.
74. Bube, Richard H. *Photovoltaic Materials (Series on Properties of Semiconductor Materials*. s.l. : Imperial College Press, 1998.

75. BIPVBOOST (This project has received funding from the European Union’s Horizon 2020 research and innovation programme under grant agreement N° 817991). *Bringing down costs of building-integrated photovoltaic (BIPV) solutions and processes along the value chain, enabling widespread nZEBs implementation*. 2019.
76. IEA PVPS Task 13 - Subtask 3.3. *Review on Infrared and Electroluminescence Imaging for PV Field Applications*. 2018.
77. *Micro cracks distribution and power degradation of polycrystalline solar cells wafer: Observations constructed from the analysis of 4000 samples*. Dhimish, Mahmoud. s.l. : Elsevier, 2019, Renewable Energy .
78. *PV module damages caused by hail impact and non-uniform snow load*. G. Mathiak, J. Sommer, W. Herrmann, N. Bogdanski, J. Althaus, F. Reil. Munich : s.n., 2016. 32nd European Photovoltaic Solar Energy Conference and Exhibition.
79. Teule, Thirza, et al. *The vulnerability of solar panels to hail*. Vrije Universiteit Amsterdam. 2019.
80. *Testing of Flat Plate Photovoltaic Modules for Terrestrial Environments*. Hoffman, A., Arnett, J., & Ross, R. Berlin : s.n., 1978. Proceedings of the 2nd E.C. Photovoltaic Solar Energy Conference.
81. Yousif, E., Haddad, R. Photodegradation and photostabilization of polymers, especially polystyrene: review. 2013.
82. European Committee for Standardization. EN ISO 12543-4:2021. *Glass in building - Laminated glass and laminated safety glass - Part 4: Test methods for durability*. 2021.
83. D. Delincé, J. Belis, G. Zarmati, B. Parmentier. Structural Behaviour of Laminated Glass Elements – A Step Towards Standardization. Tampere, Finland : s.n., 2007.
84. T. Serafinavičius, J.-P. Lebet, C. Louter, A. Kuranovas, T. Lenkimas. The effects of environmental impacts on durability of laminated glass plates with interlayers (SG, EVA, PVB). 2014.
85. Kensuke Nishioka, Kazuyuki Miyamura, Yasuyuki Ota, Minoru Akitomi, Yasuo Chiba, and Atsushi Masuda. Accurate measurement and estimation of solar cell temperature in photovoltaic module operating in real environmental conditions. *Japanese Journal of Applied Physic*. 2018.
86. 2020, BIPVBOOST - Horizon. Functional samples of multifunctional BIPV façade cladding system with integrated insulation complying with specifications. *D4.1*. 2021.
87. Mostafa M. El-Shami, Scott Norville, Yasser E. Ibrahim. *Stress analysis of laminated glass with different interlayer materials*. 2012.
88. Tomáš Hána, Tomáš Janda, Jaroslav Schmidt, Alena Zemanová, Michal Šejnoha. Experimental and Numerical Study of Viscoelastic Properties of Polymeric Interlayers Used for Laminated Glass: Determination of Material Parameters. 2019.
89. C W Lantman, W J MacKnight, R D Lundberg. Structural Properties of Ionomers. *Annual Review of Materials Science*. 2019.
90. International Electrotechnical Commission. IEC 60269-6:2010 . *Low-voltage fuses - Part 6: Supplementary requirements for fuse-links for the protection of solar photovoltaic energy systems*.
91. European Commission. Eurocodes. *EN 1990: Basis of structural design*. 2002/A1:2005.
92. (CENELEC), European Committee for Electrotechnical Standardization. EN 50583 Series. *Photovoltaics in buildings*.
93. International Electrotechnical Commission;. PT IEC 63092-2 ED1 - Photovoltaics in buildings – Part 2: Building integrated photovoltaic systems.

94. EUROPEAN COMMISSION. DIRECTIVE 2014/35/EU (LVD). *Harmonisation of the laws of the Member States relating to the making available on the market of electrical equipment designed for use within certain voltage limits*. 2014.
95. (ISO), International Organization for Standardization. ISO 12543 Series. *Glass in building — Laminated glass and laminated safety glass* .
96. International Electrotechnical Commission (IEC). IEC 61730-1:2016 Series. *Photovoltaic (PV) module safety qualification*.
97. —. IEC 61215-1:2016 Series. *Terrestrial photovoltaic (PV) modules - Design qualification and type approval* .
98. BIPVBOOST, Horizon 2020. European project - This project has received funding from the European Union's Horizon 2020 research and innovation programme under grant agreement No 817991. *BIPVBOOST - "Bringing down costs of BIPV multifunctional solutions and processes along the value chain, enabling widespread nZEBs implementation"*. 2019.
99. International Electrotechnical Commission. IEC TS 62782. *Photovoltaic (PV) modules – Cyclic (dynamic) mechanical load testing*. 2016.
100. European Committee for Standardization. EN 356:1999. *Glass in building - Security glazing - Testing and classification of resistance against manual attack*. 1999.
101. —. EN 1990:2002/A1:2005. *Eurocode - Basis of structural design*. 2005.

10 ACKNOWLEDGMENTS

The Authors thank all the industrial partners involved, and especially Onyx, PIZ, Tullips, Flisom, and Schweizer for providing the samples.